

Slipforming of Vertical Concrete Structures

Friction between concrete and slipform panel

by

Kjell Tore Fosså

Dr.ing thesis

**Department of Structural Engineering
The Norwegian University of Science and Technology
N-7491 Trondheim
Norway**

June 2001

Acknowledgements

I would like to express my gratitude to my main supervisor Professor Magne Maage for his personal commitment, interesting discussions and valuable advice. Magne has been continuously encouraging and patient throughout my study. I will also express my gratitude to supervisor Sverre Smeplass for the support and valuable advice throughout my study. Also the support and good advice from supervisor Malvin Sandvik is sincerely appreciated. Furthermore, special thanks to my colleagues at the Department of Structural Engineering and especially to Erik Sellevold for interesting discussions.

This work was made possible by the financial support from Aker Engineering AS, Selmer Skanska AS, NCC Anlegg AS, Veidekke ASA, Norcem AS, Gleitbau Ges.m.b.H. and the Research Council of Norway. The companies together with Norwegian Public Road Administration have been represented in a reference group, which have followed the research program and given comments and valuable advice throughout the execution of the research program.

The experimental program has comprised planning and construction of test rigs and also a test panel for installation in a slipform. Special thanks to T. Meltzer, J. Sandnes, J. Troset, Ø. Langnes, B. Ingebrigtsen, O. Loraas, O. Haldorsen, K. Kristiansen, H. Rødsjø and in particular S. Lorentzen for planning and construction of these rigs and also for the assistance during execution of the tests.

Furthermore, I am also grateful to S. Perlestenbakken and Interform AS for the opportunity to carry out field investigation during slipforming on site. This investigation went very well because of the successfully cooperation and assistance from Interform AS during the test period on site.

Special thanks to former Aker Norwegian Contractors (now a part of Aker Maritime ASA) for initiating this research project. Without this initiative, this research project would not be started. Also a special thanks to the many conversations and interesting discussions with former and present colleagues in the company.

I am also grateful to my family and friends for the support, encouragement and patience during these four years.

Trondheim, June 2001

Kjell T. Fosså

Table of contents

Acknowledgements	iii
Table of contents	iv
Abstract	x
Notations	xiii
Definitions	xv
1 INTRODUCTION	1
1.1 Background	1
1.2 Principles of a slipform	1
1.3 Differences between slipform and fixed formwork	3
1.4 Objectives	3
1.5 Scope of work	4
2 LITERATURE REVIEW	5
2.1 Introduction	5
2.2 Fresh concrete properties	5
2.2.1 Introduction	5
2.2.2 Shear strength in concrete	7
2.2.3 Effective pressure	9
2.2.4 Pore water pressure	11
2.2.4.1 General	11
2.2.4.2 Settlement and bleeding	12
2.2.4.3 Effect of hydration – chemical shrinkage	12
2.2.4.4 Drying of surface	15
2.2.4.5 Break-through pressure	17
2.2.5 Summary fresh concrete properties	19
2.3 Lifting force and concrete pressure during slipforming	21
2.3.1 Introduction	21
2.3.2 Concrete in a slipform	21
2.3.3 Static and sliding friction	22
2.3.4 The slipforming rate	23

2.3.5	Concrete pressure on the panel	25
2.3.6	Effect of the concrete mix composition	28
2.3.7	Surface - slipform panel	29
2.3.8	Stress distribution during lifting	31
2.3.9	Surface defects	32
2.3.10	Summary lifting force and concrete pressure during slipforming	34
2.4	Hardened properties	35
2.4.1	General	35
2.4.2	Compressive strength	36
2.4.3	Measurements of dynamic modulus of elasticity	39
2.4.4	Density of the concrete	40
2.4.5	Tensile splitting strength	42
2.4.6	Durability investigation – carbonation measurements	43
2.4.7	Chloride diffusion coefficient	46
2.4.8	Summary hardened properties	47
3	HYPOTHESES	49
4	EXPERIMENTAL PROGRAM	52
4.1	General	52
4.2	Description of the test rigs	52
4.2.1	Friction rig	52
4.2.1.1	Objectives	52
4.2.1.2	Reinforcement	53
4.2.1.3	Slipform panel	53
4.2.1.4	Pressure on top	53
4.2.1.5	The position measurements	54
4.2.1.6	Inductive displacement sensors	54
4.2.1.7	Pore water pressure gauge	54
4.2.1.8	Temperature measurements	55
4.2.1.9	Control and measurement system	55
4.2.2	Vertical slipform rig	55
4.2.2.1	Objectives	55
4.2.2.2	Steel framework	56
4.2.2.3	Concrete container	56
4.2.2.4	Reinforcement	58
4.2.2.5	The slipform panel	58
4.2.2.6	Pressure lid on top	58
4.2.2.7	Normal force measurements	59
4.2.2.8	The position measurements	60
4.2.2.9	Inductive displacement sensor	60
4.2.2.10	Pore water pressure gauges	61
4.2.2.11	Temperature measurements	62
4.2.2.12	Control and measurement system	62
4.2.3	Test panel used during field investigations	62
4.2.3.1	Design	62

4.2.3.2	Measurement gauges	63
4.2.3.3	Control and measurement system	64
4.3	Concrete constituency	65
4.3.1	Introduction	65
4.3.2	Concrete mixes	65
4.3.2.1	Friction rig	65
4.3.2.2	Vertical slipform rig	66
4.3.2.3	Field investigations	67
4.3.3	Aggregate	68
4.3.4	Cement	70
4.3.5	Admixtures	70
4.4	Test program	71
4.4.1	Friction rig	71
4.4.1.1	Program	71
4.4.1.2	Execution method of the tests	73
4.4.2	Vertical slipform rig	73
4.4.2.1	Program	73
4.4.2.2	Execution method of the single layer tests	75
4.4.2.3	3-layers concrete tests	75
4.4.3	Field investigations	76
4.4.4	Testing on hardened concrete	76
4.4.4.1	Capillary water absorption tests	76
5	CALIBRATION AND VERIFICATION	78
5.1	General	78
5.2	Friction rig	78
5.2.1	Calibration of the measuring units	78
5.2.2	The slipform rig rate during movement	78
5.2.3	Control of the surface roughness	79
5.2.4	Sliding friction in the friction rig	81
5.2.5	Reproducibility test	82
5.3	Vertical slipform rig	83
5.3.1	Calibration of the measuring units	83
5.3.2	Control of the spring steel	84
5.3.3	The rate of the slipform panel during lifting	84
5.3.4	Control of the surface roughness	85
5.3.5	Sliding friction in the vertical rig	85
5.3.6	Reproducibility test	86
5.4	Test panel	90

6	METHOD OF EVALUATION AND PRESENTATION OF THE MEASUREMENTS	91
6.1	Lifting force	91
6.2	Effective pressure in the concrete	93
6.3	The friction coefficient	95
6.3.1	Definitions of terms used to describe the pore water pressure development	98
6.3.1.1	Pore water pressure decrease rate	98
6.3.1.2	Minimum pore water pressure	99
7	RESULTS AND DISCUSSIONS	100
7.1	Effective pressure	100
7.1.1	Friction law	100
7.1.2	The correlation between the net lifting stress and the effective pressure	101
7.1.3	Statistical evaluation of the effective pressure	104
7.1.3.1	Correlation between the effective pressure and the lifting stress	104
7.1.4	The friction coefficient	105
7.1.4.1	Concrete tests carried out on the vertical slipform rig	105
7.1.4.2	Concrete tests carried out on the friction rig	107
7.1.5	Observation during the regression analyses	108
7.1.6	Summary	110
7.2	The pressure in the pore water	111
7.2.1	Introduction	111
7.2.2	Particle concentration	113
7.2.2.1	The effect of silica fume	113
7.2.3	The effect of the air content	115
7.2.3.1	Air entraining agents	115
7.2.3.2	The effect of vibration	116
7.2.3.3	The effect of lightweight aggregate	118
7.2.3.4	The effect of the binder volume	120
7.2.4	Water communication	122
7.2.4.1	Water flow between concrete layers	122
7.2.4.2	Surface drying	125
7.2.5	The effect of normal pressure	126
7.2.5.1	Correlation between minimum pore water pressure and normal pressure	129
7.2.6	The effect of the slipform technical parameters	130
7.2.7	Parameters affecting the minimum pore water pressure	132
7.2.8	Summary	133
7.3	The normal pressure	136
7.3.1	Introduction	136
7.3.2	The effect of the concrete density and the placing method	136
7.3.3	The effect of the panel stiffness	137
7.3.4	The effect of the inclination	139
7.3.5	Summary	140

7.4	The impact of the material properties in the shear zone	141
7.4.1	Introduction	141
7.4.2	The lubricant properties	141
7.4.3	Rough slipform panel	143
7.4.4	Summary	146
7.5	Operational parameters	147
7.5.1	Introduction	147
7.5.2	Lifting frequency	147
7.5.2.1	Tests with normal weight concrete	147
7.5.2.2	Tests with lightweight concrete	149
7.5.3	The effect of the lifting height	149
7.5.4	Calculation of the maximum lifting stress at different lifting heights	151
7.5.5	Summary for the lifting height and the lifting frequency	153
7.5.6	The effect of the lifting stress on the concrete surface	154
7.5.7	One layer - several concrete layers	155
7.5.7.1	Introduction	155
7.5.7.2	Interaction between the concrete layers	155
7.5.7.3	Verification procedure	156
7.5.7.4	The same type of concrete in all layers	158
7.5.7.5	Concrete with different properties	160
7.5.7.6	With inclination of the slipform panel	162
7.5.8	Summary several layers	165
7.6	Field investigations	166
7.6.1	Introduction	166
7.6.2	Measured lifting stress and normal pressure during slipform operation	166
7.6.3	Concrete tested in the slipform rig	169
7.6.4	Surface quality	171
7.6.4.1	Tukthus site	171
7.6.4.2	Sørkedalsv site	173
7.6.5	Summary	174
8	SUMMARY	176
8.1	Objectives and Scope	176
8.2	The friction law	176
8.3	The pore water pressure	177
8.4	Operational parameters	179
8.5	Connection between lifting stress (friction) and surface damages	179
8.6	The effect of combination of the parameters on the lifting stress	179
8.7	Confirmation of the hypotheses	180

9 CONCLUSIONS	181
REFERENCES	182
APPENDIX A Overview of the tests from the test rigs	186
APPENDIX B Results from the capillary testing	191
APPENDIX C Key results from each test used in the report	193

Abstract

Slipforming is a construction method that has been used in several decades for production of concrete structures. It is a wide range of different structures that are slipformed, but typical are vertical structures such as towers, bridge columns and offshore platforms. Slipforming are not only used for straight vertical concrete structures, but also on structures where the geometry of the structure and the wall thickness is changed. Slipforming is normally a continuous working operation (24 hours a day), which require a well-planned supply of materials. Problems that occur during this process needs to be solved instantly. Slipforming is a rather complicated operation compared to other construction techniques. The requirements to the materials, personnel and the execution of the work are therefore accordingly higher.

Slipforming of concrete structures has in most cases been carried out successfully with no or only minor supplementary work. However, in some cases, surface damages have occurred during slipforming. Typical surface damages are lifting cracks and vertical lined damages caused by lumps formed on the slipform panel. These problems have during recent years caused discussion and partly also scepticism to slipforming as a reliable construction technique. The Norwegian Public Roads Administration has recommended in Publication 77 that some concrete structures should not be slipformed depending on the environmental impact at the location, geometric degree of difficulties of the concrete structure and the type of concrete. Also in other countries there are scepticism to slipforming as a construction technique.

The prime objective of the research program is to improve the understanding of the slipform technique as a construction method in order to ensure high quality concrete structures. The objective is to identify the parameters affecting the net lifting stress (friction) that occur during lifting of the slipform panel. Focus is given to the importance of the concrete properties that will influence the forces that occur between the slipform panel and the concrete. Also any connection between the friction level and the surface damages is investigated. Based on the result it should be possible to define requirements for materials, mix composition and method of execution to ensure that the specified quality in the structure is obtained.

The lifting stress can be divided in static lifting stress and sliding lifting stress, where the static lifting stress represents the friction that has to be overcome in order to start sliding and the sliding lifting stress is the minimum friction that occurs during sliding. The difference between the static and sliding lifting stress is caused by the decreasing effective pressure during lifting at the sliding zone and the adhesion that occurs because of no movement of the slipform panel between two lifts. Both static and sliding lifting stress are closely related, but the static lifting stress can be extremely large compared to the sliding lifting stress.

The friction law can be used to describe the correlation between the net lifting stress and the effective pressure. This correlation is almost linear and applicable for both the net static and sliding lifting stress. The effective pressure, which represents the pressure between the solid particles and the slipform panel, is the difference between the normal pressure (concrete pressure against the slipform panel) and the pore water pressure. It is primarily the pressure in the pore water that is responsible for most of the variation in the effective pressure during the plastic phase and the transition period, which means that it is mainly the variation in the pore water pressure that controls

the level of the lifting stress. The pore water pressure is decreasing slightly in early phase because of the settlement in the concrete. During the elastic phase, the pore water pressure start to decrease faster as an effect of the chemical shrinkage that occurs because of the cement reaction.

The pore water pressure development can be characterised by the decrease rate of the pore water pressure and the minimum pore water pressure. The minimum pore water pressure is defined as the pore water pressure at the time of maximum lifting stress. The minimum pore water pressure occurs just before the pressure is increasing at the sliding zone close to the slipform panel. It is primarily the level of the minimum pore water pressure that will decide the maximum level of the static and sliding lifting stress. The pore water pressure decrease rate and the minimum pore water pressure depends on the particle concentration and particle size distribution for the finer particles and also the air content in the concrete. Higher particle concentration and finer particle size distribution will both result in a faster pore water pressure decrease rate and a lower minimum pore water pressure. A higher air content will reduce the effect from the chemical shrinkage because the existing air volume will act as a pressure release volume, resulting in a lower pore water pressure decrease rate and a higher minimum pore water pressure.

Also the compaction method will have an impact on the decrease rate of the pore water pressure and the minimum pore water pressure, because the air content will be reduced with prolonged vibration time. Prolonged vibration will in general result in a higher lifting stress, depending on the response on the concrete during vibration. When lightweight aggregate is used in the concrete, the entrapped air in the lightweight aggregate will increase the pore water pressure and result in a lower lifting stress. Porous lightweight aggregate will have larger impact on the pore water pressure than denser lightweight aggregate.

Pressure gradients that occur between two concrete layers will affect the decrease rate of the pore water pressure. Water will “flow” from layers with younger concrete without any negative pressure to concrete layers with lower pore water pressure. This will reduce the decrease rate in the concrete layer that receives the water. In later stage the same concrete that supplied the concrete layer below with water will receive water from the concrete layer above. The pressure gradient at the joint (between two concrete layers) will be more even as a result of the water communications between the concrete layers. Evaporation of water from a fresh concrete surface will result in a faster decrease rate and a lower minimum pore water pressure because of the drying process will form menisci near the surface. The water communication is in general good in the concrete in this phase.

The time at which the minimum pore water pressure occurs will also have an impact on the minimum pressure level. A shorter period of time from the minimum pore water pressure occur to the time of initial set will result in a relatively higher minimum pore water pressure and a lower lifting stress. The minimum pore water pressure has occurred earlier when water has evaporated from an exposed concrete surface. Also when very rough slipform panel is used, the incipient vacuum between the slipform panel and the concrete is punctured early (collapse of the capillary system at the sliding zone) because of the rough panel surface and will result in a relative low lifting stress.

Both the lifting frequency and the lifting height has a considerable effect on the static lifting stress. Lower lifting height or decreased lifting frequency will both result in a lower pore water pressure

and a higher static lifting stress. This is probably because the interface zone is disturbed each time the slipform panel is lifted. Less disturbance of the interface will result in a lower minimum pore water pressure. The lifting stress is decreasing during lifting as an effect of the decreasing effective pressure at the sliding zone and the reduced adhesion. The effective pressure at the sliding zone is probably at minimum and the adhesion is completely broken when the lifting stress is stabilized on a minimum level. The sliding lifting stress is also affected of the lifting frequency and the lifting height if not the minimum level is reached during the lift.

Surface damages caused by high lifting stress are not demonstrated in the vertical slipform rig. However, similar concrete mix design that has been used in a field project, where surface damages occurred, has been tested in the vertical slipform rig. The concrete mix in this field project was replaced with a new concrete mix, where no or only minor surface damages occurred after the replacement. Both concrete mixes is tested in the vertical slipform rig and the result show a considerable higher static and sliding lifting stress for the concrete mix that was used when surface damages occurred. This indicates that there are a connection between high lifting stress and risk for surface damages. This means also that concrete mixes that obtains high lifting stress in the vertical slipform rig is more exposed to surface damages than concrete mixes that has obtained lower lifting stress.

Notations

a_1	estimated regression coefficient
a_2	estimated regression coefficient
A	the contact area between the concrete and the slipform panel
A_c	particle contact area
A_G	contact area
b_1	estimated regression coefficient
b_2	estimated regression coefficient
c	cohesion
c_1	estimated system resistance
c_2	estimated friction coefficient
C	cement content
dP_{0kPa}	pore water pressure difference during dt at 0 kPa
dP_{-10kPa}	pore water pressure difference during dt at -10 kPa
dt	time period
$f_{\text{core-90 days}}$	compressive strength
$f_{\text{cube-90 days}}$	compressive strength
F	friction force
F_A	net lifting stress
F_{AG}	the net sliding lifting stress or sliding friction
F_{AGM}	the maximum net sliding lifting stress or maximum sliding friction
F_{AH}	the net static lifting stress or static friction
F_{AHM}	the maximum net static lifting stress or maximum static friction
F_E	rig friction
F_G	the net sliding lifting force or sliding friction
F_H	the net static lifting force or static friction
F_{MG}	measured sliding lifting force
F_{MH}	measured static lifting force
F_{RA}	calculated net lifting stress based on the regression model
G	shear modulus
h	height of the disc
h_{act}	height of the contact zone
h_1	the distance from the top of the slipform panel to the average curing front
h_2	the distance from top of the slipform panel to the average freeboard
l_h	lifting height
L	thickness of sample
$\ln\phi$	$p^g/p_0^g =$ relative vapor pressure
k	capillary number
K_1	compaction coefficient
m	resistance number
M_s	modulus of plastic shrinkage
n	number of measurements
N	normal force
$P(t)$	capillary pressure
p	effective pressure at failure

p^a	the air pressure (Kelvin-Laplace)
p^l	pressure in capillary condensed water (Kelvin-Laplace)
Q_{cap}	absorbed water
R	gas constant
R_a	surface roughness
R_c	compressive strength when leaving the form
r_k	Kelvin menisci radius \rightarrow pore radius
r	roughness (the average distance from top to lowest point on the surface)
t	time
t_c	time when the break-through pressure is reached
t_l	time period between the lifts
t_s	setting time
t_t	time from mixing of the concrete to placing
t_{cap}	time for the water front reach the height h
T	temperature
$\tan \varphi$	$\mu =$ friction coefficient
u	pore water pressure
U_M	minimum pore water pressure
V_{cs}	chemical shrinkage
V_{pl}	pore water pressure decrease rate
v_l	molar volume (liquid)
V_s	slipform rate
W	amount of evaporated water
W_c	energy that is required to separate two particles in a phase
W_n	non- evaporable (chemical bond) water
z_i	height from centre line
α	degree of hydration
α_f	the ratio between core and cube strength
γ	shear strain
γ_A	surface stress
Γ	function that describes the geometry of the equivalent pore
ΔG_G	difference in Gibb's free energy
ΔP	change in capillary pressure
$\Delta \varepsilon_s$	total relative deformation due to capillary forces
$\Delta \mu_G$	difference in sliding friction coefficient
μ	friction coefficient
μ_G	sliding friction coefficient
μ_H	static friction coefficient
μ_{OG}	sliding friction coefficient for an ideal smooth panel
ρ_w	density of water
σ	total pressure or normal pressure
σ'	effective pressure
σ^{lg}	surface tension (water – air)
τ	shear stress
τ_k	shear strength

Definitions

backsliding	concrete with no strength that slides towards the inclined slipform panel
concrete collapse	concrete with no strength that loose the support from the slipform panel and falls out
delamination	part of the concrete is separated from adjacent concrete
effective pressure	the pressure between the solid particles and the slipform panel
freeboard	the distance from top of the form to the concrete surface
hardened front	the distance from top of the form to the concrete layer that has passed initial set
interface zone	the zone between the concrete and the slipform panel
lifting cracks	thin horizontal cracks on the slipformed concrete surface
lump formation	lumps that sticks to the slipform panel
net lifting stress	friction, lifting stress subtracted the dead weight of the slipform panel and the resistance from the rig
normal pressure	the pressure between the concrete and the slipform panel
panel inclination	the inclination of the slipform panel compared to the lifting direction (not the vertical axis)
pore water pressure	the pressure in the liquid phase in the concrete
sliding friction	the resistance against sliding
sliding friction coefficient	the correlation between the sliding friction and the effective pressure
slipform rate	the rate of the slipform lifting per hour or day
static friction	the friction that must be overcome in order to start sliding
static friction coefficient	the correlation between the static friction and the effective pressure
strain capacity	the maximum strain that result in failure

surface roughness

how smooth or uneven/rough the slipform panel is on the surface

trowel

surface finishing by a trowel on the newly hardened concrete

1 INTRODUCTION

1.1 Background

Slipforming is a construction technique that facilitates concrete structures without any horizontal construction joints. The construction technique has been used in several decades for production of a wide range of different structures. Typical projects are vertical structures such as towers, bridge columns and offshore platforms. Slipforming is not only used on straight vertical concrete structures, but also on structures where the geometry of the structure and the wall thickness are changed during the operations.

Slipforming is normally a continuous working operation (24 hours a day), which require a well-planned supply of materials and personnel present at all times. Slipforming is a rather complicated operation compared to other construction techniques. The requirements to the materials, personnel and the execution of the work are therefore accordingly higher.

Slipforming of concrete structures has in most cases been carried out successfully with no or only minor supplementary work. However, in some cases, surface damages have occurred during slipforming. Typical surface damages are lifting cracks and vertical surface damages caused by lumps formed on the slipform panel. The causes of these surface damages are not always easy to determine and the problems are therefore sometimes difficult to solve. These problems have during recent years caused discussion and partly also scepticism to slipforming as a reliable construction technique. The Norwegian Public Roads Administration has recommended in Publication 77 (Kompen, 1995) that some concrete structures should not be slipformed depending on the location, geometric proportions of the concrete structure and the type of concrete. Also in other countries there are scepticism to slipforming as a construction technique.

1.2 Principles of a slipform

A slipform consist of a framework of horizontal walings and vertical yokes. The slipform panels are connected to each other on the inside of the walings. Each side of the slipform is connected to vertical yokes that keep the panels in position. The jacks for lifting of the form are installed on the horizontal crossbeam between the yokes. When the slipform is lifted, all the jacks are activated at the same time. Hydraulic driven jack is the most common type of jack used. The slipform panel is normally between 1.1 and 1.3 meters high and made of, or covered with, steel plates. Figure 1.1 shows the principle of the slipform.

The slipform panel will normally have an inclination in the vertical plane in order to make the panel self-clearing in relation to the concrete wall. The inclination depends also on the stiffness of the slipform panel and the concrete pressure. The slipform panel has variable stiffness depending on the position and dimension of each yokes and walings.

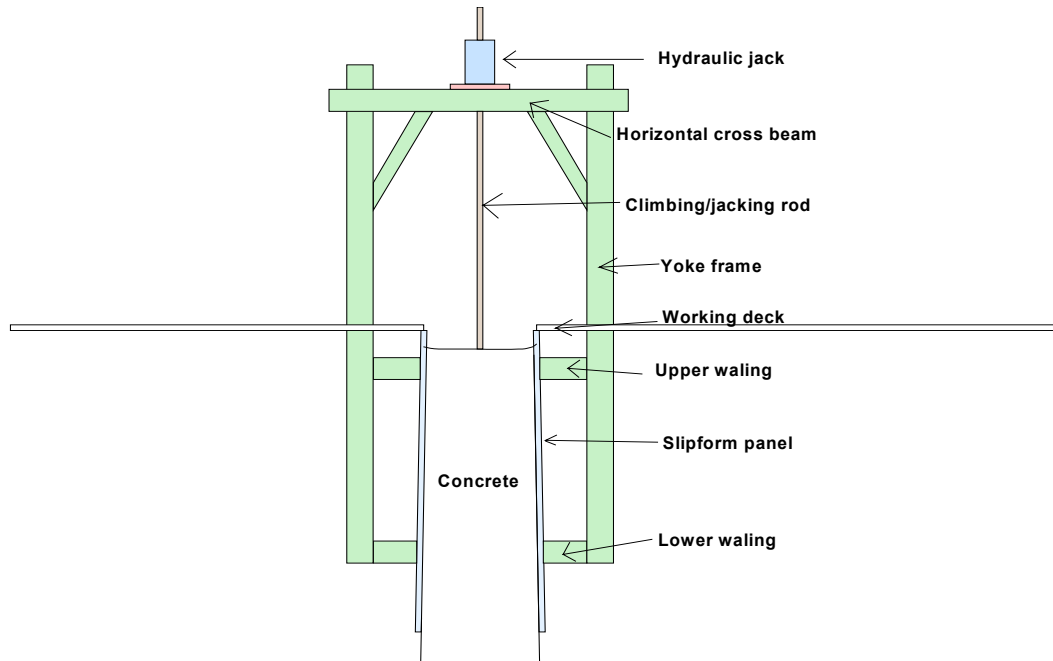


Figure 1.1: The principles of a slipform.

A slipform operation is a continuous working process where the slipform is kept close to full of concrete while it is lifted stepwise. The concrete is placed in 100 to 250 mm thick layers whenever the freeboard height is sufficient. Usually the slipform rate is adjusted so that the initial set in the concrete occur between 200 to 400 mm above the bottom of the panel. Depending on the inclination of the panel, the concrete will detach the slipform panel above the hardening front where the concrete skeleton is rigid enough to resist backsliding.

The slipform rate is planned based on the concrete structure complexity, manning, the skills of the work force and limitation in the material supply. The setting time of the concrete is adjusted to fit the planned slipform rate. The setting time of the concrete depends on the temperature, concrete composition and the properties of the cement. The concrete setting time can also be adjusted by using retarding or accelerating admixtures. The relation between the concrete setting time and the slipform rate can be calculated by using the following equation:

$$\text{Eq. 1.1} \quad V_s = (h_1 - h_2) / (t_s - t_t)$$

where

- V_s = Slipform rate [mm/h]
- h_1 = The distance from the top of the slipform panel to the average curing front [mm]
- h_2 = The distance from top of the slipform panel to the average freeboard [mm]
- t_s = Setting time [h]
- t_t = Time from mixing of the concrete to placing [h]

When calculating the setting time for the concrete in a slipform, the temperature and transfer of heat from the lower concrete layers has to be taken into consideration.

The lifting of the panel is carried out at regular intervals depending on the slipform rate. The lifting height can be adjusted from 10 to 25 mm depending on the desired frequency of the lifting. With a hydraulic system, the lifting operation is carried out by increasing the oil pressure. When the oil pressure is sufficient to overcome the friction and the weight of the form, the slipform will start to lift. After the slipform is lifted, the form is let down until the breaks in the jacks are activated, normally 2 mm downwards.

1.3 Differences between slipform and fixed formwork

Differences between slipform and fixed formwork will indicate possible causes for surface damages that can occur during slipforming. The main differences between slipforming and fixed formwork is listed below:

- The height of a fixed formwork might be several meters and stays in the same position until demoulding. A slipform is normally 1.1 – 1.3 meter high and are lifted slowly whilst the form is kept close to full of concrete.
- Reinforcement and embedments are preinstalled prior to start of the pouring operation for fixed formwork. For slipforming, the reinforcement and embedments are installed during the operation.
- The concrete layer thickness is normally smaller during a slipform operation compared to the layer thickness normally used in a fixed formwork.
- The time period between each concrete layer can be longer in a slipform operation compared to operation with fixed formwork.
- During slipforming a vertical force will affect the cover zone during each lift of the slipform. In a fixed formwork, no force from the formwork will affect the cover zone.
- The time of exposure of the slipformed concrete is normally just after setting. For concrete placed in a fixed formwork, the time of exposure is normally much later.

Based on the above list, it is the friction caused by lifting of the slipform panel that is the main difference between slipforming and fixed formwork. Other parameters such as concrete layer thickness and time period between the layers might affect the friction that occurs when the slipform panel is lifted.

Any surface damages occur most likely when the slipform panel is lifted. The friction force will be transferred as shear force into the concrete cover zone during lifting, and surface damages will occur if the concrete strain capacity is exceeded.

1.4 Objectives

The prime objective of the research program is to improve the understanding of the slipform technique as a construction method in order to ensure high quality concrete structures.

The objective is to identify the parameters affecting the friction that occur during lifting of the slipform panel. Focus will be given to the importance of the concrete properties that will influence the forces that occur between the slipform panel and the concrete.

It is assumed that there is a correlation between the level of the friction and surface damages. When the parameters affecting the friction is known, it is possible to point out the cause of the surface damages when this occur. It is assumed that the risk for any surface damages is increased with higher friction. Based on this investigation it should be possible to define requirements for materials, mix composition and method of execution to ensure that the specified quality in structure is obtained.

1.5 Scope of work

The experimental program is organized in two parts where the first and main part, has the focus on parameters that affect the friction. The second part has the focus on the connection between the friction and any surface damages. This part will primarily be carried out during the field investigations.

In a full-scale slipform with several concrete layers of different age, a number of parameters will affect the friction force. The friction response of each layer will vary because of the different stages of hardening. In addition, the inclination of the slipform panel might affect the concrete pressure as the slipform is lifted. In order to simplify the test method, it is necessary to design slipform rigs that can simulate the conditions one single layer of concrete is subjected to in a full-scale slipform. The parameters affecting a single layer can be grouped in concrete mix, the slipform (panel surface, inclination etc.) and the slipform technique.

The result from the parameter study carried out on the slipform rigs will be used in evaluation of the results from the field projects.

2 LITERATURE REVIEW

2.1 Introduction

The literature study comprises a review of the parameters in the fresh concrete that might affect the friction during slipforming. It is during the hardening period towards initial set, that the concrete is exposed for friction forces during lifting of the slipform panel.

Published reports from research programs carried out on slipforming are also studied. It is focused on parameters that affect the friction force during slipforming and the effect slipforming has on the hardened concrete. It is the lifting operation that is the main difference between concrete poured in a conventionally fixed formwork and slipformed concrete. It is therefore reasonable to compare the hardened properties between these two construction techniques in order to identify any effect caused by slipforming.

It is rather few reported investigation that is carried out on slipforming of concrete. Most of the investigation projects are carried out at German universities. Some investigations are carried out in Scandinavia, but mainly on testing of compressive strength and durability testing.

2.2 Fresh concrete properties

2.2.1 Introduction

During slipforming, the fresh concrete in the interfacial zone will be exposed to shear stresses as a consequence of the friction that occurs during lifting of the slipform panel. If the friction force is at the same level as the shear strength, the concrete will displace or flow in the interfacial zone when the panel is lifted. When the friction force is lower than the shear strength, the friction force will be transferred as shear stress into the cover zone.

However, it is only the particles in the fresh concrete that can resist and transfer the shear stress. The water can not transfer shear stress, but it can transfer pressure (positive as well as negative). Since the shear stress depends on the actual particle pressure, the parameters affecting the pressure between the particles has to be taken into consideration when evaluating the shear stress in the concrete.

Liquid phase

The concrete properties will change considerably during the period towards initial set. The period can be divided into two phases, the liquid phase and the semi-liquid phase, respectively (Hammer, 1999).

The liquid phase starts when the concrete is mixed and placed. The concrete in this phase is workable and can not withstand any significant stress or deformation. The duration of this phase depends on the concrete mix design and the temperature. The cement properties are of particular importance.

Settlements will occur in the fresh concrete because of the force of gravity. The heaviest constituencies will move in a downward direction and the water will move towards the surface. The latter is called bleeding when it appears on the concrete surface. If the concrete surface is unprotected, the water on top will evaporate. If the evaporation exceeds the bleeding rate, forming of capillary tension will give further consolidation on the surface layer since the concrete can not resist any stress in this phase. The hydration rate is slow in this dormant period, and consequently also the volume reduction due to the chemical shrinkage. However, this minor volume reduction will appear as a part of the settlement of the fresh concrete. Figure 2.1 show and idealized relation between chemical shrinkage, settlement (external vertical deformation) and linear autogenous shrinkage (external horizontal deformation) proposed by Hammer (1999) for a sealed sample without bleeding.

Semi liquid phase

The semi-liquid phase starts when the concrete skeleton is sufficiently rigid to carry its own weight. The stiffness development will gradually prevent any further external contraction and empty pores will be developed in the concrete as the hydration proceeds. The empty pores will result in a lower pore water pressure and because of this the bleeding water on top (if any) will be reabsorbed into the concrete because of development of capillary tension in the pore water. Also evaporation of water will result in capillary tension at the surface layer and plastic shrinkage will occur in the concrete. Plastic shrinkage is directly caused by evaporation of water from the concrete surface.

The semi liquid phase ends when the hydration and the heat development are increasing rapidly. According to ASTM C403 the initial and final setting in concrete can be determined by measuring the penetration resistance. Initial setting is defined as the penetration resistance equal to 3.5 MPa and the final setting when the resistance is equal to 27.6 MPa. It should be noted that these values do not indicate the strength of concrete, which are about 0 and 0.5 MPa at initial and final set, respectively. Another method that is frequently used to determine initial set, is temperature measurement in the fresh concrete. The time of initial set is based on a temperature increase of 2 °C in the fresh concrete. This method might give a slightly different initial set compared to the mechanical measurement by penetration resistance.

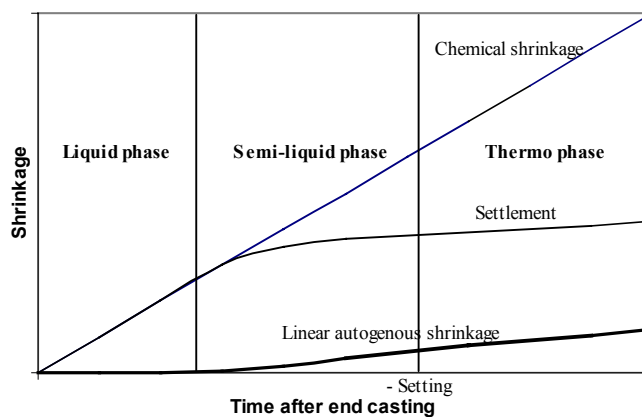


Figure 2.1: Idealized relation between chemical shrinkage, settlement and autogenous linear shrinkage in a sealed sample without bleeding (Hammer, 1999).

2.2.2 Shear strength in concrete

Fresh concrete is a material that instantaneously imposes shear strain when stress is applied. When the shear stress is below the yield value, the concrete behaves like an elastic solid. With higher shear stress, the bond strength between the particles is insufficient to prevent flow and the concrete will gradually change to a more liquid like consistence (Bache, 1977, Lane et al.,1993).

The yield value in the fresh concrete is low in the liquid phase, but it will increase as the workability is decreasing and the hydration proceeds. When the concrete is exposed to shear, it can be assumed that the concrete will have an ideal elastic and an ideal plastic behaviour as shown in Figure 2.2. In this model, the yield value and the shear strength will be the same.

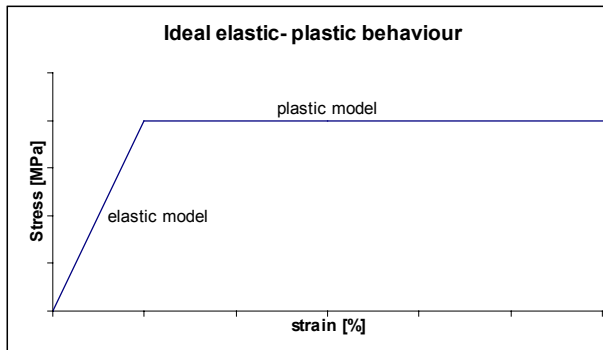


Figure 2.2: Ideal elastic and plastic behaviour

The fresh concrete can be assumed to follow linear elastic model below the yield value. Hook's law for a linear elastic material states that:

$$\text{Eq.2.1} \quad \tau = \gamma \cdot G$$

where τ = shear stress [Pa]
 γ = shear strain
 G = shear modulus [Pa]

When the applied stress is above the yield value, the concrete will start to flow. The Mohr-Coulomb flow model can be used to describe the shear strength related to the effective pressure at failure (Bache, 1987):

$$\text{Eq.2.2} \quad \tau_k = c + p\mu \quad \text{or} \quad \tau_k = c + p \tan \varphi$$

where τ_k = shear strength [Pa]
 c = cohesion [Pa]
 p = effective pressure at failure [Pa]
 $\tan \varphi = \mu$ = coefficient of friction

It is the effective pressure (p) that is used in Eq. 2.2, because the shear force can only be transferred through the particles. This is further commented in Section 2.2.4.

The shear strength in concrete is a result of internal friction and cohesion mainly from bonding because of the cement hydration. According to Alexandridis et al. (1981), the Mohr-Coulomb model is fundamentally incorrect because the fresh concrete has a dilatant behaviour during shearing. Nevertheless, he has concluded that the model adequately express the shear stress that the fresh concrete is exposed to.

Internal friction

Internal friction (Bache, 1977) in a particulate system require strain to be mobilised. The size of the internal friction depends on the shape of the particles, particle size distribution, packing of the particles and the friction coefficient when sliding between the particles. The angle of friction (ϕ) will increase with increased sharpness and roughness of the particles, increased packing and increased friction coefficient. The internal friction will also increase with increasing effective pressure.

Immediately after mixing the shear strength of fresh concrete is mainly due to the internal friction as a result of particle interaction. The internal friction remains constant with set time and temperature change (Alexandridis et al., 1981). However, this is measured in a triaxial test where the pore water pressure is drained before testing (specimens with diameter 82 mm exposed to air before installation) and during testing (drained tests).

Cohesion in concrete

The main source of cohesion in concrete is chemical bonding as a result of the hydration of the cement. The chemical bonding will be small when the concrete is fresh and increase with time as the hydration proceeds (Alexandridis et al., 1981).

Electrostatic attraction occurs due to interaction between double layers of opposite sign, when the particle edges and surfaces are oppositely charged. This force is independent of particle size and becomes significant (greater than 7 kN/m^2) for separation distances less than 25 \AA .

Electrostatic forces are developing very high repulsion at contact point between particles. This repulsion results from overlap between electron clouds, and it is sufficiently great to prevent the interpenetrating of matter. At separation distance beyond the region of direct interference between adsorbed ions and between hydration water molecules, double layer interaction provide the major source of interparticle repulsion. Electrostatic forces or van der Waals forces are a source of tensile strength only between closely spaced particles of very small size ($< 1 \text{ \mu m}$), see Figure 2.3.

Capillary stresses are not a true cohesion, but friction strength generated by the positive effective pressure created by the negative pore water pressure (Michelle, 1993). The pore water pressure is further commented in Section 2.2.4.

In general, the cohesion will increase with decreasing particle size, because the ratio between the surface area divided by volume is increasing. This is also independent of the mechanisms effecting the cohesion in the concrete, see Eq.2.3 (Dupré equation).

$$\text{Eq. 2.3} \quad W_c = 2\gamma_A = \frac{\Delta G_G}{A_G}$$

W_c is the energy that is required to separate two particles in a phase and γ_A is the surface stress. ΔG_G is the difference in Gibb's free energy and A_G is the contact area (from Mørk, 1997; Shaw, 1992).

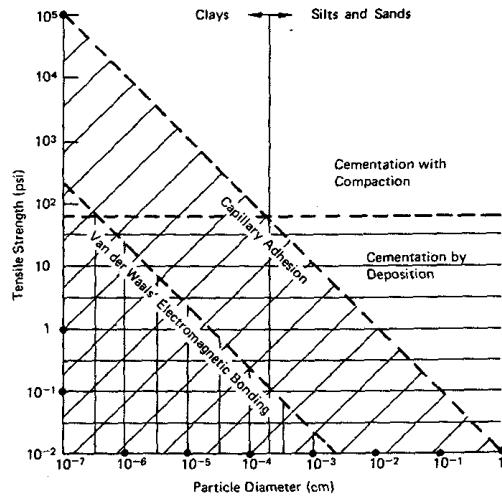


Figure 2.3: Theoretical tension forces for different particle sizes by capillary forces and van der Walls forces (Michelle, 1993).

The cohesion effect in the concrete is called adhesion in the literature when it occurs between the slipform panel and the concrete (Kordina, 1990; Reichverger, 1979).

2.2.3 Effective pressure

The concrete can be divided into two phases, the particle phase and the water phase. The water phase can transfer pressure (positive as well as negative), but it can not resist shear forces. The effective pressure is transmitted through the points of contact between the particles. The particle phase can also resist shear forces and therefore the shear force in the fresh concrete will be based on the effective pressure.

The effective pressure represents the average grain to grain pressure and can be calculated based on the following equation:

$$\text{Eq.2.4} \quad \sigma' = \sigma - u \left(\frac{A - A_c}{A} \right)$$

where

σ = total pressure
 σ' = effective pressure
 u = pore water pressure
 A = total area
 A_c = particle contact area

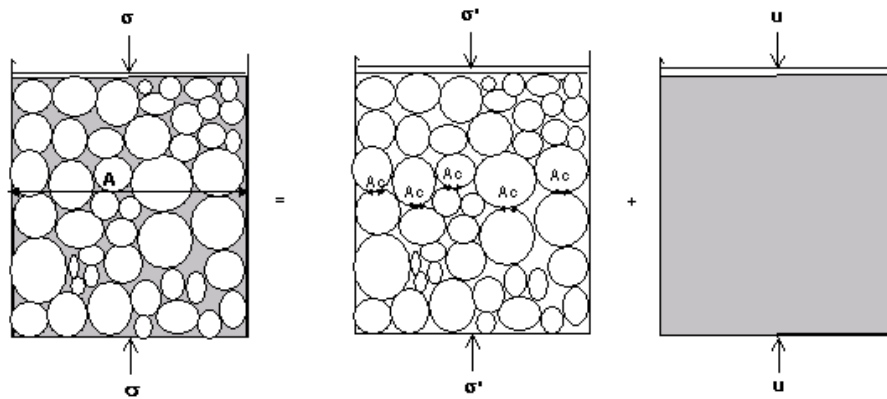


Figure 2.4: The pressure through the particles and water phase.

The contact area (A_c) is normally assumed to be very small compared to the total area (A). For a soil system it can be assumed that A_c is zero without any significant error (Yong, 1966). Also for concrete in early phase, it can be assumed that A_c is very small, even when it is assumed that it will increase as the hydration proceeds. If $A_c = 0$ the Eq. 2.4 simplifies to:

$$\text{Eq.2.5} \quad \sigma' = \sigma - u$$

This is the equation recognized by Terzaghi and describes the relationship between the total pressure and the effective pressure. The pressure for the two phases in a particulate system, can be seen in Figure 2.4. The total pressure (σ) consist of the pressure through the particles (effective pressure σ') and the pressure in the water (u). The effective pressure is the average grain to grain pressure. When water is in tension (negative pore water pressure), the effective pressure will be positive and “force” the particles together (like vacuum-packed beans). The pressure between the particles will contribute to the strength and stability of the fresh concrete. A positive pore water pressure will result in a low effective pressure. When the effective pressure is zero, the shear strength in the fresh concrete will be very low and the concrete will not be able to resist any stress or deformation.

Also at the interface between the concrete and the slipform panel, the pore water pressure is assumed to affect the effective pressure. With increasing effective pressure, the particles in the

concrete will probably be forced with increasing pressure against the slipform panel. This will be further evaluated in Chapter 7.

2.2.4 Pore water pressure

2.2.4.1 General

The pore water pressure will vary in the concrete during the period toward setting. In the liquid phase, it is the settlement of the solid particles and bleeding that will affect the pore water pressure. During the semi-liquid phase it is the cement hydration, re-absorption of water and surface drying that will affect this pressure. The pore water pressure development during the period towards setting and early hardening is shown in Figure 2.5 for concrete paste.

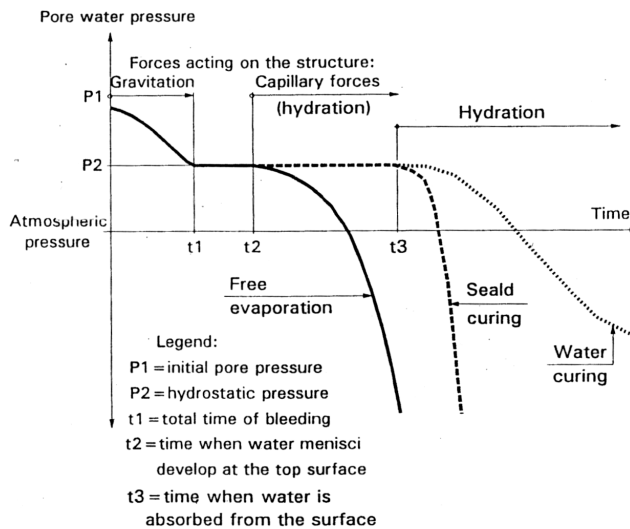


Figure 2.5: Pore water pressure development in cement paste (Radocea, 1994 B).

The pore water pressure will decrease from P1 to P2 due to settlement of the cement grains after placing. In the same period, bleeding will also occur at the surface. The initial pressure P1 depends on the density of the paste and the depth of the measurement. The surface is covered with bleeding water during the period from t1 to t2 and the pore water pressure will remain stable. At time t2, the surface start to dry out because of free evaporation and the pore water pressure will decrease. The pore water pressure will decrease because of formation of meniscus at the surface and the hydration of the cement. The effect of cement hydration can be seen at t3 where the pore pressure is decreasing in a sealed sample. If the specimens are water cured, the rate of pore water pressure decrease will be reduced because the water will be transferred into the specimens due to suction caused by the lower pore water pressure (Radocea, 1994 B).

2.2.4.2 Settlement and bleeding

After the concrete is mixed and placed, the pore water pressure depends on how the particles are distributed in the concrete. The water carries the particles when the water pressure corresponds to the weight of the concrete at the measuring point. After placing, the concrete will start to settle and bleeding might be seen on the top surface after a while.

Radocea (1992) have carried out experiments with cement paste. He concluded that the settlement and bleeding rate will be affected by the particle size distribution, particle concentration, use of plasticizer etc. The pore pressure will decrease during settlement due to direct contact between the solid particles.

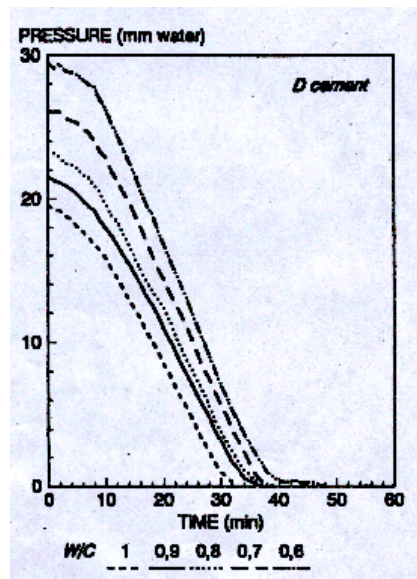


Figure 2.6: Pore water pressure development with different w/c-ratios in cement paste (Radocea, 1992).

Figure 2.6 shows that higher concentration of the cement in the paste will result in a higher initial pore water pressure because of the density of the paste is highest for the paste with highest cement concentration. In this instance, the rate of settlement is almost the same in all tests.

The settlement and bleeding period will end no later than at the beginning of the semi liquid phase. At that time the concrete will be rigid enough to withstand any further internal deformation primarily caused by the force of gravity.

2.2.4.3 Effect of hydration – chemical shrinkage

The chemical shrinkage is initiated upon the contact between cement and water (Justnes et al., 1999). However, it is during the semi-liquid phase, when the concrete skeleton is rigid enough to carry its own weight that the empty pores will develop. In the same period, the volume of the solid (cement paste – reactants) will decrease. During this period, the largest capillary pores will gradually

start to dry because of the cement hydration and the water in the capillary pores will gradually be replaced by vapour. The gel pores that are formed during hydration, will drain water from the coarsest capillary pores, because the free water is held by forces that are inversely proportional to the diameter (Aitken, 1999). This process is known as self-desiccation and is strongly related to the formation of the microstructure (Tarzawa et al., 1999). The consequence of the self-desiccation is formation of meniscus in the interface water/vapor and decreasing relative humidity in the pore system. The meniscus will give a lower negative capillary pressure in the pore water.

The capillary tension of the pore water will increase as the hydration proceeds. Lower w/c-ratio and finer microstructure will increase the capillary tension (Brooks et al., 1999). This means that the pore water pressure development will depend on the composition of the concrete constituency. More cement or higher content of fines will both result in higher rate of pore water pressure reduction.

The relation between the capillary pressure, relative humidity and menisci radius can be described by Kelvin-Laplace equation:

For spherical menisci:

$$\text{Eq. 2.6} \quad p^a - p^l = -\frac{RT}{v^l} \cdot \ln \phi = 2 \cdot \frac{\sigma^{lg}}{r_k}$$

where
 p^a = gas pressure
 p^l = pressure in the capillary condensed water
 R = gas constant
 T = temperature
 v^l = molar volume (liquid)
 $\ln \phi = p^g/p_0^g$ = relative vapor pressure
 σ^{lg} = surface tension (water – air)
 r_k = Kelvin menisci radius (= pore radius)

Powers found that the chemical shrinkage (V_{cs}) could be estimated by assuming that the reacted water loses approximately 23 % of its volume and also that each gram cement consumes approximately 0.25 g water when it is fully hydrated. The chemical shrinkage (V_{cs}) can be calculated on the following equations:

$$\text{Eq. 2.7} \quad V_{cs} = 0.254 \cdot W_n / \rho_w$$

where
 W_n = non- evaporable (chemical bond) water
 ρ_w = density of water

$$\text{Eq. 2.8} \quad W_n = \alpha \cdot 0.23 \cdot C$$

where
 α = degree of hydration
 C = cement content

According to Eq. 2.7 and Eq. 2.8 the chemical shrinkage for a cement-water mix with one kg cement is $(0.058 \cdot \alpha)$ litre assuming enough water for the hydration.

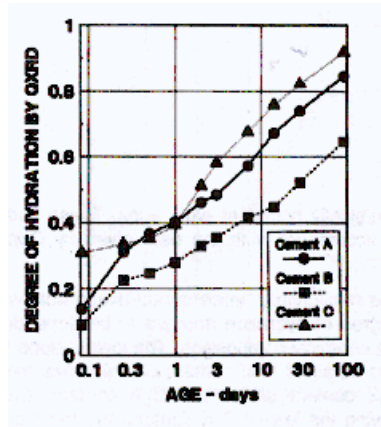


Figure 2.7: Degree of hydration related to age in cement paste. Quantitative X-ray diffraction analysis is used during testing (Parrott et al. 1990). Cement A seems to represent an average Portland cement.

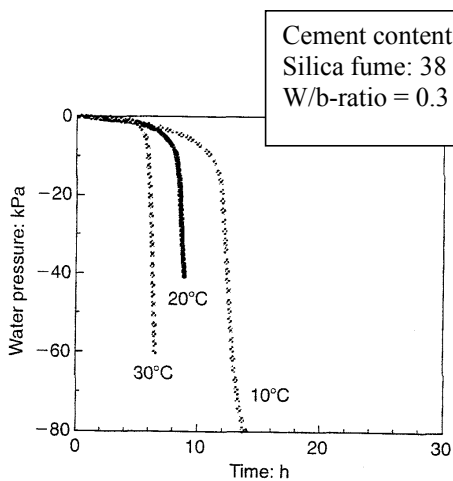


Figure 2.8: Development of pore water pressure in sealed samples of concrete at different temperatures (Radocea, 1998).

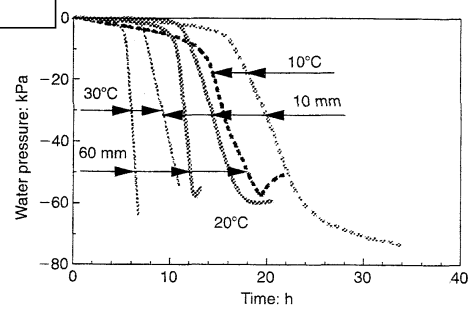


Figure 2.9: Development of pore water pressure in water cured samples at different temperatures (Radocea, 1998).

If it is assumed that the degree of hydration after 6 hours (0.3 days) is 0.3 as shown in Figure 2.7 and the cement content is 400 kg, the volume reduction due to chemical shrinkage will be approximately 7 litres ($0.058 \cdot 400 \cdot 0.3 = 6.96$). This volume reduction will be distributed equally around in the pore system (coarsest capillary pores first) and the fineness of the pore system and the meniscus radius will probably determine the capillary effect in the pore water.

It can be seen in Figure 2.8 that the pore water pressure in sealed samples is decreasing slowly at the beginning followed by a period with very high decreasing rate. The sample at 30 °C has an earlier decrease compared to the sample at 10 °C. This corresponds to the faster cement hydration at higher temperatures. For water cured samples in Figure 2.9, the pressure decrease is slightly different. The pore water pressure reduction 10 mm below the surface is slower compared to 60 mm below the surface. This is because the water from outside will increase the pore water pressure in the sample and in particular near the surface.

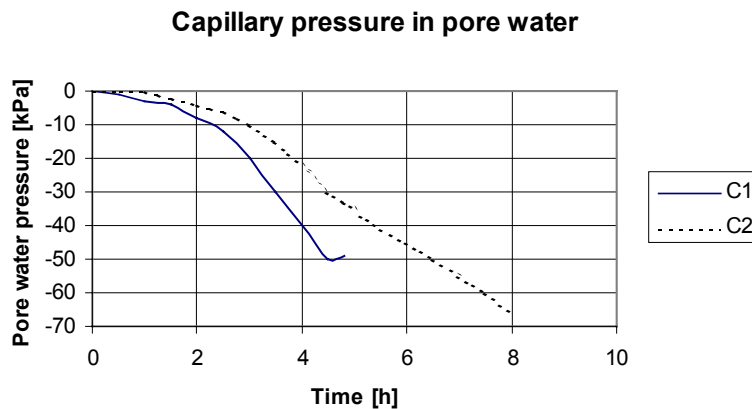


Figure 2.10 development of capillary pressure in concrete (Radocea, 1992).
 Concrete C1 – $w/c=0.4$, 380 kg Portland cement, 2.5 kg Mighty 100.
 Concrete C2 – $w/c=0.7$, 270 kg Portland cement, no admixtures.

The effect of different w/c -ratios and cement content is demonstrated in Figure 2.10. Concrete C1 has a lower w/c -ratio and more cement compared to concrete C2. The pore water pressure start to decrease earlier and with a higher rate for concrete C1. The lower w/c -ratio in this concrete has probably given a lower bleeding at the beginning, and consequently also an earlier decrease in the pore water pressure. The higher rate of the pore water pressure reduction for concrete C1 is probably because of more cement and in general lower initial porosity.

2.2.4.4 Drying of surface

The capillary pressure of the pore water will decrease when the concrete surface starts to dry out. The rate of evaporation from the wet surface depends on the temperature of the water at the surface, the ambient air temperature, humidity and the wind velocity (Radochea, 1994 A). When the concrete becomes so rigid that further consolidation is prevented, the water on top will be absorbed into the concrete and result in lateral contraction of the surface. This will result in plastic shrinkage (Powers, 1960). This happens when meniscus is formed at the surface and result in capillary pressure in the pore system. The physical system in drying of concrete is very much the same as for chemical shrinkage, but chemical shrinkage happen without any mass loss and does not develop any relative humidity gradients in the concrete.

The shape and size of the spaces between the particles will determine the size of the curvature of the menisci (Power, 1960). Which means that the particle size and the distance between the particles will affect the capillary pressure. The pressure development is dependent on the rate of evaporation and the geometry of the spaces between the particles at the surface (Radocea, 1992). The development of the capillary pressure in a saturated material exposed to drying is characterised by the existence of three periods (from Radocea, 1992):

1. A period of a low rate of pressure development, which in the case of materials in the form of powders may coincide with the formation of the consolidated skin at the surface of evaporation.
2. A period of high and almost constant rate, which indicates that the water menisci are depressed into the spaces between the particles at the surface.
3. A period of decreasing rate when the water menisci cannot find stable positions between the particles in the bulk (break-through pressure).

The development of the capillary pressure due to surface drying depends on several parameters. Radocea (1992) has developed the following model that describes the development of the capillary pressure in the pore water:

$$\text{Eq: 2.9} \quad P(t) = \int_0^t \frac{1}{\left(\Gamma + \frac{\rho_w L}{M_s}\right)} \frac{dW}{dt} dt$$

where

$P(t)$ = Capillary pressure (Pa)

Γ = function that describes the geometry of the equivalent pore (kg/N)

ρ_w = density of water (kg/m³)

L = thickness of the sample (m)

M_s = modulus of plastic shrinkage (Pa)

W = amount of evaporated water (kg/m²)

The function Γ describes the pore structure of a system that does not shrink. Γ expresses the amount of water in kg/m² that must evaporate in order to produce a change in pressure of 1 N/m². Plastic shrinkage (M_s) expresses the relation between the pressure and the total deformation:

$$\text{Eq.2.10:} \quad M_s = \frac{\Delta P}{\Delta \epsilon_s}$$

Where

ΔP = change in capillary pressure [Pa]

$\Delta \epsilon_s$ = total relative deformation due to change in capillary pressure

The model in Eq.2.9 means that the rate of pressure development depends on the rate of evaporation, the geometry of the pores at the surface, the thickness of the sample and the modulus of plastic shrinkage. This model is described in detail by Radocea, 1992.

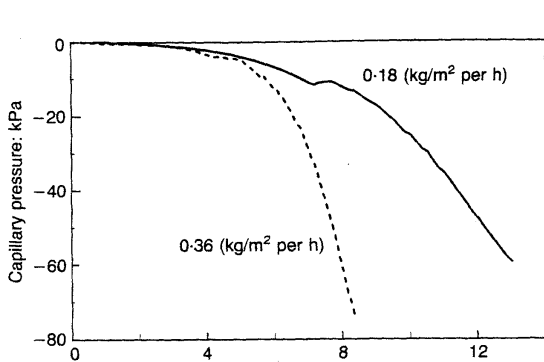


Figure 2.11 Development of capillary pressure at different rates of evaporation in fly ash slurry (Radocea, 1994 A)

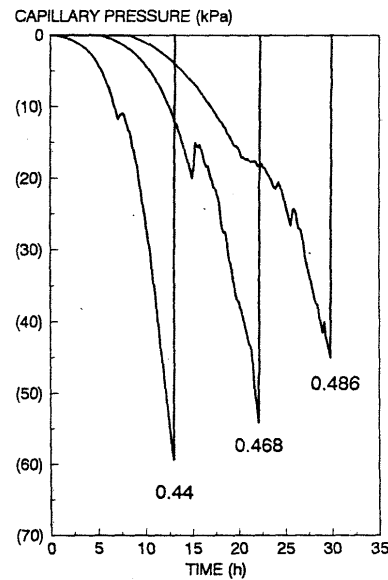


Figure 2.12: Effect of initial porosity on the development of capillary pressure. Rate of evaporation = 0.18 kg/m² per hour (Radocea, 1994 A).

An example of the effect of the evaporation rate is shown in Figure 2.11. The results show as expected, that the reduction of the capillary pressure has a higher rate when the evaporation rate is higher. In Figure 2.12, the results show that a higher initial porosity will affect the capillary pressure development. A lower initial porosity give a faster decrease in the pore water pressure compared to a mass with higher porosity. Common to both Figures is that the tests is carried out on fly ash slurry and consequently not affected by any chemical reactions.

2.2.4.5 Break-through pressure

The pore water pressure is decreasing with time because of surface drying or hydration of the cement or a combination. The free water in the concrete will after a while decrease to such a low content, that the water meniscus cannot find new stable positions. Because of this the capillary pressure cannot be maintained in such a case and the water system becomes discontinuous. This stage is represented by a collapse of the capillary pressure, and is called the break through pressure. Break-through pressure is the minimum pore water pressure where the remaining water can no longer make a continuous system in the concrete according to Wittman (1976).

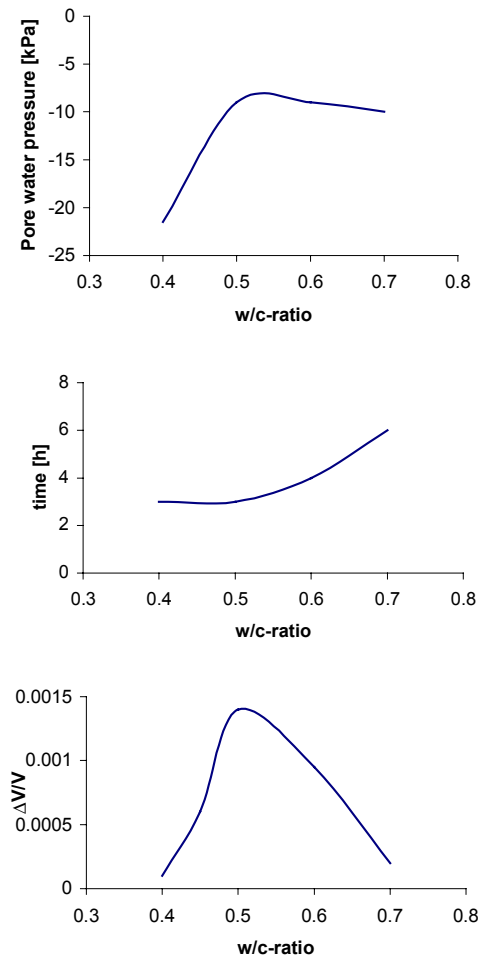


Figure 2.13 Break through pressure, time and volume shrinkage (Wittmann, 1976).

Wittman (1976) has concluded that plastic shrinkage is originated by the capillary pressure. He carried out tests on specimens exposed to wind speed of 4 m/s at 20 °C and 50 % relative humidity. The results in Figure 2.13 show that the time (t_c) when the break-through pressure is reached depends on the amount of water in the mix. The time (t_c) is increasing from about three hours at $w/c=0.4$ to more than six hours at $w/c = 0.7$. The distance between the particles is low at $w/c = 0.4$, and because of this the break-through pressure is lowest at this w/c -ratio. For the same reason, the volumetric shrinkage is also limited. With increasing w/c -ratio, the break-through pressure is increasing because of a coarser pore system. Even with a lower break-through pressure, the volume change is increasing when the w/c -ratio is increasing. At w/c -ratio 0.55, the time (t_c) is increasing and because of this, the break-through pressure is reached when the fresh concrete has developed

some strength. The volumetric shrinkage will therefore decrease as shown in Figure 2.13 (Wittman, 1976).

Radocea (1992) has concluded that the measured break-through pressure represents only a limited part of the sample adjacent to the pressure gauge. When the break-through pressure is reached, it is because of discontinuity in the water system surrounding the pressure gauge and it is actually a plastic crack.

Radocea has divided the break-through pressure in four different types:

1. a high rate of pressure development suddenly interrupted, which is the most usual case
2. a period of diminishing rate suddenly interrupted
3. a high rate followed by a period of instability
4. a smooth transition from a high rate to a period of more or less constant pressure

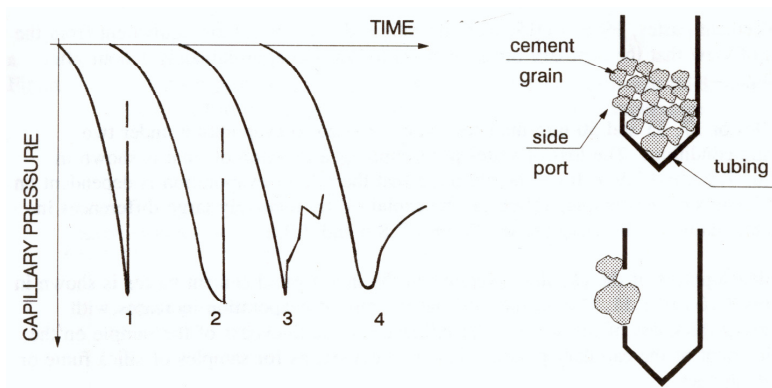


Figure 2.14: Left - Types of pressure development before and after the break-through pressure. Right - Condition at the side port of the pressure gauge.(Radocea, 1992).

The first and third types in Figure 2.14, can be considered to be typical examples of a discontinuity between the water system of the paste and the pressure gauge, which is caused by the inhomogeneity of the paste, and the limitation of the method of testing. For curves 2 and 4, a period of diminishing rate is usual for higher magnitudes of the capillary pressure. The short period of diminishing rate can be caused by the development of air bubbles. For a curve of type 4, the pressure gauge retains normally the current pressure also after the tube is removed from the concrete.

2.2.5 Summary fresh concrete properties

The concrete properties will change considerable from the time of placing to the initial set. During the liquid phase, the concrete will have a fluently or plastic consistence and the shear strength is low. The low shear strength is because of low cohesion and low internal friction between the

particles in this period. During the semi-liquid phase, the shear strength in the concrete will increase. Primarily because of the higher effective pressure, but also because of the cement reactions. Higher effective pressure will result in higher internal friction and the cement reaction will give increased cohesion between the particles in the concrete.

The effective pressure is calculated based on the measured total pressure and the pore water pressure. While the total pressure in the concrete remains constant in principle, the pore water pressure is decreasing because of development of capillary forces. Capillary forces are made in the pore water because of self-desiccation in the concrete or drying at the surface. For self-desiccation, the decrease in pore water pressure will depend primary on the cement type and content, w/c-ratio and total amount of fines in the concrete mix. A finer pore system will give a higher rate of decrease in pore water pressure compared to coarser pore system. For surface drying, the pressure development depends primarily on the rate of evaporation, pore system and the particle geometry at the concrete surface. The free water in the concrete will after a while decrease to such a low content, that the water meniscus cannot find new stable position. Because of this the capillary pressure cannot be retained in such a case and the water system becomes discontinuous. This stage is represented by a collapse of the capillary pressure, and is called the break through pressure.

2.3 Lifting force and concrete pressure during slipforming

2.3.1 Introduction

When the slipform panel is sliding on a fresh or green concrete surface, friction will arise as a consequence of the contact between the moving panel and the concrete. The nature of the materials involved (concrete and slipform panel) will determine the magnitude of the friction force. In the early phase, the friction depends on the fresh concrete properties and its ability to create a lubricant layer on the panel surface and the surface roughness of the panel. In the later phase, it is assumed that the effective pressure and the cohesion in the lubricant layer from the cement hydration and its adhesion to the panel surface affects the friction.

Skew lifting, asymmetric loading of the working deck and other unplanned parameter might effect both the concrete pressure and the friction. These parameters will not be considered here.

2.3.2 Concrete in a slipform

The shear strength in the fresh concrete is a result of frictional resistance, interlocking of the particles and bonding because of the cement hydration. Frictional resistance and interlocking of the particles are called internal friction. Chemical bonding as a result of the cement hydration is the main source to cohesion in concrete. Cohesion is small when the concrete is fresh and will increase with time as the hydration proceeds. In general the cohesion will increase with decreasing particle size, because the ratio between the surface area divided by the volume is increasing. This is independent of the type of mechanisms effecting, i.e. electrostatic forces and capillary stresses (see Section 2.2.2).

It is assumed that capillary stress, because of chemical shrinkage, have more influence on the development of friction than initially believed. No literature has so far been found that includes measurements of the pore water pressure in the concrete together with friction measurements. This is a central part of this thesis and is presented in Section 2.2.

A lubricant layer will be made between the panel and concrete during placing and vibration. Especially the vibration process will consolidate the concrete and envelop the larger aggregate in a slurry of binder and the finer aggregate particles. This slurry will behave like a lubricant during sliding when the concrete is still fresh. According to Spech (1973) the actual physical phenomenon in the sense of reduction of friction is because the lubricant is making a pressure pillow, which separate the sliding surfaces and decrease the friction. Near setting the lubricant will change its character and behave like a glue (Reichverger, 1979). This is caused by the increasing cohesion in the concrete and its adhesion to the slipform panel. The concrete properties and its ability to create a lubricant layer depend on the concrete composition and the compaction method.

2.3.3 Static and sliding friction

Before the slipform panel is lifted, the lifting force must overcome the friction between the concrete and the slipform panel. This friction force is defined as the smallest driving force, which initiates sliding and is called static friction. When the panel starts to slide on the concrete, the friction level is decreasing. The lower friction level is called sliding friction. The relation between the friction force and the normal force (lateral force) can be described by the general friction equation:

$$\text{Eq. 2.11} \quad F = \mu \cdot N,$$

where F = friction force,
 N = normal force
 μ = friction coefficient. The friction coefficient is the coefficient of static friction or sliding friction.

$$\text{Eq. 2.12} \quad \mu_H > \mu_G,$$

where μ_H is static friction coefficient
 μ_G is sliding friction coefficient

These two terms can be measured on trials with one layer of concrete, e.g. laboratory trials. On a full-scale slipform, it is difficult to separate those two terms because the friction is measured on several concrete layers at the same time. Each concrete layer will give different friction response because of different age and lateral pressure. The maximum lifting force during each lift on a full-scale slipform is normally recorded. This force is called friction force or lifting force in the literature. The weight of the slipform is normally deducted for both terms.

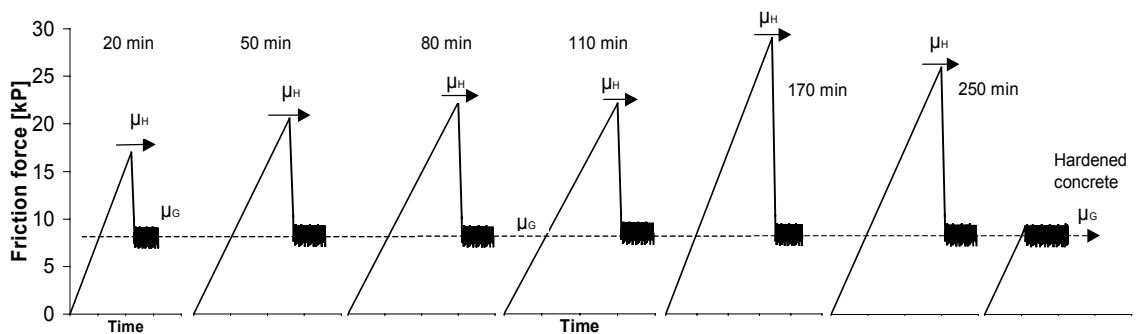


Figure 2.15: A typical results from the friction measurements, μ_H is static friction and μ_G is sliding friction (Spech, 1973).

Spech (1973) carried out several trials in order to identify the difference between the static and the sliding friction. A typical result is shown in Figure 2.15, where the static friction is the peak value at the beginning and the sliding friction is the lower value after sliding has started. The sliding length for these particular trials was approximately 100 mm.

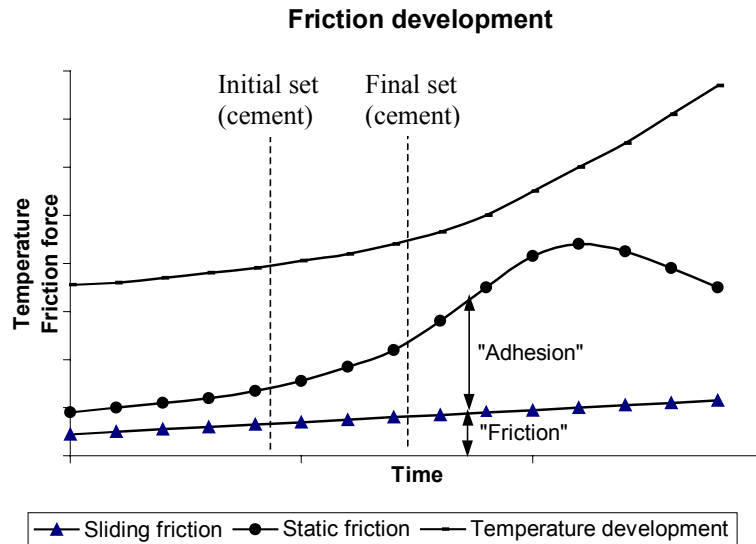


Figure 2.16: Principle sketch of friction development with time (Kordina et al., 1990).

Kordina et al. (1990) has also carried out measurements on static friction and sliding friction. The tests are carried out on different specimens that were tested only once. The principle sketch of the static and sliding friction is shown in Figure 2.16.

The static friction is in general increasing as the hydration proceeds until the maximum value is reached during the period of setting. The sliding friction according to Figure 2.15 and 2.16 will remain almost at the same level during the whole period. This means that the sliding friction is practically independent of the condition of the concrete, either fresh or hardened.

2.3.4 The slipforming rate

The static friction is increased when the lifting frequency is reduced, because of the adhesion force in the interface between the concrete and the panel is increasing with time in rest. The static friction is low when the concrete is fresh and becomes high near setting, see Figure 2.15 and 2.16. It is assumed that the highest static friction will be in the concrete layer just above the detach zone on the slipform panel.

Reichverger et al.(1982) have found that the lifting force is decreasing with increasing slipforming rate, even when the concrete pressure against the slipform panel is increasing with increasing

slipforming rate, see Figure 2.17 and Table 2.1. Increased concrete pressure will normally give a higher lifting force, while increased lifting frequency will decrease the lifting force. This means that the lifting frequency has a much higher contribution to the friction force than the concrete pressure on the slipform panel. The lifting frequency has varied from 4 lifts of 25 mm per hour (10 cm/h) to 12 lifts of 25 mm per hour (30 cm/h). With double slipform rate or frequency, the lifting force is reduced by 30 – 40 % when the concrete is hand compacted and 25 – 30 % when vibrated. This relationship is applicable for smooth panels with Polyethylene cover and steel panels. Polyethylene is a smooth plastic material.

Table 2.1: Total lifting force when the concrete is hand compacted and vibrated (Reichverger et al., 1982)

Mode of compaction	Slipforming rate cm/h	Total maximum lifting force [N]					
		Uninterrupted movements (25 mm lifts)		60 min stop		120 min stop	
		Steel	PE	Steel	PE	Steel	PE
Hand compacted	10	3400 (100%)	2800 (82%)	4700 (100%)	3800 (81%)	5400 (100%)	4200 (78%)
	20	2100 (100%)	1850 (88%)	4950 (100%)	3900 (79%)	6700 (100%)	5100 (76%)
	30	1400 (100%)	1250 (90%)	5050 (100%)	4150 (82%)	>7000*	6050
Vibration	10	4750 (100%)	3700 (78%)	6050 (100%)	4800 (79%)	6900 (100%)	5500 (80%)
	20	3300 (100%)	2750 (83%)	6600 (100%)	5100 (77%)	>7000**	6800
	30*	2400 (100%)	2100 (88%)	7000 (100%)	5400 (77%)	>7000**	>7000**

* Concrete collapsed under form during vibration.

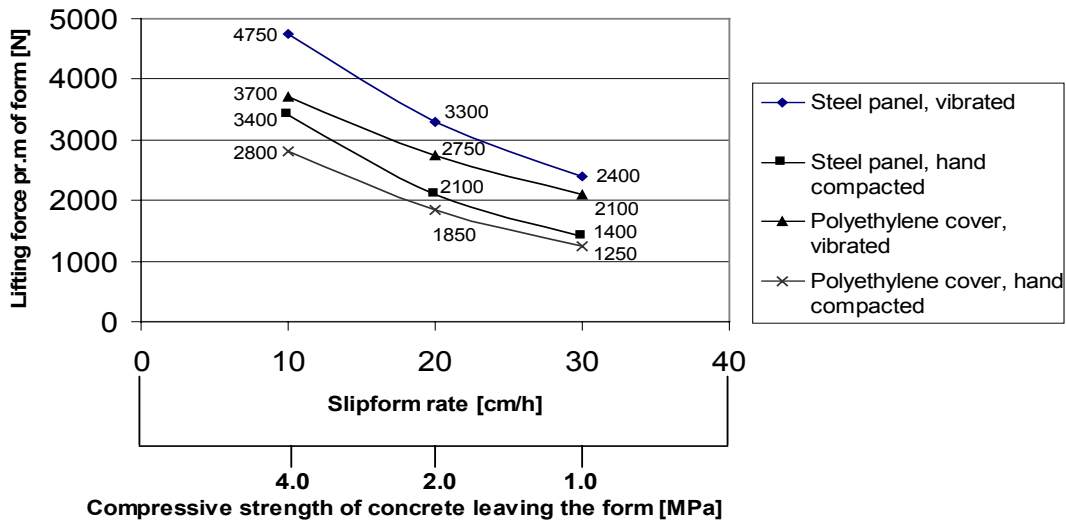
**Maximum weight reading was 7000 N.

PE – Polyethylene.

The results in Table 2.1 and Figure 2.17 shows that the highest lifting force is obtained with a steel panel, vibrated concrete and a low slipform rate (4 lifts of 25 mm per hour). The lowest lifting force is obtained when using smooth Polyethylene cover on the panel, hand compacted and high slipform rate (12 lifts of 25 mm per hour). Type of compaction has a considerable importance for the measured lifting force.

The lifting force after 60 and 120 minutes stop depends also on the initial slipform rate before the stop. The lifting force is higher when the lifting rate is initially high before the stop, see Table 2.1. According to Reichverger et al.(1982), this is caused by a larger contact area and a higher concrete pressure, when the slipform rate is initially higher, see Table 2.2 and 2.3.

Steinecke et al. (1964) has reported that when the time between two lifts was increased to 45 minutes, a wide crack was formed on the concrete surface above a horizontal bar. This means that



the friction force exceeded the concrete strain capacity.

Figure 2.17: Total lifting force at different slipform rates, uninterrupted movements – 25 mm lifting heights (Reichverger et al., 1982)

2.3.5 Concrete pressure on the panel

The lateral pressure depends on the concrete properties of the different layers. Concrete that keeps the mobility for a long time will give a higher lateral pressure against the panel than concrete with early slump loss. The concrete will detach the slipform panel when it is stiff enough to carry its own weight. According to O'Brien (1973), the penetration resistance in the concrete at the time when the panels detach the concrete is approximately 150 kPa (ASTM C403). Reichverger (1982) found the following empirical formula describing the height of contact zone (h_{act}) as a function of the compressive strength:

$$\text{Eq. 2.13} \quad h_{act} = K_1 \cdot (1.1 - R_C) \text{ [m]}$$

where $K_1 = 1.0$ for manual compacted concrete
 $K_1 = 1.1$ for vibrated concrete
 $R_C =$ compressive strength when leaving the form [MPa]

The concrete strength, when leaving the form, will increase with lower lifting rate as shown in Figure 2.17.

The operation area of the vibrator might affect the contact height of the concrete (Steinecke et al., 1964). Vibration will affect layers further down, which are already hardening. The small binding force is destroyed in the concrete and the concrete will backslide against the panel. According to Steinecke et al. (1964), the magnitude of the pressure exerted on the formwork is determined by the contact area of the freshly placed concrete. The larger this area is, the greater total pressure is obtained. Also when conical slipform is used to make geometry changes like increasing wall thickness, it will often involve higher pressure because the panel is forced to change the position.

Reichverger et al. (1982) has measured the pressure with different slipform rates. The results shows that the concrete pressure and the contact area is increasing with increasing slipform rate, see Table 2.2. This is because the concrete will keep a higher workability further down in the slipform, and therefore higher concrete pressure. It is assumed that the concrete setting time is the same in all three tests.

The reported concrete pressure from all investigation project in Table 2.2 is within the same range, but slightly lower for Steinecke et al. (1964) and Kordina et al. (1990) compared to Reichverger et al. (1982).

Table 2.2: Measured concrete pressure per meter slipform, concrete vibrated.

References	Steinecke et al. 1964	Reichverger et al. 1982			Kordina et al. 1990
Panel type	Board (water tight)	Steel panel, 1 m height			Board
Slipform rate [m/h]	0.4	0.1	0.2	0.3	0.15-0.45
Contact zone [m]		0.81	0.95	Collapse	
Maximum panel pressure [N/m]	7480	6000	9800	11200*	6400
Lifting force [N/m]		4750	3300	2400	

* The concrete collapsed under the form. The pressure might be higher if the panel was higher.

Also type of compaction will influence the concrete pressure. Reichverger et al. (1982) has measured the effect of hand compacting with the same slipform rates as listed above.

Table 2.3: Measured concrete pressure per meter slipform, concrete hand compacted.

Reference	Reichverger et al. 1982		
Panel type	Steel panel, 1 m height		
Slipform rate [m/h]	0.1	0.2	0.3
Contact zone [m]	0.73	0.85	1.00
Maximum panel pressure [N/m]	4500	6200	8800
Lifting force [N/m]	3400	2100	1400

It can be seen that both the concrete pressure and the contact zone are smaller, when the concrete is hand compacted. This indicates that the consolidation of the concrete is better and results in higher concrete pressure when a vibrator is used. In Figure 2.18, the pressure distribution over the panel height for vibrated and hand compacted concrete is shown. Higher slipform rate has for vibrated concrete in general generated a higher pressure than the theoretical hydrostatic pressure (the weight of the concrete). Hand compacted concrete has in general resulted in lower concrete pressure than the hydrostatic pressure.

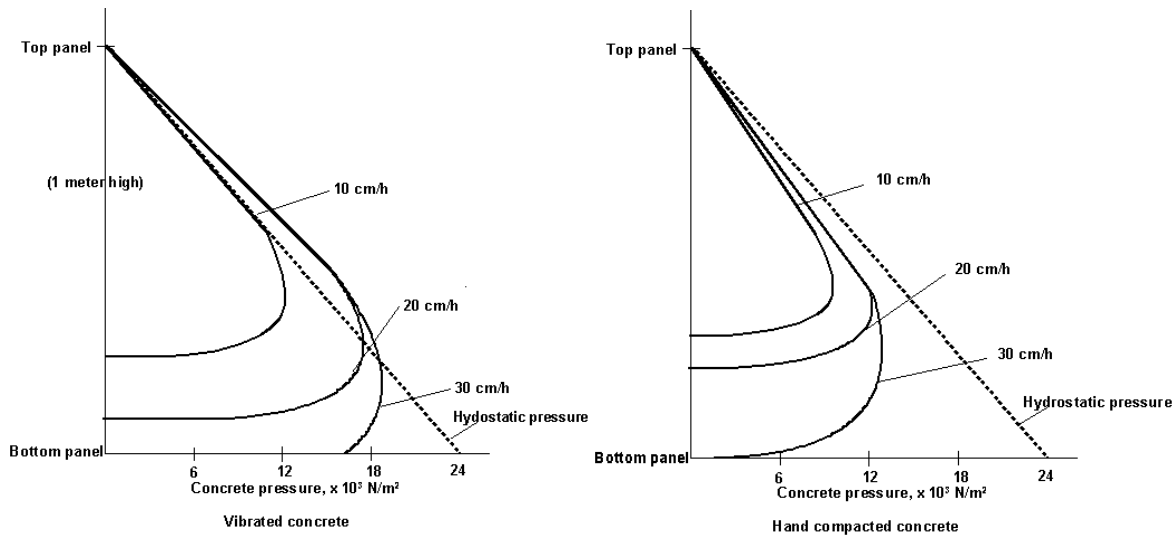


Figure 2.18 a and b: Concrete pressure distribution at different slipform rates, vibrated (a) - hand compacted concrete (b) (Reichverger et al., 1982).

The concrete pressure will also affect the friction force. Laboratory experiments show that unvibrated concrete has a considerably lower static friction than vibrated concrete (Spech, 1973). Unvibrated concrete gave approximately the same friction level for both static and sliding friction. Spech (1973) found for vibrated concrete, when the pressure was increased three times, the static friction coefficient was reduced ~33 %. The sliding friction coefficient was also reduced when the pressure was increased three times, respectively 8 % when using smooth panel and 12 % when using a rough slipform panel. This means that both the static and sliding friction coefficients depends on the total concrete pressure.

The lifting force is shown in Table 2.2 and 2.3. It can be seen that higher lifting rate involve higher concrete pressure but lower lifting force. This means that the friction is more affected of the lifting rate than the concrete pressure.

2.3.6 Effect of the concrete mix composition

During placing and vibration of the concrete, a lubricant layer will be made in the interface zone between the concrete and the panel. This layer consists of cement slurry mixed with fine sand. The thickness and properties of the lubricant layer depend on the concrete composition and the consolidation method. When the slipform panel is lifted, the shear zone in early phase will be in the lubricant layer because the shear resistance is lowest here. Later, when the lubricant layer has stiffen, the shear zone will probably go between the lubricant layer and the slipform panel (slip plane). The surface on a slipformed structure is normally covered with a layer of finer particles of sand and cement. This surface layer has probably in early phase been a part of the lubricant layer.

Kordina et al. (1990) has reported that 20 % fly ash in the concrete seems to reduce the static friction when a smooth panel is used. When a rough slipform panel is used, the tendency is more unclear. The results were compared to concrete without fly ash, but the same amount of cement.

The effect of the aggregate type was tested by Kordina et al. (1984). Several test walls were slipformed with different mix compositions. Natural round and crushed aggregate were tested in addition to the effect of fly ash in the concrete. Table 2.4 shows a summary of the different materials and the result for each wall. Note that it is only grains above 8 mm that is crushed for wall 6 and 7, the sand has a round grain shape.

In general there are two different cumulative sieve curves used. The sieve curve used in the concrete in wall 9 and 10 has a higher content of finer sand compared to the sieve curve used for concrete in wall 1, 6 and 7, see Figure 2.19. The w/c-ratio and the amount of water added is the same for all walls.

Table 2.4: Measured lifting force (from Kordina, 1984) and (Kordina, 1990)

Wall	Aggregate (grain shape)	Lifting force kN/m	Cement + PFA kg/m ³
1	Round	5.8	320 + 0
6	Crushed *	7.0	320 + 0
7	Crushed *	7.0	320 + 200
9	Round	3.6	320 + 0
10	Round	8.1	320 + 200

* Plasticizer is added for wall 6 and 7. Note that it is only the coarse aggregate that is crushed.

The result show that the lifting force is lowest when natural round aggregate is used (wall 1). The friction force is even lower when the amount of sand is increased, as shown for wall 9. Wall 10 with 200 kg fly ash showed a considerably higher friction force compared to wall 9 without fly ash. It seems that when the content of fines is too high, the friction force will increase. In this case the amount of fines is 520 kg plus the fines in sand, which in total make a considerable amount of fines. When using crushed aggregate, the lifting force is higher compared to natural round aggregate. The lifting force is not further increased when 200 kg fly is added to the mix design with crushed aggregate (wall 7).

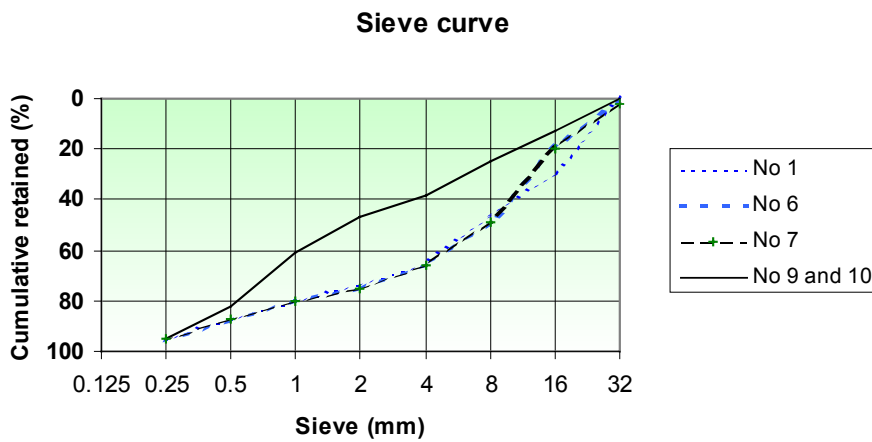


Figure 2.19: Sieve curves for aggregate used in concrete for slipformed walls according to Table 2.4.

In general there are not many reports on how the concrete properties or concrete constituency will effect the friction force. Based on the above it seems that grain shape and accumulative sieve curve is important for the friction force. Also increased amount of fines seems to give a higher friction force, but the results are not consistent. More finer particles in the interface zone will theoretically give an increased adhesion and a higher friction force.

2.3.7 Surface - slipform panel

When using a panel of wood (boards) without tongue and groove joints, some of the grout lubricant will escape and make less pressure and higher lifting force. When a wooden board is used, the face is subjected to such severe mechanical action that the planed board surface will soon becomes roughened (Steinecke et al., 1964). With watertight formwork a lubricant layer will be formed in the interface zone and result in a lower friction force.

Specht (1973) has found an almost linear relationship between the square root of the roughness factor of the slipform panel and the sliding friction coefficient.

$$\text{Eq. 2.14} \quad \Delta\mu_G = 100(\mu_G - \mu_{OG}) = \sqrt{r}$$

where μ_{OG} is the sliding friction coefficient for an ideal smooth panel
 μ_G is the sliding friction coefficient
 r is the roughness in 1/1000 mm (the average distance from top to lowest point on the surface).

This investigation was carried out in the laboratory and the results show that increased roughness will give a higher sliding friction.

Also the static friction is affected of the panel roughness. In Figure 2.20 it can be seen that the static friction vary in general between 1.5 to 2.5 times the sliding friction. It seems that the ratio between static and sliding friction has a tendency to increase with increasing panel roughness.

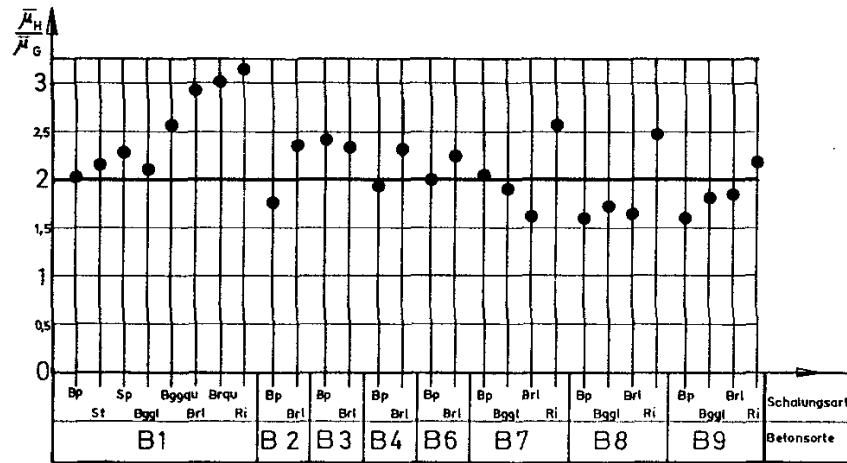


Figure 2.20: The relation between static (μ_H) and sliding (μ_G) friction coefficient (from Spech, 1973).

Panel type: *Bp and St – smooth surface,
Sp, Bggl and Bgglu – middle smooth surface,
Brgl and Brglq – rough surface
Ri – very rough surface
B1 to B9 represents different concrete mix designs.*

Also Kordina et al. (1990) have reported that there are a considerable difference in the measured friction between slipform panels with different roughness. Based on the investigation in laboratory and in field, the following friction numbers has been estimated for the different surface roughness, see Table 2.5.

Table 2.5: Friction forces on slipform panel (during slipforming) with different roughness (Kordina et al. 1990).

Formwork	Very smooth panel	Smooth panel	Wooden board	Very rough panel
Panel friction	3.4 kN/m	4.0 kN/m	6.8 kN/m	≈ 10.0 kN/m
Roughness $r \approx$	0.0225 mm	0.0625 mm	0.49 mm	1.44 mm

The friction varies considerable between very smooth and very rough panels in Table 2.5. The panel friction is estimated from the following equation (from Kordina et al. 1990):

$$\text{Eq. 2.15} \quad F = 25 * (0.1 + 0.25\sqrt{r})$$

where F = panel friction as a function of the surface roughness (r)
 r = the average distance from top to lowest point

Reichverger (1979) have carried out measurements on friction between different kind of surfaces like steel, PVC, Linoleum, and Polyethylene. In addition the friction on fouled or dirty surface is also tested. The results show that fouled surface (the panel surface covered with a thin layer of cement) gave the highest static and sliding friction, the values was doubled even after 5 minutes frequency compared to steel surface. The lowest friction was obtained with surface of Polyethylene (plastic). The result is presented earlier in Table 2.1 with surfaces of Polyethylene and steel. The results show that the lifting force when using Polyethylene surface is 80 % of the corresponding lifting force for steel panel with a slipform rate of 0.1 m/h and 90 % at higher slipform rates. For stops of 60 and 120 minutes the lifting force with Polyethylene is approximately 80 % of the corresponding lifting force for a steel surface. These results indicate that the panel roughness and type of panel have a considerable influence on the level of the friction force.

2.3.8 Stress distribution during lifting

When the slipform panel is lifted, the concrete surface will be exposed to tensile strain and tensile stress because of the friction force. The strain depends on the friction force and the elastic response from the concrete. In early phase, the concrete has no strength and the concrete will start to flow when the panel is lifted.

After the concrete has lost the workability and obtained a certain strength, the shear forces will be distributed further into the concrete. Figure 2.21 show an overview on how the stress is distributed in the cover zone during a lift. The reinforcement is working as a barrier and will reduce the effect of the tensile strain in the concrete. According to Adam (1976), the tension zone will be reduced with less concrete cover. This will reduce the effect of the friction force, even though the size of the friction force will not be reduced.

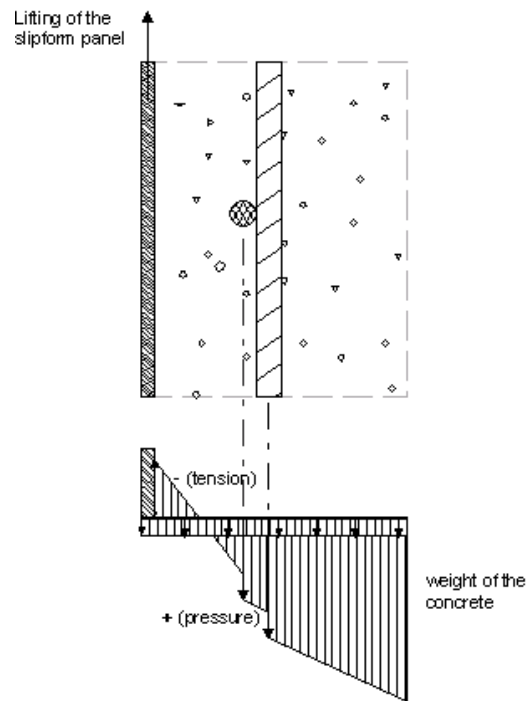


Figure 2.21: Stress distribution in the cover zone during lifting (Adam, 1976).

The weight of the concrete is also an important parameter. If the friction force becomes higher than the sum of the weight and the strength of the concrete, especially in a unreinforced wall, the concrete in contact with the panel will be lifted up (Steinecke 1964). The weight of the concrete depends on the wall thickness and the concrete density. If the wall thickness becomes to low, the weight including the strength will be lower than the friction force. This means that the minimum wall thickness depends on the level of the friction force during lifting.

2.3.9 Surface defects

The worst result on the hardened structure during slipforming is the development of damages caused by movement of the slipform panel. The damages occur when the concrete strain capacity is exceeded. Any damage is initiated during the period from the concrete has lost the workability to the slipform panel is detached from the concrete. It is also in this period the concrete strain capacity is low, see Figure 2.22.

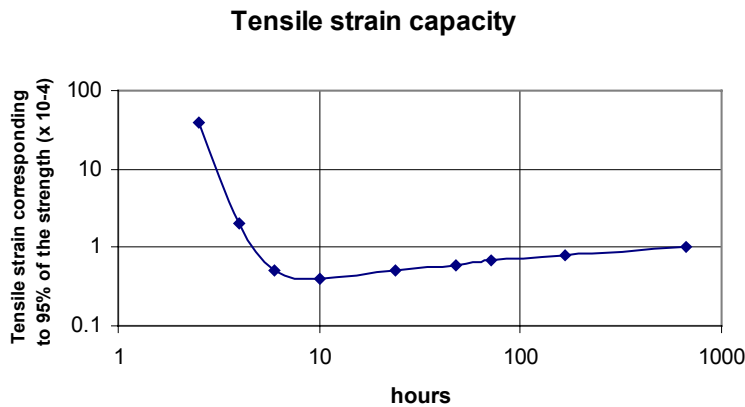


Figure 2.22: A typical curve of the tensile strain capacity in concrete, Kasai et al.1972.

There is not much literature that describes the different kind of damages that may happens during slipforming and why it happens. Most of the literature that deals with damages and condition control in slipformed structures describes the damages in a general manner. However, based on observations and some few reported damages, the following groups were identified.

1. Lifting cracks:

Horizontal (long) cracks on the wall face perpendicular to the lifting direction, are normally lifting cracks. The depth and width of these cracks may vary from thin and shallow to deep and wide. The reason for formation of lifting cracks is normally related to:

- long interval between concrete layers
- long interval between lifts

Lifting cracks are associated with forces during lifting of the slipform panel. Shaking or vibration of the slipform can also make cracks, but this is not really lifting cracks. Lifting cracks that occur during slipforming has often been assumed to be the main cause for the poor concrete quality for some slipformed concrete structures (Redlund, 1994).

2. Delamination:

Delamination of the concrete in the cover zone is concrete separated or displaced from the substrate. A vertical crack in the cover zone parallel to the reinforcement, and sometimes invisible on the surface, is delamination of concrete. Delamination is also areas where the concrete in the cover zone is lifted together with the panel and makes the cover deficiency on the wall face clearly visible. Delamination is often related to:

- Problems during start up,
- geometry changes,
- area above embedment plates and block outs
- the slipform is not in level

Delamination may happen when the friction force is greater than the weight of the concrete offering restraint in the cover zone (Kordina et al., 1984).

3. Lump formation:

Lump formation starts as a thin layer of grout sticking to the form panel. It continues to grow layer by layer until a lump is formed. After the lump is hardened it continues to grow horizontally and vertically. A lump can after a while easily be seen on the wall when the fresh concrete in the cover zone is pushed up (during lifting) and a clear visible cover deficiency is made. Lump formation is not fully comprehended. Lump formation is often related to:

- High ambient temperature
- High static friction
- Poor cleaning of the panel before start-up
- Not fully filled form

4. Concrete collapse:

Backsliding of concrete or concrete collapses happen when the slipform panel does not support the concrete any longer and the concrete strength is too low to carry its own weight. This problem is often related to:

- Uneven concrete layers
- Too high slipform rate
- Too long setting time

2.3.10 Summary lifting force and concrete pressure during slipforming

A lubricant layer will be formed between the panel and concrete during placing and vibration. Especially the vibration process will consolidate the concrete and envelop the larger aggregate in a slurry of binder and finer aggregate particles. This slurry will behave like a lubricant during lifting when the concrete is still fresh. Near setting of the concrete the lubricant will change its character and increase the adhesion between the concrete (lubricant) and the slipform panel. The thickness and properties of the lubricant layer will depend on the concrete composition and the consolidation method. When the slipform panel is lifted, the shear zone in early phase will be in the lubricant layer because the shear resistance is lowest here. Later, when the lubricant layer has stiffened, the shear zone will probably go between the lubricant layer and the slipform panel (slip plan)

Static friction is the smallest driving force which allowing sliding to be initiated. When sliding starts, the friction level is decreasing and this lower friction is called sliding friction. The static friction is increasing as the hydration proceeds until the maximum peak value is reached during the period of setting. The sliding friction will remain at almost the same level during the whole period, which means that the sliding friction is independent of the condition of the concrete (fresh or hardened). The static friction is increased with lower lifting frequency, since the adhesion force between the concrete and the panel is increasing with time in rest. In a slipform with several

concrete layers of different age, the highest static friction will probably occur in the concrete layer above the detach zone.

The concrete properties and the consolidation method will affect the concrete pressure against the panel. Higher slipform rate will give a higher concrete pressure. Higher concrete pressure will give higher static and sliding friction, but the friction coefficient based on the measured total pressure and friction will probably be reduced with increasing pressure.

The friction force during lifting will increase with increasing panel roughness. The difference in friction between a smooth and rough surface can be considerable. When natural round aggregate is used in the concrete, the friction force becomes lower compared to when crushed aggregate is used in the concrete. The total amount of fines will also affect the friction force. It seems that the lowest friction is obtained with sufficient amount of fines in the concrete. Too much fines has generally given a higher friction forces.

During lifting, the friction force from the panel will be transferred to the concrete. If the friction force is larger than the sum of the weight and the strength of the concrete, the concrete wall can be lifted up. The concrete weight depends on the wall thickness and the concrete density. The minimum wall thickness is therefore a function of the level of the friction force.

The worst result on the hardened structure during slipforming is the development of damages caused by movement of the slipform panel. The damages happen when the concrete strain capacity is exceeded. It is initiated during the period after the concrete has lost the workability and before it is detached from the slipform panel. The only exception is concrete collapse, which is caused by too low strength in the concrete at the bottom of the slipform panel. The other types of damages can be grouped in lifting cracks, delamination and lump formation. Common for all three groups seems to be high friction force and the concrete strain capacity exceeded.

2.4 Hardened properties

2.4.1 General

The hardened concrete properties in samples from slipformed structure can be compared with samples from a non-slipformed structure. The differences will indicate the impact of the construction technique, provided that the same concrete is used. Differences in hardened properties can be caused by factors such as non-uniformity, porosity or micro cracks in the concrete. In order to identify the influence the slipforming has on the properties of the hardened concrete, a comparison with non-slipformed concrete (fixed formwork) is preferred.

Most of the investigation projects referred to in this section has been carried out in Germany. Common for these projects is a wall thickness of 20 to 30 cm and a concrete cover from 20 to 34 mm. All slipformed walls have been made by using a slipform technique with a lifting height up to 30 cm and a very low lifting frequency, often more than an hour between the lifts. One exception is the wall no 13 in Braunschweig (Kordina et al. 1984) with an average lifting height of 5 cm and average lifting frequency of 12 minutes. For comparison, the lifting height during slipforming in Norway is normally between 10 and 30 mm and the lifting frequency between 5 and 15 min.

2.4.2 Compressive strength

An investigation of compressive strength is carried out by Ingvarsson (1979) on four slipformed concreted piers at the Angerad Bridge in Gothenburg, Sweden.

Cores were drilled after 60 days and tested after approximately 70 days. The cores were 100 mm in diameter and approximately 300 mm long. The cores were cut in two samples, the first 100 mm representing the cover zone (fcc1) and the other part representing the centre of the wall (fcc2).

Table 2.6: Observed compressive strength of the concrete, from Ingvarsson (1979).

	fca MPa	fcB MPa	fcc1 MPa	fcc2 MPa	fcR MPa
	K400 and 7 samples				
Mean compressive strength	47.5	33.9	39.2	40.3	44.2
Standard deviation	2.6	4.2	2.4	4.9	6.1
Characteristic strength (mean - 1.64* st.dev)	43.2	27.0	35.3	32.3	34.2
Minimum strength	42.2	26.8	36.5	31.9	38.7
Maximum strength	49.7	39.0	42.3	47.8	55.9
	K500 and 17 samples				
Mean compressive strength	53.2	39.0	41.8	46.5	44.2
Standard deviation	1.9	3.1	5.9	5.7	4.9
Characteristic strength (mean - 1.64* st.dev)	50.1	33.9	32.1	37.2	36.1
Minimum strength	49.3	33.3	35.7	39.1	37.1
Maximum strength	56.3	44.6	58.3	59.4	58.3

fca - standard cubes 150 mm (28 days)

fcB - cubes stored at site 150 mm (28 days)

fcc1 - drilled cores from cover zone (70 days), adjusted to 28 days strength.

fcc2 - drilled cores from centre of the wall (70 days), adjusted to 28 days strength.

fcR - calculated strength based on the measured values from rebound hammer.

The conclusion in the report is that the observed level of strength is in agreement with the strength obtained at other conventionally poured concrete structures. As shown in Table 2.6, the cores from the cover zone has a lower compressive strength (8 %) than cores from the centre of the wall.

Ingvarsson has (1979) also carried out an investigation on the strength gradient by using a rebound hammer. The thick line in Figure 2.23 shows the average measured compressive strength. According to Ingvarsson (1979), the carbonation of the cores has probably influenced the rebound hammer test values. For that reason the strength at the surface is probably lower (dotted line).

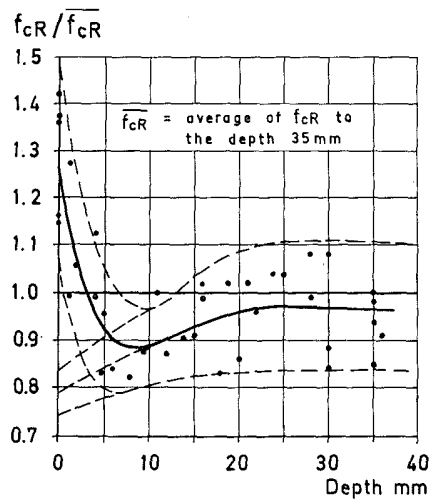


Figure 2.23: Variation of the compressive strength of the concrete near the surface of the pier walls determined by the rebound hammer tests. The dashed line above and below the mean curve (thick solid drawn line) denotes the dispersion zone.

At Norwegian Contractors an in-situ program have been carried out on 8 concrete platforms. More than 1300 cores have been drilled, mostly from slipformed walls and non-slipformed domes. On Gullfaks B (Danielsen, 1987) and Oseberg A (Danielsen, 1989), the skirts have been made with fixed formwork (non slipformed). The samples from these walls have been used to determine the α_f -factor for non-slipformed concrete in Table 2.7, see equation below. Other parts of the same concrete structure have been used to determine the α_f -factor representing the slipformed concrete.

$$\text{Eq 2.16: } \alpha_f = \frac{f_{\text{core-90 days}}}{f_{\text{cube-90 days}}}$$

- $f_{\text{core-90 days}}$ is the compressive strength in drilled core with a diameter of 75 mm and a height of 75 mm.
- $f_{\text{cube-90 days}}$ is the compressive strength in a 100 mm cube with the same concrete as in the core (stored in water at 20° C)

Table 2.7: α_f -factor

	α_f - factor	No of cores
Gullfaks B		
Skirt (non-slipf.)	0.80	16
Slipformed	0.92	125
Oseberg A		
Skirt (non-slipf.)	0.91	13
Slipformed	0.93	131

According to the α_f -factor in Table 2.7, the slipformed walls have in average a higher relative compressive strength than in non-slipformed walls. It is assumed that the main reason for this difference is better consolidation of the concrete in slipformed structures.

The compressive strength has also been measured for both slipformed and non-slipformed walls by Kluge (1986). Table 2.8 shows the average strength measured in out-sawed cubes (100 mm).

Table 2.8: Measured compressive strength in out-sawed cubes from Köln (Kluge, 1986)

	Age Days	No of cubes	Compressive strength N/mm ²
Non-slipf.	44	5	35,8
	51	6	39,5
Slipformed	44	6	41,0
	63	12	43,6

In Table 2.8, it can be seen the same tendency of higher compressive strength in the slipformed wall. The most probably reason for the lower strength in the non-slipformed wall is due to less consolidated concrete as mentioned above. It is reported that the concrete layer thickness during placing for the non-slipformed wall, was approximately 1 meter.

Based on the above results, it seems that the compressive strength in a slipformed concrete structure can be at the same level or higher than comparable non-slipformed structure. Since the compressive strength usually gives an overall picture of the quality of the concrete, it can be assumed that the concrete porosity and crack formation is in general equal for both construction techniques.

Drozella (1984, p.403-404) have measured the porosity gradient by Mercury intrusion in cores from a slipformed structure. He concluded that the porosity in the concrete is approximately equal for both construction techniques. The details on the investigated slipform structure and number of samples taken are not reported.

2.4.3 Measurements of dynamic modulus of elasticity

The dynamic modulus of elasticity is measured in concrete samples from slipformed and non-slipformed structures. Also the type of panel surface during slipforming has varied between the walls. The 100 mm core samples were cut to 10 mm thick discs and dried to constant weight before testing. The dynamic E-modulus were tested by using a “Grindo-Sonic” from Lemmens Elektronika, Belgium (Schmidt-Thrö et al. 1986,a).

The results presented in the Figure 2.24 and 2.25 are the average results from 2 or more cores from the same structure. The results have in general varied considerably between the samples from the same level and structure. Because of this variation, the average results represent more a tendency in dynamic E-modulus through the wall.

In Figure 2.24, the results in dynamic E-modulus from non-slipformed and slipformed structures are presented. Panel surfaces of coated plywood and undressed board has been used, the coated plywood represents a smooth surface and the undressed board represents a rough surface. The wall thickness is 200 mm and the concrete cover is 20 mm. The same concrete mix is used in both structures.

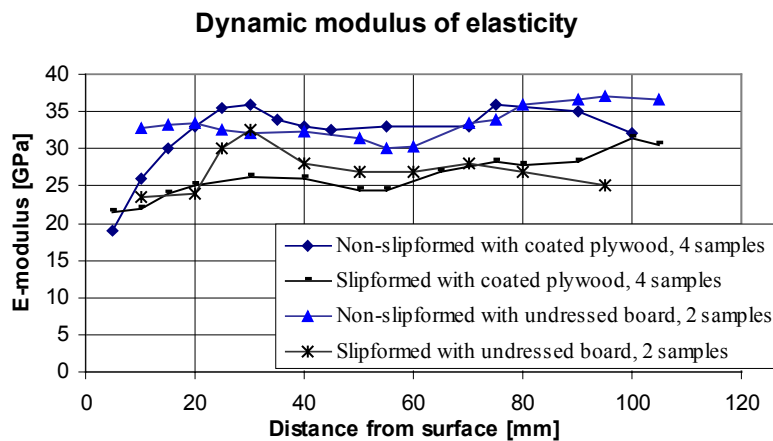


Figure 2.24: Dynamic E-modulus tested in samples from Utting (Schmidt-Thrö et al. 1986,a).

The dynamic E-modulus is approximately 20 % lower in samples from the slipformed structure compared to the samples from the non-slipformed structure. According to Schmidt-Thrö et al. (1986,a), the lower results is probably caused by the lifting of the panel in combination with a unstable slipform set-up. However, the lower dynamic E-modulus in the slipformed wall, even at the centre, indicates that the slipform operation in this instance have had a considerable impact on the quality of the concrete structure.

A rougher panel surface seems to give a higher E-modulus near the surface for both construction techniques. However, this is probably not significant and should theoretically not make any difference for concrete placed in a fixed formwork.

In general all curves in Figure 2.24 show a lower E- modulus near the surface. This can be explained by the increased amount of fines near the surface because of the wall effect. The wall effect means an increase of finer particles such as cement and sand at the surface area. Also curing of the concrete can have effected the E-modulus near the surface.

In Figure 2.25, the results from two slipformed walls with panel surface of steel and dressed board is presented. The wall thickness is 200 mm and the concrete cover is 20 and 30 mm. The concrete in wall 11 has 200 kg/m³ with fly ash and less aggregate (aggregate is replaced by fly ash) compared to the concrete without fly ash for wall 4.

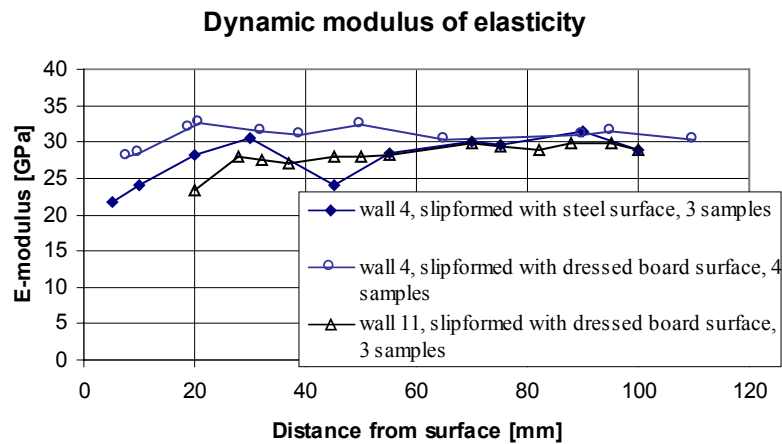


Figure 2.25: Dynamic E-modulus tested in samples from Braunschweig (Schmidt-Thrö et al. 1986,a).

The results in Figure 2.25 show that the dynamic E-modulus is in general higher for wall 4 compared to wall 11. According to Schmidt-Thrö et al. (1986,a), when the compressive strength is taken into consideration, the E-modulus result is as expected. It is also stated that the increased stickiness and unsuitable mixture in wall 11, caused by the high amount of fly ash, has not significantly affected the E -modulus.

Wall 4, slipformed with panel surface of steel, has in general a lower E-modulus near the surface compared to the concrete structure slipformed with dressed board. However, further inside the structure, the E-modulus is almost the same for all walls. The same tendency can be seen here as for Figure 2.24, with lower E-modulus near the surface.

2.4.4 Density of the concrete

The same samples used for the dynamic E-modulus measurements were also used to determine the density in the concrete at different depth. In Figure 2.26 and 2.27, the average density is shown.

In Figure 2.26, the densities from non-slipformed and slipformed structure are presented. The results show in total a large variation in the measured density. The expected drop in density near the surface caused by the increased amount of fines, which has a lower average density, can not be seen. Any significant difference in the density between samples from non-slipformed and slipformed concrete can not be identified. Also between the different panel surface, no clear differences in density can be observed.

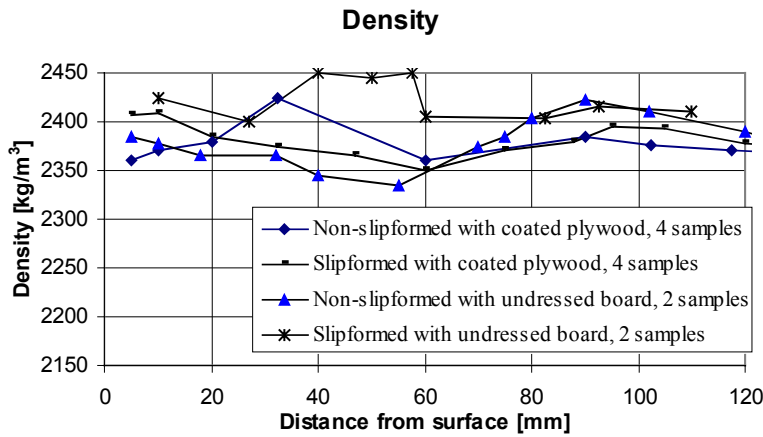


Figure 2.26: Measured concrete density in samples from Utting, (Schmidt-Thrö et al. 1986,a)

In Figure 2.27, the result from slipformed structures with different panel surface is shown. The result show in this instance, a lower density near the surface. The density is slightly higher in the samples from the slipformed wall with a panel surface of dressed board. However, this is not significant when also the results in Figure 2.26 is taken into consideration.

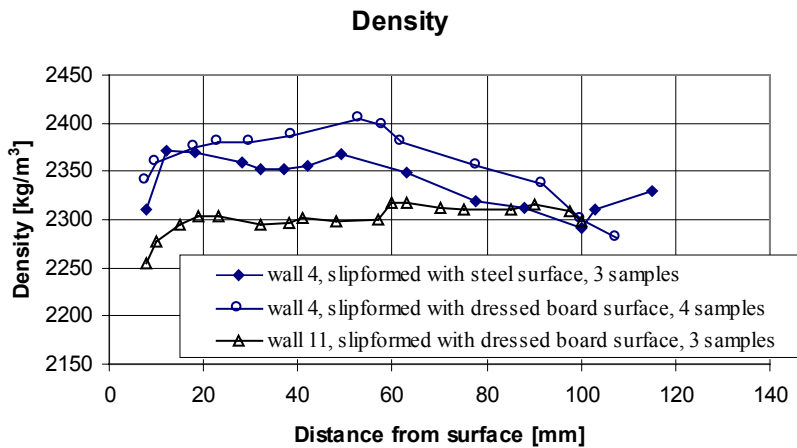


Figure 2.27: Measured concrete density in samples from Braunschweig (Schmidt-Thrö et al. 1986,a)

The results in Figure 2.27 show a lower density at centre of wall 4. According to Schmidt-Thrö et al. (1986,a), the lower density at wall centre is probably due to deep vibration of the concrete during slipforming. If this is correct, the vibration has been deep and also the dynamic E-module for the same samples should be lower. This is not the case, so the reason for the lower density must be more related to parameters such as placing method and the accuracy of the measurements.

The density variation is considerable for about all walls independent of the construction techniques and the panel surface. This indicates primarily that the samples are too small for representative results or the concrete in general is non-uniform.

The measured density of the fresh concrete for each wall is as follows:

- Utting:	2470 kg/m ³
- Braunschweig wall 4	2430 kg/m ³
- Braunschweig wall 11	2390 kg/m ³

The densities of the fresh concrete correspond well to average densities of the concrete samples in Figure 2.26 and 2.27.

2.4.5 Tensile splitting strength

The tensile splitting strength has been measured on samples from slipformed and non-slipformed structures. The tensile splitting strength is measured on cores with a length of 100 to 200 mm and represents an average strength from the surface to the centre of the wall, see Table 2.9. Only one sample from wall 11 Braunschweig, represents the wall centre. The tensile splitting strength in this sample is much higher than in other samples representing the wall part from the surface to the centre of the wall.

Table 2.9: Tensile Splitting Strength in slipformed and non-slipformed samples (Schmidt-Thrö et al. 1986,a and Kluge et al.,1986)

	Panel surface	Age	Dimensions, no of cores	Tensile splitting strength, N/mm ²	Direction
Utting					
Non-slipf.	Plywood	1-2 years	100/100, 4	4,37	Horizontal
Slipformed	Plywood	1-2 years	100/100, 3	3,03	Horizontal
Braunschweig					
Slipf. wall 4	Steel	1-2 years	100/100, 2	3.67	Horizontal
Slipf. wall 4	Board	1-2 years	100/100, 2	3.92	Horizontal
Slipf. wall 11	Board	1-2 years	100/100, 1	5.11 *	Horizontal
Köln					
Non-slipf.		52 days	150/200, 3	2,55	Horizontal
		52 days	150/200, 3	2,19	Vertical
Slipformed		52 days	150/200, 3	2,70	Horizontal
		52 days	150/200, 3	2,37	Vertical

* Core from centre of the wall

The results from Utting show that the samples from the non-slipformed structure have considerably higher values than the samples from the slipformed structure. Based on the results presented earlier, the lower tensile splitting strength was expected for the slipformed wall. However, in samples from another project (Köln), it can be seen that the results from the slipformed wall are higher than the comparable samples from the non-slipformed wall. Cores drilled in a vertical direction (concrete placing direction) show a lower tensile splitting strength.

In general, the results from the tensile splitting strength testing vary. It seems that the results depend on how the slipform operation is carried out. Disturbance of the fresh concrete during lifting will probably affect the results.

2.4.6 Durability investigation – carbonation measurements

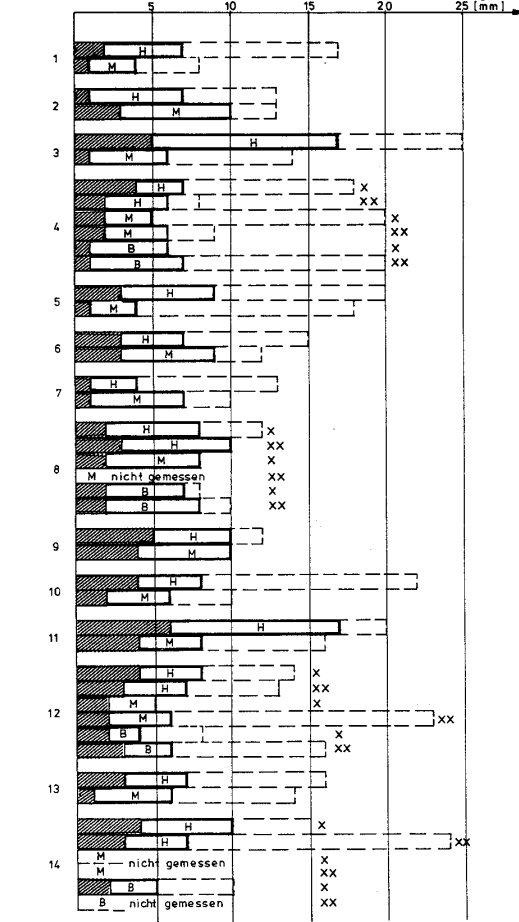
Kordina et al. (1984) has carried out an investigation to identify the effect slipforming has on the carbonation depth in the concrete structure. In total 14 different test walls were made (all slipformed).




After 19 months outdoor exposure, the test-walls were covered by plastic and the surrounding air filled with higher concentration of CO₂. This treatment was carried out during a 7-month period and the concentration of CO₂ varied between 0.1 to 2.0 % (volume). According to the report, this treatment should approximately correspond to the same exposure as for a 15 years old structure stored in outdoor condition.

After the CO₂-treatment the carbonation depth was measured in all walls by using 2 % solution phenolphthalein. The minimum, maximum and average carbonation depth was recorded (pH < 9). Figure 2.28 and 2.29 shows the recorded maximum carbonation depth on troweled and non-troweled concrete surface. The troweling was carried out on green concrete (in its own “juice”) just after the surface was exposed underneath the panel. The concrete cover is 20 and 30 mm and marked with X and XX, respectively.

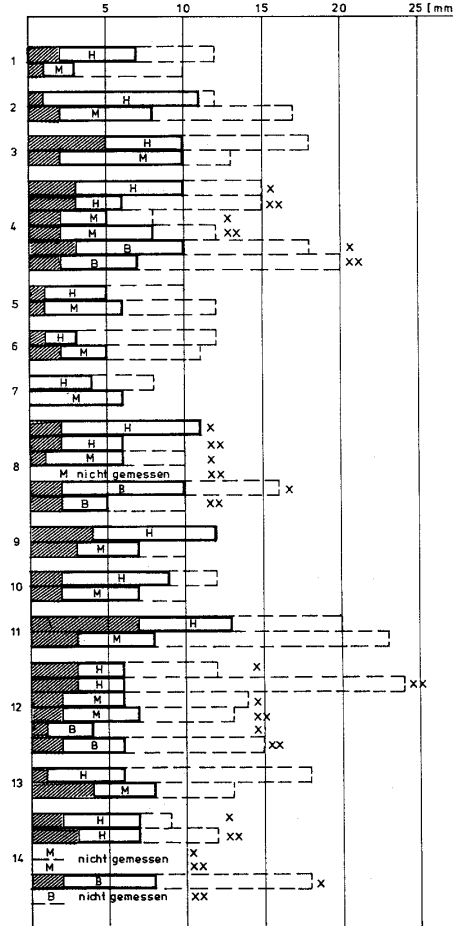
The results in Figure 2.28 and 2.29 show that the carbonation depth was higher in the concrete when a rough panel (wood) was used compared to smooth panel (steel or plywood). When a panel of wood is used and the concrete surface troweled, the carbonation depth was decreased. When smooth panels of steel were used and the concrete surface troweled, the result was partially opposite with increased carbonation depth. Based on the results, it seems that rough panels make a less dense concrete surface and gives a higher carbonation depth compared to the carbonation depth when a smooth panel is used. Troweling will make the concrete surface denser when a rough panel is used. When a smooth panel is used, the concrete surface is already dense and additional surface finishing will not improve but rather reduce the surface quality. This tendency of lower surface quality is measured by Teigland (1991) in samples with lightweight concrete. The samples were drilled from a concrete structure that was slipformed with panel surface of steel. A higher water intrusion depth was obtained on concrete from a troweled concrete surface compared to concrete where no surface finishing on the concrete surface had been carried out.

Carbonation depth (not surface treated)



 Carbonation depth
 Carbonation tip
 Carbonation tip close to aggregate

Carbonation depth (troweled surface)



H – Wooden board
 M – Plywood
 B – Steel plate
 X – Cover to reinforcement = 20 mm
 XX – Cover to reinforcement = 30 mm

Figure 2.28: Measured maximum carbonation depth, concrete surface not treated. Braunschweig (Kordina et al.,1984).

Figure 2.29: Measured maximum carbonation depth, concrete surface troweled. Braunschweig (Kordina et al.,1984).

Different lifting rates were used during slipforming of the wall. The rate varied between 0.1 to 0.3 m/hour. No difference in the carbonation intrusion could be observed in walls when the slipform rate was changed.

Slipformed concrete with fly ash has not given any difference in carbonation. The carbonation depth was slightly higher when blast-furnace slag cement was used in the concrete mix compared to concrete without slag cement. According to Kordina et al. (1984), this is probably because of the lower content of $\text{Ca}(\text{OH})_2$ when using slag cement. Less content of $\text{Ca}(\text{OH})_2$ might give a faster carbonation process and a deeper carbonation front.

According to Kordina et al.(1984), the concrete cover has no significant effect on the carbonation depth.

The carbonation depth is higher when using round coarse aggregate compared to crushed coarse aggregate. In Kordina et al. (1984) the following theory is suggested to explain the connection between carbonation depth and the coarse grain form. During lifting a vertical force and a torque will effect the fresh concrete in the cover zone, see Figure 2.30 and 2.31. The torque will try to rotate the coarse aggregate close to the surface, but if the aggregate is sharp edged (crushed) the surrounding mortar will restrain the aggregate. For that reason the interface zone between aggregate and mortar will still be intact and not destructed when crushed aggregate is used. According to Kordina et al. (1984) this theory might explain why the carbonation depth is considerable lower when using crushed coarse aggregate (even with higher friction force) and higher when using round aggregate. The same theory is proposed as an explanation why wall no 9 (high sand content) and wall no 13 (high lifting frequency) with low friction (both with round coarse aggregate) have not obtain better results.

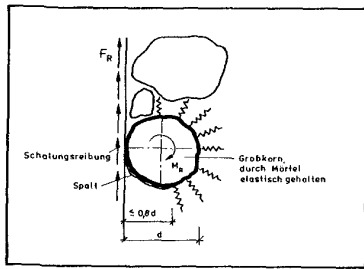


Figure 2.30: Gap formation underneath the coarse aggregate (Kordina et al.,1984).

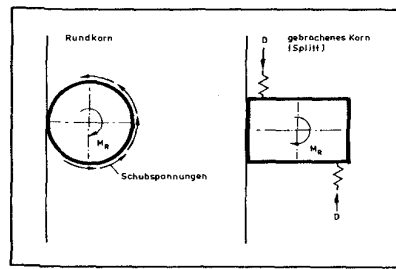


Figure 2.31: Vertical force and torque on the coarse aggregate (Kordina et al.,1984).

Based on the information in Figure 2.28 and 2.29, it is difficult to verify this theory. Wall no 6 and 7 has been made with crushed aggregate and the comparable walls with natural round aggregate are wall 1 and 2. It is only the result from wall no 7 with troweled surface, that has obtained a considerable lower carbonation depth than the comparable wall no 2. However, also the lower D_{\max} for the crushed aggregate (22 mm compared to 32 mm) should be taken into consideration when evaluating the results.

Also in samples produced in Utting, the carbonation depth have been measured by Schmidt-Thrö et al.(1986 b). The samples were stored indoors between 1 and 2 years in dry environment before testing.

Table 2.10: Measured carbonation depth in samples produced in Utting, slipformed and non-slipformed (Schmidt-Thrö et al., 1986 b).

	No of samples	Average max mm	Average min mm	Average mm
Utting Non slipformed Coated plywood	4	12	6	9
Utting Slipformed Coated plywood	3	11	5	7

The results show that the carbonation depth is lower in samples from slipformed concrete compared to the results in non-slipformed concrete. However, the difference is probably not statistically significant. It is indicated in the report that possible explanations for the good results in the samples from slipformed walls are surface finishing or how the core was cut. However, it is not explained how core cutting can influence the carbonation measurements on all three samples.

2.4.7 Chloride diffusion coefficient

In Figure 2.32 the average diffusion coefficient in concrete from different bridge structures is presented (Østmoen, 1999). In general, the main columns on bridges are constructed by slipforming and secondary columns are constructed by using fixed formwork.

The diffusion coefficient can only be compared when the condition of exposure is identical. This means that results from the same bridge can be compared if the measurements are taken from the same elevation and the same direction (North, East etc.). We assume that the number of samples taken from each bridge make the average number comparable between the different construction techniques (slipformed and non-slipformed).

The results show (Figure 2.32) that the highest diffusion coefficient was obtained in the slipformed part for four of the bridges. Based on this, it can not be documented any connection between the concrete resistance against chlorides and the construction method. More information is needed in order to make any conclusion.

Slipformed concrete structures installed in the North Sea have generally shown a high resistance against chloride ingress (Sandvik, 1997). Only minor corrosion of reinforcement has been observed on some platforms during the service time in the hostile North Sea environment. These corrosion areas of local nature have been characterised by reduced concrete cover or/and inadequate concrete quality caused by erroneously construction and poor workmanship.

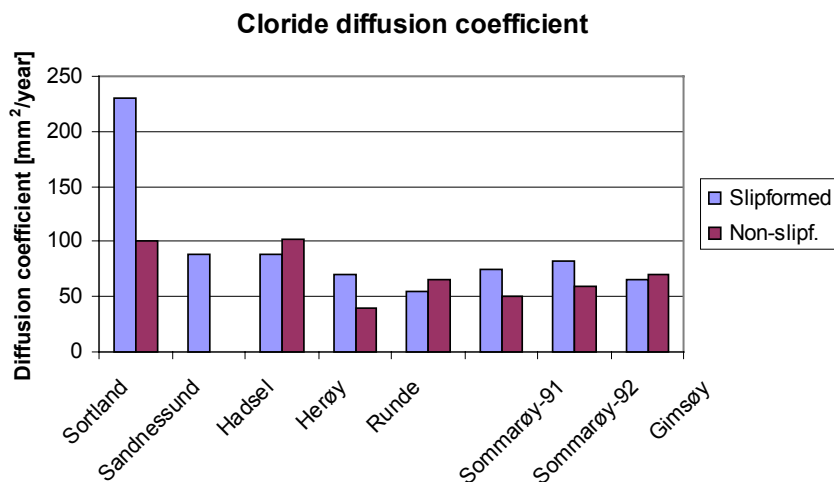


Figure 2.32: Diffusion coefficient in slipformed and non-slipformed bridges (Østmoen, 1999).

2.4.8 Summary hardened properties

The focus in this section has primarily been on how the properties in the hardened concrete structure are effected by slipforming compared to fixed formwork. In practice the consequence of slipforming can in the worst case lead to considerable surface damages. The different types of damages are described more detailed in Section 2.3.9. These damages are initiated by the panel movement and the creation of friction force in the interfacial zone between concrete and the panel. The damages happen when the concrete tension strain capacity is exceeded. Also during a "successful slipforming operation" the cover zone will be influenced by the friction force, but without any visible surface damage.

The results from Germany are based on a slipform technique that is different from the technique normally used in Norway and elsewhere. The main differences is the lifting height of 20-25 cm and a lifting frequency of up to 1 hour in Germany while in Norway, the normal lifting height is 10-25 mm and a frequency of approximately 10 minutes. It is measured up to 50 % higher adhesion between form panel and concrete when the time between two movements is increased from 10 minutes to 60 minutes. A higher friction/adhesion force will produce higher tension forces in the concrete, and the possibility of development of surface defects and cracks is considerably increased. It is assumed that this, in combination with typical concrete cover of 20 to 30 mm, high D_{max} and thin wall thickness, have given a negative influence on the results for the German slipform tests.

The results from mechanical testing vary, especially some of the results from the German investigations. Compressive strength and tensile splitting strength tests carried out on drilled cores from the cover zone show approximately the same result for both construction techniques. Dynamic modulus of elasticity shows a lower value for slipformed structures compared to non-slipformed structures.

The differences between the two construction techniques, based on the few reported measurements, are probably minor when the special relationship discussed above is taken into consideration. But it has to be emphasized that friction forces or other disturbances during slipforming, can give reduced quality of the hardened concrete.

The results from the durability measurement show that the carbonation depth depends considerable on the type of panel used during slipforming. Lower carbonation depth is obtained when smoother panels are used during slipforming. Also troweling carried out on a slipformed (green) concrete surface might have a considerable impact on the surface quality. When a slipform panel with rough surface is used, the carbonation depth will be decreased if troweling is carried out. This is because the concrete surface will be denser. When using steel panel, the concrete surface is smoother and additional treatment, such as surface finishing with trowel, will not further improve the surface quality, but reduce it.

It is difficult to make any conclusion for any connections between the concrete resistance against chloride ingress and the two construction techniques for concrete structures in Norway (bridges). However, slipformed concrete structures in the North Sea have in general shown a high resistance against chloride ingress.

3 HYPOTHESES

This section presents the hypotheses for this research program. The hypotheses are based on the literature review and pre-tests.

Hypothesis 1:

The risk of defects on the concrete surface is increased with increasing friction force during slipforming, i.e. a lower friction coefficient, or a lower effective pressure. It is assumed that the friction will increase with increased effective pressure. The effective pressure represents the pressure between the solid particles and the slipform panel (see Hypothesis 2) and is the difference between the normal pressure (concrete pressure against the slipform panel) and the pore water pressure in the concrete.

The damages is initiated during the period from the concrete has lost the workability to the slipform panel detach the concrete surface. Surface damages may occur when the friction between the panel and the concrete results in an exceeded strain capacity. Type of damages that may occur are lump forming and delamination of the concrete structure (type 2 and 3 in Section 2.3.9). Uneven friction between the slipform panel and the concrete (limited area with considerable higher friction) may result in lifting cracks (type 1 in Section 2.3.9).

Hypothesis 2:

The effective concrete pressure will increase when the pore water pressure is decreasing in the concrete. It is assumed that the effective pressure will be the same at the interface zone close to the slipform panel as for the bulk concrete. It is assumed that the particles at the interface will be pressed with higher pressure against the slipform panel, as the effective pressure is increasing. Higher effective pressure is assumed to increase the friction force during lifting.

The air content in the concrete is assumed to be in equilibrium with the liquid system in the concrete. When chemical shrinkage is developing, new space is formed (contraction pores) since the reaction products have a smaller volume than the reacting materials. If no air were present in the concrete, the chemical shrinkage would have resulted in an instant reduction of the negative pore water pressure. The air content, and settlement of the concrete, will reduce the effect of chemical shrinkage on the pore water pressure and result in a lower decrease rate of the pore water pressure. The air content in the concrete is probably the dominating factor and increasing air content is expected to increase the minimum pore water pressure and reduce the pore water pressure decrease rate.

The effect of the chemical shrinkage on the pore water pressure is assumed to depend, besides the cement hydration and the air content, also on the pore system that is formed. The pore water pressure, and development of the meniscus in the pore system, will depend on the particle size

distribution and the particle concentration. A system with higher particle concentration and finer pore system is assumed to result in a faster decrease in the pore water pressure compared to a coarser system. The pressure in the pore water will decrease, as the meniscus radius becomes smaller in pores where the menisci are formed.

Hypothesis 3:

There are two theories that might explain why the pore water pressure is increasing after a while at the sliding zone:

Theory 1:

The free water content in the concrete at the sliding zone at the slipform panel will be reduced as the cement hydration proceeds. When the water content is decreased to such a low content that the water meniscus cannot find new stable positions, the capillary system will collapse and the pore water pressure will increase or just disappear. The minimum pore water pressure is expected to occur just before the collapse of the capillary system at the sliding zone.

Theory 2:

The pore water pressure at the sliding zone is decreasing during lifting of the slipform panel. It is assumed that the pressure in the pore water at the sliding zone is increasing, because of an improved communication channel along the slipform panel during lifting. The pore water pressure at the sliding zone will, between two lifts, decrease until it is in equilibrium again with the pore water pressure in the bulk concrete. When the concrete start to be denser and the water communication slower, the time period will increase before the pore water pressure at the sliding zone will reach equilibrium again with the pore water pressure in the bulk concrete. The minimum pore water pressure is probably reached when the time period for equilibrium is longer than the period between two lifts. The pore water pressure at the sliding zone will thereafter probably increase.

Hypothesis 4:

The friction can be divided into two phases, sliding and static friction. The static friction is the resistance that has to be overcome in order to start sliding and the sliding friction represents the resistance during sliding.

The sliding friction is expected to be affected by the parameters in the concrete sliding zone at the slipform panel. Rougher slipform panel and crushed aggregate (sharp edged) will, according to the literature, increase the sliding friction. Also the pressure between the particles (effective pressure) will have a direct impact on the sliding friction (hypothesis 2). It is assumed that the friction law can be used to describe the correlation between the effective pressure and the sliding friction.

The static friction is more related to the adhesion that occur in the sliding zone. The adhesion is mainly because of the cement bonding that occur during the cement hydration. The cement hydration is low the first hours, but when it is increasing also the adhesion and the static friction will increase. Also the pore water pressure might affect the static friction. It is assumed that the negative

pore water pressure at the sliding zone will increase during lifting. Increased time between the lifts will most likely increase the static friction.

4 EXPERIMENTAL PROGRAM

4.1 General

The purpose of the experimental program is to carry out tests in order to investigate and possible verifies the hypotheses in Chapter 3. The test program is organized mainly in two parts where the first part has the focus on parameters that affect the friction and the second part has the focus on the connection between the friction and any surface damages. The second part of the test program will primarily be carried out during the field investigations.

In a full-scale slipform with several concrete layers of different age, a number of parameters will affect the friction force. The friction response of each layer will vary because of the different stages of hardening. In addition, the inclination of the slipform panel might affect the concrete pressure as the slipform is lifted. In order to simplify the test method, it is necessary to make a slipform rig that can simulate the conditions one single layer of concrete is subjected to in a full-scale slipform.

The first slipform rig was made simple and easy to rebuild (if necessary), in order to gain more experience with the parameters affecting the friction force. This first rig has a horizontal slipform panel and is called the friction rig. The experience from testing in this rig is used in planning of the vertical slipform rig, which is considered to be the main rig in this test program. The vertical slipform rig is planned to simulate the most relevant slipform conditions and loads that one or several concrete layer are exposed for. The design of these rigs is described in detail in the following.

4.2 Description of the test rigs

4.2.1 Friction rig

4.2.1.1 Objectives

The objective of the friction rig is to identify the parameters affecting the friction that occur during panel movement. This includes also a study on how the parameters affect the friction. The test program will be focused on parameters in the fresh concrete and slipform technical parameters such as movement frequency and sliding length. Different concrete pressure is also included in the test program.

The friction rig will be able to simulate all kind of “lifting heights”, “lifting” frequencies and normal pressures against the slipform panel. Since the panel is installed horizontally, the concrete pressure is independent of the concrete properties. The drawback for this rig might be that the concrete is restrained in the concrete box because of the end plate at the front, see Figure 4.1. Because of the horizontal slipform panel, the bleeding and segregation of the concrete might also give a different effect on the friction force compared to a vertical slipform panel.

The friction rig is made for testing of only one layer of concrete during each test. The concrete is placed in a plywood box that is 600 mm long, 300 mm wide and 150 mm high. Approximately 30 litres of concrete is used to fill the box. A pneumatic controlled lid on top can push the concrete and increase the concrete pressure against the slipform panel.

4.2.1.2 Reinforcement

Reinforcement mesh is used during the tests. This mesh consists of 10 mm bars spot welded c/c 100 mm in both directions. The mesh is installed with the longitudinal bars on top and in a distance of 50 mm from the slipform panel.

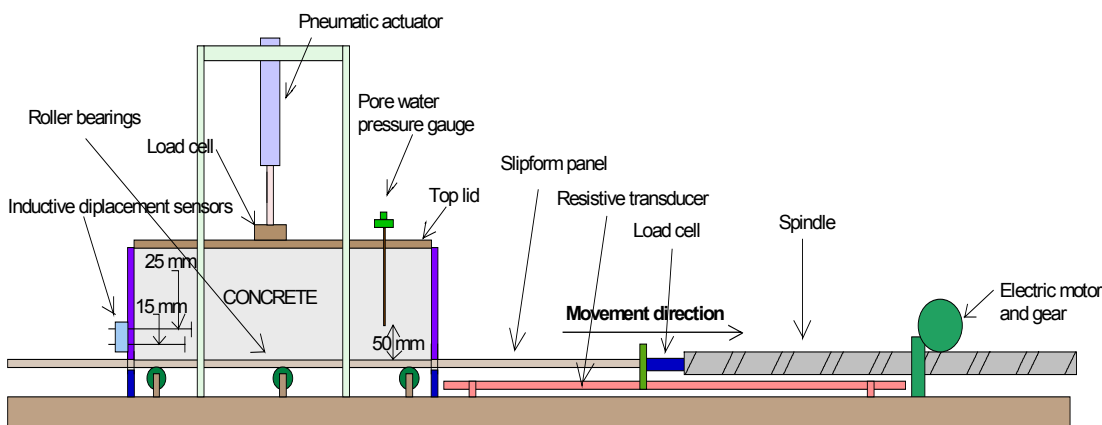


Figure 4.1: A principle drawing of the horizontal model rig

4.2.1.3 Slipform panel

The slipform panel is approximately 1200 mm long and 300 mm wide. The panel consists of a 20 mm thick plywood with 2 mm steel plate on top. The panel is supported by three rigid roller bearings at the bottom of the box. The maximum movement length of the slipform panel is 57 cm. Movement of the slipform panel is carried out by an electric motor connected to a spindle through a gear. When the motor is running, the spindle pulls the slipform panel. Between the spindle and the slipform panel, a load cell is installed for measuring the friction force. A frequency converter controls the speed of the motor.

4.2.1.4 Pressure on top

The lid on top can pressurise the concrete in order to simulate additional concrete layers. The lid is pressurised by the connected pneumatic actuator, see Figure 4.1.

4.2.1.5 The position measurements

Two resistive displacement transducers are installed on the rig, one on each side of the slipform panel. The resistive transducer measures the position of the slipform panel during the operation.

4.2.1.6 Inductive displacement sensors

In order to measure any displacement of the concrete in the cover zone, two “nails” are embedded in the concrete respectively 15 and 25 mm above the slipform panel. The nails are of different length, respectively 130 and 150 mm measured from the rear end of the box. The nails are placed in a sleeve in order to prevent any friction from the surrounding concrete. The head of the nail is approximately 10 x 10 mm in area. One inductive displacement sensor is connected to each nail, see Figure 4.1 and 4.2.

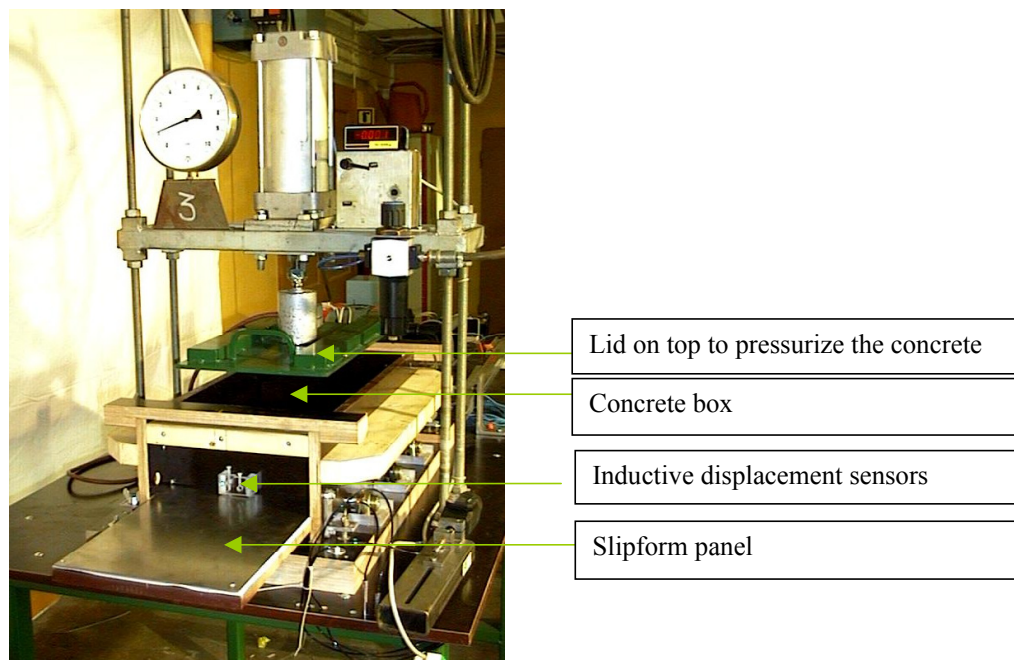


Figure 4.2: The friction rig

4.2.1.7 Pore water pressure gauge

The purpose of the pore water pressure gauge is to measure the pore water pressure in the concrete pore water. A pore water pressure gauge consists of a thin tube connected to a pressure transducer. The pressure gauges is installed at the centre on top of the concrete and it measure the pressure in the pore water approximately 50 mm above the slipform panel, see Figure 4.1. The pressure transducer (model AB HP15 \pm 15 psig) is supplied by Data Instruments.

The pore water pressure gauges were introduced after the test program was started and therefore only the last tests has been carried out with pore water pressure measurements.

4.2.1.8 Temperature measurements

The concrete temperature is measured during the tests by using a thermocouple of type T (Copper - Constantan). The thermocouple is located during testing approximately 100 mm below the centre of the top concrete surface.

4.2.1.9 Control and measurement system

Start and stop of the motor and the frequency converter are fully managed by Labtech Notebook, a computer program for data acquisition and control. This software also carries out measurements and logging of the results. Datascan 7250 measurement processor with 12 bit resolution is connected to the measurement units and is controlled by the Labtech Notebook.

The following parameters are measured during the test.

- The friction force
- Concrete temperature
- The position of the slipform panel
- Displacement of the concrete in the cover zone
- The pore water pressure in the concrete
- The load on top of the fresh concrete

The sampling rate is 10 measurements/second during the panel movements and 1 measurement/10 seconds between each movement. All data is continuously logged and stored in the computer.

4.2.2 Vertical slipform rig

4.2.2.1 Objectives

The objective of the vertical slipform rig is to identify parameters affecting the friction. This includes also a study on how the parameters affect the friction. Connection between friction and any surface damages will also be investigated (if possible). The test program will be focused on parameters in the fresh concrete and slipform technical parameters such as lifting height and frequency.

The purpose for the rig is to simulate realistic loads that one or several layer of concrete is exposed to during slipforming. Additional layer can be simulated by using the top lid to pressurise the concrete on top. The slipform panel is installed vertically, which means that the concrete pressure will depend on the concrete properties and the inclination and stiffness of the slipform panel. The panel has the possibility to adjust both the inclination and the stiffness in order to simulate different slipform set-ups.

4.2.2.2 Steel framework

The vertical slipform rig is made of steel framework consisting of 50 x 50 mm rectangular hollow sections, see Figure 4.3 and Figure 4.4. The framework is 3.6 meter high and 1.0 x 1.0 m wide. Inside the frame a 1.6-meter high slipform panel and a container for concrete are installed. Most of the measuring equipment is fastened to the framework.



Figure 4.3: The vertical slipform rig.

4.2.2.3 Concrete container

The concrete container is located inside the steel framework 850 mm above the floor. It is 600 mm wide and 300 mm deep. The height of the container is 955 mm and makes it possible to place 6 concrete layers of 150 mm. In addition the concrete can be pressurised on top in order to simulate additional layers. The dimension of the concrete container is decided based on the capacity of the laboratory mixers.

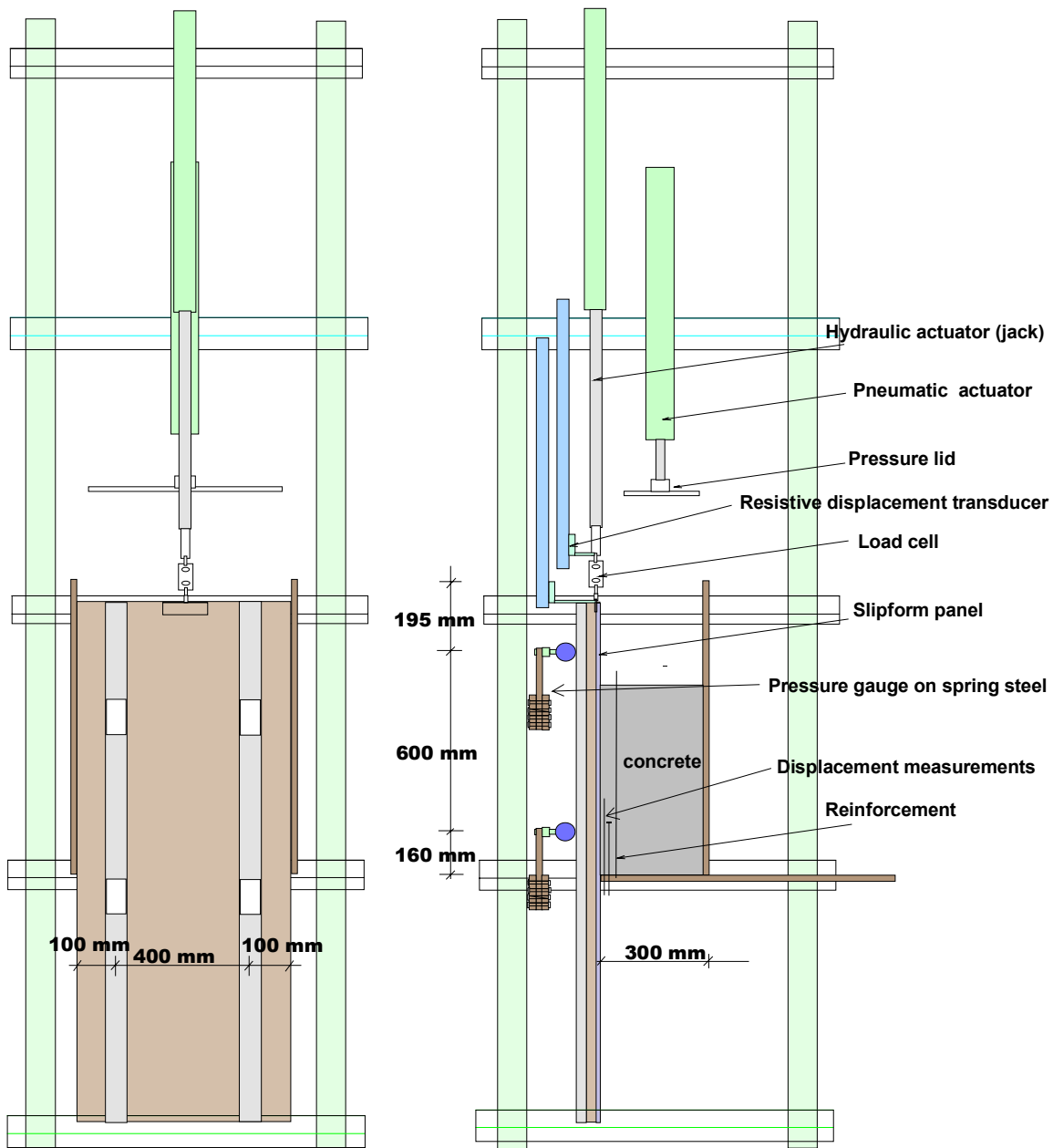


Figure 4.4: The vertical slipform rig, rear and side face

4.2.2.4 Reinforcement

Reinforcement mesh is used during the tests. This mesh consists of 10 mm bars spot welded c/c 85 mm in vertical and horizontal direction. The mesh is installed with the vertical bars inwards (against the centre of the wall) and in a distance of 40 mm from the slipform panel, see Figure 4.5.

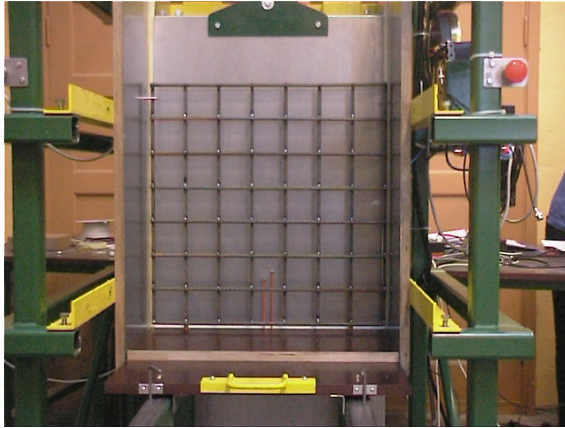


Figure 4.5: The reinforcement mesh in the concrete container.

4.2.2.5 The slipform panel

The slipform panel is 1600 mm long and 600 mm wide. The height is chosen in order to ensure that the lifting can start without any concrete fallout during the test. The maximum movement length of the jack (actuator) is 1000 mm during a test, which will be the limitation of the total lifting height.

The slipform panel is made of 20 mm thick plywood with a 2 mm thin steel plate on the sliding face. The width of the panel is 600 mm. Two sections of steel T-beam is mounted on the outside face of the panel. Along each T-beam, a flat steel bar is bolted to provide adjustment of the inclination. The flat steel bar is rolling against the roller on the load cells (measuring the concrete pressure) installed on the steel framework (see Figure 4.7 and 4.8).

The hydraulic jack mounted on the top of the framework will lift the slipform panel. A load cell installed between the slipform panel and the jack measures the lifting force.

4.2.2.6 Pressure lid on top

The pressure lid is used to pressurize the concrete when simulating additional concrete layers, see Figure 4.6). In order to prevent the concrete in the cover zone from being restrained when using this pressure lid, a 50 mm thick mineral wool mat is used between the concrete and the lid. The lid itself fills the whole space between the side faces, except for a 30 mm gap along the slipform panel (above the cover zone).



Figure 4.6: The lid for pressurizing the concrete.

A pneumatic actuator provides the pressure on the lid. A load cell is installed between the lid and the actuator for measuring the pressure.

4.2.2.7 Normal force measurements

On the outside face of the slipform panel, four load cells are installed. The upper two load cells are installed 760 mm above the bottom of the container and the lower load cells are installed 160 mm above the bottom. The load cells are rolling along the flat steel where the inclination can be adjusted relatively to the slipform panel, see Figure 4.7 and 4.8.

The four load cells will measure the concrete pressure and the pressure distribution against the slipform panel.

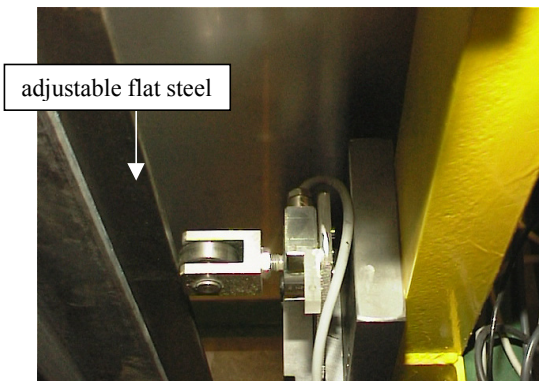


Figure 4.7: The flat bar steel is rolling against the roller on the load cells



Figure 4.8: The load cell installed on the spring steel

The spring steel is 51 mm wide and 7 mm thick and the cantilever arm of the spring steel can be adjusted as shown in Figure 4.9. Shorter cantilever arm on the spring steel gives a higher stiffness on the pressure gauge that rolls against the slipform panel. The stiffness is adjusted by moving the brackets up and down. The load cells have a fixed position relative to the concrete. Any deformation

of the spring steel will not increase the inclination of the slipform panel (related to the lifting direction), because the slipform panel is rolling against the load cells connected to the spring steel.

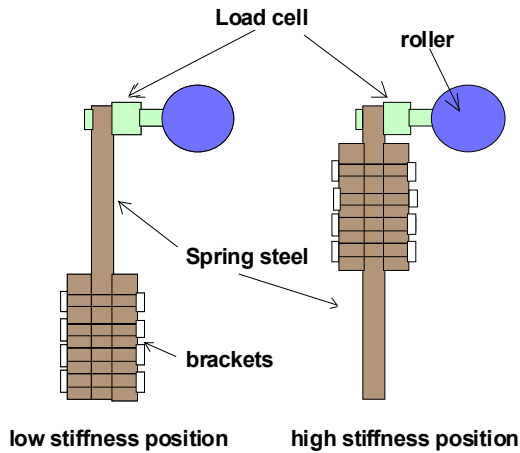


Figure 4.9: The position of the spring steel decides the stiffness of the slipform panel.

4.2.2.8 The position measurements

Two resistive displacement transducers are installed on the slipform rig, see Figure 4.4. The first displacement transducer controls the position of the jack during lifting (closed loop displacement control) and the second displacement transducer measures the actual position of the slipform panel. The closed loop displacement control is further commented in Section 4.2.2.12.

4.2.2.9 Inductive displacement sensor

In order to measure any displacement of concrete in the cover zone, two “nails” are embedded in the concrete 15 and 25 mm respectively from the slipform panel, see Figure 4.10. The nails are of different length, respectively 170 and 400 mm measured from the bottom of the container. The nails are placed into a plastic sleeve in order to prevent any friction from the surrounding concrete. The head of the nail is approximately 10 x 10 mm in area. Inductive displacement sensors installed underneath the box are connected to each nail.

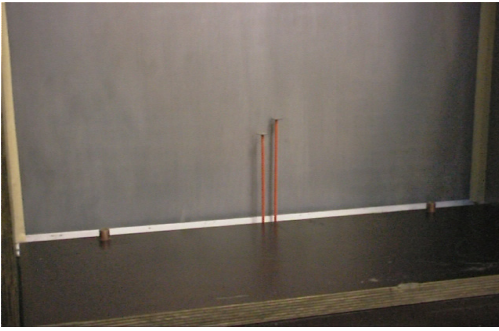


Figure 4.10: Inductive displacement sensors

4.2.2.10 Pore water pressure gauges

The pressure in the concrete pore water is measured by pore water pressure gauges. The pore water pressure gauge consists of a thin tube connected to a pressure transducer. The gauges are installed on top of the newly placed concrete and from underneath the bottom as shown in Figure 4.11.

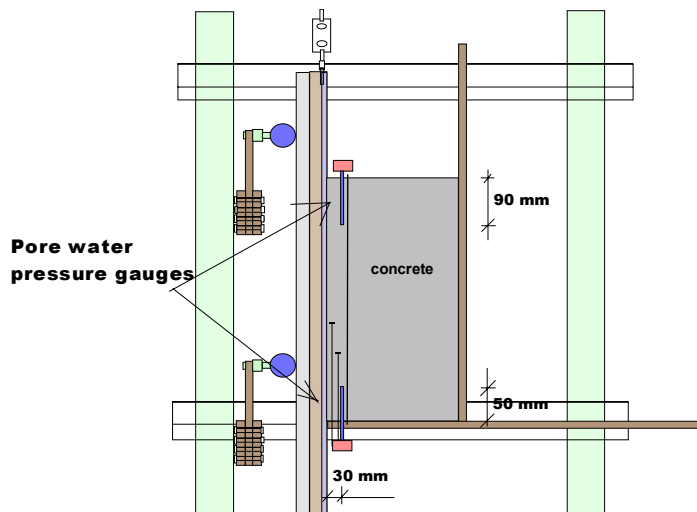


Figure 4.11: The position of the pore water pressure gauges.

By using two gauges, it is possible to measure the difference in pore water pressure between the upper and lower part of the concrete.

4.2.2.11 Temperature measurements

The ambient and concrete temperature is measured by using a thermocouple of type T (Copper - Constantan). The thermocouple in the concrete is located normally approximately 100 mm below the centre of the top surface.

4.2.2.12 Control and measurement system

The lifting jack is operated in closed loop displacement control. The command signal comes from a Datascan 7250 measurement processor with 12-bit resolution, which will give step of approximately 0.25 mm of the jack. Some filtering has been applied to the signal to smoothen the movements. The Datascan system is controlled by a computer running Labtech Notebook, a program for data acquisition and control. A table describing the movement of the jack is loaded into the computer and read out by the Datascan 7250. The system also consists of a Datascan 7221, which has no outputs but is connected directly to load cells. Each measuring unit is connected to one of these Datascan units. The data are stored in the computer.

The following parameters are measured during the tests.

- The lifting force
- The normal force from the concrete (4 load cells in total, 2 on upper and 2 on lower part).
- Concrete and ambient temperature
- The position of the slipform panel
- The concrete displacement in the cover zone
- The pore water pressure in the concrete
- The load on top from the pressure lid

The sampling rate is 10 measurement/second during lifting and 1 measurement/ 10 second between each lift. The log file consists of the above data in addition to the elapsed time since start-up.

The chosen standard lifting heights are respectively 10 mm and 20 mm. A timer connected to the control panel controls the frequency of the lifts.

4.2.3 Test panel used during field investigations

4.2.3.1 Design

The test panel is made for measuring the concrete pressure and the friction force during full-scale slipforming operations, see Figure 4.12. It is equipped with load cells and installed as an integrated part of the slipform. The test panel is 500 mm wide and 1100 mm high. To prevent adjacent panels to affect the measurements, thin strips of POM – plastic (Polyoxymethylene) is installed on both sides of the joint between the panels, see Figure 4.13. The POM – plastic is a low friction material.

In order to measure the concrete pressure on the slipform panel and the friction force during lifts, the load cells transfer all loads between the panel and the walings. There are no direct physical contact between the walings and the test panel.

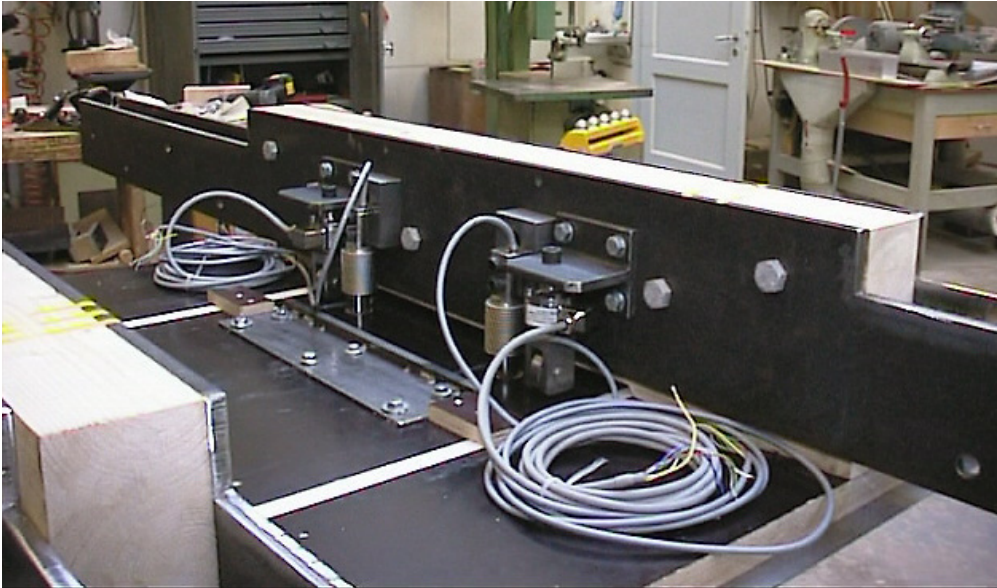


Figure 4.12: Test panel equipped with load cells.

The test panel was used on two full-scale slipform operations at Tukthus site in Oslo, Norway. The slipform panel was made originally of 20 mm thick plywood and covered by a 0.9 mm steel plate on the “sliding face” of the plywood. The plywood was replaced by 20 mm thick vertical boards on the test panel during the second slipform operation.

4.2.3.2 Measurement gauges

The test panel is equipped with in total 6 load cells, where all loads are theoretically passing through these load cells. Of these load cells, 4 measure the concrete pressure against the slipform panel. The load cells are located 50 mm below the upper and lower walings and will therefore give slightly different normal force distribution compared to when the walings are connected directly to the slipform panel. However, the total concrete pressure will be the same.

The 2 last load cells are installed between the test panel and the upper waling. When the slipform is lifted, the walings connected to the adjacent slipform panels lift the test panel through the load cells. The measured load should in principle be equal to the friction force that occurs between the test panel and the concrete.

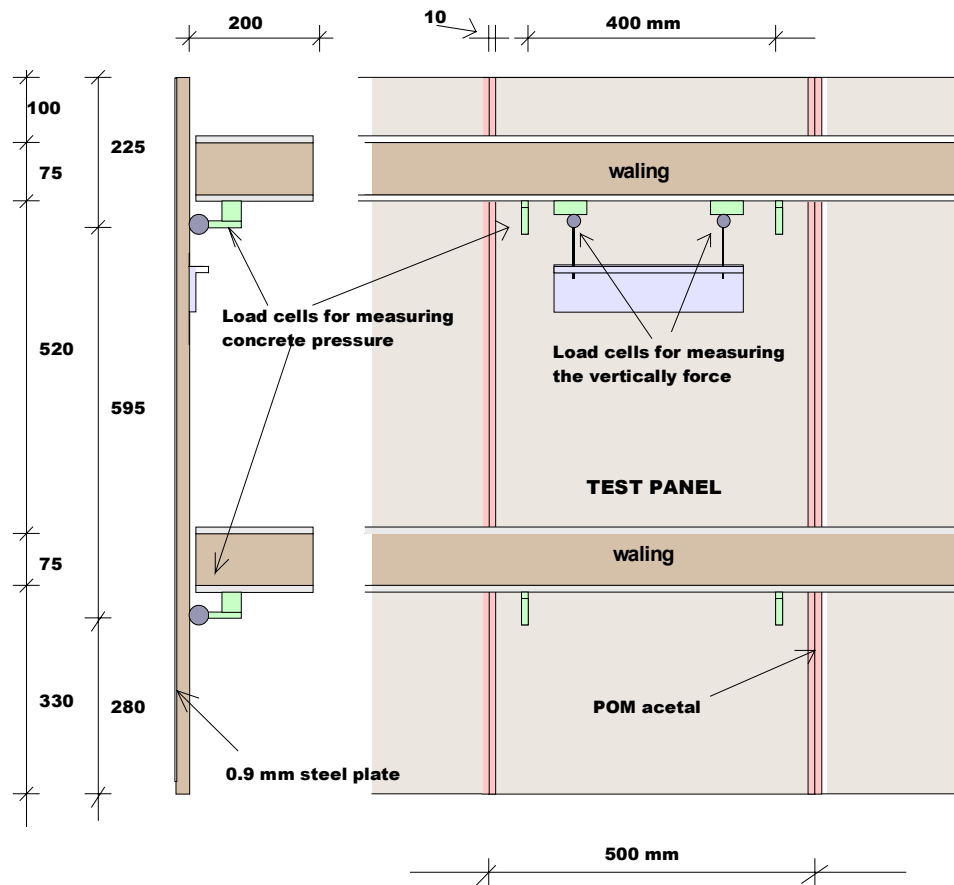


Figure 4.13: The test panel for installation in a slipform

4.2.3.3 Control and measurement system

Labtech acquisition and control software is used for registration of the results. Each time the slipform is lifted, the trigger give a signal to the software that again starts the measurements. It is the start of the oil pump for the hydraulic jacking system that is used as a trigger. The measurement frequency is 10 times in a second during a lift. After the lifting is completed, the frequency of the measurements is changed to one measurement pr 10 second. After 60 seconds the measurements are terminated. The measurement sequence can also be started manually, when extra measurements are desired, e.g. during vibration.

4.3 Concrete constituency

4.3.1 Introduction

The mix design and the constituency of the tested concretes represents typical concretes that are used in slipformed structures such as bridges, towers and offshore structures. Both normal weight concrete and lightweight concrete are used in the test program. Addition of superplasticizer and silica fume in the concrete are frequently used in these kind of concrete structures and is also used in the concrete for this program. The basis concrete used in both the friction rig and the vertical slipform rig has a w/b-ratio of 0.40 and 5 % silica fume. The characteristic strength of this concrete is 65 MPa.

4.3.2 Concrete mixes

4.3.2.1 Friction rig

The basis concrete mix used in the friction rig is listed in Table 4.1. This concrete is used when testing the effect of different slipform techniques including the normal pressure on the measured friction. The basis concrete is also used during the reproducibility testing carried out for this rig, see Chapter 5. With new supply of aggregates, the amount of aggregate in each fraction is sometimes changed in order to keep the same cumulative sieve curve in Figure 4.14.

Table 4.1: Basis concrete

[kg/m ³]	Basis
Norcem Anlegg	392
Silica fume	5 %
Sand 0-2 mm	247
Sand 0-8 mm	713
Coarse aggr. 8-11 mm	342
Coarse aggr. 11-16 mm	519
w/b-ratio	0.4
SP-admixture *	Glenium51
Binder content [litre/m ³]	300

* Air admixture has also been used in some concrete tests.

The basis concrete is varied in order to detect the effect on the friction. The following parameters in the concrete are varied:

- air content
- w/b-ratio
- content of silica fume
- lower binder content
- coarser sieve curve
- crushed aggregate

The variations of the basis mix are shown in Table 4.2 and in detail for each test in Appendix A-1. The slump is kept between 15-25 cm for all tests.

Table 4.2: Concrete mixes used in the friction rig

[kg/m ³]	Mix I (silica fume)	Mix II (binder)	Mix III (sieve curve)	Mix IV (w/b-ratio)	Mix V (crushed aggregate)
Norcem Anlegg	416/336	327	392	308/455	392
Silica fume	0 / 20 %	5 %	5 %	5 %	5%
Sand 0-2 mm	247	265	0	247	*
Sand 0-8 mm	713	765	961	713	*
Coarse aggr. 8-11 mm	342	366	341	342	*
Coarse aggr. 11-16 mm	519	557	519	519	*
w/b-ratio	0.4	0.4	0.4	0.6 / 0.3	0.4
SP-admixture	Glenium 51				
Binder content [litre/m ³]	300	250	300	300	300

* Mylonitt aggregate from Tau has been used. See Appendix A-1 for details.

4.3.2.2 Vertical slipform rig

The basis concrete mix used in the vertical slipform rig is listed in Table 4.3. This is the same basis mix as used in the friction rig. This concrete is used when the effects of the slipform technical parameters on the friction are tested. The basis concrete is also used during the reproducibility testing, see Chapter 5. With new supply of aggregates, the amount of aggregate in each fraction is changed in order to keep the same cumulative sieve curve in Figure 4.14.

The basis concrete has mostly been a self-compacting concrete where no further consolidation is needed. Sika ViscoCrete 3 and Scancem SSP2000 are used as superplasticizer admixtures to obtain the self-compacting properties in the concrete.

Table 4.3: Basis concrete

[kg/m ³]	Basis
Norcem Anlegg	392
Silica fume	5 %
Sand 0-2 mm	348
Sand 0-8 mm	672
Coarse aggr. 8-11 mm	283
Coarse aggr. 11-16 mm	519
w/b-ratio	0.4
SP-admixtures	Sika ViscoCrete 3, Scancem SSP 2000, Sikament 92
Binder content [litre/m ³]	300

The basis concrete is varied in order to detect the effect on the friction. The following parameters in the concrete are varied:

- binder content
- content of silica fume
- coarser cumulative sieve curve
- crushed aggregate
- lightweight aggregate

Also some concrete mixes used at the field projects are tested in the vertical slipform rig. These concrete mixes are listed in Table 4.5 and Table 4.6. It is the concrete denoted C45 at Tukthus site (Table 4.5) and both concrete mixes used on Sørkedalsv site (Table 4.6) that are tested.

The variations of the basis mix are shown in Table 4.4 and in detail for each test in Appendix A-2. The slump is kept between 10 and 15 cm for concrete tests that are vibrated. The slump for the self-compacting concrete has been approximately 25 – 26 cm.

Table 4.4: Concrete mixes used in the vertical slipform rig.

[kg/m ³]	Mix I (silica fume)	Mix II (binder)	Mix III (sieve curve)	Mix IV (crushed aggregate)	Lightweight concrete			
Norcem Anlegg	392	359/457	392	392	394			
Silica fume	10 / 20%	5 %	5 %	5 %	5 %			
Sand 0-2 mm	348	364/326	0	* ¹	306	254	362	351
Sand 0-8 mm	672	703/630	1030	* ¹	153	431	562	678
Coarse aggr. 8-11mm	283	297/266	286	* ¹				
Coarse aggr. 11-16mm	519	544/487	525	* ¹				
Leca 1-4 mm					115	89	75	0
Liapor 7 4-10 mm					383	332	250	351
w/b-ratio	0.4	0.4	0.4	0.4	0.4	0.4	0.4	0.4
SP-admixture * ²	SV3	SV3	SSP2	S92	SV3			
Binder content [litre/m ³]	300	275/350	300	300	300			

*¹ Mylonitt aggregate from Tau has been used. See Appendix A-2 for details.

*² SV3 – Sika ViscoCrete 3, SSP2 – Scancem SSP2000, S92 – Sikament 92

4.3.2.3 Field investigations

The field investigation is mainly carried out at Tukthus site where the test panel was installed as a part of the slipform. The concrete used at Tukthus site is listed in Table 4.5. The field investigation was also carried out at Sørkedals site where the concrete mixes are listed in Table 4.6. All these concretes have also been tested in the vertical slipform rig except for the concrete denoted C35 in Table 4.5.

Table 4.5: Concrete mixtures used on Tukthus site

[kg/m ³]	Tukthus site	
	C35	C45
Norcem Standard	365	456
Sand 0-7 mm	478	461
Sand 0-8 mm	463	465
Coarse aggregate 8-16mm	880	828
w/b-ratio	0.56	0.44
Admixture	Scancem SP-1	

Table 4.6: Concrete used on Sørkedalsv site

[kg/m ³]	Sørkedalsv site	
	mix 1	Mix 2
Norcem Standard FA	370	394
Silica fume	10	12
Sand 0-8 mm	910	895
Coarse aggregate 8-14 mm	910	562
Coarse aggr. 14-24 mm	0	298
w/b-ratio	0.48	0.48
Admixtures	Melstab 21	Sika ViskoCrete 3

The slump in the concrete to Tukthus site has not been measured, but the consistence has in general varied from stiff to more fluid like. The concrete delivered for Tukthus site was produced by A/S Lettbetong, Oslo. The concrete delivered for Sørkedalsv site was produced by Unicon AS.

4.3.3 Aggregate

The aggregate used in the concrete for the friction and vertical slipform rig is granite-gneiss from Årdal and has mostly a natural round grain form. All fractions are washed and most of the particles less than 30 µm are removed from the sand. Also concrete with Mylonitt from Tau is used in both rigs. This aggregate is called Durasplitt and is more crushed and sharp-edged than the Årdal-aggregates.

Data on the aggregate used in the lightweight concrete is listed in Table 4.7.

Table 4.7: The lightweight aggregate.

	Specific density, Kg/m ³	Bulk density, kg/m ³	1 hour absorption, * mass %	Saturated, ** mass %	Actual moisture content, *** mass %
Leca 1-4 mm	606	300	16	73	1.0
Liapor 7 4-10 mm	1206	700	8	27	6.4

* 1 hour absorption is the amount of water that the aggregate absorb during 1 hour in water.

** Saturated is the amount absorbed when complete filled with water.

*** Actual moisture content is the moisture in the aggregate before mixing.

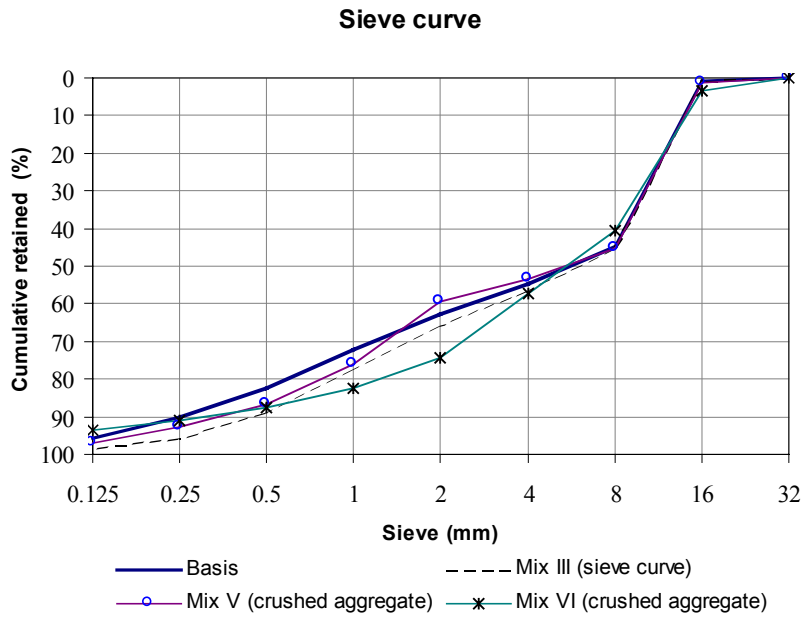


Figure 4.14: The cumulative sieve curve for the aggregates used in the slipform rigs.

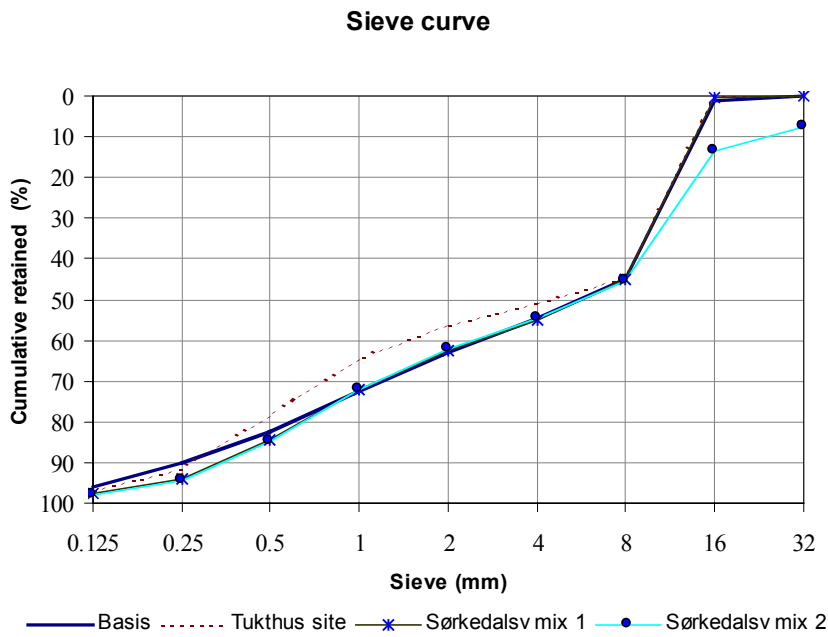


Figure 4.15: The cumulative sieve curve for the aggregates used in the field projects.

The four different fractions of aggregate used are delivered to the laboratory several times with slightly different sieve curves each time. However, even when the single curve has slightly varied between each delivery, it is tried to maintain the cumulative sieve curve by adjusting the amount of aggregate from the different fractions. The total cumulative sieve curve for each concrete composition is shown in Figure 4.14.

Brødremoen Sand AS and Fossens eift AS have delivered the aggregate used in the concrete for the Tukthus site and Svelvik aggregate is used in the concrete for Sørkedalsv site. The total cumulative sieve curve for the aggregates used in these field projects are shown in Figure 4.15.

4.3.4 Cement

It is primarily Norcem Anlegg that is used during the tests carried out at the slipform rigs. But also Norcem Standard and Norcem Standard FA have been used. The standard production values are listed in Table 4.8. All cements are supplied by Norcem AS in Brevik, Norway.

Table 4.8: Standard production values for the cement

	Norcem Anlegg	Norcem Standard	Norcem Standard FA
Type	CEM I 52,5 LA	CEM I 42,5R	CEM II A/V 42,5R
Typical mineral content:			
C ₃ S [%]	60	60	60
C ₂ S [%]	19	15	15
C ₃ A [%]	6	7.5	7.4
C ₄ AF [%]	10	10	10
Na ₂ O equivalent (alkalis) [%]	0.55	0.95	0.85
Physical properties:			
Fineness [m ² /kg]	360	350	400
Specific weight [kg/m ³]	3.12	3.12	2.95
Initial set [min]	120	130	130

4.3.5 Admixtures

Different types of admixtures have been used in the concrete during the tests. The admixtures are listed in Table 4.9 with a short description of the main components according the manufacturers data sheet.

Table 4.9: Admixtures used in the concrete

Admixtures	Type	The main component(s) according to the manufactures data sheet
Glenium 51	Superplasticizer	modified polycarboxyleter without formaldehyde
Sikament 92	Superplasticizer	modified polycarboxyleter
Sika ViscoCrete 3	Superplasticizer/stabilizer	modified polycarboxyleter with stabilizer
Scancem SSP2000	Superplasticizer	polymers from metacryl acid
Scancem SP1	Superplasticizer	sulfonated naphthalene-formaldehyde and melamine condensate
Melstab 21	Superplasticizer/stabilizer	melamine condensate with stabilizer
Scancem L(M) Micro air	Air entraining admixtures	
Rescon R	Retardation admixtures	sodium gluconate
Sika R	Retardation admixtures	modified phosphate basis

4.4 Test program

4.4.1 Friction rig

4.4.1.1 Program

The test program for the friction rig has focused on the effect of the variables in the concrete and the slipform technical variables have on the friction between the slipform panel and the concrete.

The variables in the concrete will affect the particle concentration, particle size distribution and the air content, see Table 4.10. Tests will be carried out in order to verify the effect of these parameters on the pore water pressure, see the hypotheses in Chapter 3. The concrete mixes used in this part of the program are listed in Table 4.2.

Table 4.10: The concrete variables

	Pore water pressure	
	Particle concentration and size distribution	Air content
Silica fume	x	
W/b-ratio	x	
Binder content	x	
Coarse sieve curve	x	
Air content		x

The effective pressure, which is the difference between the normal pressure (force) and the pore water pressure, is assumed to affect the sliding friction as indicated in Table 4.11. Also crushed aggregate and a rougher slipform surface will be tested in order to verify the effect on the sliding friction. The effect of different sliding length and frequency will also be tested in order to verify the impact on the static friction, see the hypotheses in Chapter 3.

Table 4.11: The parameters assumed to affect the friction

	Sliding friction	Static friction
Pore water pressure	x	x
Normal force	x	x
Movement height and frequency		x
Crushed aggregate	x	
Rough slipform panel	x	

The normal force has varied from 600 N to 2500 N, as shown in Table 4.12. The weight of the 14 cm concrete layer in the friction rig is approximately 600 N and the weight of 60 cm concrete is approximately 2500 N. The normal force of 2500 N is used as standard setting during the concrete parameter tests.

The slipform technical parameters (frequency and sliding length) have varied from 10 mm sliding each 8 minutes to 35 mm sliding each 30 minutes, see Table 4.12. The standard setting used when the concrete parameters are tested, has been 10 mm sliding each 8 minutes.

A detailed overview of the tests is shown in Appendix A-1.

Table 4.12: Slipform technical test program

Setting*	Basis concrete
Frequency: 8 min between the movements and 10 mm sliding length	x
Frequency: 30 min between the movements and 35 mm sliding length	x
Normal force 600 N	x
Normal force 1600 N	x
Normal force 2500 N	x
Normal force 600 N – 2500N – 600 N	x
Smooth panel	x
Rough panel	x

* *Standard settings are marked bold.*

The following parameters are measured during each test:

- The friction force
- Additional pressure applied on top of the concrete

- Displacement of the concrete in the cover zone
- The concrete temperature
- The pore water pressure in the concrete (only the last part of the program)

4.4.1.2 Execution method of the tests

For mixing the concrete, a 50 litre laboratory mixer (Eirich) is used. Each batch consists of 30 to 40 litres of concrete. The used mixing sequence is:

- 1 min dry mixing,
- 1 min mixing after water and admixture are added,
- 2 min complete stop
- 1 min mixing.

The workability of the concrete is kept in the range of 15-25 cm slump. The concrete is placed in one layer of approximately 13-14 cm thickness and than carefully vibrated.

The test is started approximately 1 hour after mixing. Each panel movement ends with 1 second backward movement of the panel. The testing is terminated after the concrete has passed initial set. The total duration time for a test is approximately 7 - 8 hours.

The normal force on top of the concrete has normally been applied 1.5 hours after concrete mixing. All tests are carried out in the laboratory with ambient temperature of 19 – 23 °C.

4.4.2 Vertical slipform rig

4.4.2.1 Program

The program for the vertical slipform rig has been based on the results from the tests carried out on the friction rig. The program has focused on the effect of the slipform technical variables and the concrete properties on the friction force.

Tests will be carried out in order to verify the effect of the particle concentration, particle size distribution and the air content on the pore water pressure, see the hypotheses in Chapter 3. The concrete variables tested are listed in Table 4.13. The concrete mixes used in this part of the program are listed in Table 4.4.

Table 4.13: The concrete variables

	Pore water pressure	
	Particle concentration and size distribution	Air content
Silica fume	x	
Binder content	x	
Coarse sieve curve	x	
Lightweight aggregate		x

The effective pressure, which is the difference between the normal pressure and the pore water pressure, is assumed to affect the sliding friction as indicated in Table 4.14. Also crushed aggregate and a rougher slipform surface will be tested in order to verify the effect on the sliding friction. Lifting height and frequency will also be tested in order to verify the effect on the static friction, see hypotheses in Chapter 3.

Table 4.14: The parameters assumed to affect the friction

	Sliding friction	Static friction
Pore water pressure	x	x
Normal pressure	x	x
Lifting height and frequency		x
Crushed aggregate	x	
Rough slipform panel	x	

The slipform technical parameters have been varied as listed in Table 4.15. The standard settings marked bold are used during the concrete parameter tests. The basis concrete (Table 4.3) and also partly the lightweight concrete (Table 4.4) are used when testing the effect of the slipform technical parameters in Table 4.15. A detailed overview of the tests is shown in Appendix A-2.

Table 4.15: Slipform technical test program

Setting *	Basis concrete	Lightweight concrete
Frequency 5 min and 10 mm sliding	x	
Frequency 8 min and 10 mm sliding	x	
Frequency 15 min and 10 mm sliding	x	x
Frequency 20 min and 10 mm sliding	x	x
Frequency 30 min and 10 mm sliding	x	x
Stiffness 11588 N/mm in each spring steel	x	
Stiffness 1568 N/mm in each spring steel	x	
Stiffness 405 N/mm in each spring steel	x	x
Stiffness 253 N/mm in each spring	x	
Stiffness 145 N/mm in each spring	x	
Panel inclination -1.5 mm/m	x	x
Panel inclination 0 mm/m	x	
Panel inclination 1.9 mm/m	x	
Panel inclination 5.6 mm/m	x	
Smooth panel	x	x
Rough panel	x	
Self compacting concrete	x	
Vibration 2 x 15 sec	x	
Vibration 2 x 30 sec	x	x
Vibration 2 x 60 sec	x	
3-layers concrete tests	x	

* Standard settings are marked bold.

The concrete for this rig has normally been self-compacting concrete in order to obtain the same degree of consolidation each time, but also the effect of the vibration is tested as shown in Table 4.15.

The following parameter are measured during each test:

- The lifting force
- The concrete pressure on the slipform panel
- The concrete and ambient temperature
- Displacement of the concrete in the cover zone
- The load on top of the concrete from the pressure lid
- The pore water pressure

4.4.2.2 Execution method of the single layer tests

A 250-litre laboratory mixer (Eirich) mixes the concrete. Each batch consists of approximately 120 litres of concrete, which give a concrete layer of ~60 cm. The mixing sequence used is the same as for the smaller laboratory mixer referred to in Section 4.4.1.2.

The workability of the concrete is kept approximately equal to 25 – 27 cm slump for self-compacting concrete and approximately 10 – 15 cm slump for vibrated concrete.

Before the concrete is placed into the concrete box, the reinforcement mesh is installed with a concrete cover of 40 mm. The concrete is placed in one layer when self-compacting concrete is used. When concrete that needs vibration is used, the concrete is placed and vibrated in two layers of approximately 30 cm height. After the concrete is placed, the top of the concrete is covered by plastic in order to prevent any water evaporation.

The test is started just after the concrete is placed and the measuring equipment installed. The test is terminated when the concrete has passed initial set, approximately after 8-9 hours. All tests are carried out in the laboratory with ambient temperature of 19 – 23 °C.

4.4.2.3 3-layers concrete tests

A 50-litre laboratory mixer (Eirich) mixes the concrete. The first batch is 50 litres, which will give a layer thickness of 25 cm. The next two batches are 40 litres, which will give a layer thickness of 20 cm. The mixing sequence used is the same as described in Section 4.4.1.2.

The concrete is placed with 2 hours between the layers. The concrete is vibrated after each layer when concrete with lower slump is used. Self-compacting concrete is normally not vibrated. After the last layer is placed, the top of the concrete is covered by plastic in order to prevent any water evaporation.

The test is started just after the concrete in the first layer is placed and the measuring equipment installed. The test is terminated when the concrete has passed initial set for the last layer placed, approximately after 11-12 hours. All tests are carried out in the laboratory with ambient temperature of 19 – 23 °C.

4.4.3 Field investigations

The test program for the field investigations are focused on the friction and the normal forces the concrete is exposed for during slipforming. Also identification of any connection between measured friction and surface damages are a part of the test program. The result from the field investigation will be compared with the result from the rig testing in the laboratory.

The test panel is installed in two slipform operations at Tukthus site in order to measure the friction force and the concrete pressure against the panel. During the slipform operation, the finished concrete surface below the slipform is visually inspected for any surface defects. The freeboard and curing front are also measured on regular basis throughout the slipform operations.

A field investigation is also carried out at Sørkedalsv site. The field investigation consists mainly of surface inspection of the slipformed concrete structure.

The concrete used at Sørkedalsv site and Tukthus site is also tested in the vertical slipform rig in order to compare the different concrete types used (Table 4.5 and Table 4.6). This result will also be connected to any observation of surface damages during slipforming on site.

4.4.4 Testing on hardened concrete

4.4.4.1 Capillary water absorption tests

The capillary suction test is a non-stationary test method, described by Sintef internal procedure KS 70 110. Concrete discs of 20 mm thickness are dried at 105 °C during 4 days before the absorption testing start. The concrete discs are exposed to one-dimensional water absorption and the weight increase of the discs are measured regular during 4 days. The water front will reach the top of the discs during the measurement period. After absorption, the discs are immersed in water, and then pressure saturated at 50 MPa water pressure. A typical absorption curve is shown in Figure 4.16.

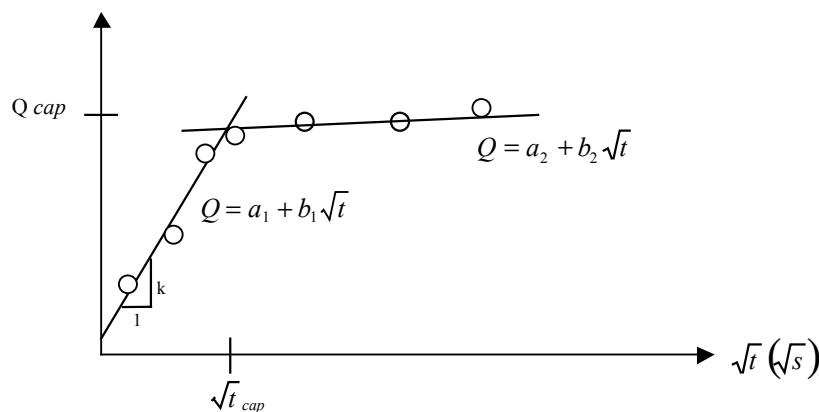


Figure 4.16: Absorption curve (Smeplass, 1988)

The relation between the absorbed amount of water (Q_{cap}) and the square root of the time (t_{cap}) may be calculated by linear regression. The slope of the first part of the graph, which expresses the water absorption before the water front reaches the top, gives the capillary number k (Eq. 4.1). The capillary number is an expression of the rate of water absorption.

$$\text{Eq. 4.1} \quad k = \frac{Q_{cap}}{\sqrt{t_{cap}}}$$

$$\text{Eq. 4.2} \quad m = \frac{t_{cap}}{h^2}$$

Equation 4.2 gives the resistance number. The resistance number expresses the time (related to the thickness of the specimens) the water front uses to reach a height h . The resistance number reflects the fineness of the pore system and is therefore correlated to the w/b-ratio. From the recorded weights, the following may be calculated: bulk dry density, solid density, air/macro-porosity, suction porosity, capillary number (Eq. 4.1) and resistance number (Eq. 4.2).

The resistance number and capillary number are directly related. In contrast to the resistance number, the capillary number depends on the pore volume in the concrete, and also the volume ratio of aggregate/binder. The resistance number is more suitable to characterize the concrete quality than the capillary number, since it is not necessary to know the binder volume.

It is necessary to pre-dry the discs in order to carry out the capillary water absorption test. In these tests the drying of the discs is carried out at 105 °C.

5 CALIBRATION AND VERIFICATION

5.1 General

The scope of the calibration program is to ensure that the slipform rigs and the test panel are able to measure correctly the forces that occur during the tests. This is especially important here in this program where the slipform rigs are new and have no experience record.

The first part of the calibration program deals with calibration of the measuring units. All measuring units are standard products that are frequently used for similar measurements in all kind of rigs.

The second part of the calibration program deals with calibration of the equipment made for these rigs. This includes in particular verification and control of the slipform panel.

The third part comprises the reproducibility testing of the rigs. This is carried out in order to verify that the rigs are able to reproduce the results when all parameters are the same.

5.2 Friction rig

5.2.1 Calibration of the measuring units

Each measuring unit used on the horizontal rig is calibrated and controlled. The operation range and calibration frequency for each unit is:

- Inductive displacement sensors for measurement of the concrete displacement in the cover zone. Operation range is 0 - 10 mm. The calibration was carried out before installation.
- Resistive displacement transducers for measurement of the panel movement. Operation range is 0 – 1000 mm. The calibration was carried out before installation. The transducers are controlled frequently during operation.
- Load cell on top lid. Operation range is 0 – 10 000 N. The calibration is carried out before installation and thereafter controlled frequently during operation.
- Load cell for measurement of the friction force. Operation range is 0 – 6 000 N. Calibration is carried out frequently during operation.
- Pore water pressure gauge. Operation range - 80 – 20 kPa. Calibration is carried out weekly during operation.
- Thermocouples for measuring the temperature. Operation range -100 – 300 °C. The thermocouples are frequently controlled.

5.2.2 The slipform rig rate during movement

The movement of the slipform panel is deformation controlled, which means that the slipform rate during the movements is independent of the load. On a full-scale slipform with a hydraulic system,

the lifting of the panel is pressure controlled, which means that the rate depends on the hydraulic pressure and the total lifting weight.

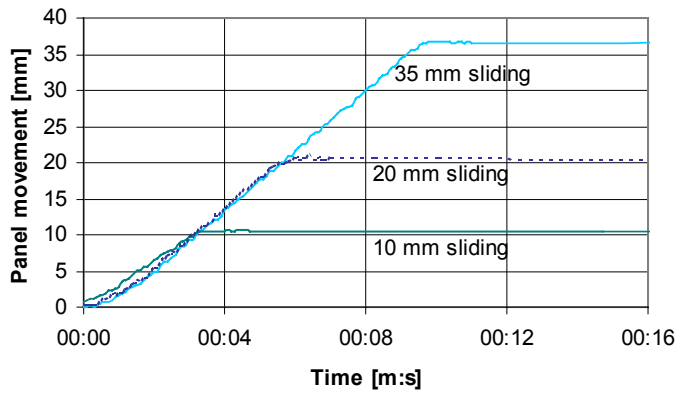


Figure 5.1: Rate of the slipform panel

The results in Figure 5.1 shows that the slipform rate during the movements is almost constant and independent of the movement length. The slipform rate during a lift is 3.75 mm/second for this rig, which is within the range for a full-scale slipform (2-5 second for 10 mm lifts). At the end of each movement, the motor is reversed for 1 second. This backwards movement can not be seen in Figure 5.1, which means that the stress between the panel and motor is relieved without any further movement of the panel.

5.2.3 Control of the surface roughness

The surface roughness of the panel is measured when it is new and after it has been used during approximately 35 tests. The surface profile for a new panel is presented in Figure 5.2 and for used panel in Figures 5.3 – 5.5. The R_a -factor is calculated for each profile during a measurement length of approximately 5mm. The R_a -factor is the arithmetic mean of the distance from the centre line to the top of each peak, see Eq. 5.1.

Eq. 5.1:
$$R_a = \frac{1}{n} \sum_{i=1}^n |z_i|$$

where z = height from the centre line. The centre line is the average of all measuring points.
 n = number of measurements



Figure 5.2: Surface profile for a new panel. The distance between the horizontal grid lines is $1\mu\text{m}$ and it is $250\mu\text{m}$ between the vertical grid lines. $R_a = 0.9\mu\text{m}$.

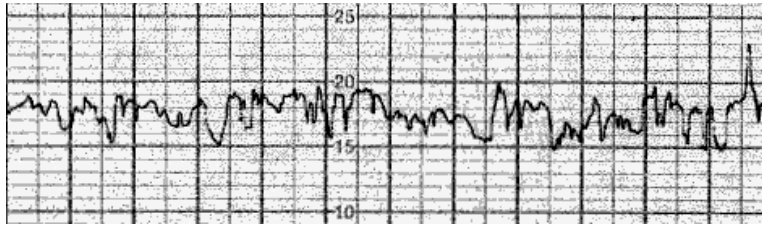


Figure 5.3: Surface profile for a used panel – longitudinal measurement. The distance between the horizontal grid lines is $1\mu\text{m}$ and it is $250\mu\text{m}$ between the vertical grid lines. $R_a = 0.9\mu\text{m}$.

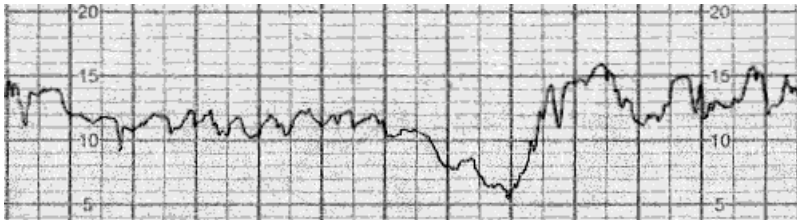


Figure 5.4: Surface profile for a used panel – across measurement at the start* point on the slipform panel for slipform tests. The distance between the horizontal grid lines is $1\mu\text{m}$ and it is $250\mu\text{m}$ between the vertical grid lines. $R_a = 1,05\mu\text{m}$.

* The start point represents an area on the panel where the concrete at the start of the test is in contact with the panel.

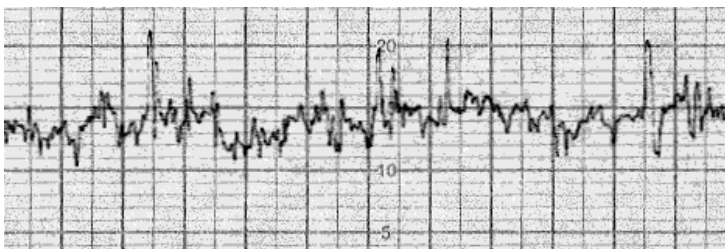


Figure 5.5: Surface profile for a used panel – across measurement at the termination* point on the slipform panel for the slipform tests. The distance between the horizontal grid lines is $1\mu\text{m}$ and it is $250\mu\text{m}$ between the vertical grid lines. $R_a = 0,95\mu\text{m}$.

* The termination point represents an area on the panel where the concrete at the end of the test is in contact with the panel.

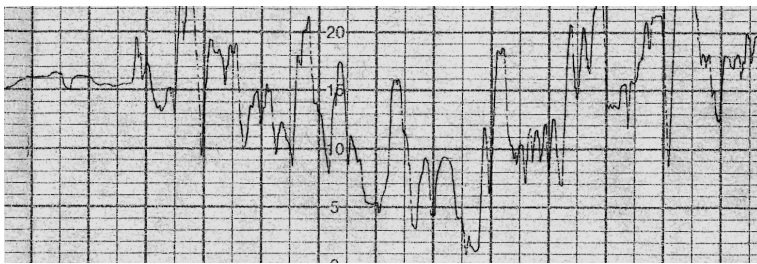


Figure 5.6: Surface profile for a non-used rough panel – longitudinal measurements. The distance between the horizontal grid lines is $4\mu\text{m}$ and it is $250\mu\text{m}$ between the vertical grid lines. $R_a \sim 10\mu\text{m}$.

The result shows that R_a is $0.9\mu\text{m}$ when the panel is new. For panels that has been used for a period of time, the R_a -factor is still $0.9\mu\text{m}$ in the longitudinal direction and between $0.95\mu\text{m}$ and $1.05\mu\text{m}$ in the across direction. Based on the result, it can be concluded that the panel roughness remains almost the same during the tests. The panel surface has a more smooth profile at the start point of the panel (Figure 5.4) compared to the termination point where the panel is sharper toothed (Figure 5.5). The start point represents an area on the panel in contact with fresh concrete and the termination point represents an area on the panel in contact with concrete that is normally hardened or soon hardened.

A slipform panel with rough surface is also used in one test. The panel surface was sand blasted in order to obtain a rough surface profile. The surface profile is shown in figure 5.6. The R_a -factor is calculated to approximately $10\mu\text{m}$.

5.2.4 Sliding friction in the friction rig

Measurement of the sliding friction created by the slipform rig itself (resistance in roller, along the edge of the slipform panel etc.) is carried out. The measurements were carried out three times with different test set-up. Teflon plates were used between the sliding faces in the first two tests. The friction force was measured at different normal forces, made by the top lid that pressurised the panel with Teflon plates. The result is presented in Figure 5.7 with no lubricants and applied lubricants between the Teflon plates. The result show that the sliding friction force in both instances are increasing almost linear with increasing normal force, but the friction is considerable lower when dry Teflon plates are used.

A third test was also carried out with “not fasten” weights. The weights were placed on top of the slipform panel and followed the panel during the movements. The measured friction was in this instance considerable lower compared to the previous tests. This means that most of the friction that was measured was actually caused by friction between the Teflon plates, which was not expected.

It was concluded that the friction created by the rollers and the edge effect is probably more like what measured in the third tests, approximately 100 N at the different normal forces. Based on these

results, 100 N is subtracted from the measured results when calculating the friction force between the slipform panel and the concrete.

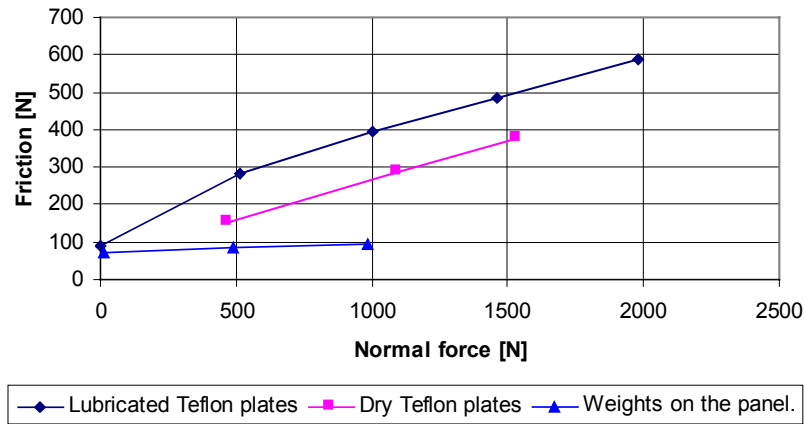


Figure 5.7: Calibration of the friction rig.

5.2.5 Reproducibility test

A reproducibility test is carried out on the friction rig in order to ensure that the rig is able to reproduce the results. The same basis concrete mix (Table 4.1) and slipform set-up was used in all tests. The panel was moving 10 mm each 8 minutes during the tests. The result is presented in Figures 5.8 to 5.11 and shows the measured friction, normal force and temperature versus the elapsed time since concrete mixing.

The presented friction force represents the measured raw data, and is not compensated for the rig friction measured in Section 5.2.4. The concrete force against the slipform panel was increased to 2500 N after approximately 1-2 hours in all tests.

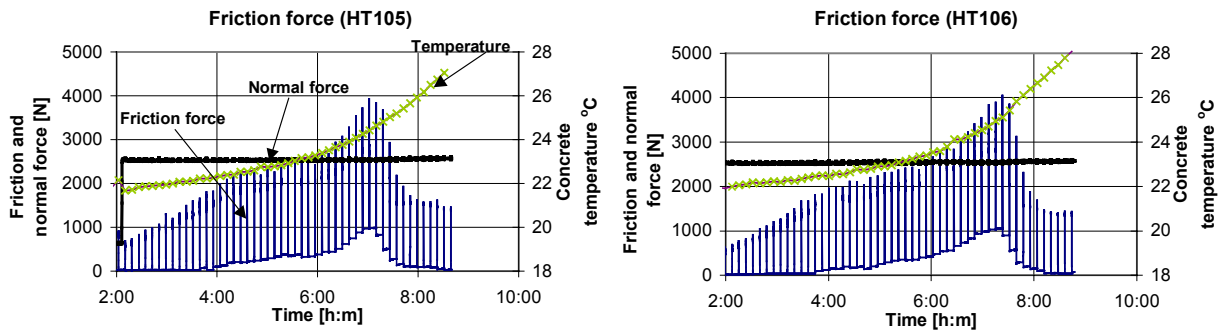


Figure 5.8 and 5.9: Reproducibility test of the friction rig (HT105 and HT106)

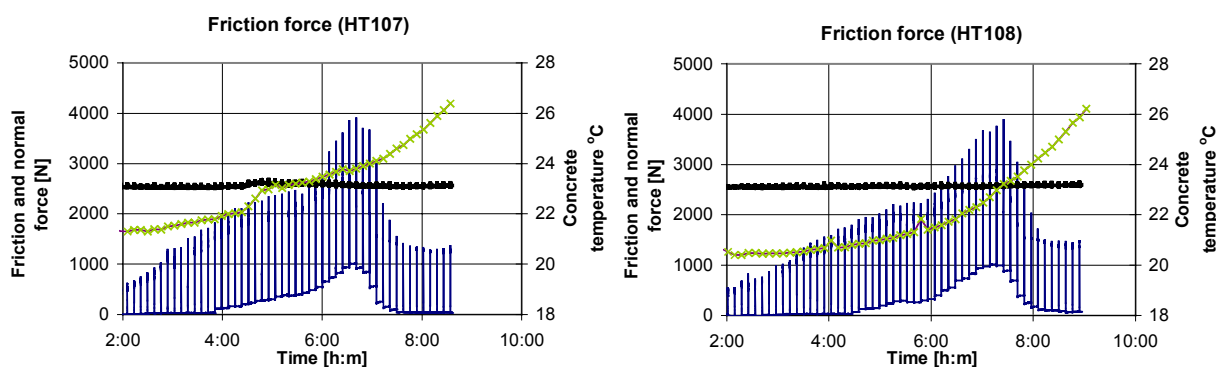


Figure 5.10 and 5.11: Reproducibility test of the friction rig (HT107 and HT108)

The measured friction curve consists of vertically lines that represents start and stop of the slipform panel. At 2 hours, the measured peak friction is approximately 600 – 700 N for all 4 tests. After 2 hours, the peak friction is increasing evenly up to approximately 2400 N at 5 hours. After ~ 6 hours, the friction is increasing up to a maximum with a range of 3886 – 4050 N for all tests. This gives an average of 3942 N and a standard deviation of 75 N ($\approx 1.9\%$). It can be seen that the maximum friction occurs slightly at different times for the tests, from 6 hours and 35 min after mixing for HT107 (Figure 5.10) to 7 hours and 15 min for HT108 (Figure 5.11). However, the difference in the friction level is so insignificant that it can be concluded that the friction rig is able to reproduce the results within acceptable limits.

5.3 Vertical slipform rig

5.3.1 Calibration of the measuring units

Each measuring unit used on the vertical rig is calibrated and controlled. The operation range and calibration frequency for each unit is:

- Inductive displacement sensors for measurement of the concrete displacement in the cover zone. Operation range is 0 - 10 mm. The calibration was carried out before installation.
- Resistive displacement transducers for measurement of the panel movement. Operation range is 0 – 1000 mm. The calibration was carried out before installation. The transducers are controlled frequently during operation.
- Load cells for measurement of the normal force. Operation range is 0 – 5 000 N. The calibration is carried out before installation and thereafter controlled frequently.
- Load cell on top lid. Operation range is 0 – 10 000 N. The calibration is carried out before installation and thereafter controlled frequently during operation.
- Load cell for measurement of the friction force. Operation range is 0 – 12 000 N. Calibration is carried out frequently during operation.

- Pore water pressure gauge. Operation range - 80 – 20 kPa. Calibration is carried out weekly during operation.
- Thermocouples for measuring the temperature. Operation range -100 – 300 °C. The thermocouples are frequently controlled.

5.3.2 Control of the spring steel

The stiffness of the slipform panel is adjusted by the 4 spring steels connected to the load cells on the rear side of the panel. The spring steel was tested with cantilever arms. The deformation in the spring steel was measured by inductive displacement sensors installed on the brackets. The result from the stiffness measurements is shown in Table 5.1 with different cantilever arms.

Table 5.1: Measured stiffness in the spring steel.

Cantilever arm [mm]	Measured Stiffness [N/mm]	Theoretical Stiffness [N/mm]
38	11588	18900
80	1568	2026
130	405	472
180	253	277
215	145	162

The measured stiffness in Table 5.1 represents the load necessary to obtain a deformation of 1 mm. The result shows as expected that a shorter cantilever arm will give a higher stiffness and a less deformation compared to longer cantilever arm. The stiffness is also calculated theoretically in Table 5.1. A comparison between the calculated and measured stiffness shows that the calculated stiffness is higher. This is probably because the bracket that keeps the spring steel in place is not fully clamped.

5.3.3 The rate of the slipform panel during lifting

The slipform rate during a lift is 3.4 mm/second. This will give approximately a duration time of 4 and 7 second for respectively 10 and 20 mm lifting height. At the end of each lift, the jack has a 2 mm downward movement, which is similar to the downward movement when the break is activated on a full-scale slipform. Also in this rig, the lifts are deformation controlled, which means that the lifting rate is constant and independent of the load.

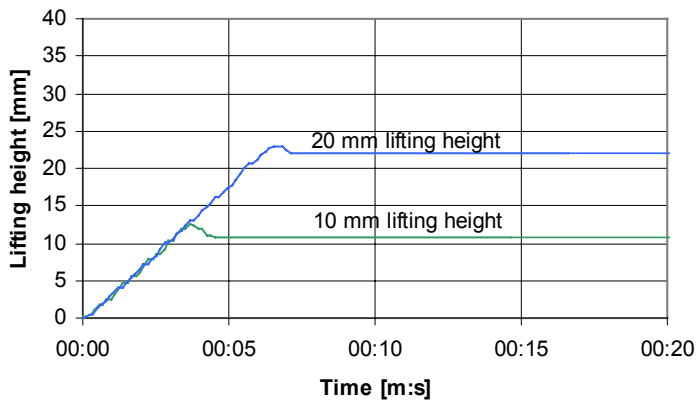


Figure 5.11: Lifting height and rate in the vertical slipform rig.

5.3.4 Control of the surface roughness

Since it is the same kind of steel panel used in the vertical rig as for the friction rig, it can be concluded that the surface roughness will be approximately the same during the period of use. The normal pressure for the vertical rig is also normally lower compared to the pressure used in the friction rig.

5.3.5 Sliding friction in the vertical rig

Friction will occur along the edges of the slipform panel and at the rollers on the rear side during lifting. In order to identify this friction force, a lid with a pneumatic actuator was installed horizontally to press the slipform panel during lifting. Between the lid and the panel, two layers of dry Teflon plates were installed to minimize any additional friction.

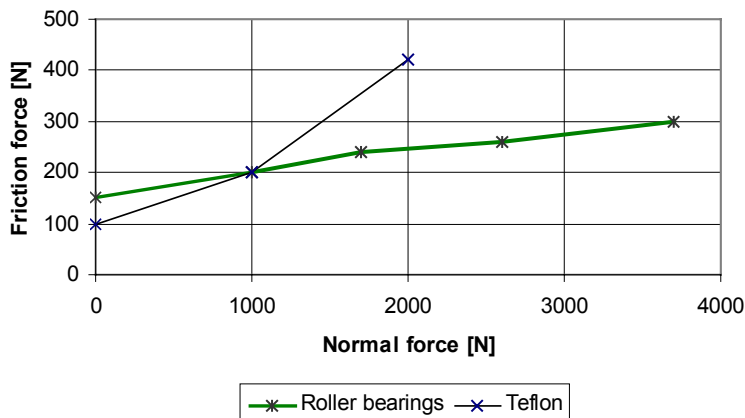


Figure 5.12: Sliding friction in the vertical rig.

The result in Figure 5.12 presents the applied normal force and the measured friction force. The weight of the slipform panel is subtracted from the measured friction (lifting) force. The result shows that the friction force is increasing considerable when the normal force is doubled from 1000 N to 2000 N when using Teflon as sliding faces. Based on previous experience from the friction rig, it was decided to carry out another test where the Teflon plates were replaced with roller bearings. The roller bearings consisted of five rollers with diameter of 20 mm and were installed between the pressure lid and the slipform panel. In this instance, the measured friction force were considerable lower compared to the previous results at normal force of 2000 N.

Based on the results it was concluded that 250 N should be subtracted from the measured lifting force in order to calculate the net lifting force, which is the same as the friction between the concrete and the slipform panel. Since the zero reading represents an unloaded load cell, also the weight of the slipform panel (750 N) must be subtracted from the measured lifting force.

5.3.6 Reproducibility test

A reproducibility test is carried out on the vertical slipform rig in order to ensure that the rig is able to reproduce the results. The same basic concrete mix (Table 4.3) and slipform set-up was used in all tests. The panel was lifted 10 mm each 8 minutes during the test. The result is presented in Figures 5.13 to 5.16 and shows the measured friction and normal force versus the elapsed time since concrete mixing.

The presented friction force represents the measured raw data, and is not compensated for the rig friction measured in Section 5.3.5.

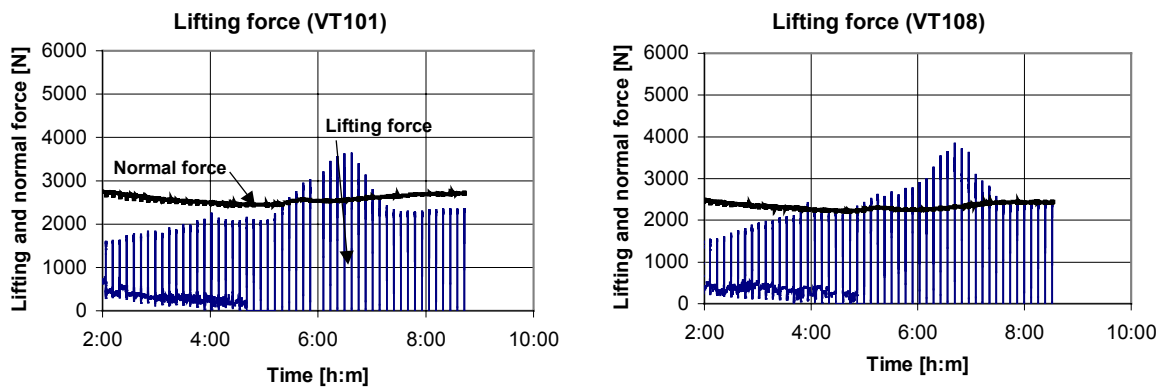


Figure 5.13 and 5.14: reproducibility test of the vertical slipform rig (VT101 and VT108)

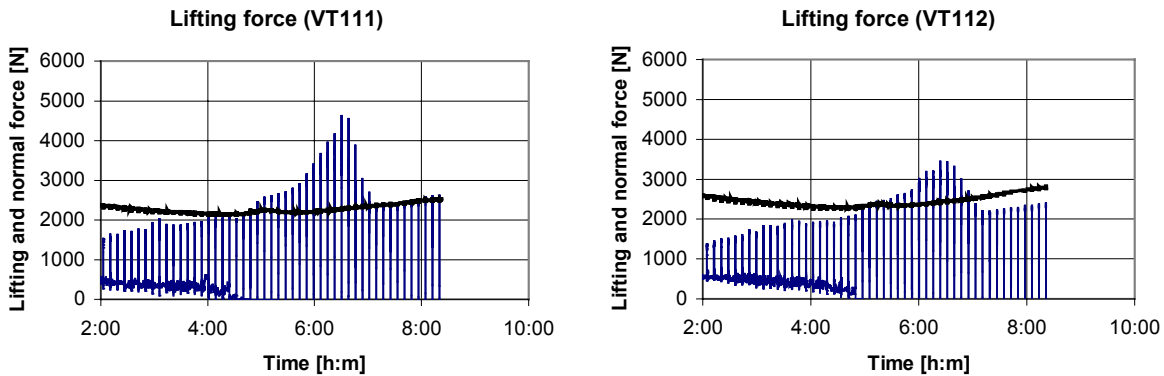


Figure 5.15 and 5.16: Reproducibility test of the vertical slipform rig (VT111 and VT112)

The curve for the lifting force (Figures 5.13 – 5.16) consists of vertically lines that represents start and stop of the slipform panel. At 2 hours, the peak value of the lifting force is approximately 1500 N for the different tests. From 2 hours to 4 hours, the peak value is evenly increased before it is levelled at 2000-2200 N. After 5 hours, the peak value continue to increase up to a maximum value, which vary from 3467 – 4610 N. The time when this maximum value occur vary from 6 hour and 25 minutes to 6 hour and 40 minutes. However, the variations in the maximum values give an average of 3884 N and a standard deviation of 506 N ($\approx 13\%$), which is too large for a reproducibility test.

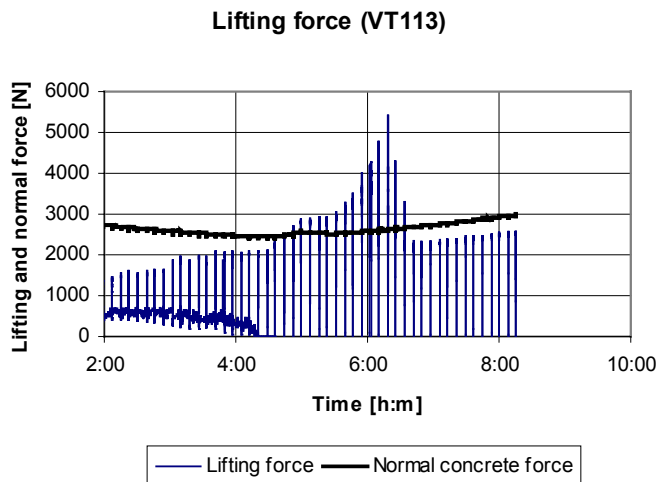


Figure 5.17: Test with heavy vibrated concrete.

Observations during the testing have indicated that the compaction of the concrete might have an impact on the measured lifting force. This means that parameters such as slump value, fresh concrete stability properties and vibration might affect the lifting force. In order to verify this, a new test was carried out where the concrete after placing was heavy vibrated (Figure 5.17).

The result in Figure 5.17 shows that more vibration of the concrete seems to have an impact on the maximum lifting force. The maximum lifting force is increasing in this instance to approximately 5400 N, which is considerable higher than the previous 4 tests. However, it seems that the normal force and the peak value of the lifting force the first five hours is not affected of the heavy vibrated concrete.

Based on the results, it was concluded that the reproducibility tests need to be carried out with concrete that give the same level of compaction each time. It was chosen to carry out a new reproducibility test with self-compacting concrete. Self-compacting concrete will not need any additional consolidation because the fluid consistence of the concrete will ensure proper and hopefully equal consolidation.

A new test series with self-compacting concrete were used during the reproducibility test. The same basis concrete (Table 4.3) was used, but now with another superplasticizer, which resulted in a slump value of approximately 25 – 27 cm. The panel was lifted in these tests 10 mm each 15 minutes. The results are presented in Figure 5.18 to Figure 5.21.

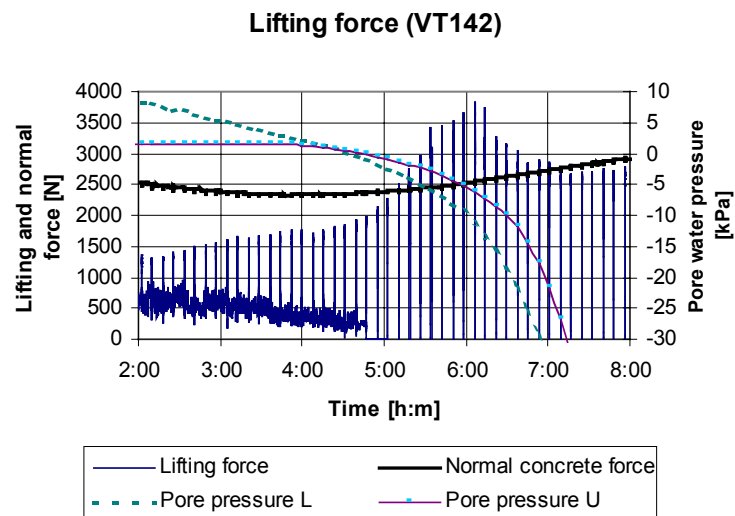


Figure 5.18: The reproducibility test with self-compacting concrete (VT142).

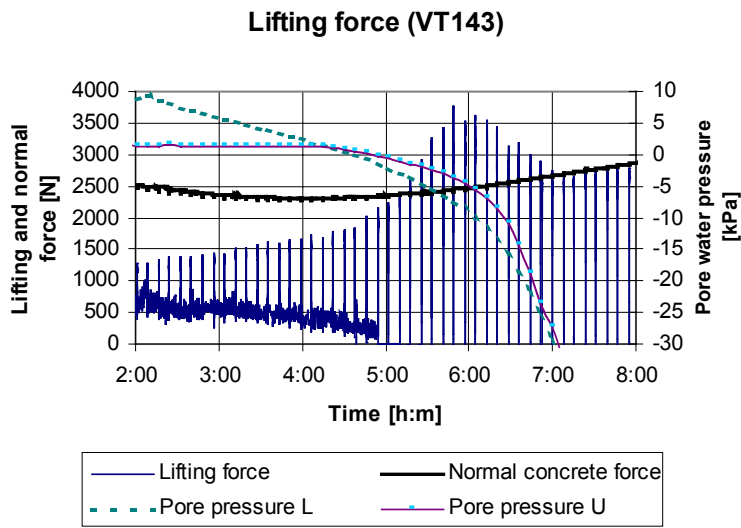


Figure 5.19: The reproducibility test with self-compacting concrete (VT143).

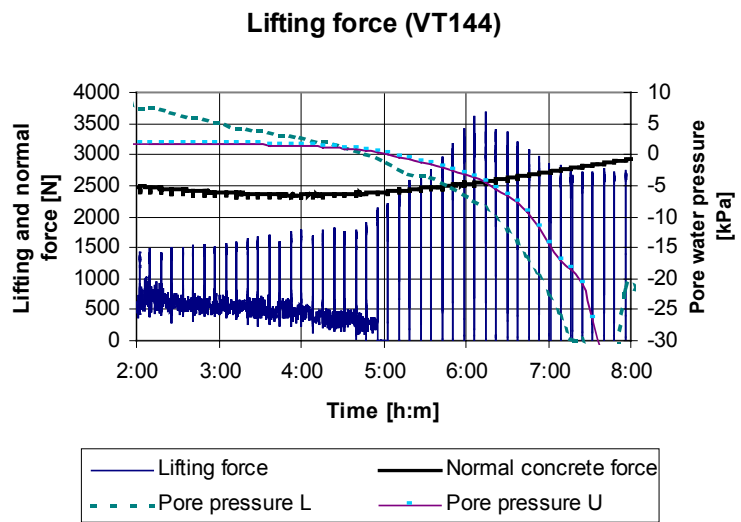


Figure 5.20: The reproducibility test with self-compacting concrete (VT144).

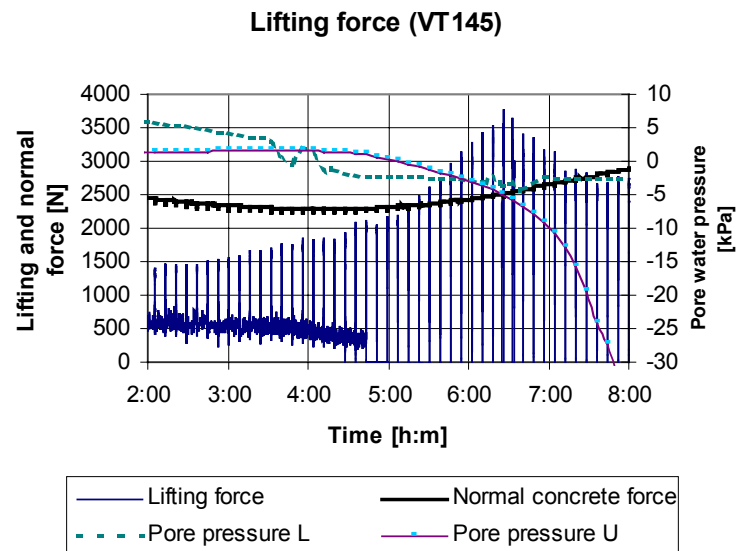


Figure 5.21: The reproducibility test with self-compacting concrete (VT145).

At 2 hours, the peak values of the lifting force vary from 1300 to 1500 N in the tests. The peak value of friction is evenly increasing from 2 hours until 5 hours where it is increasing faster up to the maximum. The maximum lifting force varies from 3680 to 3830 N between the tests. This gives an average of 3769 N and a standard deviation of 64 N ($\approx 1.7\%$), which is a considerable improvement compared to the previous reproducibility test. The maximum lifting forces occur in the tests from 5 hours and 30 minutes to 6 hours and 50 minutes. The maximum lifting force is assumed to be more related to stiffening and hardening process of the concrete than the elapsed time since mixing. The time between maximum lifting force and when the upper pore water pressure gauge is passing zero pressure varies from 1 to 1.5 hours, which is much less time range compared to the range in elapsed time. In total it can be concluded based on the results, that the reproducibility test is acceptable.

5.4 Test panel

The test panel for installation on a full-scale slipform is equipped with 6 load cells. Each load cell was calibrated before installation. The operation range for each load cell is 0 – 5 000 N.

After installation of the test panel in the slipform, the 4 load cells for measuring the concrete pressure were adjusted to zero before the slipform operation started and concrete filled into the form. The 2 load cells for measurements of the friction force were zero adjusted before installation.

After complete field investigation, the load cells were again controlled.

6 METHOD OF EVALUATION AND PRESENTATION OF THE MEASUREMENTS

6.1 Lifting force

The raw data from the tests carried out on the friction rig (HT-series) and the vertical slipform rig (VT-series) need to be further calculated before presentation and evaluation. An example of the measured lifting force (raw data) from a complete test is shown in Figure 6.1. The measurement period starts when the concrete is fresh and workable and ends after it has passed initial set and the concrete is hard. The lifting force will increase and decrease as the lifting of the slipform panel proceeds during the test. Each vertical line in this figure represents start and stop of the slipform panel. In this instance, the test is started 30 minutes after concrete mixing and thereafter the panel is lifted each 15 minutes. The correlation between the lifting height and the corresponding time after water addition is shown in Figure 6.1.

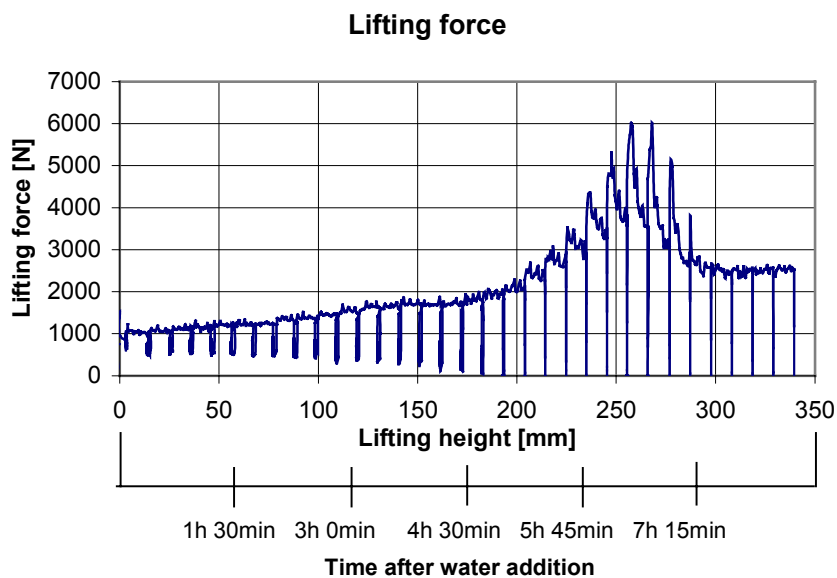


Figure 6.1: The variation in lifting force with time (VT151).

When studying a single lift, the lifting force must overcome the adhesion and the friction between the panel and the concrete before the sliding starts. In the same moment as the panel starts sliding, the lifting force is at maximum. This maximum lifting force is called static lifting force. During sliding, the lifting force will stay at the same level or decrease. The lowest level of the lifting force during lifting is called sliding lifting force. An example on identification of the static and sliding lifting force for a single lift is shown in Figure 6.2.

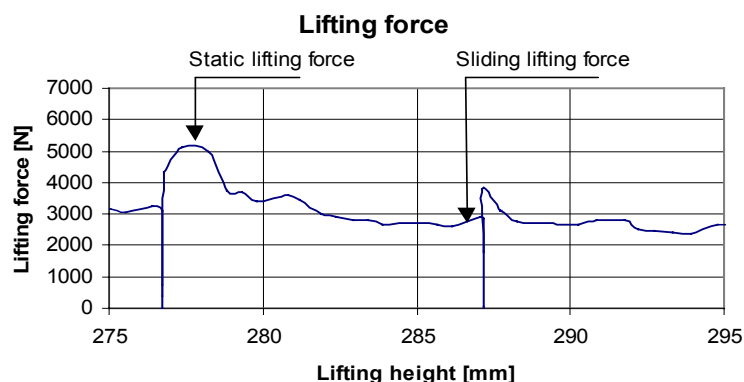


Figure 6.2: The static and sliding lifting force for a single lift (VT151)

Enveloped curves can be made based on the static and the sliding lifting force values from each lift, see Figure 6.3. The upper enveloped curve represents the static lifting force and the lower enveloped curve represents the sliding lifting force. In this instance, the results show that the sliding and static lifting force is almost identical the first 180 mm or approximately 5 hours. Thereafter the curves are separated for a period before they are again merged. This “separation” period is also the transition period from plastic to elastic/solid phase in the concrete.

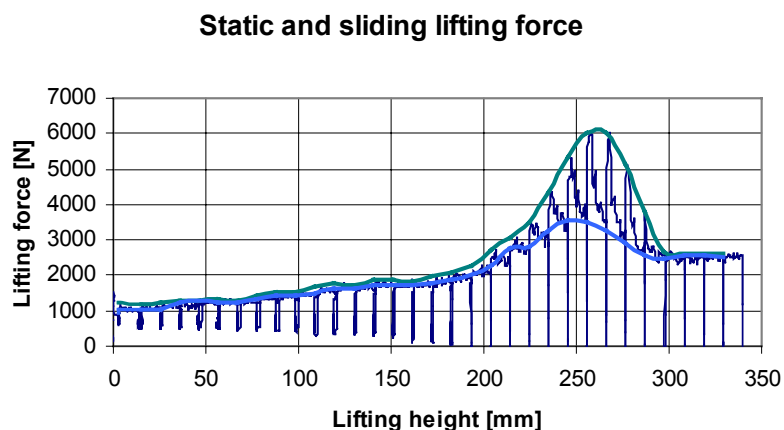


Figure 6.3: The enveloped curve for the static and sliding lifting force (VT151)

In order to calculate the friction between the panel and the concrete during sliding, the friction in the rig and the weight of the panel must be subtracted (only vertical slipform rig) from the measured lifting force.

Eq. 6.1 $F_H = F_{MH} - F_E$

Eq. 6.2 $F_G = F_{MG} - F_E$

where F_H = the net static lifting force or static friction [N]
 F_G = the net sliding lifting force or sliding friction [N]
 F_{MH} = measured static lifting force [N]
 F_{MG} = measured sliding lifting force [N]
 F_E = rig friction [N],
 F_E (horizontal slipform rig) = 100 N and
 F_E (vertical slipform rig) = 1000 N

The friction per square meter can be calculated by the following equations:

Eq. 6.3 $F_{AH} = F_H/A$

Eq. 6.4 $F_{AG} = F_G/A$

where F_{AH} = the net static lifting stress or static friction [Pa]
 F_{AG} = the net sliding lifting stress or sliding friction [Pa]
 A = the contact area between the concrete and the slipform panel.

6.2 Effective pressure in the concrete

The effective pressure represents the average pressure between the solid particles in the concrete. This pressure is calculated based on the following equation (from Section 2.2.3, Eq. 2.5):

Eq. 6.5 $\sigma' = \sigma - u$

where σ' = effective pressure [Pa]
 σ = normal pressure [Pa]
 u = pore water pressure [Pa]

and

Eq. 6.6 $\sigma = \frac{N}{A}$

where N = normal force [N]
 A = the contact area between the concrete and the panel

The normal force (N) is the concrete force against the slipform panel. For the friction rig where the panel is horizontally installed, the normal force is theoretically equal the weight of the concrete above, including additional force from the lid on top of the concrete. In the vertical slipform rig,

where the slipform panel is installed vertically, the normal force is the lateral concrete force against the panel. A typical example on the measured normal force is shown in Figure 6.4 (it is from the same test as used in Figures 6.1 – 6.3). This is measured in the vertical slipform rig with an initial panel inclination of -1.5 mm/m and a panel stiffness of $(4 \times 405) 1620 \text{ N/mm}$, see Table 5.1. The normal force is decreasing slightly during the first period until the concrete is rigid enough to resist any further deformation. The normal force will then increase because of the initial negative inclination.

The pore water pressure is measured in the fresh concrete and represents the pressure in the pore water. The pressure gauge is installed 30 mm from the slipform panel and a typical example of the measured pore water pressure can be seen in Figure 6.4. The pore water pressure measured at the bottom gauge (B) is decreasing evenly during the first period because of settlement of the solid particles. After a while, the pore water pressure in both gauges passes zero pressure and continues to decrease even faster. At the time of approximately zero pore water pressure (after 180 mm), the concrete is rigid enough to resist any further deformation/settlement. Further development of the chemical shrinkage in the concrete will instead affect the pore water pressure. The time of zero pore water pressure can also be defined as the time when the concrete transforms from plastic to elastic phase.

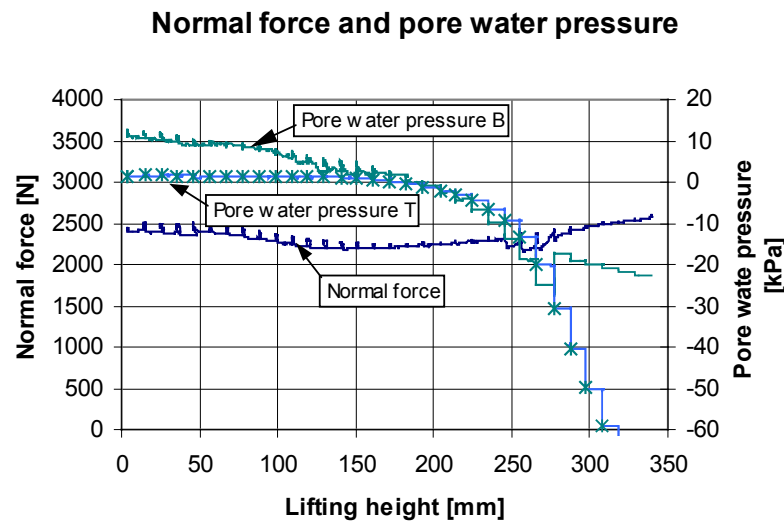


Figure 6.4: The measured normal force and the pore water pressure (VT151)

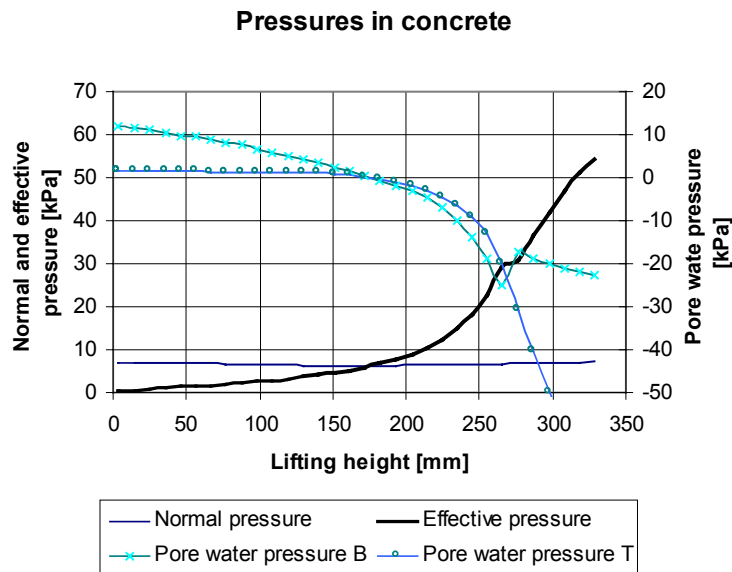


Figure 6.5: The effective, normal and pore water pressures in the concrete (VT151)

The calculated effective pressure is shown in Figure 6.5. Note that the scale is the same for the normal pressure and the pore water pressure. It can be seen that it is mainly the pore water pressure development that increases the effective pressure during the presented period, see Eq. 6.5.

6.3 The friction coefficient

The friction coefficient describes the relationship between the measured net lifting stress and the calculated effective pressure. The static and sliding friction coefficient are calculated based on the following equations:

$$\text{Eq. 6.7} \quad \mu_H = \frac{F_{AH}}{\sigma'}$$

$$\text{Eq. 6.8} \quad \mu_G = \frac{F_{AG}}{\sigma'}$$

where μ_H = static friction coefficient
 μ_G = sliding friction coefficient

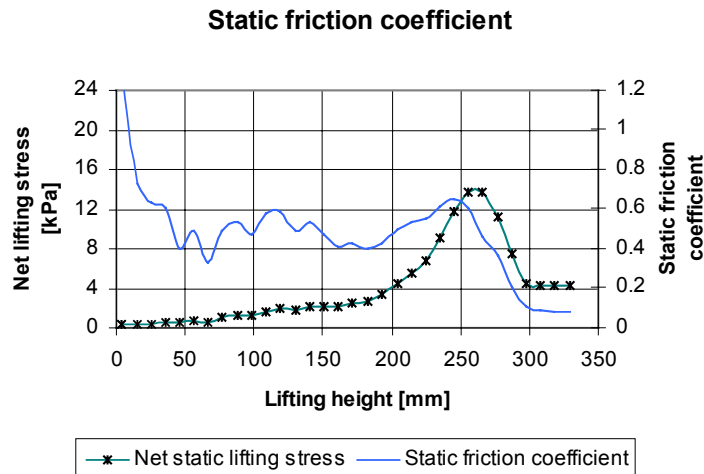


Figure 6.6: Static friction coefficient (VT151)

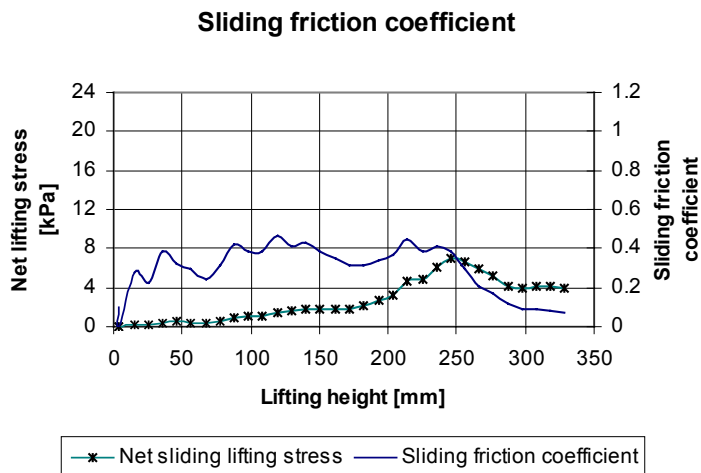


Figure 6.7: Sliding friction coefficient (VT151)

The calculated static and sliding friction coefficient is presented in Figures 6.6 and 6.7 respectively. Both static and sliding friction coefficients are fluctuating, especially during the first phase. This is caused by small variations in either the effective pressure or the net lifting stress. Small variations in these curves will have a large effect on the curve of the calculated friction coefficient. After the maximum net lifting stress is reached (static as well as sliding), the friction coefficient is decreasing as shown in Figures 6.6 and 6.7. It is chosen to terminate both the effective pressure curve and the friction coefficient curve when the maximum net lifting stress occurs because the measured pore

water pressure does not represent the actual situation at the sliding zone. It is assumed that the maximum lifting stress occurs when the pore water pressure starts to increase at the interface. This will be further discussed in Chapter 7. A final presentation of the friction coefficient and the two parameters affecting (effective pressure and the net lifting stress), is shown in Figures 6.8 and Figure 6.9.

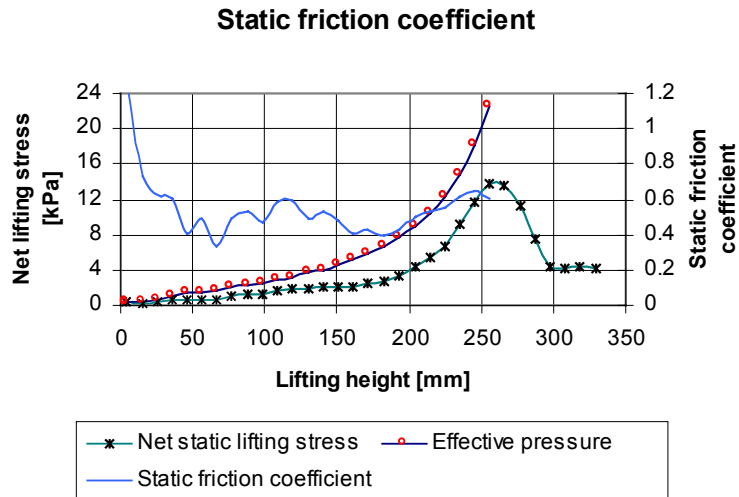


Figure 6.8: The static friction coefficient together with the static net lifting stress and the effective pressure (VT151)

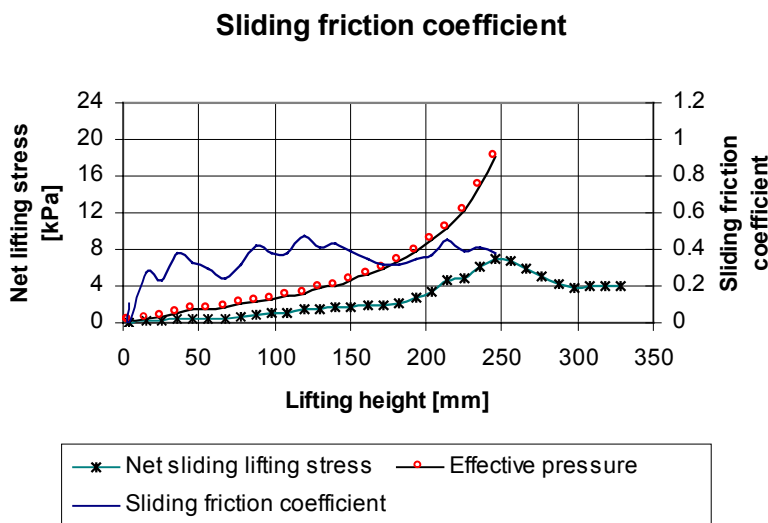


Figure 6.9: The sliding friction coefficient together with the sliding net lifting stress and the effective pressure (VT151).

6.3.1 Definitions of terms used to describe the pore water pressure development

6.3.1.1 Pore water pressure decrease rate

In order to compare the decrease rate of the pore water pressure between different tests, the pore water pressure decrease rate is defined and calculated at 0 kPa and -10 kPa pore water pressure. These levels are chosen because the 0 kPa pressure is the approximately level where the pore water pressure start to decrease faster and -10 kPa pore water pressure represents approximately the level where the maximum lifting stress occur for most of the single layer tests. The pore water pressure decrease rate is calculated as the average decrease rate at these two pore water pressures, see Eq. 6.9 and Figure 6.10.

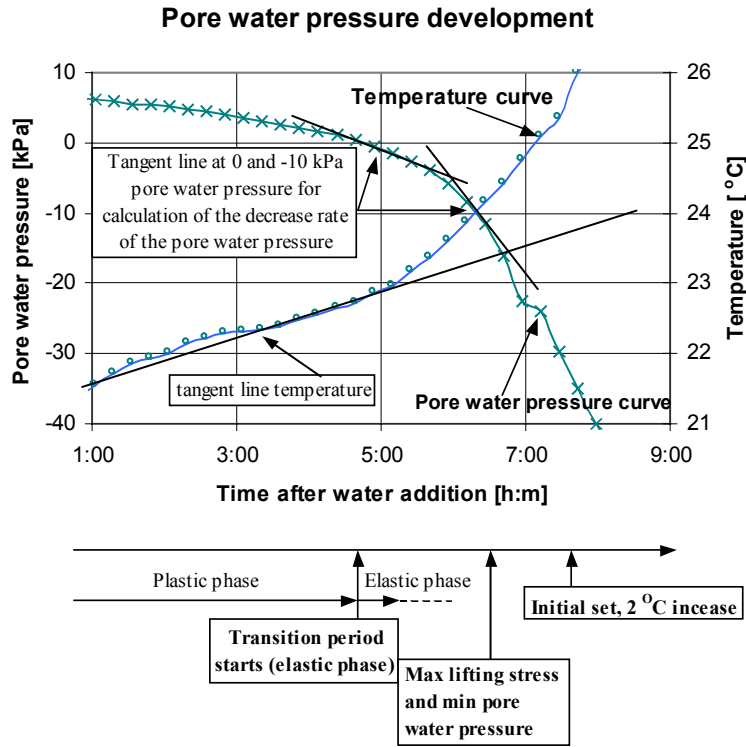


Figure 6.10: The pore water pressure development

$$\text{Eq. 6.9: } V_{Pl} = \frac{1}{2} \left(\frac{dP_{0kPa}}{dt} + \frac{dP_{-10kPa}}{dt} \right)$$

where V_{PL} = pore water pressure decrease rate [Pa/min]
 dP_{0kPa} = Pore water pressure difference during dt at 0 kPa
 dP_{-10kPa} = Pore water pressure difference during dt at -10 kPa

The average pore water pressure used in this calculation is the average of the measured pore water pressure at top and bottom of the concrete block.

6.3.1.2 Minimum pore water pressure

The minimum pore water pressure is defined as the pore water pressure at maximum sliding lifting stress. It is assumed that the minimum pore water pressure is the lowest pore water pressure before the pressure is increasing at the interface (concrete – slipform panel). This will be further discussed in Section 7.2. The minimum pore water pressure occurs in this instance 1 hour before the initial set.

The initial set is defined as 2 °C temperature increases from the tangent line for the temperature, see Figure 6.10.

7 RESULTS AND DISCUSSIONS

7.1 Effective pressure

7.1.1 Friction law

Friction is defined as the resistance against sliding between the slipform panel and the concrete. The friction (net lifting stress) is normally relatively low during lifting when the concrete is fresh and newly placed. The friction will increase gradually when the concrete loses its workability and becomes stiffer, but the major friction increase occurs when the elastic phase starts. Any deformation caused by settlement in the concrete in this phase will be resisted and the pressure in the pore water will start to decrease.

A typical net lifting stress development from a single layer test in the vertical slipform rig is shown in Figure 7.1 (see Chapter 6). The net lifting stress can be divided in static and sliding lifting stress. The static friction is the resistance that has to be overcome in order to start sliding and the sliding friction is the resistance during sliding. It can be seen that the net static and sliding lifting stress is almost identical the first 4.5 hours, and then the enveloped curves are separated during the transition period where the concrete has elastic properties. After the transition period, the net static and sliding lifting stress is almost equal, see Figure 7.1.

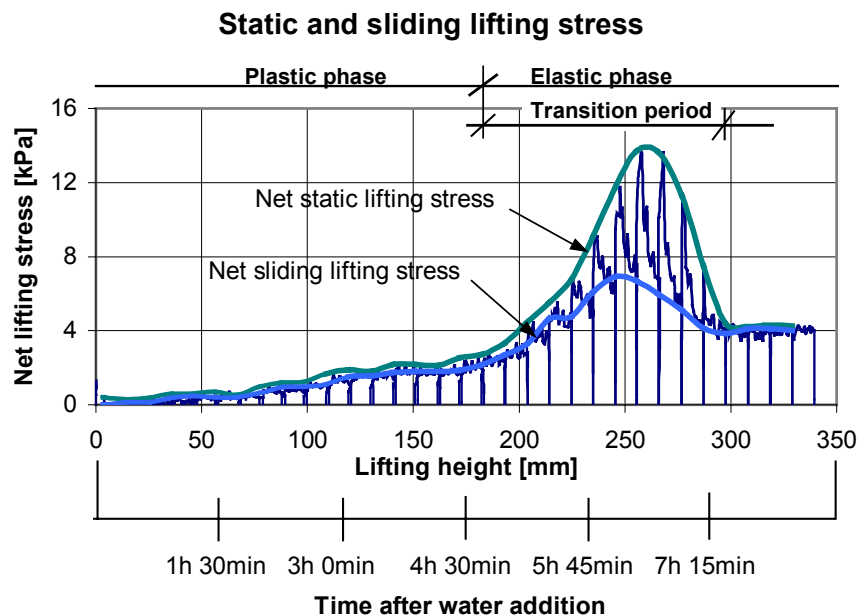


Figure 7.1: Static and sliding lifting stress for a single layer test in the vertical slipform rig (from Chapter 6).

The general friction law is frequently used in the literature to describe the correlation between the friction and the normal force between two solid materials. The friction law can also be used for concrete, but since the fresh concrete consists of a particulate mass in a liquid matrix, the normal pressure must be replaced with the effective pressure. The effective pressure represents the pressure between the particles and it is only the solid particles in the concrete that can resist shear stress and contribute to friction. The effective pressure is calculated by subtracting the pressure in the pore water from the normal pressure. The normal pressure, which is the concrete pressure against the slipform panel, is normally constant during the single layer tests. On the other hand the pressure in the pore water varies from a positive level in early stage to a lower negative level at a later stage. It is therefore primarily the variation in the pore water pressure that contributes to the variation in the effective pressure throughout a test. The friction law is shown in Eq. 7.1 (from Eq. 6.7 and Eq. 6.8 in Chapter 6).

Friction law:

$$\text{Eq. 7.1} \quad F_A = \mu \cdot \sigma' = \mu \cdot (\sigma - u)$$

where F_A = net lifting stress [kPa]
 σ' = effective pressure [kPa]
 σ = normal pressure [kPa]
 μ = friction coefficient
 u = pressure in the pore water [kPa]

The regression model in Eq. 7.2 will be used during the statistical analysis in order to verify the correlation between the friction/net lifting stress and the effective pressure. The regression constant c_1 is the system resistance exclusive the dead weight and c_2 represents the friction coefficient μ .

Regression model:

$$\text{Eq. 7.2:} \quad F_{RA} = c_1 + c_2 \cdot (\sigma - u)$$

where F_{RA} = Calculated net lifting stress based on the regression model [kPa]
 c_1 = estimated system resistance [kPa]
 c_2 = estimated friction coefficient

7.1.2 The correlation between the net lifting stress and the effective pressure

In order to show the correlation between the net lifting stress and the effective pressure, repeated tests carried out in the vertical slipform rig with the same concrete mix (the amount of superplasticizer has varied), lifting frequency and lifting height are selected. It is assumed that the correlation between the net lifting stress and the effective pressure is linear, which means according to the regression model in Eq. 7.2 that the estimated friction coefficient is constant.

The difference between the static and sliding lifting stress (see the enveloped curves in Figure 7.1) is probably caused by the adhesion (bonding from the cement hydration), but also the variation in the effective pressure (pore water pressure) during lifting may affect. This is further discussed in Section 7.2.7.

The net lifting stresses versus the effective pressure are plotted in Figure 7.2 and 7.3 for each test from approximately 3 hours after water addition to maximum net lifting stress. The workability has varied from high flow concrete with self-compacting properties to low workability where the compaction has been carried out by vibration. For some tests also the panel stiffness and inclination of the panel is changed, which have affected the normal pressure against the slipform panel.

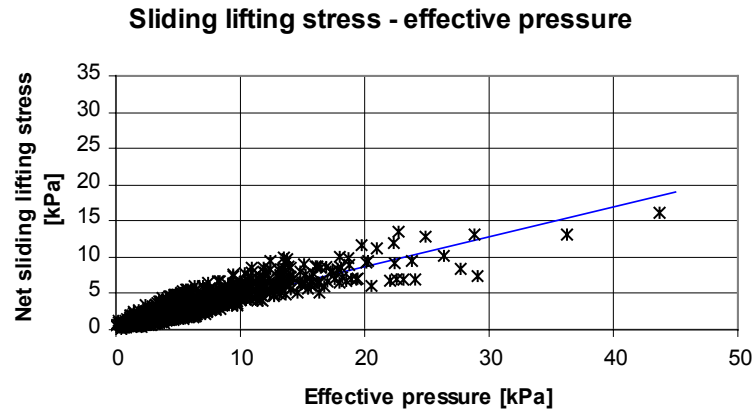


Figure 7.2: Net sliding lifting stress versus effective pressure

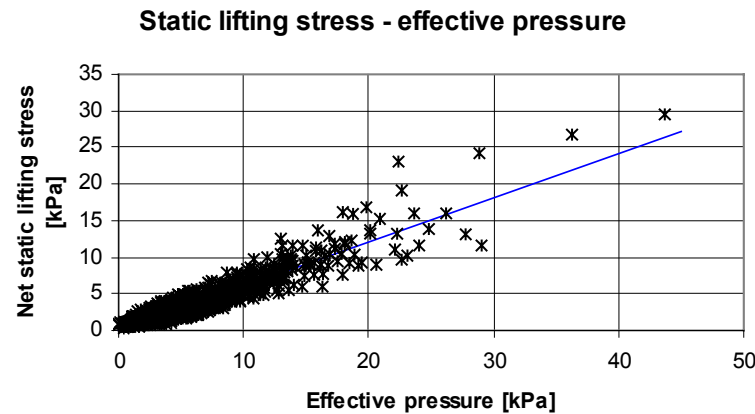


Figure 7.3: Net static lifting stress versus effective pressure

The results in Figure 7.2 show that the net sliding lifting stress is increasing almost linearly with increasing effective pressure. Also the result in Figure 7.3 show an almost linear correlation between the net static lifting stress and the effective pressure, but the static lifting stress is increasing more than the sliding lifting stress above approximately 8 – 10 kPa effective pressure. The linear correlation between the net static lifting stress and the effective pressure indicate that the static

lifting stress is more related to the effective pressure than the adhesion. The adhesion should be more related to hydration process than the level of the effective pressure. Any variation in concrete workability and normal pressure seems not to have any affect on the correlation between the net lifting stress and effective pressure. Statistical analysis on the static and sliding friction coefficient are presented in Section 7.1.3.

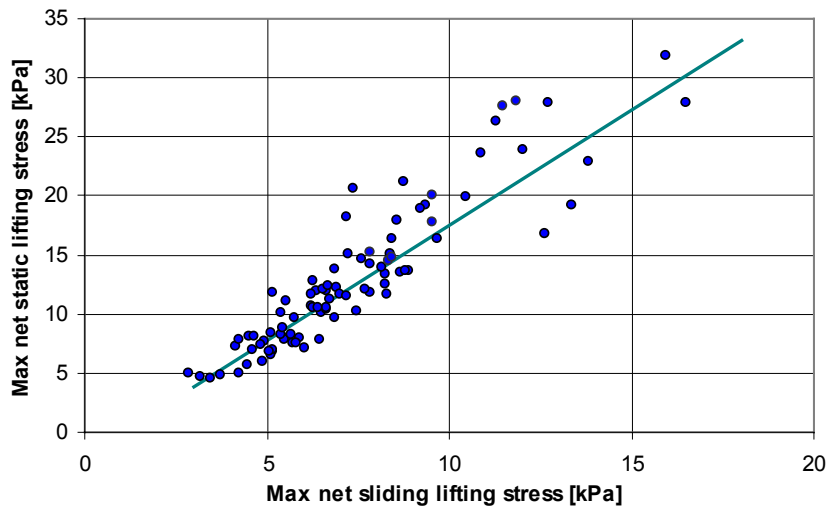


Figure 7.4: The correlation between the maximum static and maximum sliding lifting stress for all single layer tests.

The correlation between the maximum net static and sliding lifting stress is shown in Figure 7.4. The results show that the maximum net static lifting stress has an almost linear correlation to the maximum sliding lifting stress. This result confirms that the static lifting stress is evenly increased with increasing sliding lifting stress and implicit with increased effective pressure. This means that it is not only the period between two lifts that controls the difference between static and sliding lifting stress, but also the level of the effective pressure. The difference between static and sliding lifting stress is further discussed in Section 7.2.7 and Section 7.5.

It can be concluded that the friction law in Eq. 7.1 can be used to describe the linear correlation between both the net static lifting stress versus the effective pressure and the net sliding lifting stress versus the effective pressure. The friction law can be used in calculations from approximately zero effective pressure, when the concrete is fresh, to maximum lifting stress. Any variation in concrete workability and normal pressure seems not to have any affect on the correlation between the net lifting stress and effective pressure. The pressure in the pore water is responsible for most of the variation in the effective pressure during the early hardening period. Knowledge on the parameters affecting the development of the pressure in the pore water is therefore very important. This will be further discussed in Section 7.2.

7.1.3 Statistical evaluation of the effective pressure

7.1.3.1 Correlation between the effective pressure and the lifting stress

Statistical analyses are carried out in order to verify the relationship between the lifting stress and the effective pressure. The regression model in Eq.7.2 is used in the regression analysis to calculate the regression coefficients. The concrete tests selected are presented in Figure 7.2 – 7.3. The same concrete mix (amount of superplasticizer is varied), lifting frequency and lifting height are used for all tests, but the workability and the compaction method have varied. Also the normal pressure has varied in some few tests because of variation in the panel inclination and stiffness. It is assumed that the selected tests should give the same linear correlation between the lifting stress and the effective pressure.

The regression analysis is carried out on all measured data from approximately 3 hours after water addition to maximum lifting stress. The result from the statistical analysis is presented in Table 7.1.

Table 7.1: Regression equation for the net static and sliding lifting stress.

	Regression equation according to Eq.7.2	R²-coefficient [%]	Standard deviation [kPa]
Net sliding lifting stress [kPa]	$F_{AG} = 0.56 + 0.41 \cdot \sigma'$	83	0.89
Net static lifting stress [kPa]	$F_{AH} = 0.04 + 0.60 \cdot \sigma'$	87	1.09

The results show that the R²-coefficients vary from 83 to 87 %, which confirm that there is a linear correlation between the lifting stress and the effective pressure. However as shown in Figures 7.2 and 7.3, the variation in the lifting stress is increasing with higher effective pressure, which results in decreased R²-coefficients and increased standard deviation for both regression equations in Table 7.1. This will be further evaluated in Section 7.1.5.

The estimated system resistance c_1 in Eq. 7.2 is close to zero in both the static and sliding equations and can therefore be ignored. The estimated friction coefficient c_2 is 0.41 for the sliding lifting stress and 0.60 for the static lifting stress. This friction coefficient describes the correlation between the net lifting stress and the effective pressure and represents the angle of the regression line in Figure 7.2 and 7.3.

The result in Table 7.1 confirms that the friction law in Eq. 7.1 can be used to describe the linear correlation between the lifting stress (both static and sliding) and the effective pressure. The friction law can be used in calculations up to maximum lifting stress for both the static and sliding lifting stress. It is assumed that this is also applicable for other concrete mixes as well.

7.1.4 The friction coefficient

The friction coefficient is calculated according to Eq.7.1 for each lift in each single layer test from approximately 3 hours after water addition to maximum lifting stress. Both the sliding friction coefficient and the static friction coefficient are calculated for all single layer tests carried out on the friction rig and the vertical slipform rig. It is assumed that both the static and sliding friction coefficient are constant for each single layer test.

The value of the friction coefficient will probably depend on variations in the slipform technique, panel surface and type of concrete. Note that only small variations in the lifting stress will result in a relative large variation in the friction coefficient. E.g. a sliding lifting stress of 10 kPa and a effective pressure of 20 kPa will result in friction coefficient of 0.50, but 10 % increase in the sliding lifting stress from 10 to 11 kPa, which is a relative small variation in these tests, will result in a friction coefficient of 0.55. For comparison, the variation in the reproducibility test in Section 5.3.6 is 0.4 kPa.

7.1.4.1 Concrete tests carried out on the vertical slipform rig

The results show that the average sliding friction coefficient for each test has varied mostly between 0.35 and 0.60 with an average for all the tests of 0.48, see Figure 7.5. The average static friction coefficient is approximately 0.10 higher and vary mostly between 0.45 and 0.70. The average static friction coefficient for all tests is 0.60.

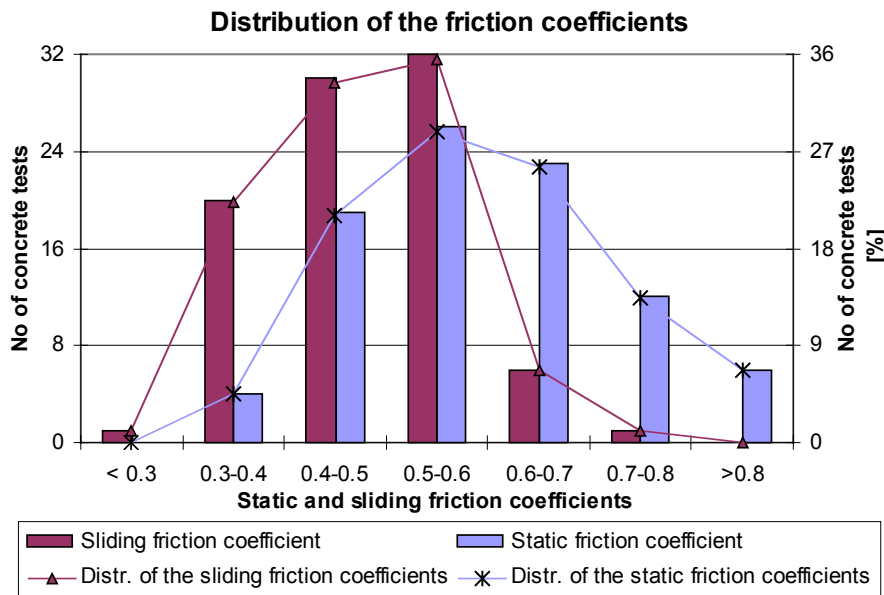


Figure 7.5: Distribution of the friction coefficients for tests from the vertical slipform rig.

The ranges of the friction coefficients are wide, but this is a consequence of the span in the experimental program. Concrete tests with e.g. high content of silica fume have obtained a low

friction coefficient, while tests carried out on a rough surface panel have obtained a high friction coefficient. The effect of rough surface panel will be discussed in Section 7.4.3.

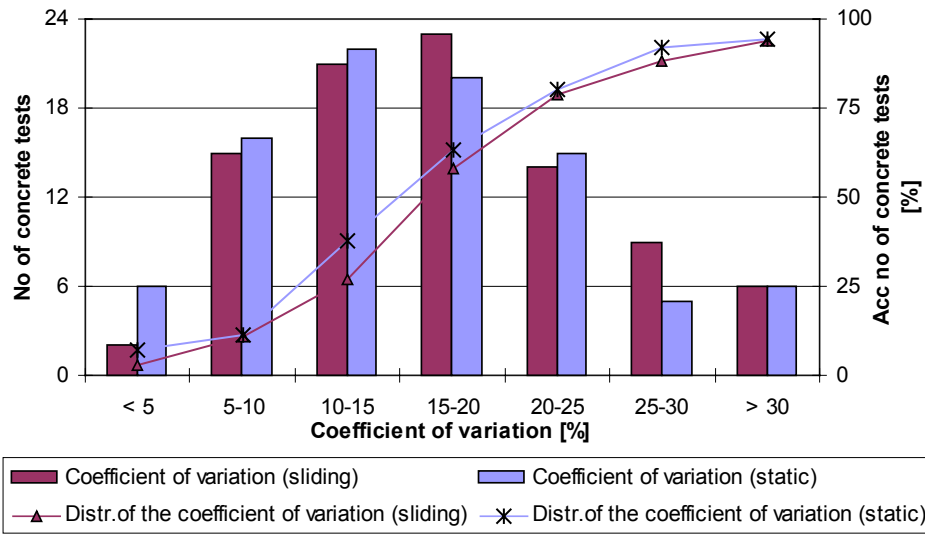


Figure 7.6: Coefficient of variation (standard deviation/mean friction coefficient) for tests from the vertical slipform rig.

The coefficient of variation of each test, which is the standard deviation divided by the mean of the friction coefficient, is calculated and presented in Figure 7.6. The results show that approximately 75 % of the tests have a coefficient of variation lower than 20 % for both the static and sliding friction coefficients. Only 25 % of the tests have a coefficient of variation lower than approximately 10 %.

The results show that there is a linear correlation between the lifting stress and the effective pressure (both static as well as sliding) for the single layer tests. However, some single tests have a high coefficient of variation and it seems that this coefficient is also increasing with increased effective pressure and maximum lifting stress, see Figure 7.7. In particular the static lifting stress above 20 kPa have in general obtained a high coefficient of variation. Possible reason for the high coefficient of variation is discussed in Section 7.1.5.

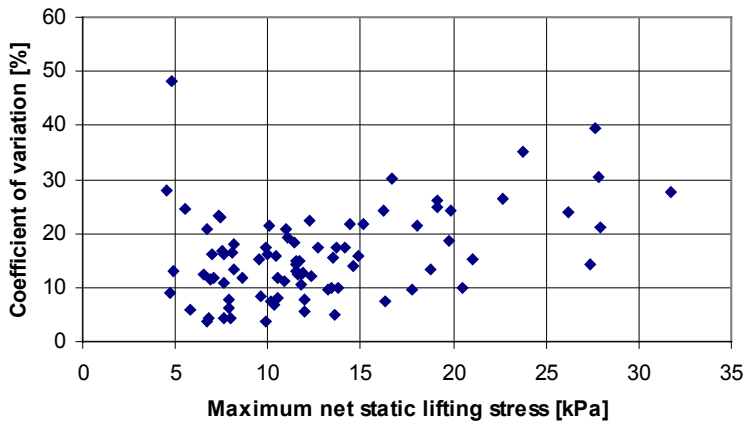


Figure 7.7: Coefficient of variation versus the net maximum net static lifting stress.

7.1.4.2 Concrete tests carried out on the friction rig

The sliding friction coefficients for the concrete tests carried out on the friction rig are shown in Figure 7.8. The sliding friction coefficient varies from 0.47 to 0.80 with an average for all tests of 0.62 while the static friction coefficient varies from 0.56 to 0.97 with an average of 0.78. The range in the friction coefficient is a result of the span in the experimental program. Also in this rig, the highest friction coefficient is obtained when using a rough slipform panel.

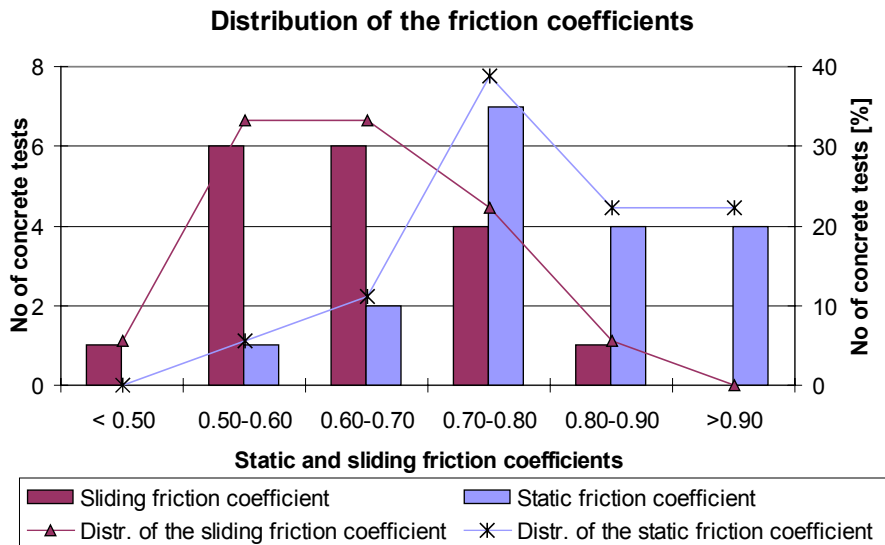


Figure 7.8: Distribution of the friction coefficients for tests from the friction rig.

In general the friction coefficients are approximately 0.15 higher in this rig compared to the vertical slipform rig. A possible reason is because the coarse aggregates is segregating and replace the lubricants in the sliding zone. During panel movements, the coarse aggregates will then cause a higher static and sliding friction.

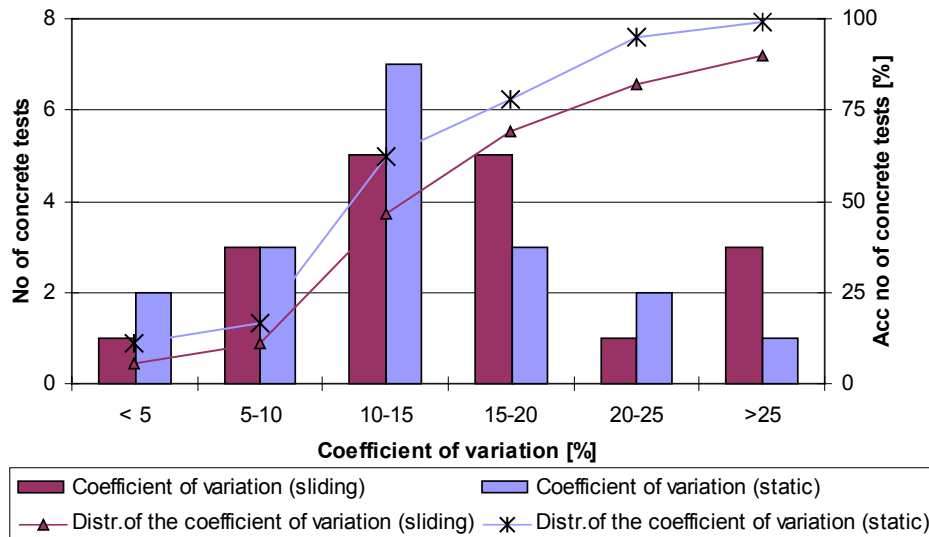


Figure 7.9: Coefficient of variation for tests from the friction rig.

The coefficient of variation of each test is calculated and presented in Figure 7.9. The results show that approximately 75 % of the tests have a coefficient of variation lower than 20 % for both the static and sliding friction coefficients. This is approximately at the same level as for the tests carried out in the vertical slipform rig. The high coefficient of variation for some tests indicates that the friction is not increasing linearly with the effective pressure. This is further discussed in Section 7.1.5.

7.1.5 Observation during the regression analyses

It has been observed that the variation in the static lifting stress is increasing with increased static lifting stress (increased effective pressure) as shown in Figure 7.7. The main reason seems to be that the lifting stress is increasing slower the last period before maximum, while the effective pressure continues to increase at the same rate or faster, see Figure 7.10 and 7.11. This is probably because of the calculated effective pressure, which is based on the measured pore water pressure, does not represent the actual pressure at the interface zone during the last period before maximum lifting stress.

It is assumed that the pore water pressure is the same in the bulk concrete as in the interface zone between the slipform panel and the concrete. However, when the concrete becomes denser because

of the cement hydration, the water communication in the concrete will decrease. This can result in a pressure gradient in the cover zone between the measuring point and the interface zone, which means that the measured pore water pressure 30 mm inside does not represent the actual pore water pressure at the interface. This can be the cause of the deviation in the linear correlation between the net lifting stress and the effective pressure for some tests. It can be seen in Figure 7.10 and 7.11 that the correlation between the lifting stress and the effective pressure is almost linear except for the last period. It is assumed that this is caused by a lower pore water pressure at the gauge compared to the actual pressure at the sliding zone at the interface. Both the static and sliding lifting stress curves will be affected by this situation.

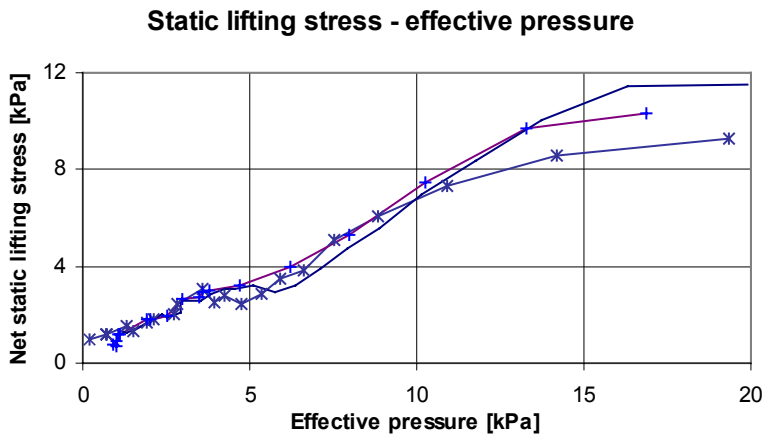


Figure 7.10: Typical examples on how the net static lifting stress curve culminates before maximum.

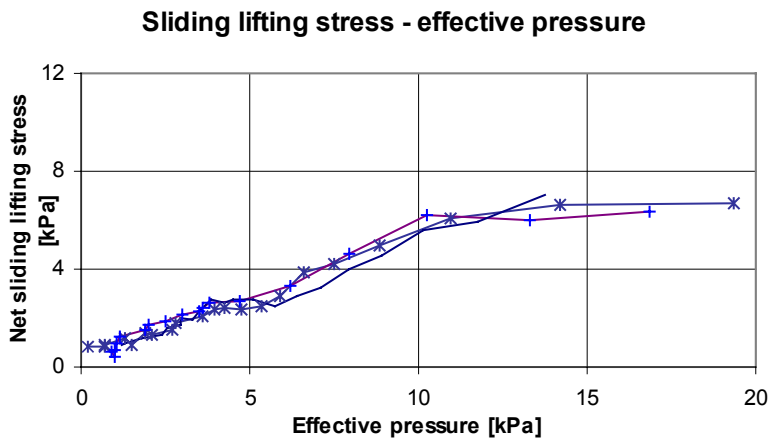


Figure 7.11: Typical examples on how the net sliding lifting stress curve culminates before maximum.

It is primarily the minimum pore water pressure, which occur just before the pressure in the pore water disappear at the sliding zone, that can be difficult to determine when this situation occurs. However, the determination of the minimum pore water pressure will follow the same procedure for all tests as described in Chapter 6. This will probably give fairly comparable minimum pore water pressures between the tests.

7.1.6 Summary

The friction law presented in Eq. 7.1 can be used to describe the linear correlation between both the net static lifting stress versus the effective pressure and the sliding lifting stress versus the effective pressure. The effective pressure, which represents the pressure between the solid particles and the slipform panel is the difference between the normal pressure and the pore water pressure. The normal pressure, which is the concrete pressure against the slipform panel, is normally almost constant in these single layer tests. It is primarily the pressure in the pore water that is responsible for most of the variation in the effective pressure during the plastic phase and the setting period.

The difference between the static and sliding lifting stress starts at the beginning of the transition period and is increasing evenly with larger effective pressure until the maximum lifting stress. The difference is probably caused by bonding from the cement hydration (adhesion), but also variation in the effective pressure (pore water pressure) during lifting may affect.

The high coefficient of variation for some tests seems to be because the measured pore water pressure is not representing the actual pore water pressure at the interface zone when the concrete becomes dense. It is primarily the minimum pore water pressure that can be difficult to determine when this situation occurs.

7.2 The pressure in the pore water

7.2.1 Introduction

The chemical shrinkage caused by the cement hydration is the primarily driving force for the change in the pore water pressure. The pore water pressure is positive after mixing and corresponds approximately to the hydrostatic pressure in the concrete. It is decreasing slowly during the plastic phase, but during the transition period in the elastic phase, the pore water pressure will become negative and start to decrease faster. The focus in this section will be on the pore water pressure development during the transition period.

As explained in Chapter 3 - Hypotheses, the effect of the chemical shrinkage on the pore water pressure is assumed to depend, besides the cement hydration, also on the geometry of the pore system that is formed and the pressure equilibrium between air and water. The pore system that is formed is mainly depending on the particle concentration and the particle size distribution and this will affect the size of the capillaries that is formed. When chemical shrinkage is developing, contraction pores are formed since the reaction products have a smaller volume than the reacting materials. The pore water pressure will decrease as a result of the developed contraction pores.

The existing air content in the concrete will theoretically affect the pressure in the pore water by acting as a pressure release volume. This will reduce the effect of the chemical shrinkage on the pore water pressure because of the air content in the concrete is assumed to be in equilibrium with the liquid system in the concrete. With increased air content, the minimum pore water pressure will be higher and the decrease rate of the pore water pressure will probably be lower. A calculation shows that the chemical shrinkage with 400 kg cement will give approximately 3.5 litres reduced volume when it is assumed that the chemical shrinkage is 25 % of the chemical bound water and the degree of hydration is 15 % at the time of minimum pore water pressure.

The pore water pressure will also be effected of the development of the meniscus in the capillary pores, which will depend on the size of the capillary system (pore size distribution). A system that consists of a higher particle concentration will probably result in a faster decrease of the pore water pressure than a lower particle concentration. The pressure will decrease as the meniscus radius becomes smaller in the pores where the meniscus is formed. Also when the cement content is increased in a system with the same pore size distribution (e.g. filler substituted with cement), the cement hydration will increase and probably increase the decrease rate of the pore water pressure.

It is assumed that the minimum pore water pressure occur just before it increase or just disappear at the sliding zone close to the slipform panel. The first theory is that the pressure will disappear because of the capillary system is collapsing when the water content is reduced to such a low level that the menisci cannot find new and stable positions. An alternative theory is that the pore water pressure at the sliding zone is decreasing during lifting of the slipform panel. When the concrete start to be denser and the water communication slower, the period will be longer before the pore water pressure at the sliding zone will reach equilibrium again with the pore water pressure in the adjacent concrete. When the period for reaching equilibrium is longer than the period between two lifts, the pore water pressure (just before each new lift) at the sliding zone will probably flatten out

and thereafter increase. The minimum pore water pressure will be the lowest pore water pressure at the sliding zone before it increase or disappear.

The minimum pore water pressure and the pore water decrease rate are both a results of the chemical reaction, the pore system and the air content. These two parameters are therefore closely connected. With a faster pore water decrease rate, it is assumed that the minimum pore water pressure will be lower and opposite with a slower pore water pressure decrease rate.

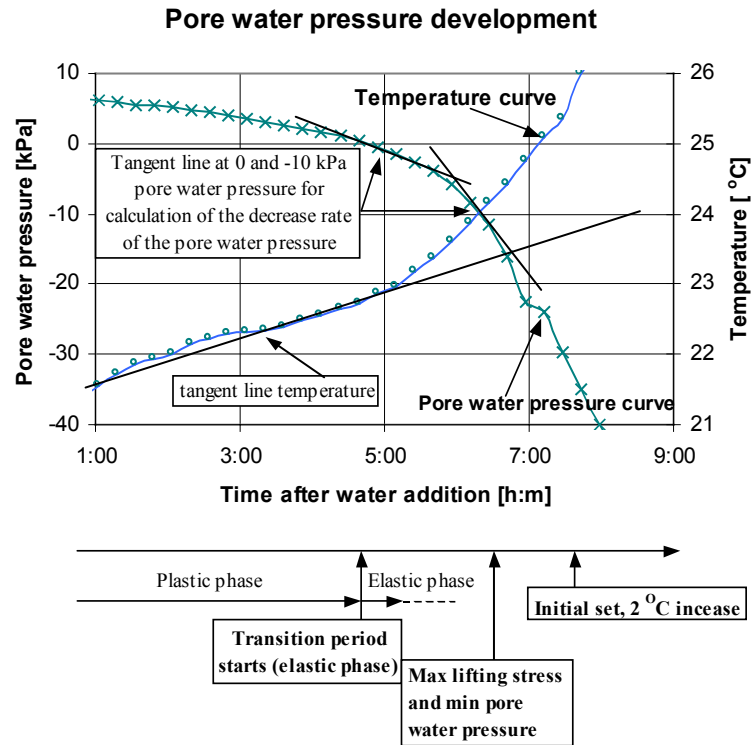


Figure 7.12: Typical example on the pore water pressure decrease and temperature increase during a test (from Chapter 6).

The two main notations that will be used in this section are the rate of the pore water pressure decrease and the minimum pore water pressure. The rate of the pore water decrease is calculated as the average rate at the pressures 0 kPa and -10 kPa, see Figure 7.12. These levels are chosen because of the 0 kPa pressure is the approximately level where the pore water pressure start to decrease faster and -10 kPa pressure represents the level when the minimum pore water pressure approximately occur for most of the single layer tests. The minimum pore water pressure and the rate of the pore water pressure decrease will give an indication on the pore size distribution in the concrete. The minimum pore water pressure is the pore water pressure at the time of maximum lifting stress and it is assumed that this pressure represents the lowest pressure before it increase or just disappear at the sliding zone. In the typical example shown in Figure 7.12, the initial set (2 °C

difference between tangent line and temperature curve) occur approximately 1 hour after the time for minimum pore water pressure. The definition and calculation of the pore water pressure decrease rate and minimum pore water pressure are also given in Chapter 6.

7.2.2 Particle concentration

7.2.2.1 The effect of silica fume

The silica fume grains have an average diameter of approximately 0.1 μm , which is about 1/100 of an average cement grain. Addition of silica fume will therefore have a considerable impact on the particle size distribution and also on the particle concentration. According to Hammer (2000), increased amount of silica fume will result in a faster decrease rate of the pore water pressure. The minimum pore water pressure is assumed to be lower with increased amount of silica fume.

The effect of the silica fume is tested at 5 %, 10 % and 20 % levels of the cement content (mass), see Table 7.2. Since the specific gravity is slightly lower for the silica fume compared to the cement, the total mass is increasing with higher content of silica fume when the binder content (volume) in the concrete is kept constant for all tests.

In total 8 concrete tests were tested, but three of these tests were carried out with a lower frequency between the lifts than the others and can therefore not be used in the evaluation of the effect of silica fume on the minimum pore water pressure. It is assumed that the minimum pore water pressure is affected of the slipform rate, this is further discussed in Section 7.2.6.

Table 7.2: The effect of silica fume on the pore water pressure

Silica fume content	VT188 5%	VT212 5%	VT205 10%	VT215 20%	VT226 20%	VT217 20%	VT220 20%	VT225 20%
Average pore water pressure decrease rate [Pa/min]	140	149	143	169	172	183	183	188
Min pore water pressure [kPa]	-5.9	-6.3	-22.7	-41.8	-35.3	*	*	*

* *Different slipform rate*

In Figure 7.13, the decrease rate of the pore water pressure is presented. The result shows that the pore water pressure is decreasing faster with 20 % silica fume compared to concrete with 10 and 5 % silica fume. The rate of pore water pressure decrease is within the same range for concrete with 5 and 10 % silica fume. The result shows also that silica fume has a higher effect on the decrease rate of the pore water pressure than the cement (silica fume replaces cement by the mass percent).

A linear regression between the silica content and the average decrease rate of the pore water pressure is carried out. The R^2 -coefficient is calculated to 83 % and the regression is significant at 0.05 significance level. This confirms that the pore water pressure will decrease faster with increased silica fume addition in the concrete.

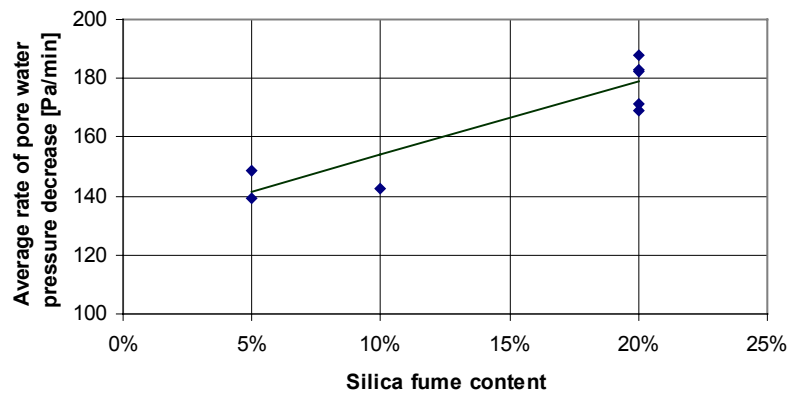


Figure 7.13: The average rate of the pressure decrease in the pore water versus the silica fume content

In Figure 7.14, the minimum pore water pressure versus the silica fume content is shown. The results show that the amount of silica fume has a considerable effect on the minimum pore water pressure. The minimum pore water pressure is approximately -40 kPa in tests with 20 % silica fume, which is a rather low pressure compared to approximately -6 kPa in tests with 5 % silica fume. The result confirm that increased addition of silica fume, which will result in a faster decrease rate of the pore water pressure, have a considerable impact on the minimum pore water pressure. The result shows also that silica fume have a larger effect on the minimum pore water pressure than the cement. The correlation between the minimum pore water pressure and the amount of silica fume in percent of the cement content (volume binder content constant) is almost linear. The R^2 -coefficient is 96 % and the regression model is significant at 0.05 significance level with an ample margin.

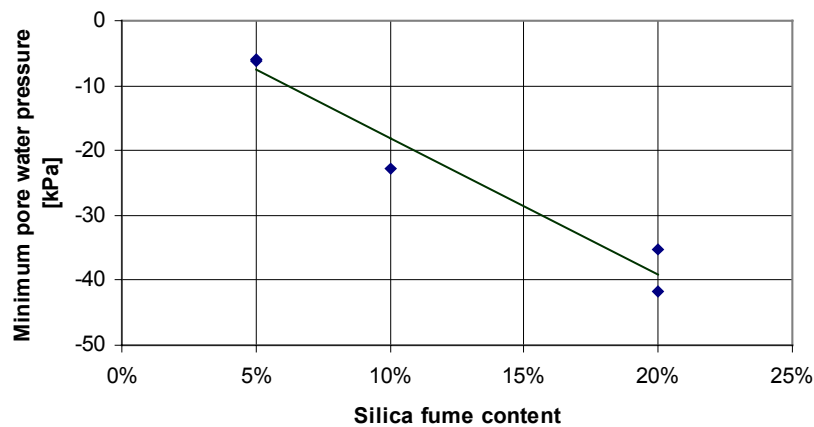


Figure 7.14: Minimum pore water pressure versus the silica fume content

It can be concluded based on the results that increased amount of silica fume will result in a faster decrease rate of the pore water pressure because of finer particle size distribution and a higher particle concentration. Also the minimum pore water pressure will be affected by the silica fume. The minimum pressure is decreasing with increased content of silica fume and it supports the theory that finer particle size distribution and a higher particle concentration, will result in a faster pore water decrease rate and a lower minimum pore water pressure.

7.2.3 The effect of the air content

7.2.3.1 Air entraining agents

The air voids system in the concrete will theoretically affect the pore water pressure development as explained in Chapter 3. When the negative pressure occur in the concrete pore water, the existing air volume will act as a pressure release volume. Due to this, the effect of the chemical shrinkage will be reduced with increased air content. This means that the decrease rate of the pore water pressure should be reduced and the minimum pore water pressure should be higher with increased content of air.

Air entraining agents are used in all mixes except mixes HT168 and HT169. The air content has varied from 2.6 to 9 %, see Table 7.3. The compaction of the concrete might have affected the actual air content, but this is ignored in this discussion.

Table 7.3: The effect of air on the pore water pressure

	HT169	HT168	HT170	HT172	HT160
Air content [%]	2.6	3.1	4.3	8.0	9.0
Average pore water pressure decrease rate [Pa/min]	228	221	163	94	93
Minimum pore water pressure [kPa]	-5.6	-10.4	-7.9	-2.0	-1.1

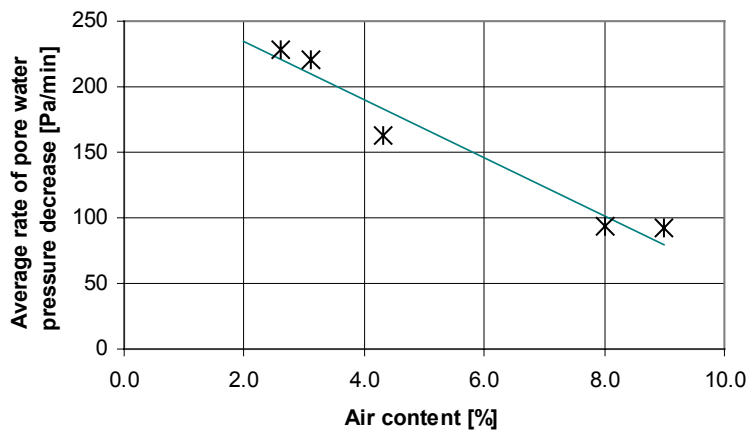


Figure 7.15: The average pressure decrease rate in the pore water versus the air content

The average pore water pressure decrease rate versus the air content is presented in Figure 7.15. The results show that the average pore water pressure decrease rate is decreasing with increasing air content, which supports the theory that also the air content is affecting the response of the chemical shrinkage on the pore water pressure development. The correlation between the decrease rate of the pore water pressure and the air content is almost linear. The R^2 -coefficient is 95 % and the regression is significant at 0.05 significance level. The results in Figure 7.15 show that the average pore water pressure rate is decreasing by 22 Pa/min for each percent increased air content in the concrete.

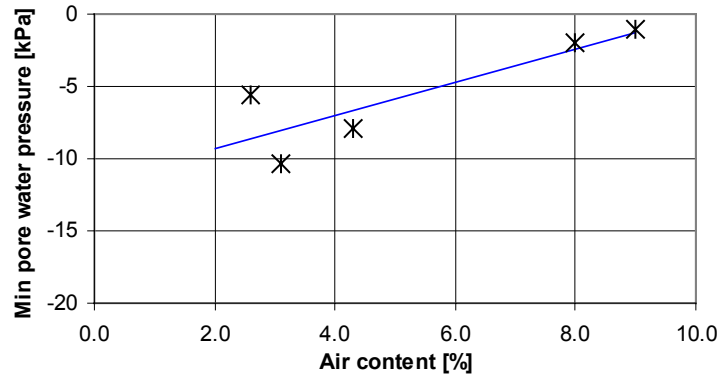


Figure 7.16: Minimum pore water pressure versus the air content

The minimum pore water pressure versus the air content is shown in Figure 7.16. The result shows that the minimum pore water pressure is increasing with increased air content. The trend line is increasing with 1.2 kPa for each percent higher air content. These results confirm the theory that the air content is also affecting the minimum pore water pressure.

Based on the results, it can be concluded that the air content in the concrete will affect the decrease rate of the pore water pressure and the minimum pore water pressure. This support the theory that the increasing air content will reduce the effect of the chemical shrinkage on the pore water pressure because the air content is acting as a pressure release volume.

7.2.3.2 The effect of vibration

The purpose of vibration is to consolidate the fresh concrete by removing entrapped air. During vibration, the solid particles in the concrete are put into motion by the vibrator and entrapped air will during this process be removed. The air content will decrease with increased vibration time and it is expected that this will result in a faster decrease rate of the pore water pressure and a lower minimum pore water pressure.

The effect of the vibration time is investigated in tests where the vibration times have varied from 2x15 sec to 2x60 sec. The concrete is placed and vibrated in two layers with thickness of approximately 30 cm each. Two different superplasticizers are used, Scancem SSP2000 and Sika ViscoCrete 3 respectively, see Table 7.4.

Table 7.4: The effect of vibration on the pore water pressure

	VT184	VT185	VT187	VT186	VT194
Admixture	Sika ViscoCrete 3		Scancem SSP2000		
Vibration (time)	2 x 15 sec	2 x 30 sec	2 x 15 sec	2 x 30 sec	2 x 60 sec
Average pore water pressure decrease rate [Pa/min]	152	173	169	176	216
Min pore water pressure [kPa]	-13	-15	-33	-15	-43

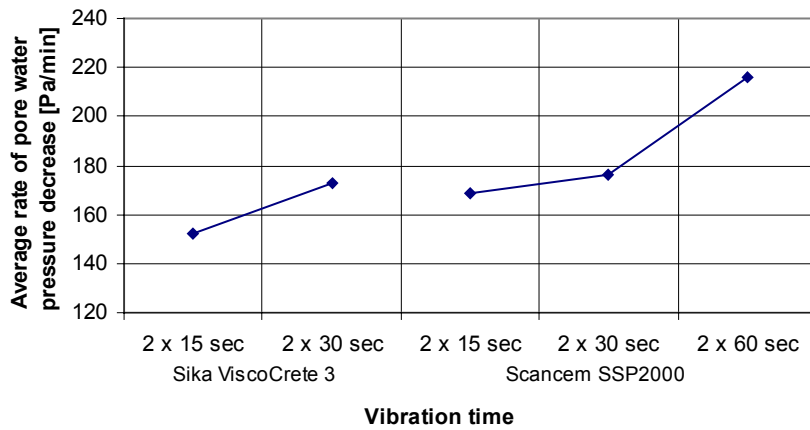


Figure 7.17: The pore water pressure decrease rate versus the vibration time

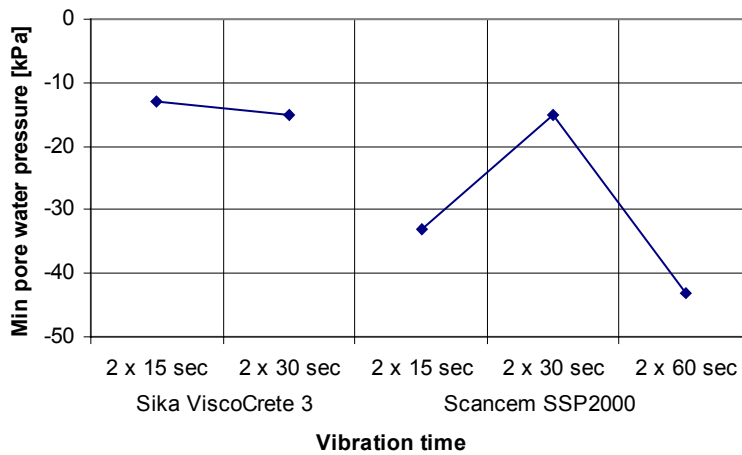


Figure 7.18: Minimum pore water pressure versus the vibration time

The decrease rate of the pore water pressure is presented for each concrete test in Figure 7.17. The results show that increased vibration time has resulted in a faster decrease rate of the pore water pressure. This is in accordance to the result from previous sections that lower air content has resulted in a faster decrease rate. The rate of decrease is slightly higher for concrete with Scancem SSP2000 compared to concrete with Sika ViscoCrete 3. A possible reason is the stabilizer in the Sika ViscoCrete 3, which probably have maintained a higher air content in the concrete during vibration. The same concrete with self-compacting properties show a decrease rate of the pore water pressure at approximately 140 Pa/min. Compared to the result in this section, it can be seen that even 2 x15 sec vibration show a higher decrease rate than comparable nonvibrated self-compacting concrete. This demonstrates the major response of the vibration on the fresh concrete properties.

In Figure 7.18, the minimum pore water pressure versus the vibration time is shown. The results show a tendency of lower minimum pore water pressure with increased vibration time. This is in accordance with the previous result, that increased vibration will reduce the air content and decrease the minimum pore water pressure. The test with 2x15 sec vibration time and Scancem SSP2000 show a lower minimum pore water pressure than expected. It was expected that the minimum pore water pressure should be between -10 and -15 kPa. However, the results indicate that the tests should be carried out several times in order to avoid errors.

It can be concluded based on the results that increased vibration time is affecting both the decrease rate of the pore water pressure and the minimum pore water pressure. The longer vibration time has reduced the air content, which has affected the response of the chemical shrinkage on the pore water pressure.

7.2.3.3 The effect of lightweight aggregate

When lightweight aggregate is introduced into the concrete, it is supposed that the effect of the chemical shrinkage on the pore water pressure will be reduced. It is assumed that the high porous lightweight aggregate will function as a pressure release volume. With negative pressure in the pore water, the entrapped air volume in the lightweight aggregate will result in a reduced decrease rate of the pore water pressure and a higher minimum pore water pressure.

The volume of the lightweight aggregate has varied from 291 litres to 508 litres. Leca 1-4 mm and Liapor 7 4-12 mm has been used in all tests except for in one test where Liapor 7 was used only. The amount of aggregate used in each test is listed in Table 7.5.

Table 7.5: Average decrease rate in the pressure in the pore water

	VT169	VT170	VT171	VT172	VT201	VT202
	LWA	LWA	LWA	LWA	LWA	LWA
Air content [%]	5	4.3	4	2.6	4.2	3.9
LWA volume [litres]	508	423	331	291	331	331
Leca 1-4 mm [kg/m ³]	115	89	75	0	75	75
Liapor 7 [kg/m ³]	383	332	250	351	250	250
Average pore water pressure decrease rate [Pa/min]	23	23	29	51	40	42
Minimum pore water pressure [kPa]	-4.7	-3.3	-3.1	-8.6	*	*

* Different slipform rates

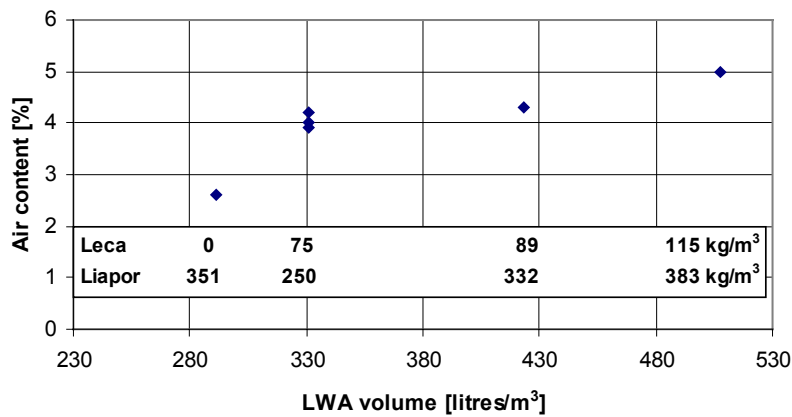


Figure 7.19: Air content versus the volume of lightweight aggregate

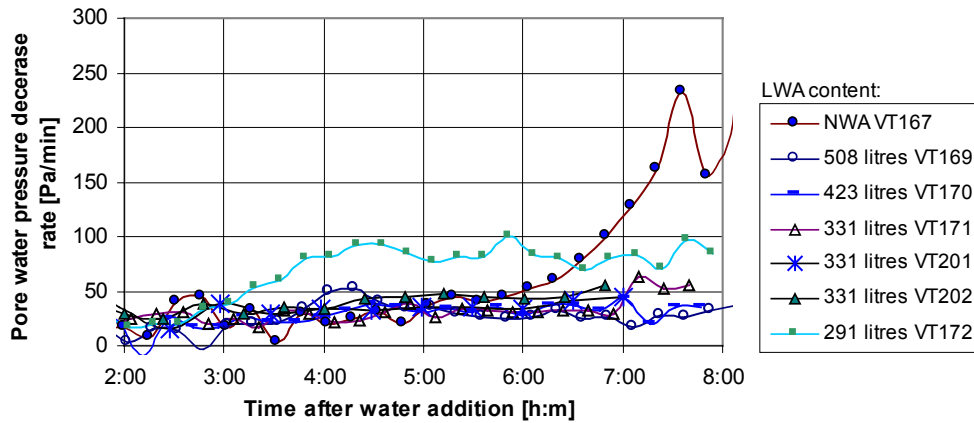


Figure 7.20: The rate of the pore water pressure decrease.

In Figure 7.19 it can be seen that the air content is increasing with larger volume of lightweight aggregate (no air entraining admixtures is added). It seems that it is primarily the content of Leca that have affected the air content in the concrete. Probably because the Leca have a lower initial moisture content, is more porous and have less dense surface compared to Liapor 7, see Table 4.7.

The decrease rate of the pore water pressure is presented in Figure 7.20. The lightweight concretes with both Leca and Liapor 7 show an almost constant and low decrease rate of the pore water pressure (23 – 42 Pa/min). The test with only Liapor 7 (VT172) show that the rate of decrease is in general higher compared to the other tests with lightweight concrete (51 Pa/min). It can be seen that the Leca have larger effect on the decrease rate of the pore water than Liapor 7. This is probably because the Leca aggregate has a higher volume of air because it is more porous. It seems also that it

is the properties of the lightweight aggregate that control the response of the chemical shrinkage on the pore water pressure and not the quantity of the lightweight aggregate. The decrease rate of the pore water pressure is considerably lower for lightweight concrete than for normal weight concrete also when the air content is taken into consideration, see Figure 7.15 in Section 7.2.3.1. This means that it is the properties of the lightweight aggregate that are the main reason for the lower decrease rate of the pore water pressure.

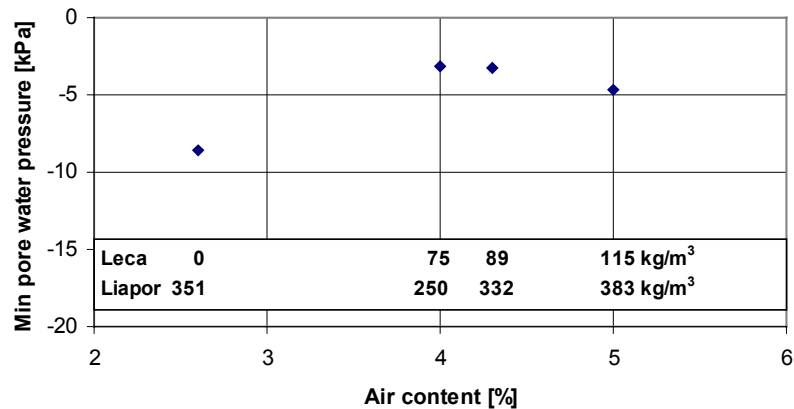


Figure 7.21: Minimum pore water pressure versus the lightweight aggregate content

The minimum pore water pressure for the concrete tests with both Liapor 7 and Leca is in general high and vary between -3.1 and -4.7 kPa, see Figure 7.21. With only Liapor 7, the minimum pore water pressure is -8.6 kPa. This is approximately the same level as for the normal weight concrete and is probably caused by the lower air content.

The result shows that the lightweight aggregate has a considerable impact on the decrease rate of the pore water pressure and the minimum pore water pressure. This is caused by the porous aggregate, which function as air reservoir and will reduce the effect of the chemical shrinkage on the pore water pressure. The entrapped air in the lightweight aggregate acts as a pressure release volume when the pore water pressure is decreasing. It seems that the porosity of the lightweight aggregate has a larger impact on the pore water pressure than the quantity of the lightweight aggregate.

7.2.3.4 The effect of the binder volume

The binder volume will theoretically not affect the particle concentration of cement and silica because the ratio between the binder and the water volume is constant. However, when the binder volume is increased also the volume of chemical shrinkage is increased, but if the air content is increasing proportional with the binder volume, the decrease rate of the pore water pressure and the minimum pore water pressure should be the same.

Table 7.6: The effect of the binder volume on the pore water pressure

Binder volume	VT192 275 litres	VT188 300 litres	VT212 300 litres	VT190 350 litres	VT191 350 litres
Air content of concrete volume[%]	1.5	1.2	1.0	0.6	1.0
Air content of binder volume [%]	5.5	4.0	3.3	1.7	2.9
Pore water pressure decrease rate [Pa/min]	168	140	149	171	163
Min pore water pressure [kPa]	-6.1	-5.9	-6.3	-11.0	-17.2

The binder volume has varied from 275 to 350 litres, see Table 7.6. All tests were carried out with self-compacting concrete, but the test with the lowest binder volume of 275 litres had rather low self-compacting properties and additional compaction was carried out in order to obtain a proper consolidation of the fresh concrete. An opposite tendency was observed for the tests with binder volume of 350 litres, where the concrete had high self-compacting properties.

The air content (percent of concrete volume) shows a variation from 0.6 to 1.5 % for the tests. When calculating the air content in percent of the binder volume, the result show a tendency of decreasing air content with increased binder volume. It is expected that the decrease rate of the pore water pressure will be faster and the minimum pore water pressure lower with decreasing air content in percent of the binder volume.

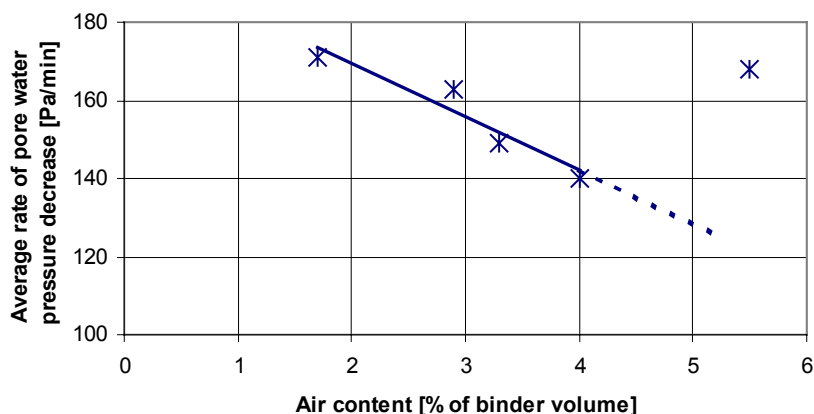


Figure 7.22: The average rate of the pressure decrease in the pore water versus the air content

The average decrease rate of the pore water pressure is shown in Figure 7.22. The result shows that lower air content will result in a higher decrease rate. The test with 275 litres of binder shows a higher decrease rate than expected based on the trend line in Figure 7.22. This is probably because the additional compaction that was carried out for this test, which have probably reduced the air content during placing. The correlation between the binder volume versus the rate of the pore water

pressure decrease is significant at 0.05 significance level even with few data (the test with 275 litres of binder not taken into consideration).

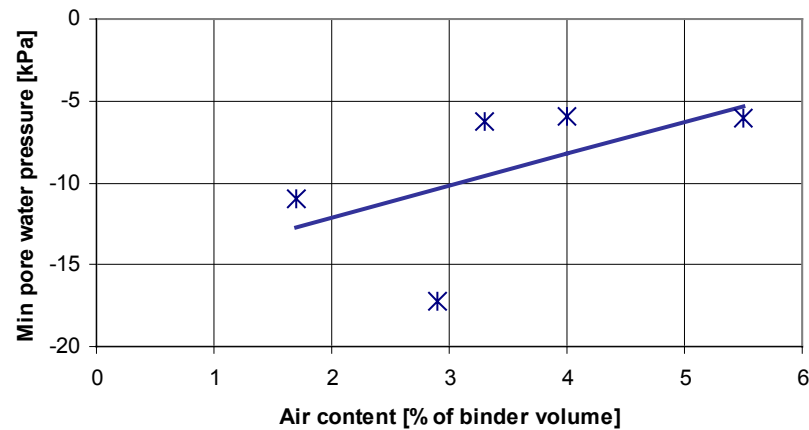


Figure 7.23: The minimum pore water pressure versus the air content

The results in Figure 7.23 show a tendency of decreasing minimum pore water pressure with lower air content. One of the tests with 350 litres of binder shows a deviation from the trend line. This is probably more an effect of the uncertainty in the method than a correct value. However, the result shows a clear tendency that lower air content will result in a lower minimum pore water pressure. It seems that the binder volume has a marginal effect on the pore water pressure, but this is difficult to verify because the air content is decreasing with increasing binder volume.

7.2.4 Water communication

7.2.4.1 Water flow between concrete layers

Because of the pressure gradient in the pore water between concrete layers of different age, water might flow between the concrete layers. It is assumed that water will move against the older concrete layer with lower pore water pressure. Differences in decrease rates of the pore water pressure between the single layer test of same age as the tested concrete layer in a 3-layer test is assumed to indicate water flow between the concrete layers.

The 3-layers concrete tests are carried out according to the procedure described in Section 4.4.2.3 with 2 hours between the concrete layers. The pore water pressure is measured in different locations in the concrete specimen during the testing, see Figure 7.24. The locations of the pressure gauges are also the same as for the single layer tests. The decrease rate of the pore water pressure is calculated for each measuring point in each test and presented in Table 7.7 to 7.10.

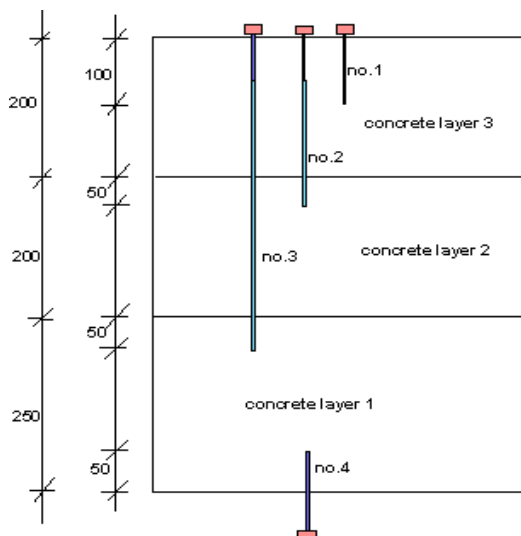


Figure 7.24: The set-up of the concrete test (from Section 4.4.2).

Table 7.7: The average decrease rate of the pore water pressure 100 mm from top in layer 3.

Pore water pressure 100 mm from top in layer 3, gauge no.1:	3-layers tests				single layer tests			
	VT208	VT211	VT216	VT219	VT206	VT209	VT223	VT224
The average decrease rate of the pore water pressure [Pa/min]	103	135	145	-	134	172	121	155
Average [Pa/min]	128				146			
Standard deviation [Pa/min]	22				23			

Table 7.8: The average decrease rate of the pore water pressure 50 mm from top in layer 2.

Pore water pressure 50 mm from top in layer 2, gauge no.2:	3-layers tests				single layer tests			
	VT208	VT211	VT216	VT219	VT200	VT221	VT223	VT224
The average decrease rate of the pore water pressure [Pa/min]	120	141	120	137	166	167	-	208
Average [Pa/min]	130				180			
Standard deviation [Pa/min]	11				24			

Table 7.9: The average decrease rate of the pore water pressure 50 mm from top in layer 1.

Pore water pressure 50 mm from top in layer 1, gauge no.3:	3-layers tests				single layer tests		
	VT208	VT211	VT216	VT219	VT221	VT223	VT224
The average decrease rate of the pore water pressure [Pa/min]	120	110	119	207	214	169	-
Average [Pa/min]	139				192		
Standard deviation [Pa/min]	46				32		

Table 7.10: The average decrease rate of the pore water pressure 50 mm from bottom in layer 1.

Pore water pressure 50 mm from bottom in layer 1, gauge 4:	3-layers tests				single layer tests		
	VT208	VT211	VT216	VT219	VT221	VT223	VT224
The average decrease rate of the pore water pressure [Pa/min]	108	86	82	123	167	133	150
Average [Pa/min]	100				150		
Standard deviation [Pa/min]	19				17		

The results from the pore water pressure measurements 100 mm from top in layer 3 is presented in Table 7.7. The result shows that the average decrease rate of the pore water pressure is slightly lower in the 3-layer tests compared to the single layer tests. This is opposite of what should be expected. It was expected approximately the same or higher decrease rate in the 3-layer tests compared to the single layer tests because of possible water flow to layer 2. The result indicates that this is not the case, maybe because of the 100 mm distance is too long (from the gauge to joint for layer 2).

The decrease rate of the pore water pressure measured 50 mm from top in layer 2 is presented in Table 7.8. These rates represent a normal situation in slipform with older concrete below and younger concrete above. The measurements are carried out close to the layer above and will therefore probably be more affected of this layer. The result shows a higher decrease rate of the pore water pressure in the single layer tests than the 3-layer tests. This indicates that water from the layer above has reduced the decrease rate of the pore water pressure in layer 2 in the 3-layer tests.

Measurements are carried out 50 mm from top and 50 mm from bottom in layer 1. The results are presented in Table 7.9 and 7.10 and show a higher average decrease rate of the pore water pressure in the single layer concrete tests, even at the bottom gauge. This indicates water flow from layer 2 to layer 1. The results is not significant for the measurements 50 mm from top in layer 1 (Table 7.9) because of high standard deviation, but it is significant at 0.05 significance level for the measurement at the bottom gauge in layer 1 (Table 7.10). It was unexpected that the result showed a lower decrease rate at gauge 4 for the 3-layer tests with a distance of 200 mm to the joint, when a distance of 100 mm to the joint in layer 3 had no effect on the decrease rate.

The high variation between some of the measurements indicates the uncertainty in the result. However, based on the number of measurements carried out and all the result from the 3-layer tests and the single layer tests, it can be concluded that the pressure gradient between the layers will affect the decrease rate of the pore water pressure. This means that water flows from layers with young concrete with positive pore water pressure and against concrete layers with lower pressure. The consequence of the pressure difference in early phase is that the concrete will lose water to the older concrete layer below. In later stage the same concrete will receive water from the layer above. The result of this is that the pressure gradient at the joint will be reduced and the pressure above and below the joint will be more even.

7.2.4.2 Surface drying

Menisci will be formed on an uncovered surface of fresh concrete exposed to water evaporation. This will result in a decreasing pore water pressure in the concrete. It can be assumed that water evaporation will result in a higher decrease rate of the pore water pressure because the effect of the water evaporation on the pore water pressure will be in addition to the effect of chemical shrinkage. Faster decrease rate of the pore water pressure is assumed to result in a lower minimum pore water pressure. However, less water might accelerate the time of minimum pore water pressure, which will reduce the effect of the higher pore water pressure decrease rate on the minimum pore water pressure.

Tests are carried out with the top surface covered by plastic (as normal) and tests without cover. An electric light was installed ~0.5 m above the concrete and heated up the fresh concrete surface in one test. The results are presented in Table 7.11. The same basis concrete was used in all tests.

Table 7.11: The effect of surface drying on the pore water pressure

	VT116 Covered surface	VT123	VT126 Uncovered surface	VT127 Uncovered surface with heat
Average pore water pressure decrease rate [Pa/min]	157	191	195	256
Minimum pore water pressure [kPa]	-14.4	-7.1	-20.8	-20.6
Time from minimum pore water pressure to initial set [minutes]	25	35	55	80

The decrease rate of the pore water pressure varies from 157 to 256 Pa/min. The lowest rates are measured in tests with covered surface and the highest rate is measured in test with uncovered surface and heat. The result show that increased water evaporation will result in a higher water communication in the pore systems and a higher decrease rate of the pore water pressure. This support the theory that water evaporation (in addition to the effect from chemical shrinkage) will result in a higher decrease rate of the pore water pressure.

The minimum pore water pressure is presented in Table 7.11. The minimum pore water pressure varies from -7.1 to -20.8 kPa and the highest minimum values are measured in the tests with cover on the top surface. This result would probably be more distinct with lower concrete height of the test block than the actual height of 60 cm. The time from minimum pore water pressure to initial set is less for tests with covered surface compared to tests with uncovered surface. This means that the minimum pore water pressure occur earlier when the surface is uncovered, which also will reduce the effect of the higher pore water pressure decrease rate on the minimum pore water pressure.

In Figure 7.25 and 7.26 the measured pore water pressure development versus time at top and bottom of the concrete block is presented. It can be seen that the test with uncovered surface and heat has a considerable earlier decrease in the pore water pressure at the top gauge compared to the pore water pressure result measured at the bottom of the concrete block. This result show that water evaporation has resulted in an earlier start of the decrease of the pore water pressure and will result in considerable pressure gradient along the height of the concrete block. In this instance the pressure gradient is about 20 kPa, see Figure 7.25 and 7.26. Also for the concrete test with uncovered surface

and no additional heat, the water evaporation has resulted in an earlier decrease of the pore water pressure. This has also caused a pressure gradient, but not as large as for the test with heat on top. The initial set occurs approximately at 6.5 hours for all tests.

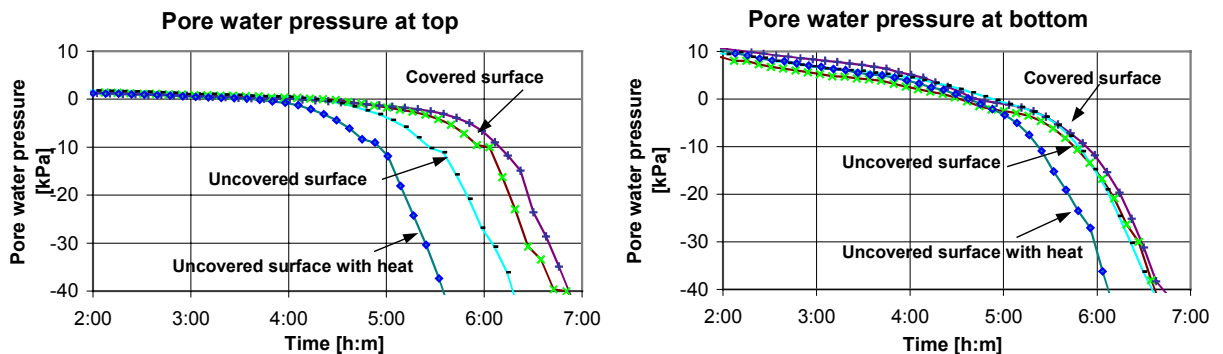


Figure 7.25 and 7.26: The pore water pressure measured at top and bottom of the concrete specimens

The result shows that the water evaporation from a fresh concrete surface seems to give a higher decrease rate of the pore water pressure, which also means that there is a good water communication in the concrete. The drying effect caused by water evaporation will result in an earlier decrease of the pore water pressure and result in a large pressure difference. Also the minimum pore water pressure will be lower with increasing water evaporation from the fresh concrete surface, but the minimum pore water pressure occur earlier for tests with uncovered surface, which have reduced the effect of the higher decrease rate on the minimum pore water pressure.

7.2.5 The effect of normal pressure

The concrete pressure in this context represents the total horizontal pressure from the concrete against the slipform panel and is the sum of the pressure from the liquid and the particles in the concrete. The focus in this section is primarily how the normal pressure will affect the development of the pore water pressure during the transition period when the concrete is in the elastic phase. The tests are carried out with 60 cm basis concrete in the rig, which have resulted in a normal pressure of approximately 7 kPa against the slipform panel after placing. This pressure corresponds approximately to the theoretical hydrostatic pressure.

When the concrete is in the elastic state, the concrete at the surface will deform slightly with increased normal pressure. This deformation of the concrete will increase the pore water pressure, slightly reduce the volume of the gas filled pores and the gas pressure will be higher. Based on this it can be assumed that the decrease rate of the pore water pressure will be lower when the normal pressure and also the deformation of the concrete are increased. The minimum pore water pressure will probably also be affected by the normal pressure. The lower decrease rate of the pore water

pressure will probably increase the minimum pore water pressure at higher normal pressure and opposite with decreasing normal pressure.

Tests with the same concrete mix are carried out where the panel stiffness and panel inclination has varied, this is described in detail in Section 7.3. The normal pressure at maximum lifting stress is listed in Table 7.12 and Table 7.13 together with the decrease rate of the pore water pressure and the minimum pore water pressure. Also the time from minimum pore water pressure occur to initial set is presented in Tables 7.12 and 7.13.

Table 7.12: The effect of the normal pressure on the pore water pressure (panel stiffness test)

	VT177	VT176	VT181	VT182	VT175	VT180
Normal pressure [kPa]	11.9	10.3	7.7	7.6	6.4	5.6
Average pore water pressure decrease rate [Pa/min]	93	112	102	127	134	162
Minimum pore water pressure [kPa]	-10.4	-10.5	-8.3	-6.6	-7.0	-3.7
Time from minimum pore water pressure to initial set [minutes]	30	10	25	10	65	60

Table 7.13: The effect of the normal pressure on the pore water pressure (panel inclination test)

	VT150	VT151	VT166	VT161	VT165	VT162	VT163	VT164
Normal pressure [kPa]	6.2	6.6	6.0	4.4	5.0	3.4	1.8	2.2
Average pore water pressure decrease rate [Pa/min]	107	118	122	123	139	155	139	126
Minimum pore water pressure [kPa]	-9.5	-11.5	-7.8	-7.5	-10.0	-6.3	-5.6	-6.2
Time from minimum pore water pressure to initial set [minutes]	90	50	70	60	65	100	85	95

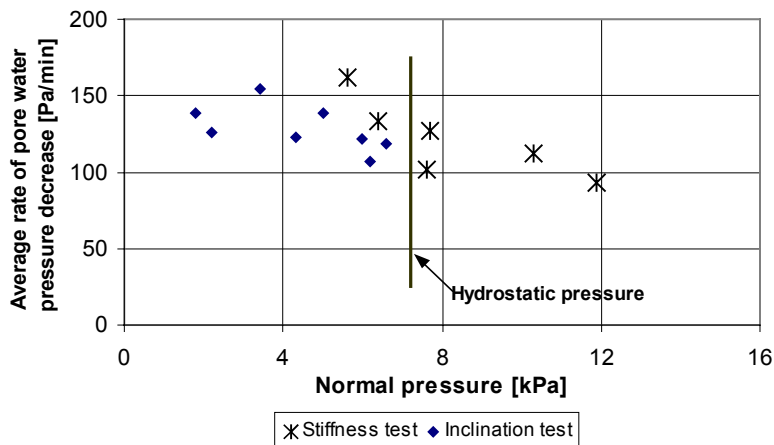


Figure 7.27: The pore water pressure decrease rate versus the normal pressure

The decrease rate of the pore water pressure versus the normal pressure is shown in Figure 7.27. The results are plotted both from the panel stiffness test (Table 7.12) and the panel inclination test (Table 7.13). The results show that the decreasing rate of the pore water pressure is slightly reduced with increasing normal pressure for both the stiffness test and also the inclination test. These results confirm the theory that higher normal pressure have increased the pressure in the pore water, which will result in a lower pore water pressure decrease rate. The results show also opposite that the decrease rate of the pore water pressure is increasing with lower normal pressure.

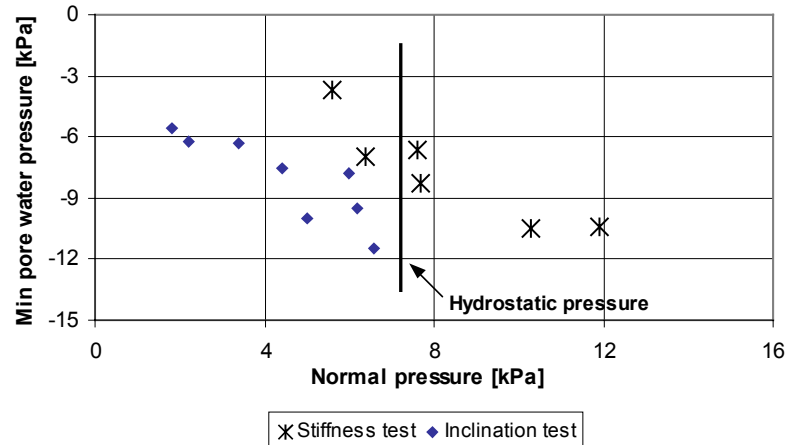


Figure 7.28: The minimum pore water pressure versus the normal pressure

The effect of the normal pressure on the minimum pore water pressure is plotted in Figure 7.28. The results show a clear tendency of decreased minimum pore water pressure with increasing normal pressure. It was expected that increased normal pressure should result in a higher minimum pore water pressure because of the lower pore water decrease rate, but this is not the case here.

It can be seen in Figure 7.29, that there is a tendency of delayed time for the minimum pore water pressure (period between the minimum pore water pressure and the initial set). A delayed time will result in lower minimum pore water pressure, which can explain the lower minimum pore water pressure even with lower decrease rate of the pore water pressure. A possible explanation is that the higher normal pressure has deformed the concrete at the sliding zone and squeezed out more water from the concrete to the surface. More water present at the sliding zone will maintain the capillary system and delay the time of minimum pore water pressure. A higher normal pressure can also result in a reduced water communication along the slipform panel, which have maintained a lower pore water pressure at the sliding zone even during lifting. Both instances can explain the delayed and lower minimum pore water pressure.

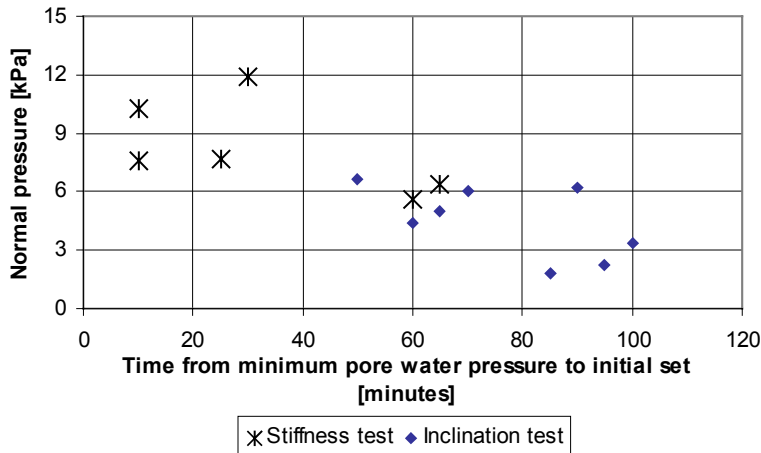


Figure 7.29: The correlation between the time from minimum pore water pressure to initial set and the normal pressure.

7.2.5.1 Correlation between minimum pore water pressure and normal pressure

Tests are carried out with different concrete height in the vertical slipform rig in order to vary the normal pressure. The result from these tests and the results from the inclination tests are plotted in Figure 7.30, which show the minimum pore water pressure versus the normal pressure. The result from the inclination tests is chosen because the normal pressure is decreasing already in early phase while the concrete is still plastic and will therefore represent concrete at different levels of normal pressure, see the normal pressure development for the inclination test in Figure 7.36.

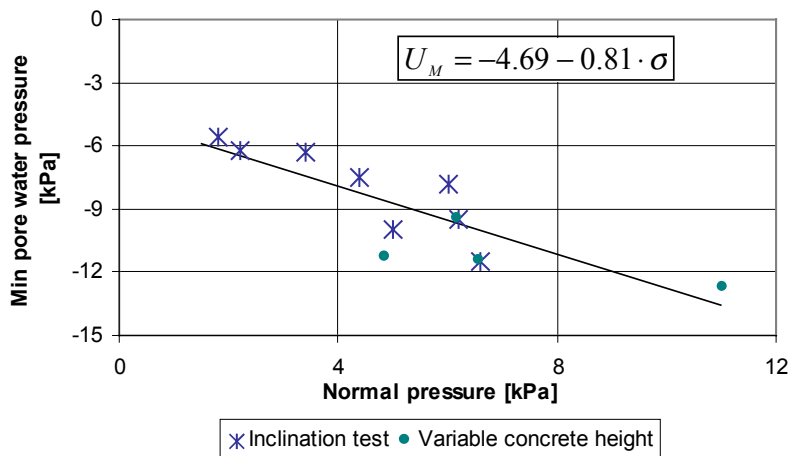


Figure 7.30: The correlation between the minimum pore water pressure and the normal pressure $U_M = \text{minimum pore water pressure [kPa]}, \sigma = \text{normal pressure [kPa]}$

The correlation between the data show that the minimum pore water pressure is decreasing with increased normal pressure. As described above, this is caused by the delayed time of minimum pore water pressure, which can explain the lower minimum pore water pressure with increased normal pressure. The linear correlation between the data in Figure 7.30 is significant at 0.05 significance level. The equation shown in the figure is used in the calculations carried out in Section 7.5.7.

7.2.6 The effect of the slipform technical parameters

The slipform technical parameters that are discussed in this section, are the effects of the lifting frequency and the lifting height on the pore water pressure. It is assumed that the decrease rate of the pore water pressure is not affected by the slipform technical parameters, primarily because the pore water pressure is measured 30 mm inside the concrete and should therefore be unaffected of any lifting of the slipform panel. The effect of the slipform technical parameters on the net static and sliding lifting stress is discussed in Section 7.5.2 and Section 7.5.3.

Table 7.14: Maximum lifting stress versus period between the lifts, 10 mm lifting height.

	VT148	VT144	VT145	VT150	VT151	VT146	VT147
Period between the lifts [min]	5	8	8	15	15	30	30
Pore water pressured decrease rate [Pa/min]	120	123	127	107	118	112	101
Min pore water pressure [kPa]	-3.1	-5.6	-4.4	-9.5	-11.5	-12.8	-14.4
Time from minimum pore water pressure to initial set [minutes]	70	70	80	90	50	45	45

Table 7.15: Maximum lifting stress versus lifting height (15 min between each lift)

	VT152	VT159	VT150	VT151	VT153
Lifting height[mm]	5	5	10	10	20
Pore water pressured decrease rate [Pa/min]	127	131	107	118	106
Min pore water pressure [kPa]	-37.3	-28.6	-9.5	-11.5	-5.7
Time from minimum pore water pressure to initial set [minutes]	10	30	90	50	75

The minimum pore water pressure is supposed to be affected by the lifting height and lifting frequency. It is assumed that longer period between the lifts will result in a lower minimum pore water pressure because the panel is disturbing the sliding zone each time it is lifted. Also lower lifting height, which will cause less disturbances at the interface compared to higher lifting heights, is assumed to decrease the minimum pore water pressure. The results are presented in Table 7.14 and 7.15. Note that the minimum pore water pressure represents the maximum sliding lifting stress and not the maximum static lifting stress, see Chapter 6.

The effect of the period between the lifts on the pore water pressure decrease rate is shown in Table 7.14. The results show that the decrease rate for the pore water pressure is somewhat reduced with lower lifting frequency, but the tendency is not consistent. The effect of the lifting height on the pore water pressure decrease rate is shown in Table 7.15. The results show a tendency of higher decrease rate of the pore water pressure when the lifting height is reduced, especially with 5 mm lifting height. This indicates that the disturbance from the lifting of the panel will somehow increase the negative pore water pressure at the sliding zone and it is more noticeable with increased lifting height.

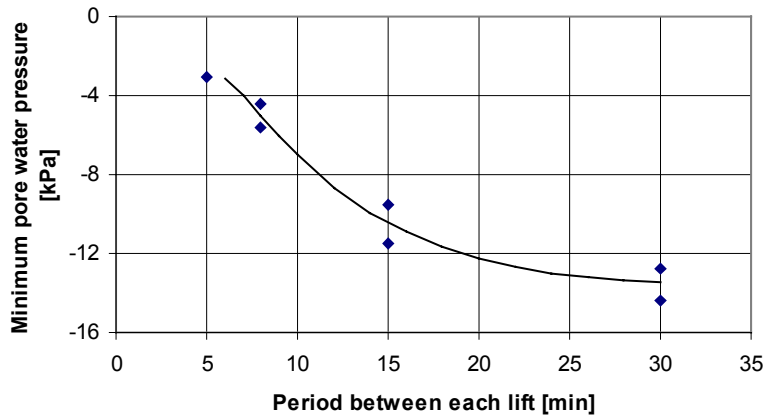


Figure 7.31: The effect of the period between the lifts on the minimum pore water pressure

The minimum pore water pressure is decreasing with increased period between the lifts, see Figure 7.31. The results show that minimum pore water pressure is decreasing from -3.1 kPa to -14.4 kPa, when the period between the lifts is increased from 5 minutes to 30 minutes. This confirms that the lifting of the panel will affect the minimum pore water pressure, because of disturbance of the sliding zone during lifting. There is also a tendency of delayed time of the minimum pore water pressure with longer periods between the lifts, which will result in a lower minimum pore water pressure.

The minimum pore water pressure is decreasing with decreased lifting height, see Figure 7.32. The results show that the minimum pore water pressure is decreasing considerably with decreased lifting height. This confirms the theory that decreased lifting height will result in less disturbance of the sliding zone compared to higher lifting height. The pore water pressure is therefore decreasing to a lower level before the pore water pressure is increasing or just disappears at the sliding zone. The period between the minimum pore water pressure and initial set show a tendency that the time of minimum pore water pressure is delayed with lower lifting height, which will result in a lower minimum pore water pressure.

The effect of the disturbance at the sliding zone and the minimum pore water pressure will also be discussed in Section 7.2.7.

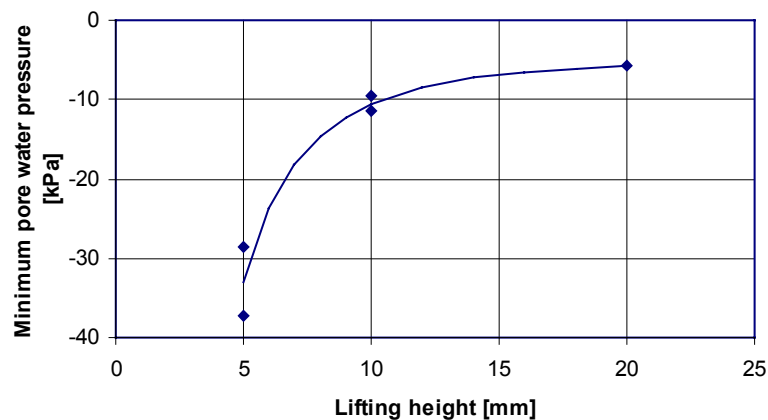


Figure 7.32: The effect of the lifting height on the minimum pore water pressure.

7.2.7 Parameters affecting the minimum pore water pressure

The minimum pore water pressure is defined as the pore water pressure at maximum sliding lifting stress. The minimum pore water pressure is probably the lowest pressure at the sliding zone and occurs just before the pore water pressure is increasing. In this Section, two theories (Hypotheses 3) will be discussed that deals with possible causes for the increase of the negative pore water pressure after minimum at the sliding zone.

Theory 1:

The free water content in the concrete at the sliding zone will be reduced as the cement hydration proceeds. When the water content is decreased to such a low content that the water meniscus cannot find new stable positions, the capillary system will collapse and the pore water pressure will increase or just disappear.

Theory 2:

The pore water pressure at the sliding zone is decreasing during lifting of the slipform panel. It is assumed that the pressure in the pore water at the sliding zone is increasing, because of an improved communication channel along the slipform panel during lifting. The pore water pressure at the sliding zone will, between two lifts, decrease until it is in equilibrium again with the pore water pressure in the bulk concrete. When the concrete start to be denser and the water communication slower, the time period will increase before the pore water pressure at the sliding zone will reach equilibrium again with the pore water pressure in the bulk concrete. The minimum pore water pressure is probably reached when the time period for equilibrium is longer than the period between two lifts. The pore water pressure will thereafter probably increase at the sliding zone.

The following observations have been found that supports Theory 2:

Figure 7.1 in Section 7.1.1 shows that the difference between the net static and sliding lifting stress is large during the transition period. After the transition period at initial set, the difference is approximately zero. It was expected that the adhesion caused by bonding should be even higher in this period. This indicates that the large difference between the static and sliding lifting stress during the transition period is not only caused by the adhesion. The pore water pressure is probably also increasing at the sliding zone during lifting, which can explain the large difference in the static and sliding lifting stress.

Figure 7.3 in Section 7.1.2 shows a linear correlation between the net static lifting stress and the effective pressure. This indicates that it is not only the adhesion that affects the difference, but also the pore water pressure, which is probably increasing at the sliding zone during lifting.

In Figure 7.10 and 7.11 in Section 7.1.5, the net static and sliding lifting stress is increasing slower the last period before maximum. This is probably because of the pore water pressure at the sliding zone is not in equilibrium with the pore water pressure in the concrete. This occurs when the concrete becomes denser and the communication in the concrete slower.

In Section 7.2.6, the minimum pore water pressure is decreased with decreasing frequency or lower lifting height. These results indicate that a communication channel is made along the slipform panel during lifting, which will result in that the negative pore water pressure is probably increasing. Higher lifting height or increased lifting frequency will probably increase the negative pore water pressure at sliding zone more than a lower lifting height or reduced lifting frequency.

Based on the above results and observations, it is most likely that the pore water pressure is increasing during lifting of the slipform panel, which can explain the large difference between static and sliding lifting stress during the transition period. When the concrete becomes dense, the period will be longer before the pore water pressure at the sliding zone is in equilibrium with the pore water pressure in the concrete. As a result of this, the pore water pressure (measured just before a new lift) at the sliding zone will be higher than the pore water pressure in the concrete. The minimum pore water pressure is probably reached when the period for equilibrium is longer than the period between two lifts. The pore water pressure at the sliding zone will thereafter increase as the slipform panel is lifted.

7.2.8 Summary

The main driving force for the pore water pressure is the chemical shrinkage that occurs because of the cement reaction. The effect of the chemical shrinkage depends on the particle concentration, the particle size distribution and the air content. But also water communication (between concrete layers, water evaporation from exposed surface etc.), the normal pressure and slipform technical parameters will affect the response of the chemical shrinkage on the pore water pressure.

The pore water pressure development can be characterised by the decrease rate of the pore water pressure and the minimum pore water pressure. The pore water pressure decrease rate is calculated as the average decrease rate at 0 kPa and at -10 kPa pore water pressure. The minimum pore water

pressure is defined as the pore water pressure at the time of maximum lifting stress. The minimum pore water pressure occurs just before the pressure is increasing or just disappear at the sliding zone. Higher particle concentration and a finer particle size distribution in the concrete will reduce the meniscus radius. Lower menisci radius will give a larger pressure gradient at the menisci and will result in a lower pore water pressure. Higher particle concentration and a finer particle size distribution (e.g. increased silica fume content) will result in a higher decrease rate of the pore water pressure and a lower minimum pore water pressure. Any delay of the minimum pore water pressure in relation to the initial set, will also result in a lower minimum pore water pressure. When the minimum pore water pressure occur earlier, the minimum pore water pressure will be higher.

The existing air in the concrete will act as a pressure release volume and reduce the effect of the chemical shrinkage on the pore water pressure. Increased air content will result in a lower decrease rate of the pore water pressure and a higher minimum pore water pressure. Addition of porous lightweight aggregate in the concrete will function as air reservoir and reduce the decrease rate of the pore water pressure. It seems that the decrease rate is more affected by the porosity of the aggregates than the quantity of the lightweight aggregate.

Pressure gradients that occur between two concrete layers will affect the decrease rate of the pore water pressure. Water will “flow” from layers with younger concrete without any negative pressure to concrete layers with lower pore water pressure. This will reduce the decrease rate in the concrete layer that receives the water. In later stage the same concrete that supplied the concrete layer below with water will receive water from the concrete layer above. The pressure gradient at the joint (between two concrete layers) will be more even as a result of the water communications between the concrete layers. The water communication is in general good in the concrete in this phase.

Water evaporation from fresh concrete surface will increase the decrease rate of the pore water pressure and large pressure gradients within the same concrete layer might occur. The minimum pore water pressure seems to decrease with increasing water evaporation from the fresh concrete surface. The water evaporation seems also to accelerate the time when the minimum pore water pressure occur, which will reduce the effect of the higher pore water pressure decrease rate on the minimum pore water pressure.

Increased normal pressure between the concrete and the slipform panel will reduce the decrease rate of the pore water pressure and the minimum pore water pressure will be lower. This is opposite of the usual correlation between the decrease rate and the minimum pore water pressure. Higher normal pressure will increase the deformation at the sliding zone and result in a higher pressure in the pore water, lower volume of the gas filled pores and higher gas pressure. This has resulted in a lower decrease rate of the pore water pressure. A higher normal pressure may result in a reduced water communication along the slipform panel, which have maintained a lower pore water pressure at the sliding zone even during lifting. This can explain the delayed and also lower minimum pore water pressure.

The lifting height and lifting frequency will affect the minimum pore water pressure. Lower lifting height and decreased lifting frequency will both result in a lower minimum pore water pressure. This is probably because the interface zone is disturbed each time the slipform panel is lifted. Less disturbance of the interface will result in a lower minimum pore water pressure.

The pore water pressure at the sliding zone is increasing during lifting of the slipform panel, which can explain the large difference between the static and sliding lifting stress during the transition period. When the concrete becomes dense, the period will be longer before the pore water pressure at the sliding zone is in equilibrium with the pore water pressure in the concrete. The minimum pore water pressure is probably reached when the period for equilibrium is longer than the period between two lifts. The pore water pressure at the sliding zone will thereafter increase as the slipform panel is lifted.

7.3 The normal pressure

7.3.1 Introduction

The concrete pressure against the vertical slipform panel is called the normal pressure. The concrete density and the concrete height (liquid head) are the main parameters controlling the normal pressure, but also concrete properties and vibration method might influence (Gardner, 1985). In a slipform, also parameters such as the inclination and the stiffness of the slipform panel, will affect the normal pressure.

7.3.2 The effect of the concrete density and the placing method

The concrete density is the main parameter that controls the normal pressure, but vibration during the concrete placement is assumed to increase the normal pressure compared to self-compacting concrete.

The initial inclination (without loads) of the slipform panel is for these tests -1.5 mm/m and the slipform rate is 40 mm/h for the lightweight concrete and 75 mm/h for the normal weight concrete. The normal weight concrete has a theoretical density of 2430 kg/m³ and the two lightweight concretes have densities of 1600 and 2005 kg/m³, respectively. The arrows in Figure 7.33 show the level of the theoretical hydrostatic pressure for each different concrete type. Also the variation in the normal pressure for each concrete test is shown. The four load cells on the rear side of the slipform panel measure the normal pressure during the tests, see Section 4.2.2.7. All tests are carried out as single layer tests.

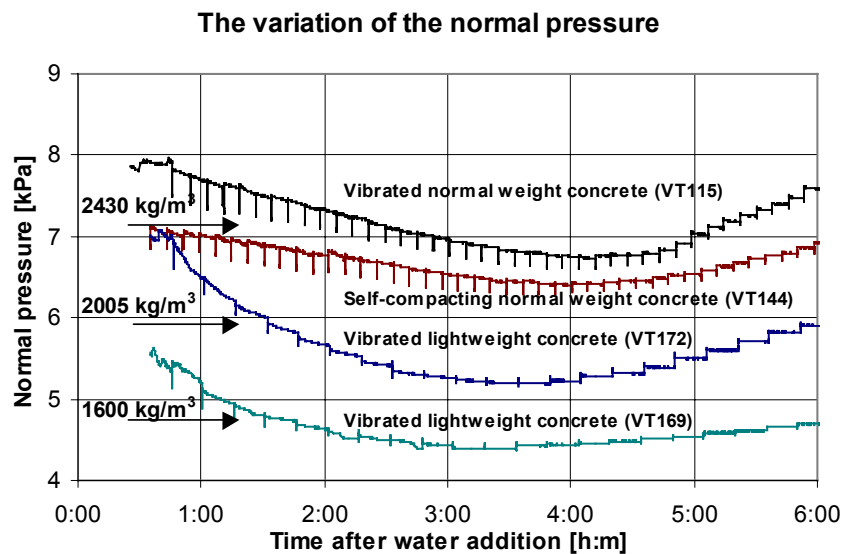


Figure 7.33: The effect of the density of the concrete and placing method on the normal pressure.

The effect of the concrete density and the placing method on the normal pressure is shown in Figure 7.33. The result shows that the normal pressure after concrete placing is 10 – 20 % higher than the theoretically hydrostatic pressure for the vibrated concrete tests, while the self-compacting concrete test show a normal pressure corresponding to the theoretical hydrostatic pressure. In spite of the negative inclination in the slipform panel, the normal pressure is decreasing as the slipform panel is lifted. It can be seen in Figure 7.34 that the normal pressure is decreasing during a single lift, but it is increasing immediately when the lifting stops and the slipform panel is moving 2 mm downwards (simulate activation of the breaks between the jacks and the jacking rod). It can be assumed that the concrete will be slightly deformed for each lift and each time the normal pressure is increasing. This deformation is probably the reason for the general decrease of the normal pressure as the panel is lifted. Concrete has normally a dilatant behaviour (Alexandridis, 1981), which means that the concrete will expand during shearing in the concrete (shearing will occur when the panel is lifted). This should result in a higher normal pressure during lifting, but this can not be detected here.

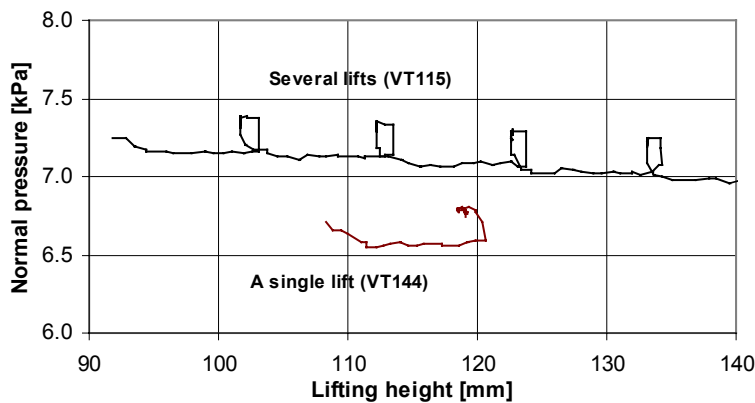


Figure 7.34: Typical variation in the normal pressure during lifting

After approximately 3.5 hours for the lightweight concrete and 4 hours for the normal concrete, the normal pressure starts to increase as the slipform panel is lifted. This is because of the concrete is in the transition period where it has elastic properties and further deformation caused by the negative initial inclination of the slipform panel will therefore be resisted.

7.3.3 The effect of the panel stiffness

The cantilever arm on each spring adjusts the stiffness of the slipform panel. The panel stiffness depends on the stiffness in each individual spring (four springs in total). Note that increased deformation in the spring will not result in a higher inclination with lifting, because the slipform panel is rolling against the spring when it is lifted, see Section 4.2.2.7. It is expected that the normal pressure will increase during the elastic phase with increased stiffness and negative inclination of the

slipform panel. The normal pressure will probably increase to a level above the theoretical pressure because the slipform panel is pushed against the concrete.

The single layer tests are carried out with stiffness in each spring that has varied from 145 N/mm to 11588 N/mm, see Table 7.16. The tests is carried out with -1.5 mm/m initial inclination of the slipform panel. The same type of self-compacting concrete has been used in all tests.

Table 7.16: The effect of the panel stiffness on the normal pressure at maximum lifting stress

	VT177	VT176	VT181	VT182	VT175	VT180
Stiffness in each spring [N/mm]	11588	1568	405	405	253	145
Normal pressure [kPa]	11.9	10.3	7.7	7.6	6.4	5.6

The effect of the stiffness of the slipform panel is presented in Figure 7.35. During the plastic phase, the normal pressure is decreasing as described in Section 7.3.2. After approximately 5 hours, the normal pressure starts to increase because of the concrete is now in the transition period where the concrete has elastic properties. The results show that the normal pressure is increasing faster with increased stiffness of the slipform panel as expected. It can also be seen that the pressure in a slipform can be considerable higher than the theoretical hydrostatic pressure, when the initial inclination of the panel is negative.

The normal pressure at maximum lifting stress is presented in Table 7.16. The result shows that increasing stiffness of the slipform panel has resulted in increased normal pressure at the time of maximum lifting stress.

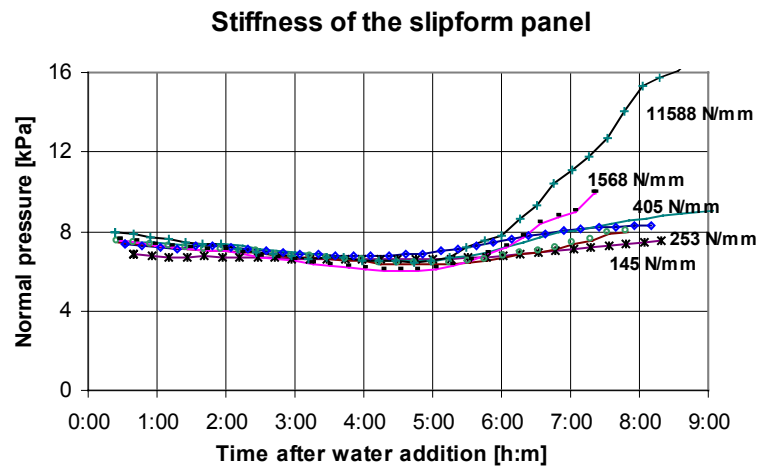


Figure 7.35: The variation in the normal pressure at different panel stiffness

7.3.4 The effect of the inclination

The inclination tests are carried out as single layer tests. The initial inclination of the slipform panel is adjusted from -1.5 mm/m to 5.5 mm/m, see Table 7.17. The panel stiffness is 405 N/mm (normal position for each spring) and self-compacting concrete is used in all tests. It is assumed that increased positive inclination will result in a decreased normal pressure as the slipform panel is lifted.

Table 7.17: The effect of the inclination on the normal pressure at maximum lifting stress

	VT 150	VT 151	VT 166	VT 161	VT 165	VT 162	VT 163	VT 164
Inclination [mm/m]	-1.5	-1.5	0	1.9	1.9	3.8	5.5	5.5
Normal pressure [kPa]	6.2	6.6	6.0	4.4	5.0	3.4	1.8	2.2

The results in Figure 7.36 show that the development of the normal pressure is almost the same for the tests the first two hours. It is probably the viscous properties in the self-compacting concrete that has dominated the development of the normal pressure. At 2 hours, the normal pressure is increasing probably because the concrete is passing a local uneven area on the slipform panel. After 2 hours, the normal pressure is decreasing faster with increased inclination of the slipform panel. The normal pressure in tests with no or negative inclination starts after approximately 5 hours to increase because of the elastic response in the concrete at this time. Positive inclination of the slipform panel has resulted in a decreased normal pressure.

The normal pressure at maximum lifting stress is presented in Table 7.17. The results show that increased positive inclination of the slipform panel has resulted in decreased normal pressure at the time of maximum lifting stress.

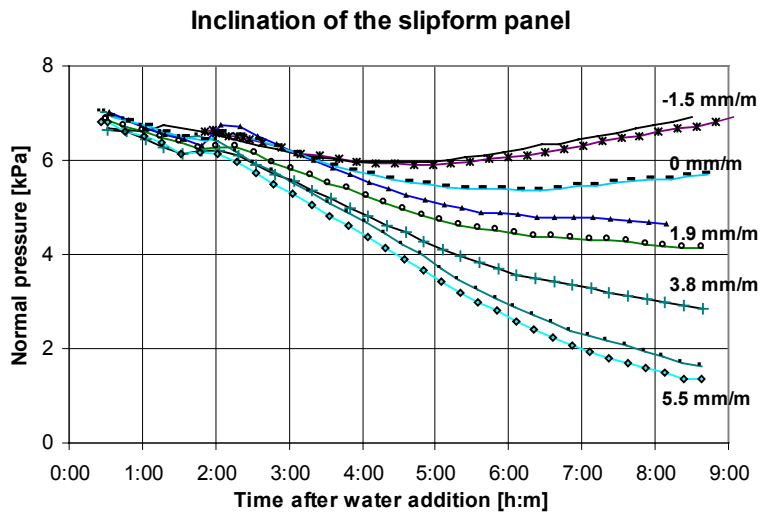


Figure 7.36: The variation in the normal pressure with different inclination of the slipform panel

7.3.5 Summary

The normal pressure against the slipform panel depends on the density of the fresh concrete and the placing method. Vibration of the concrete increases the normal pressure to a level 10 – 20 % higher than the theoretically hydrostatic pressure. For the single layer tests, the normal pressure is decreasing each time the slipform panel is lifted. The results show that the normal pressure is decreasing during the lift and is increasing when the lift is completed and the panel is moving 2 mm downwards.

The stiffness of the slipform panel seems to have no effect on the normal pressure during the plastic phase. During the transition period, where the concrete has elastic properties, the impact of the panel stiffness is significant provided a initial negative inclination of the slipform panel. The normal pressure will increase with increased stiffness in the slipform panel. The initial inclination of the panel will have an impact on the normal pressure in both the plastic and elastic phase. With increased positive inclination, the normal pressure will decrease as the panel is lifted. With no or negative inclination of the slipform panel, the normal pressure will increase during the transition period with elastic properties in the concrete. The results show that the normal pressure can be considerable higher than the theoretically hydrostatic pressure, when the slipform panel has an initial negative inclination.

These results depend on the fact that the concrete is not disturbed after placing. If revibration of the concrete is carried out in the plastic phase, the normal pressure will probably return to initial level, but this has not been verified by testing.

7.4 The impact of the material properties in the shear zone

7.4.1 Introduction

A shear zone will be formed close to the slipform panel when the panel is lifted. The shear zone consists of smaller particles (cement paste mixed with fine sand) and act as a lubricant during the plastic phase (Reichverger, 1979). The net lifting stress (friction) in this phase should depend on the internal friction and cohesion in the lubricant layer and the surface roughness of the slipform panel. The effect of the surface roughness of the slipform panel depends probably also on the thickness of the lubricant layer and location of the shear zone.

During the transition period at the beginning of the elastic phase, the shear zone will probably gradually be a sliding zone, where the slipform panel is sliding against the concrete. The surface properties of the now elastic lubricant layer in the sliding zone together with the surface roughness of the slipform panel, will decide the effect on the lifting stress. The initial roughness of the slipform panel might be changed because the surface roughness will partly be filled with grout of finer particles.

7.4.2 The lubricant properties

It is assumed that the initial workability of the concrete will affect the lifting stress during the plastic phase. Lower slump will increase the lifting stress because of higher viscosity in the lubricant layer in the shear zone. Also the particle shape will affect the internal friction. Angular particle shape (crushed aggregate) will probably increase the internal friction and result in a higher lifting stress in both the plastic and elastic phase.

The tests include concrete with self-compacting properties, low slump and concrete with crushed aggregate. The crushed aggregate is Mylonitt from Tau and the sieve curve is slightly different compared to the round shaped Gneiss-granite aggregate from Årdal that is used in all other tests (the sieve curves are shown in Figure 4.14). The slipform panel surface has a surface roughness $R_a = 1 \mu\text{m}$ and can be characterized as smooth. Information on workability of the concrete and type of aggregate used in these tests is shown in Table 7.18.

Table 7.18: Workability and type of aggregate used in the tests

	VT184	VT185	VT231	VT232	VT245	VT246
Rounded aggregate from Årdal	x	x	x	x		
Crushed aggregate from Tau					x	x
Slump [cm]	7	11.5	26	27	12	14

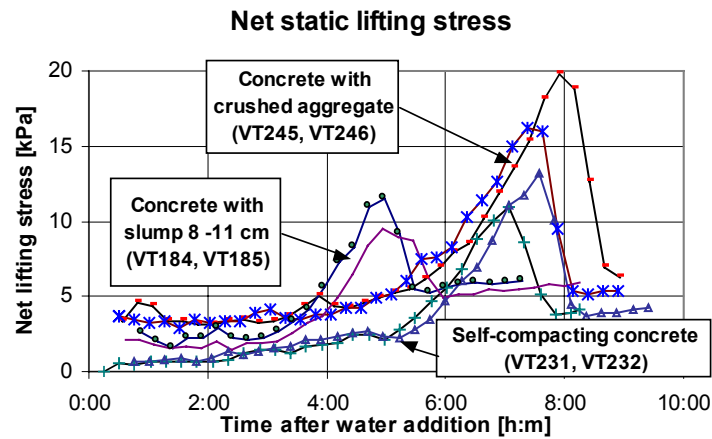


Figure 7.37: The effect of the aggregate surface on the lifting stress

The result in Figure 7.37 show that the use of crushed aggregate causes a relatively high lifting stress during the first 4 hours when the concrete is in the plastic phase. Compared to concrete with aggregate of rounded particle shape and the same level of workability (slump 8 – 14 cm), the static lifting stress is approximately 1.5 kPa lower. The lowest lifting stress is obtained in concrete tests with self-compacting properties, but the workability is decreasing with time and after approximately 6 hours, the net static lifting stress is at the same level as for the concrete test with lower slump. This means that the lifting stress is affected of both the particle shape and the workability during the plastic phase.

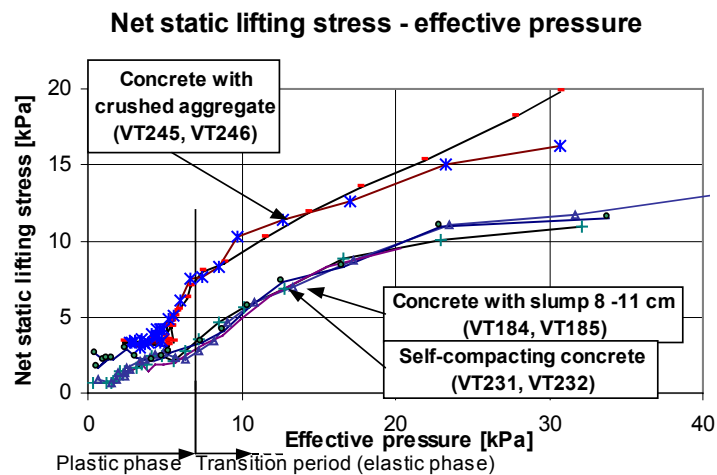


Figure 7.38: The net static lifting stress versus the effective pressure

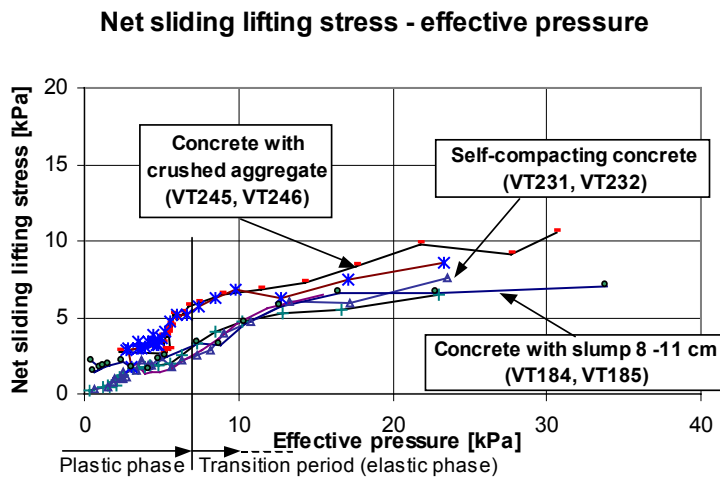


Figure 7.39: The net sliding lifting stress versus the effective pressure

The net static lifting stress versus the effective pressure is shown in Figure 7.38 and the corresponding presentation of the net sliding lifting stress is shown in Figure 7.39. The start of the transition period (marked in both figures) is defined at an effective pressure of 7 kPa (the normal pressure is approximately 7 kPa). When the effective pressure is above 7 kPa, the pore water pressure is negative, which means that the transition period has started.

During the plastic phase, it can be seen that both the static and sliding lifting stress is increasing more for concretes with crushed aggregate than concretes with rounded aggregate. Concretes with rounded aggregate have the same lifting stress at the end of the plastic phase independent of the initial workability as shown in Figure 7.38 and Figure 7.39. This means that the crushed aggregate will result in increased static and sliding lifting stress during the plastic phase, probably because of the increased shear resistance which crushed aggregate with angular particle shape probably is causing.

The static and sliding lifting stress is higher for the concretes with crushed aggregate also during the transition period where the concrete has elastic properties. At e.g. 10 kPa effective pressure, the static lifting stress for the concretes with crushed aggregate is almost twice as large compared to concretes with rounded aggregate, which means that the friction coefficient is also twice as large for the concretes with crushed aggregate.

7.4.3 Rough slipform panel

Test is carried out where the roughness of the slipform panel has been smooth ($R_a \sim 1 \mu\text{m}$) and very rough ($R_a \sim 10 \mu\text{m}$), see Section 5.2.3. The rough surface is obtained by sand blasting. It is assumed that higher surface roughness should result in a higher lifting stress both in the plastic phase and

during the transition period. The same type of self-compacting concrete is used in all tests. The results are listed in Table 7.19.

Table 7.19: The maximum net static/sliding lifting stress and the minimum pore water pressure.

	Rough panel surface			Smooth panel surface		
	VT227	VT228	VT230	VT224	VT231	VT232
Maximum net static lifting stress [kPa]	8.0	7.6	7.9	10.1	11.0	13.2
Maximum net sliding lifting stress [kPa]	4.5	4.2	4.7	7.5	6.5	7.6
Minimum pore water pressure [kPa]	0.5	0	-1.6	-15.4	-15.9	-10.2
Time from minimum pore water pressure to initial set [minutes]	110	90	105	35	40	55

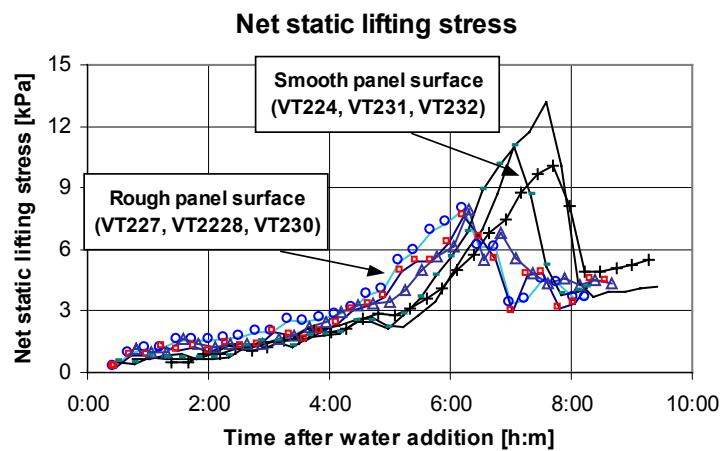


Figure 7.40: Net sliding lifting stress development

In Figure 7.40, the net static lifting stress development is shown. The results show that the static lifting stress is almost the same or only slightly higher the first 5 hours for tests carried out with rough panel surface. This is probably because of the high workability (high slump) in the self-compacting concrete that has reduced the effect of the rough panel surface. The rough surface has probably been filled with cementious grout (lubricants) from the concrete, and the shear zone has in this phase been in the remaining part of the lubricant layer between the panel and the concrete substrate. Concrete with less content of fines and thinner lubricant layer would probably have obtained a higher lifting stress.

After 5 hours, it can be seen that the static lifting stress is increasing faster for tests carried out with the rough panel surface compared to tests carried out with the smooth panel surface. This is probably because the concrete workability has decreased and the effect of the rough panel surface becomes more evident.

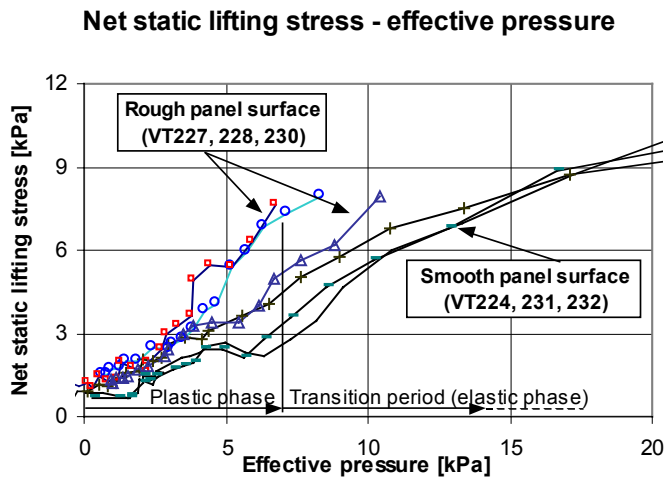


Figure 7.41: The net static lifting stress versus the effective pressure

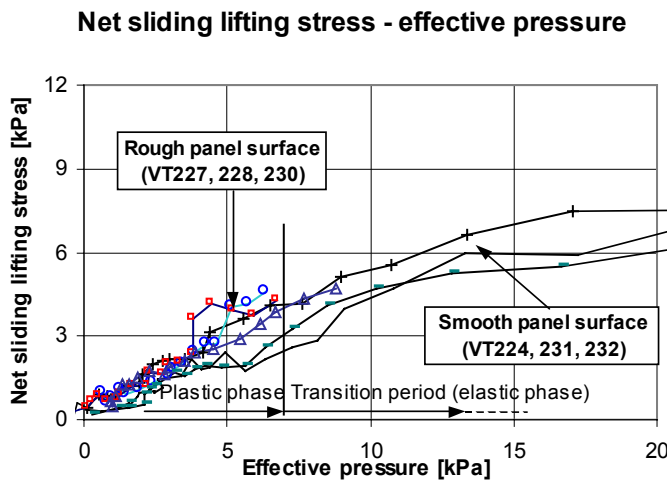


Figure 7.42: The net sliding lifting stress versus the effective pressure

In Figure 7.41 and Figure 7.42, the net static/sliding lifting stress is plotted as function of the effective pressure. It can be seen also here that the lifting stress is increasing more during the last part of the plastic phase for tests carried out with the rough panel surface than tests carried out with smooth panel. The maximum lifting stress is reached for these tests at the beginning of the transition period. This means that the maximum lifting stress has occurred at a pore water pressure of approximately 0 kPa (see also Table 7.19), which indicates that the capillary system has collapsed as a result of the high panel roughness. The collapse is probably because of air has been introduced in

the sliding zone and punctured the incipient vacuum. This has resulted in a lower effective pressure and consequently a lower maximum net static and sliding lifting stress compared to the tests carried out with a smooth slipform panel. The time from minimum pore water pressure to initial set is longer for tests carried out with a rough slipform panel, which also confirm that the rough slipform panel has punctured the incipient vacuum since the time of minimum pore water pressure occurred so early.

7.4.4 Summary

The lubricant layer that is formed in the shear zone close to the slipform panel consists probably of cement paste mixed with finer sand. Lower workability in the concrete and also in the lubricant layer will result in a higher lifting stress compared to concrete with higher workability. The lifting stress will increase with decreasing workability. During the transition period, when the concrete has elastic properties, the lifting stress seems to be independent of the initial workability. Crushed aggregate will also increase the lifting stress both in the plastic phase and during the transition period.

The lifting stress will increase when rough panel surface is used, but the effect of the rough panel will be low with high workability (high slump) in the concrete. This is because the panel surface is filled with cementitious grout (lubricants) and the shear zone is in the remaining part of the lubricant. At the end of the plastic phase, the lifting stress will be considerably higher when rough panel is used, but the maximum lifting stress occur early and at the beginning of the transition period because of the capillary system seems to be punctured by the rough panel surface. This has resulted in a lower maximum net static and sliding lifting stress for concrete carried out with rough panel compared to tests carried out with a smooth slipform panel.

7.5 Operational parameters

7.5.1 Introduction

The operational parameters that will be discussed in this section are the effect of the lifting frequency and the lifting height on the maximum net static and sliding lifting stress. Also a discussion on the effect of the lifting stress on the slipformed concrete surface is carried out. Discussion of the results from the single layer test will be included in this section in order to verify that these results represents each individual layer and implicit all layers in a slipform.

7.5.2 Lifting frequency

The difference between the static and sliding lifting stress is caused by the adhesion and the decreasing effective pressure during lifting according to the results in Section 7.2.7. The lifting frequency, which represents the time between two lifts, is assumed to affect the static lifting stress mainly during the transition period. Increased time between the lifts in this period is supposed to increase the static lifting stress. The lifting stress will during a lift decrease to a minimum that represents the sliding lifting stress. It is assumed that the sliding lifting stress should be only minor affected of the lifting frequency.

In these tests, the effect of the lifting frequency on the maximum static and sliding lifting stress is investigated. The concrete tests are carried out with both normal weight and lightweight concrete. The lifting height for all tests is 10 mm.

7.5.2.1 Tests with normal weight concrete

The period between the lifts has varied from 5 to 30 minutes for the concrete tests. The selected period between the lifts is kept constant during the whole test period for each concrete test. The same kind of self-compacting concrete is used in all tests.

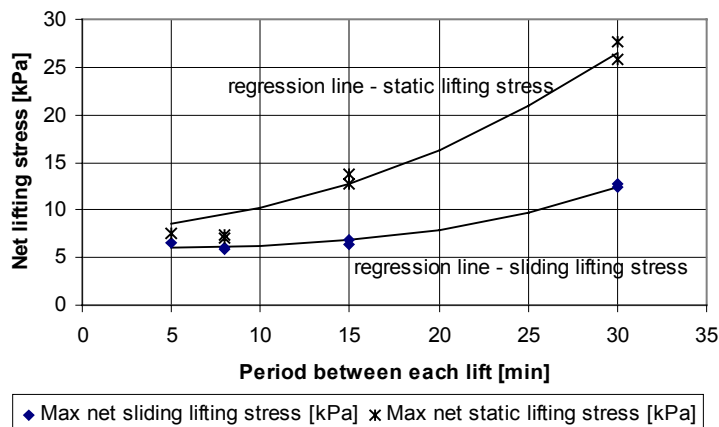


Figure 7.43: The effect of the period between the lifts (lifting frequency) on the maximum net static and sliding lifting stress (10 mm lifting height)

Table 7.20: Maximum lifting stress versus period between the lifts, 10 mm lifting height.

	VT148	VT144	VT145	VT150	VT151	VT146	VT147
Period between the lifts [min]	5	8	8	15	15	30	30
Maximum net sliding lifting stress [kPa]	6.5	6.1	5.8	6.3	6.9	12.1	12.8
Maximum net static lifting stress [kPa]	7.6	7.0	7.3	12.7	13.7	23.8	27.7

In Figure 7.43, it can be seen that the maximum net static lifting stress is increasing with increased period between the lifts. The maximum net static lifting stress is increasing more than 3 times when the period between each lift is increased from 8 to 30 minutes. The maximum net sliding lifting stress is almost constant in tests carried out with 5 to 15 minutes between the lifts, see Table 7.20 or Figure 7.43. When the period is increased to 30 minutes between the lifts, the maximum net sliding lifting stress is significantly increased. The slope of the regression line is considerably steeper for the static lifting stress compared to the sliding lifting stress. This confirms that it is primarily the maximum net static lifting stress that is affected by the period between the lifts, but also the sliding lifting stress will be affected if the period between the lifts is long, in this instance 30 minutes.

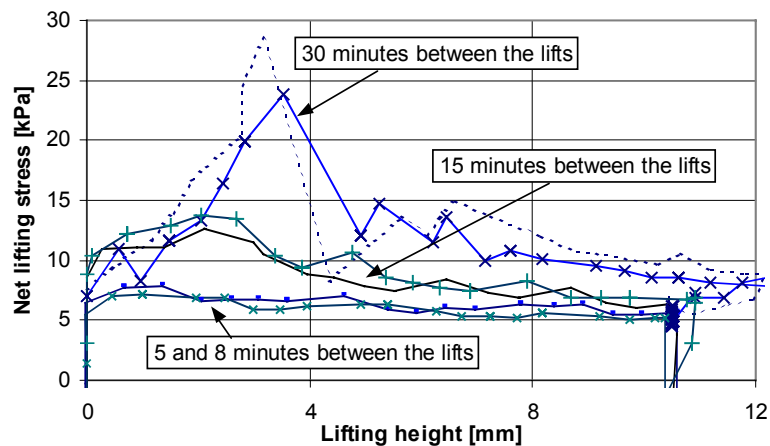


Figure 7.44: The lifting stress variation during a single lift with lifting height of 10 mm

The lifting stress variation during a single lift, measured in the transition period for each test, is presented in Figure 7.44. After the peak level is reached, the lifting stress is decreasing as the lifting proceeds. With relatively low initial static lifting stress, it seems that the lifting stress is stabilized at a minimum level during the 10 mm lift. With higher initial static lifting stresses, the 10 mm lifting height seems not to be sufficient in order to stabilize the stress at the same minimum level. The effective pressure is probably not at minimum at the sliding zone or the adhesion is not completely broken, when the sliding lifting stress is not stabilized. This is probably the reason why the net

sliding lifting stress is higher when the period between the lifts is 30 minutes. It seems that the lifting stress is not stabilized at a minimum level when the static lifting stress is too high.

The regression lines are presented in Figure 7.43 and calculated in Section 7.5.4.

7.5.2.2 Tests with lightweight concrete

The period between the lifts varied from 15 to 30 min in tests carried out with the same type of lightweight concrete. Lightweight concrete is supposed in general to obtain a lower lifting stress than normal weight concrete because of the lower effective pressure in the lightweight concrete (see Section 7.2.3.3). With lower effective pressure in the concrete will also the static lifting stress be lower according to the result in Section 7.1. It can be expected that the static lifting stress will increase with increased period between the lifts, but because of the lower effective pressure in the concrete, the static lifting stress is expected in general to be low.

Table 7.21: Maximum lifting stress versus period between lifts, 10 mm movement length.

	VT171	VT202	VT201
Period between the lifts [min]	15	24	30
Maximum net sliding lifting stress [kPa]	4.5	4.2	5.1
Maximum net static lifting stress [kPa]	5.5	7.1	8.2

The results in Table 7.21 show that the maximum net sliding lifting stress vary between 4.2 and 5.1 kPa. This variation is not systematic related to the period between the lifts, which indicate that the maximum sliding lifting stress for lightweight concrete might be independent of the period between the lifts.

The maximum net static lifting stress is increasing almost linear from 5.5 kPa to 8.2 kPa when the period between the lifts is increased from 15 to 30 minutes. The level of the maximum static lifting stress is considerable lower than for similar tests carried out with normal weight concrete. This confirms the theory that the level of the static lifting stress depends on the level of the effective pressure in the concrete.

It can be concluded that the period between the lifts has a considerable impact on the (maximum) net static lifting stress, especially when the period between the lifts is approaching 30 minutes. Lightweight concrete has in general a lower maximum net static and sliding lifting stress compared to normal weight concrete. This is because the effective pressure in lightweight concrete is in general lower than in normal weight concrete according to Section 7.2.3.3.

7.5.3 The effect of the lifting height

The lifting stress will decrease during a lift. It is assumed that the lifting stress will decrease until a certain minimum level, which represents the “true” sliding lifting stress between the materials

involved in the sliding zone. It is assumed that it is primarily the sliding lifting stress that will be effected of the lifting height.

The effect of the lifting height on the maximum static and sliding lifting stress is tested. Tests are carried out with lifting heights from 5 to 20 mm and a constant period between the lifts of 15 minutes. The results are presented in Table 7.22.

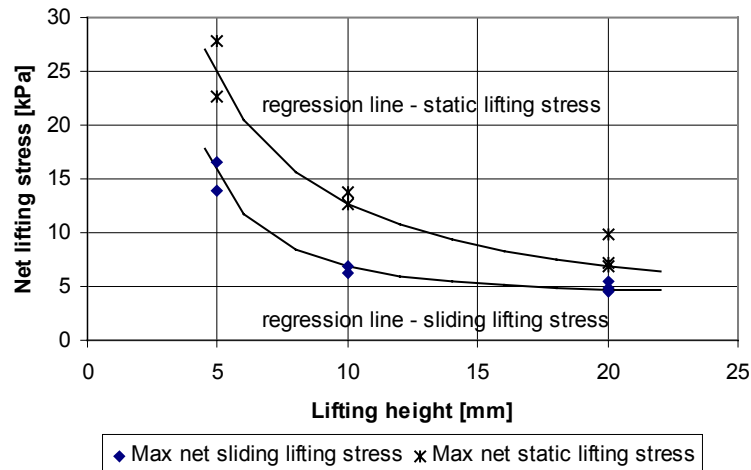


Figure 7.45: The effect of lifting height on the maximum net static and sliding lifting stress (15 minutes between the lifts)

Table 7.22: Maximum lifting stress versus lifting height (15 min between each lift)

	VT152	VT159	VT150	VT151	VT153	VT221	VT223
Lifting height[mm]	5	5	10	10	20	20	20
Maximum sliding lifting stress [kPa]	13.9	16.6	6.3	6.9	4.6	5.4	4.9
Maximum static lifting stress [kPa]	22.7	27.8	12.7	13.7	6.8	9.9	7.2

The maximum net sliding lifting stress is increasing with decreased lifting height as shown in Figure 7.45. The results show that the lifting height has an impact on the sliding lifting stress and is increasing considerably for lifting heights below 10 mm. The maximum net sliding lifting stress is decreasing slightly when the lifting height is increased from 10 to 20 mm.

The maximum net static lifting stress is also increasing with decreased lifting height. This must be because the minimum sliding lifting stress is not reached during the previous lift and the sliding lifting stress has therefore affected the level of the static lifting stress.

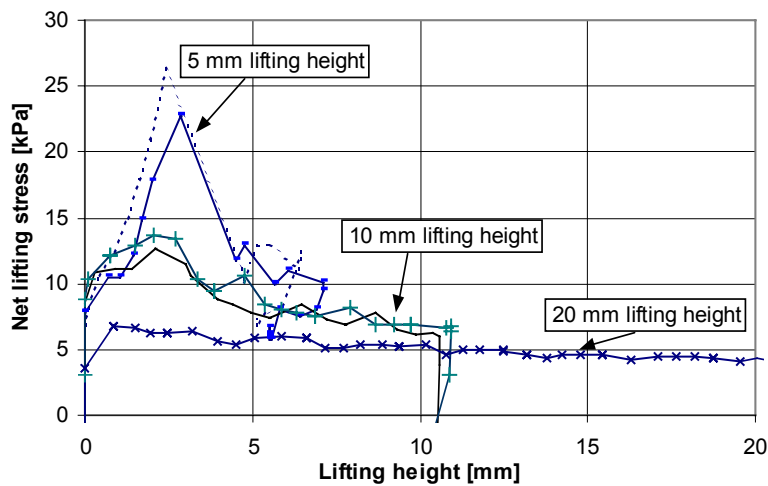


Figure 7.46: The lifting stress variation during a single lift when the period between the lifts is 15 minutes

The impact of the lifting height during the transition period can be seen in Figure 7.46. With 20 mm lifting heights, the net lifting stress is stabilized at a minimum level during the lift. It can be seen for both 10 and 5 mm lifting heights that the lifting stress is not stabilized during the lift. Extended lifting height will probably result in a lower sliding lifting stress. When the lifting stress is not stabilized during lifting, means that the effective pressure at the sliding zone is not reduced to a minimum or the adhesion is not completely broken.

Based on the result presented in Figure 7.45, it seems the sliding lifting stress is stabilized at minimum and the effect of the static lifting stress has almost disappeared when the lifting height is above approximately 15 mm. At lower lifting heights, the minimum lifting stress is not reached during a lift. The next lift will consequently start at a higher lifting stress compared to tests with larger lifting heights. This is demonstrated in Figure 7.45 and Figure 7.46.

The regression line in Figure 7.45 is calculated in next Section.

7.5.4 Calculation of the maximum lifting stress at different lifting heights

A regression analysis is carried out for the results for maximum net lifting stress and the period between the lifts in Table 7.21 and the maximum net lifting stress and the lifting height in Table 7.22. The regression is carried out in order to identify the impact of the lifting height at different slipform rates.

The regression equation for the maximum sliding lifting stress is shown in Eq. 7.3. The regression has obtained a R^2 -coefficient of 97 %, which indicates high correlation between the data. The

regression equation for the maximum static lifting stress is shown in Eq.7.4 and has a R²-coefficient of 94 %, which indicates also a high correlation between the data for the chosen regression model.

$$\text{Eq. 7.3} \quad F_{AGM} = 3.25 + 0.238 \cdot 10^{-3} \cdot t_i^3 + \frac{278}{l_h^2}$$

$$\text{Eq. 7.4} \quad F_{ASM} = -3.58 + 20.4 \cdot 10^{-3} \cdot t_i^2 + \frac{117}{l_h}$$

where F_{AGM} = maximum net sliding lifting stress [kPa]
 F_{ASM} = maximum net static lifting stress [kPa]
 t_i = period between the lifts [minutes]
 l_h = lifting height [mm]

The regression curves are presented in Figure 7.43, where the period between the lifts has varied from 5 minutes to 30 minutes and in Figure 7.45, where the lifting height has varied from 5 mm to 20 mm. In Figure 7.47 and Figure 7.48, the effect of the lifting height at different slipform rates is shown. The plotted curves in all figures are based on Eq. 7.3 or Eq. 7.4. It should be emphasized that the presented curves exceed the testing range for the period between the lifts and consequently the interpretation of the results should be careful.

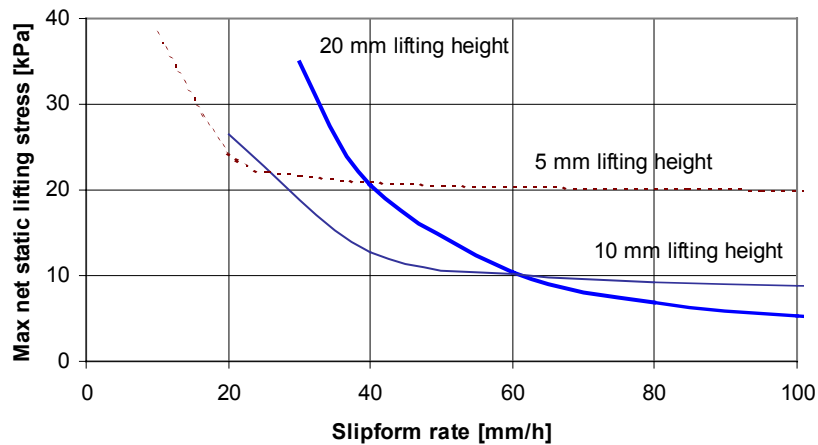


Figure 7.47: The effect of the lifting height on the maximum net static lifting stress

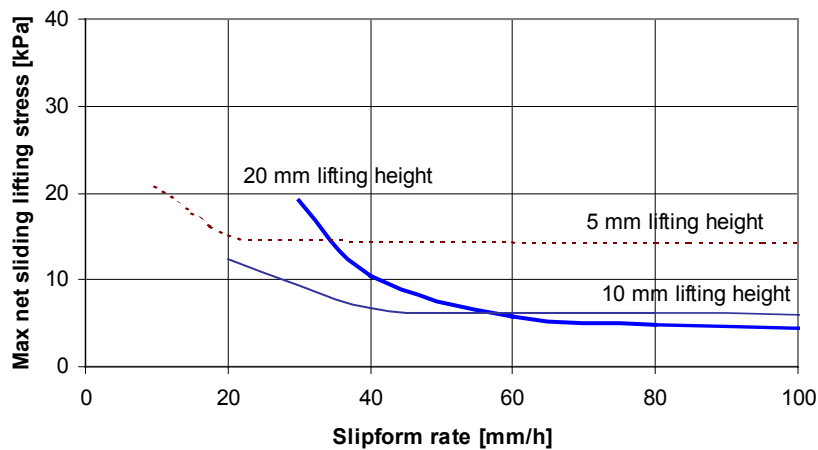


Figure 7.48: The effect of the lifting height on the maximum net sliding lifting stress

The result shows that 20 mm lifting height have obtained the lowest maximum net static and sliding lifting stress above slipform rates of 60 mm/h (1.44 m/d). This is because the lifting height is sufficient to completely break the adhesion and reduce the effective pressure to a minimum at the sliding zone, consequently both the maximum static and sliding lifting stress are reduced. The impact of the period between the lifts is more distinct at slipform rates below 60 mm/h. Also the maximum lifting stress is increasing for the 20 mm lifting height because the period between the lifts is 20 minutes or less when the slipform rate is 60 mm/h or lower.

The lowest maximum lifting stress is obtained with 10 mm lifting height at slipform rates below 60 mm/h. The maximum static and sliding lifting stress are increasing for 10 mm lifting height below slipform rate of 40 mm/h. Lifting height of 5 mm have in general given high maximum static and sliding lifting stress because the effective pressure at the sliding zone is not reduced to a minimum during the lift. This has resulted in a high maximum lifting stress even with short period between the lifts.

7.5.5 Summary for the lifting height and the lifting frequency

The result shows that the lifting height has a considerable impact on the maximum lifting stress. Lowest lifting stress is obtained at lifting height more than 15 mm (according to Section 7.5.3) for slipform rates more than 60 mm/h. For slipform rates less than 60 mm/h, 10 mm lifting height resulted in the lowest maximum static and sliding lifting stress.

The lifting frequency has a considerable impact on the level of the maximum net static lifting stress. The maximum net static lifting stress is increasing more than three times when the frequency is changed from 8 to 30 minutes between the lifts. The sliding lifting stress will also be affected by the lifting frequency if the effective pressure at the sliding zone is not reduced to a minimum during the lift. During lifting, the lifting stress is decreasing as the effective pressure is decreasing and the

effect of the adhesion is reduced at the sliding zone. When the lifting stress is stabilized on a minimum level, the adhesion is completely broken and the effective pressure is at minimum at the sliding zone zone. In order to reach a stabilized minimum sliding lifting stress, an increased lifting height is required.

7.5.6 The effect of the lifting stress on the concrete surface

The displacement of the concrete is measured in the cover zone for most of the tests carried out in the vertical slipform rig. The displacement is measured by two “nails” located 15 and 25 mm from the slipform panel, see Section 4.2.2.9. The result from these measurements is shown in Figure 7.49 for three concrete tests, which represents maximum static lifting stress from approximately 10 kPa to more than 30 kPa. Only the results from the measurements with the “nail” located 15 mm from the surface are shown.

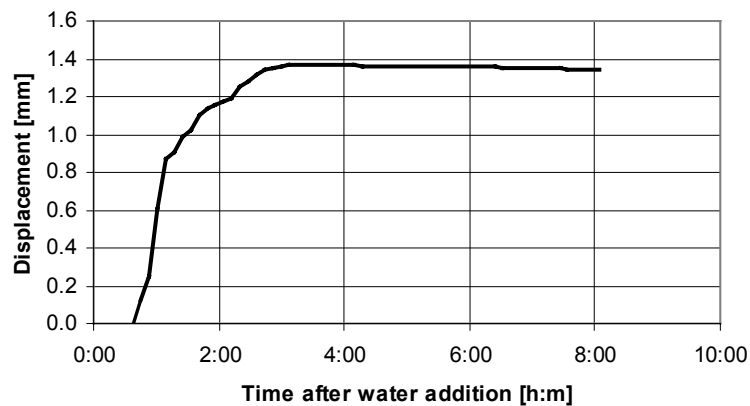


Figure 7.49: Typical displacement in the concrete 10 - 20 mm from the concrete surface in tests carried out in the vertical slipform rig.

In Figure 7.49, it can be seen that the displacement occurs during the first hours when the concrete is still plastic. In the elastic phase, which starts approximately after 5 hours, the additional displacement of the concrete is zero. The total displacement during a test is only 1.2 – 1.4 mm, which can be characterized as low. A probably reason for this low displacement is the effective pressure, which will increase the shear strength in the concrete. The same effective pressure is also causing the increased lifting stress, which means that the shear strength in the concrete is increasing when the lifting stress is increasing. Higher friction is resisted by the higher shear strength. This is probably the main reason why no surface damages have been observed during the single layer tests.

The static lifting stress for some of the single layer tests in the vertical rig has been above 30 kPa, which correspond to a lifting force above 10 000 N (contact surface area is 0.36 m²). The weight of the whole concrete block is approximately 2600 N, which means that the concrete surface has been exposed for a force almost 4 times the total concrete weight. The reason that the concrete block is not lifted is because the concrete is restrained to the three walls that surround the concrete block.

The effective pressure that is the main cause for the high lifting stress is also applicable for these three walls. This means that the static friction that needs to be overcome in order to lift the concrete block are at the same level (or probably higher) between these three walls and the concrete. In addition the contact area between the concrete and the three walls is much larger compared to the contact area between the slipform panel and the concrete, which also is a reason itself that the concrete block is kept in place.

Surface damages will theoretically occur when the static lifting stress is higher than the shear strength in the concrete or lubricant layer near the slipform panel. This seems not to be possible when operating with concrete of same age or with concrete at the same stage in the hardening process.

7.5.7 One layer - several concrete layers

7.5.7.1 Introduction

Most of the concrete tests have been carried out as a single layer test. A single layer test means a test consisting of concrete from the same batch of same age. It has been assumed that the single layer tests represent each individual layer in a slipform. In order to verify that the measured lifting stress in the single layer represents also the lifting stress in a slipform with several layers, a comparison has been carried out between the single layer tests and 3-layer concrete tests.

7.5.7.2 Interaction between the concrete layers

The lifting stress development for each concrete layer in a slipform can be calculated directly based on the result from the single-layer test. However, also the effect of the interaction between the concrete layers and the placing method must be taken into consideration when calculating the total net lifting stress. Based on the results from Section 7.2, the following parameters should be considered:

- Water communication between the concrete layers (Section 7.2.4.1)
- The normal pressure (Section 7.2.5)
- Drying of the concrete surface on top (Section 7.2.4.2)
- Vibration of the concrete (Section 7.2.3.2)

The water will flow from the younger concrete layer in the direction of the older concrete layer because of the pressure difference in the pore water between the concrete layers. This will result in a more gradual pore water pressure gradient at the joint between the concrete layers. Water will be submitted to the concrete layer below in early phase and water will be received from the layer above in later phase. It is assumed that this situation will not have any large effect on the lifting stress. In these tests the 3-layer tests might have an effect on layer 1 (first layer placed), which will not lose any water in early phase, but receive water from the layer above in later phase. The opposite situation occurs for layer 3 (last layer), which will lose water in early phase, but not receive any water in later phase. The effect of this might be that the lifting stress would be slightly lower than expected for layer 1 and slightly higher for layer 3. It is difficult to calculate this effect on the lifting

stress and any possible effect will therefor not be taken into consideration during the following calculations.

The normal pressure will also affect the lifting stress. Higher normal pressure will result in a higher lifting stress based on the result from Section 7.2.5. This effect will be taken into consideration when calculating the lifting stress.

The water at the concrete surface will evaporate when the surface is exposed for dry air. This will probably result in a higher lifting stress, if the concrete is not covered with plastic before a new concrete layer is placed on top. In these tests, the concrete surface is only covered with plastic after the last layer (layer 3) is placed, while layer 1 and 2 has been unprotected approximately 2 hours each. It is assumed that the effect in this instance is marginal (no sunlight or dry wind) and has not be taken into consideration in the calculations.

When a concrete layer is vibrated, also the layers below will be more or less affected of the vibration. This will result in improved consolidation and backsliding of the concrete layers in plastic phase below if any positive inclination of the slipform panel. This effect will not be taken into consideration because it is mostly self-compacting concrete used in these tests.

7.5.7.3 Verification procedure

The 3-layers concrete tests are carried out in the vertical slipform rig with 2 hours between the layers, see Section 4.4.2.3. The layer thickness and the theoretical hydrostatic pressure against the slipform panel for each layer are shown in Figure 7.50. The concrete density used in the calculations is 2400 kg/m^3 .

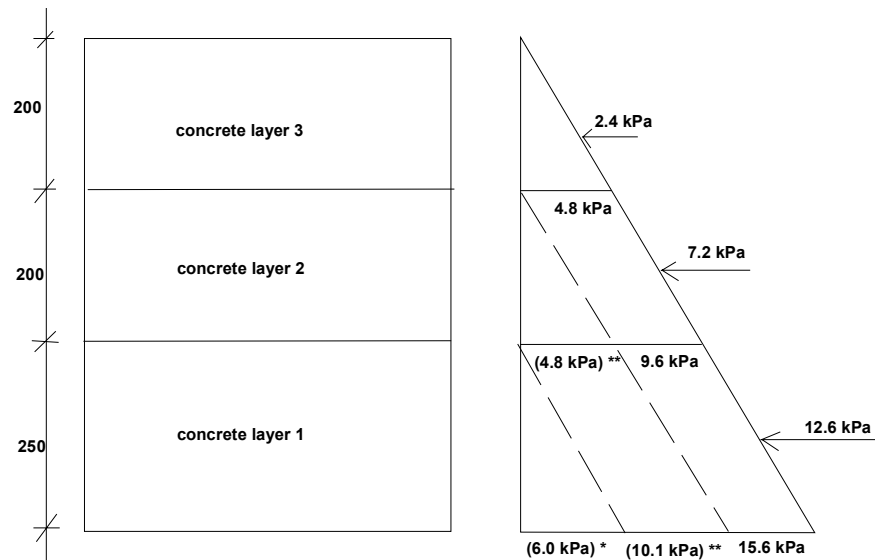


Figure 7.50: The theoretical normal pressure (hydrostatic pressure) in the 3-layer tests.

* Normal pressure when only concrete layer 1 placed.

** Normal pressure when both concrete layer 1 and 2 placed.

The results from the single layer tests will be used to calculate the lifting stress for each layer in the 3-layer test. The concrete height of the single layer tests is approximately 600 mm and the average theoretical hydrostatic pressure is 7.2 kPa. In order to calculate the maximum lifting stress, the actual normal pressure for each concrete layer must be taken into consideration. Layer 2 in the 3-layer tests will have the same average theoretical hydrostatic pressure as for the single layer tests. The position of the resultant for this pressure is different, but this will not have any affect on these calculations. Layer 1 and 3 will have a different normal pressure, which will affect the maximum net static and sliding lifting stress.

The correlation between the normal pressure and the minimum pore water pressure is calculated and shown in Figure 7.30. When this equation is added to the equations listed in Table 7.1 in Section 7.1.3.1, new equations can be made where the maximum net static and sliding lifting stress can be calculated based on the normal pressure. The equations are shown in Eq. 7.5 and Eq. 7.6 (the equations are only applicable for the basis concrete with 15 minutes between the lifts and lifting height of 10 mm).

Eq. 7.5: $F_{AHM} = 2.85 + 1.09 \cdot \sigma$

Eq. 7.6: $F_{AGM} = 2.48 + 0.74 \cdot \sigma$

where F_{AHM} = maximum net static lifting stress [kPa]
 F_{AGM} = maximum net sliding lifting stress [kPa]
 σ = normal pressure [kPa]

Verification procedure:

1. The ratio between the theoretical hydrostatic pressure and the measured normal pressure (from the single layer test) is calculated for layer 2. This ratio is used to calculate the normal pressure for layer 1 and 3 based on the theoretical hydrostatic pressure. The normal pressure is calculated for layer 1 and 3 after all layers are placed because the lifting stress is rather small during the first 4 hours.
2. Calculation of the maximum net static and sliding lifting stress for layer 1 and 3 are based on the normal pressure from pkt. 1. Eq. 7.5 and Eq. 7.6 are used in these calculations.
3. The static and sliding lifting stress curve for layer 1 and 3 are based on the measured curve for layer 2 and is drawn as shown in Figure 7.51. The curves are started at beginning of the transition period (~5 hours after water addition) and then drawn to the calculated maximum and further to the lower lifting stress level.
4. The calculated curves from each concrete layer is combined for the net static and net sliding lifting stress for the 3-layer test.

If the calculated net static and sliding lifting stress curve for the 3-layer tests correspond to the measured curve, it should be concluded that the single layer tests represent each individual layer in a slipform. This means that it is possible to calculate the total net lifting stress that occur in a slipform with several concrete layers. Also the effect on the total lifting stress when e.g. adjusting the layer thickness or changing the slipform rate can be studied provided that the necessary single layer tests is carried out.

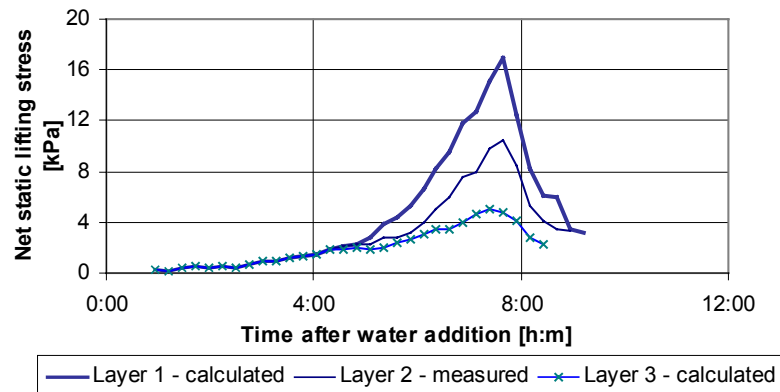


Figure 7.51: Example of calculated net static lifting stress according to the above procedure (VT212).

7.5.7.4 The same type of concrete in all layers

The 3-layer concrete test consists of the same self-compacting concrete in all 3 layers. The same setup with no inclination of the slipform panel and self-compacting concrete is used also in the single layer test. The maximum net static and sliding lifting stress is calculated for layer 1 and 3 according to the procedure in Section 7.5.7.3. The measured normal pressure and maximum net static/sliding lifting stress for the single layer test are used in layer 2. The calculated and measured normal pressure and the maximum net static and sliding lifting stress for each layer are shown in Table 7.23.

Table 7.23: Calculated normal pressure and maximum net static/sliding lifting stress

	Measured	Calculated	
	layer 2	layer 1	layer 3
Normal pressure [kPa]	7.0	12.3	2.3
Maximum net sliding lifting stress [kPa]	6.4	11.6	4.2
Maximum net static lifting stress [kPa]	10.5	16.3	5.4

The measured net static and sliding lifting stress for the single layer test is presented in Figure 7.52. The measured and calculated net static and lifting stress for the 3-layer test is presented in Figure 7.53.

The first layer in the 3-layer test will reach the maximum static and sliding lifting stress approximately 7.5 hours after water addition, see Figure 7.52. Since there are 2 hours between the layers, layer 2 and 3 will theoretically reach the maximum after 9.5 and 11.5 hours, respectively.

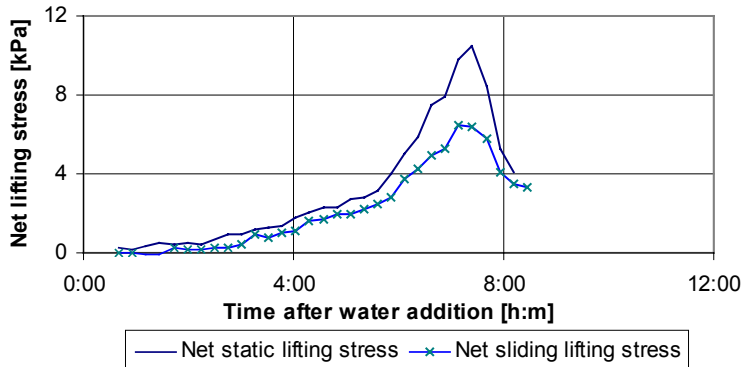


Figure 7.52: Measured net static and sliding lifting stress for the single layer test (VT212)

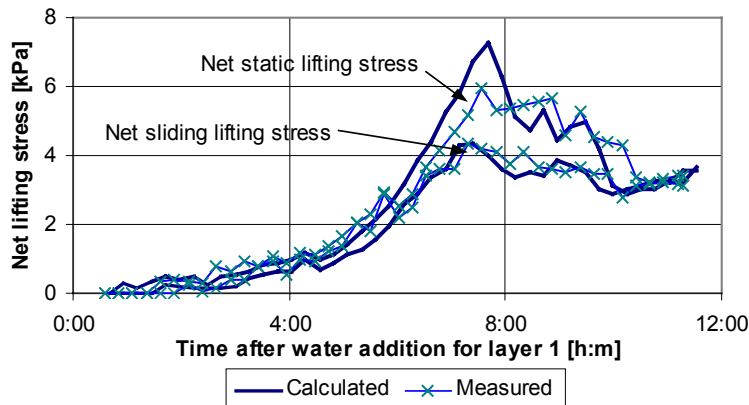


Figure 7.53: Measured and calculated net static/sliding lifting stress for the 3-layer test (VT208).

The net sliding lifting stress in Figure 7.53 shows that the calculated curve is very close to the measured curve. The first peak on the curve is after 7.5 hours and it is caused by the maximum net sliding lifting stress for layer 1. The maximum for layer 2 and 3 is difficult to identify on the measured curve, but it seems that layer 2 reach the maximum after approximately 10 hours as expected. The calculated net static lifting stress is also very close to the measured curve, but the calculated maximum net static lifting stress for layer 1 after 7.5 hours is approximately 1 kPa higher than the corresponding maximum on the measured curve. After 8 hours, the calculated curve is similar to the measured curve.

It is only the calculated maximum net static lifting stress for layer 1 that is different from the measured curve. The possible reasons for this deviation can be:

- The concrete used in the single layer test has different properties than the concrete used in the 3-layer test.
- The calculated normal pressure for the 3-layer test is different compared to the actual normal pressure.
- Errors in the equations used or the interaction between the concrete layers is larger than assumed, see Section 7.5.7.2. This is primarily the effect of the normal pressure and water communication on the lifting stress.

Since only the calculated maximum net static lifting stress and not the maximum net sliding lifting stress is higher than measured, it indicates error in the equation for the maximum net static lifting stress (Eq. 7.5) for normal pressure above a certain values. However, also since the calculated lifting stress is higher for layer 1 (first layer), it indicates that layer 1 has received water from layer 2, which might have decreased the measured maximum net static lifting stress.

However, in general it can be concluded that it is possible to calculate the lifting stress for several layers with adequately approximation based on the single layer tests. This means that the single layer test represents each individual concrete layer in a slipform.

7.5.7.5 Concrete with different properties

This test is carried out in order to verify that the net static and sliding lifting stress can be calculated also when concretes of different properties are used in the 3-layer test. The 3-layer concrete test with 2 hours between the layers, consists of the same self-compacting concrete in layer 1 and 3 as in the previous section (Section 7.5.7.4). The concrete used in layer 2 is self-compacting concrete where Scancem SSP2000 is used as superplasticizer. The single layer test for this concrete shows a high static and sliding lifting stress because of the low air content (0.3 %). The maximum net static and sliding lifting stress are calculated for layer 1 and 3 according to the procedure in Section 7.5.7.3. The measured normal pressure and maximum net static/sliding lifting stress for the single layer test presented in Figure 7.54 are used in layer 2. The calculated and measured normal pressure and the maximum net static and sliding lifting stress for each layer are shown in Table 7.24.

Table 7.24: Calculated normal pressure and maximum net static/sliding lifting stress

	Measured	Calculated	
	layer 2	layer 1	layer 3
Normal pressure [kPa]	7.9	12.3	2.3
Maximum net sliding lifting stress [kPa]	16.0	11.6	4.2
Maximum net static lifting stress [kPa]	31.7	16.3	5.4

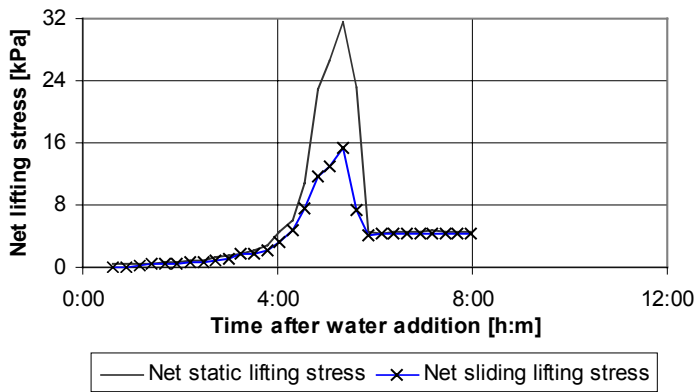


Figure 7.54: Measured net static and sliding lifting stress for the 1-layer test (VT137)

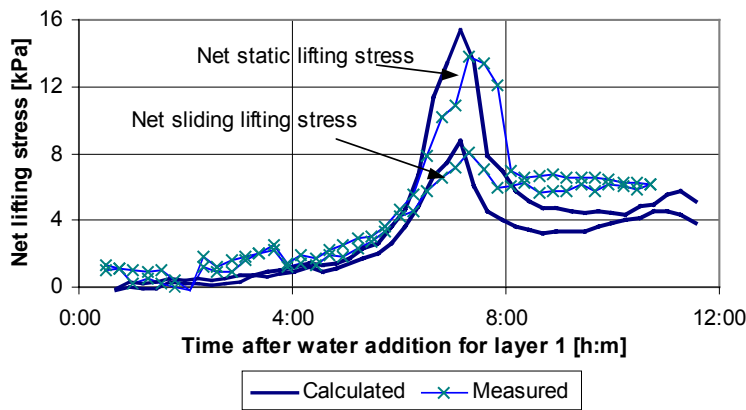


Figure 7.55: Measured and calculated net sliding lifting stress for the 3-layer test (VT218).

The measured net static and sliding lifting stress for the single layer test with the same concrete as for layer 2 in the 3-layer test is presented in Figure 7.54. The single layer test with the same concrete as in layer 1 and 3 is presented earlier in Figure 7.52. The measured and calculated net static and sliding lifting stress for the 3-layer test is presented in Figure 7.55.

The concrete in layer 1 and 3 will reach the maximum net static and sliding lifting stress approximately 7.5 hours after water addition (see Figure 7.52), but the concrete in layer 2 will reach the maximum as early as approximately 5.5 hours after water addition (see Figure 7.54). This means that the maximum net static and sliding lifting stress for layers 1 and 2 will theoretically occur at the same time, approximately 7.5 hours after water addition to the concrete in layer 1. The maximum for layer 3 will theoretically occur 11.5 hours after water addition to the concrete in layer 1.

The net sliding lifting stress in Figure 7.55 shows that the calculated curve is similar to the measured curve, but the first maximum for layer 1 and 2 occur slightly later than calculated. Nevertheless, the level of the calculated first maximum on the curve is almost the same as measured. After 8 hours, the measured curve shows a higher sliding lifting stress than calculated. A higher normal pressure in the 3-layer test than calculated is probably the reason, which will result in a higher lifting stress, see Figure 7.56. Both curves in Figure 7.56 indicate that the inclination is slightly negative, since the normal pressure is increasing. This is because it is difficult to adjust the inclination of the panel to exactly zero.

The calculated static lifting stress shows also a similar development as for the measured curve. The calculated maximum static lifting stress for layer 1 and 2 occur slightly earlier and is also approximately 1.0 – 1.5 kPa higher than the corresponding measured maximum. This indicates that the equation (Eq. 7.5) for maximum net static lifting stress gives a higher result above a certain normal pressure. Water communication between the layers can also be a possible reason for the lower maximum net static lifting stress (as described for layer 1 in previous section).

However, in general it can be concluded that it is possible to calculate the lifting stress for several concrete layers with adequately approximation based on the single layer tests. This means that the single layer test represents each individual concrete layer in a slipform.

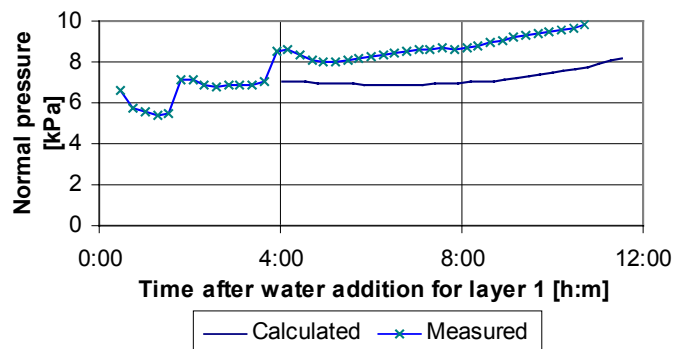


Figure 7.56: The calculated and measured normal pressure

7.5.7.6 With inclination of the slipform panel

The 3-layer concrete test consists of the same concrete self-compacting concrete as in Section 7.5.7.3, but the inclination of the panel is 3.8 mm/m for both the single layer test and the 3-layer test. The concrete is vibrated slightly during placing of each layer. The maximum net static and sliding lifting stress is calculated for layer 1 and 3 according to the procedure in Section 7.5.7.3. The measured normal pressure and maximum net static/sliding lifting stress for the single layer test is used in layer 2. The calculated and measured normal pressure and the maximum net static and sliding lifting stress for each layer are shown in Table 7.25.

Table 7.25: Calculated normal pressure and maximum static/sliding lifting stress

	Measured	Calculated	
	layer 2	layer 1	layer 3
Normal pressure [kPa]	3.4	6.0	1.1
Maximum net sliding lifting stress [kPa]	5.0	6.9	3.3
Maximum net static lifting stress [kPa]	7.5	9.4	4.0

The measured net static and sliding lifting stress for the single layer with inclination is presented in Figure 7.57. The measured and calculated static and sliding lifting stress for the 3-layers tests are presented in Figures 7.58 and 7.59. The calculated curves in each figure are based on the single layer tests with inclination (VT162), but also the result from Section 7.5.7.3 where the calculation is based on a single layer test without any inclination is presented in the figures (VT212).

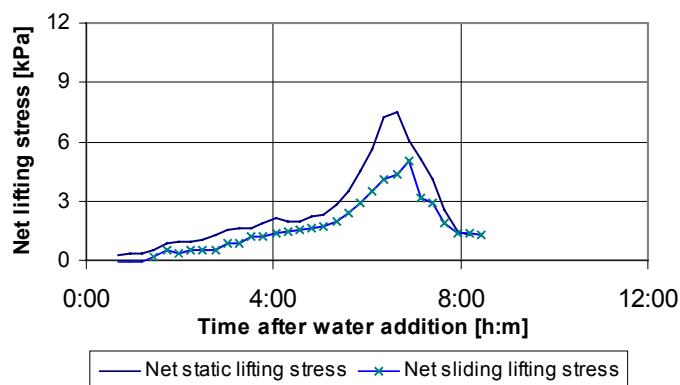


Figure 7.57: Measured net static and sliding lifting stress for the single layer test with 3.8 mm/m inclination (VT162).

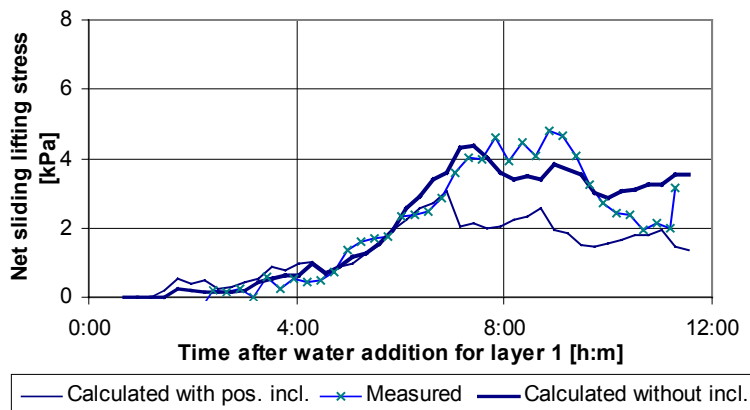


Figure 7.58: Measured and calculated net sliding lifting stress for the 3-layer test (VT219).

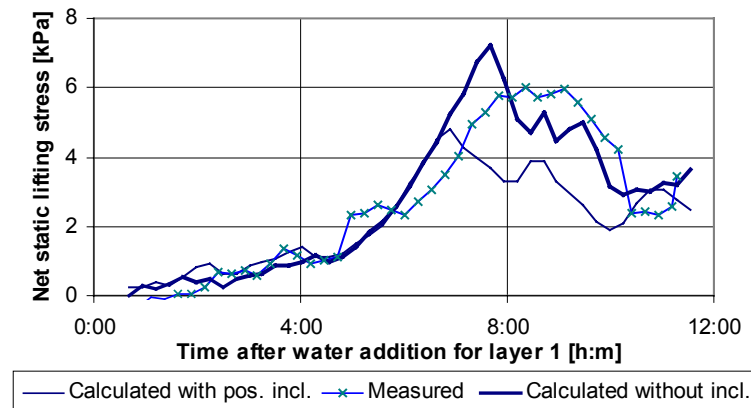


Figure 7.59: Measured and calculated net static lifting stress for the 3-layer test (VT219).

Layer 1 in the 3-layer test will reach the maximum static and sliding lifting stress approximately 7 hours after water addition according to the single layer tests with panel inclination in Figure 7.57. The maximum for layer 2 and 3 will then occur theoretically after 9 hours and 11 hours, respectively. Compared to the single layer test without inclination in Figure 7.52, the maximum lifting stress occurs approximately 0.5 hours later for each layer.

The calculated net sliding lifting stress for the test without panel inclination (Figure 7.58) is more similar to the measured net sliding lifting stress than the calculated test with panel inclination. The difference between these two curves is almost 2 kPa or 50 % after the first maximum at approximately 7 hours. The main reason for the difference between the two calculated curves is the lower normal pressure for the panel with positive inclination, see Figure 7.60. It is the vibration of the concrete during placing that seems to cause a higher and a more similar normal pressure to the calculated test without panel inclination. The calculated test without panel inclination shows an increasing normal pressure, which means that the panel has a slightly negative inclination.

Also for the net static lifting stress in Figure 7.59, the calculated test without inclination is more similar to the measured curve than the calculated test with inclination. The calculated maximum without panel inclination at approximately 7 hours is ~1 kPa higher than the measured maximum and the calculated maximum with panel inclination is more than 1.5 kPa lower than the measured maximum. As mentioned above, the higher normal pressure caused by the vibration during placing seems to be the main cause for a more similar result to the calculated test without panel inclination.

It can be concluded that the net static and sliding lifting stress can be calculated also for the vibrated 3-layer tests with positive panel inclination. The results show that the normal pressure is increasing each time a new layer is placed and vibrated, which has reduced the effect of the panel inclination. For the same reason, the single layer test with no panel inclination has been a better basis for the calculations than the single layer test with a positive inclination.

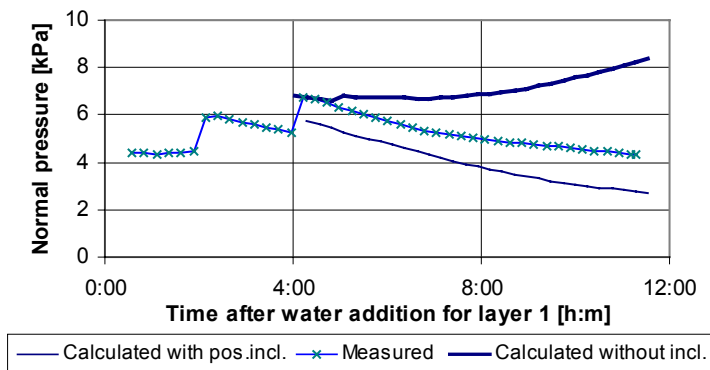


Figure 7.60: The calculated and measured normal pressure for the 3-layer test (VT219)

7.5.8 Summary several layers

The purpose of these tests was to verify that the single layer test represents the single layer in a slipform. The verification is carried out on 3-layer tests where the total lifting stress is dominated by the maximum net static and sliding lifting stress for layer 1 with the highest normal pressure. Also layer 2 with less normal pressure will have an impact on the total lifting stress when the maximum level is reached for this layer, but less compared to layer 1. This is because the normal pressure has a considerable effect on the level of the maximum net static and sliding lifting stress. Also water communication between the concrete layers might have an effect in these tests because layer 1, which is the first layer placed will not lose any water in early phase, but will in later phase receive water from layer 2. It is opposite for layer 3 (last layer) that will lose water in early phase, but not receive any water in later phase. The effect of this might be that the lifting stress would be slightly lower for layer 1 and slightly higher for layer 3. However, this situation will not occur in a slipform with continuously placing of new layers and the effect of the water communication will therefore be less.

The results show, when the procedure in Section 7.5.7.3 is used, that the net static and sliding lifting stress can be calculated with a certain accuracy for the different concrete layers. Also calculation of the lifting stress for a positive panel inclination is possible. If the concrete is vibrated, the single layer test without panel inclination should be used as basis for the calculations, because the vibration will increase the normal pressure (backsliding) for the already placed concrete layers.

It can be concluded that the single layer tests can be used in calculation of the total net lifting stress for a slipform. This means that the single layer test represents each individual concrete layer in a slipform. Also the effect on the total lifting stress when e.g. adjusting the layer thickness or changing the slipform rate can be studied provided that the necessary single layer tests are carried out.

7.6 Field investigations

7.6.1 Introduction

The purpose of the field investigation has been to measure the level of friction and normal pressure that occur during an ordinary slipform operation. The results will be compared to the results from the slipform rig testing in reported previous sections. Also the cause of the surface defects that occurred on the tested concrete structures will be discussed.

The field investigation was carried out at the Tukthus site in Oslo during May-July in 1999. The friction and normal pressure were measured during two slipform operations including inspection of the concrete surface below the slipform. Cores were also drilled at different locations on these two slipformed concrete structures after approximately 2-3 months for further laboratory analysis. The required characteristic compressive strength in the concrete used in these two structures was 45 and 35 MPa, respectively.

In another slipform operation carried out at Sørkedalsv site in Oslo during October in 2000, large surface damages occurred during start-up and the first meters of slipforming. The surface damages ended after an extensive surface cleaning of the slipform panels combined with changing of the concrete mix. Both concrete mixes had a minimum characteristic strength of 45 MPa.

The concrete mix used in the first slipform operation at Tukthus site and both types of concrete used at Sørkedalsv site are tested in the slipform rig. The results are evaluated in order to identify any differences between the concrete mixes.

7.6.2 Measured lifting stress and normal pressure during slipform operation

A test panel (0.5 m wide) was installed as an integrated part of the slipform on two operations at the Tukthus site. The test panel was equipped with load cells for measurements of the friction and normal forces during lifting of the slipform panel, see section 4.2.3.

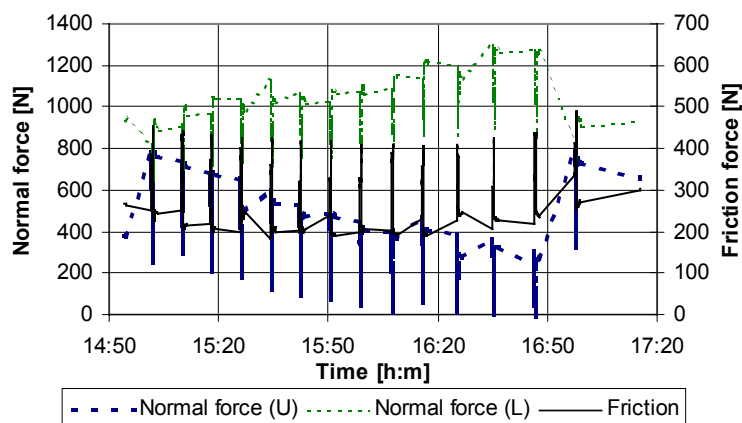


Figure 7.61: The measured friction and normal force at (U)pper load cells and (L)ower load cells.

A typical period of measurements from the first slipform operation is selected for further discussions. This period represents the general level of the measured forces at both slipform operations and is shown in Figure 7.61. The slipform rate during this period is approximately 160 mm/h and the hardening front is approximately 850 mm below the top of the slipform. The wall thickness is 200 mm and the inclination of the slipform panel is measured to be 4 mm/m. The time between each lift is in average 9.4 minutes with a lifting height of 25 mm.

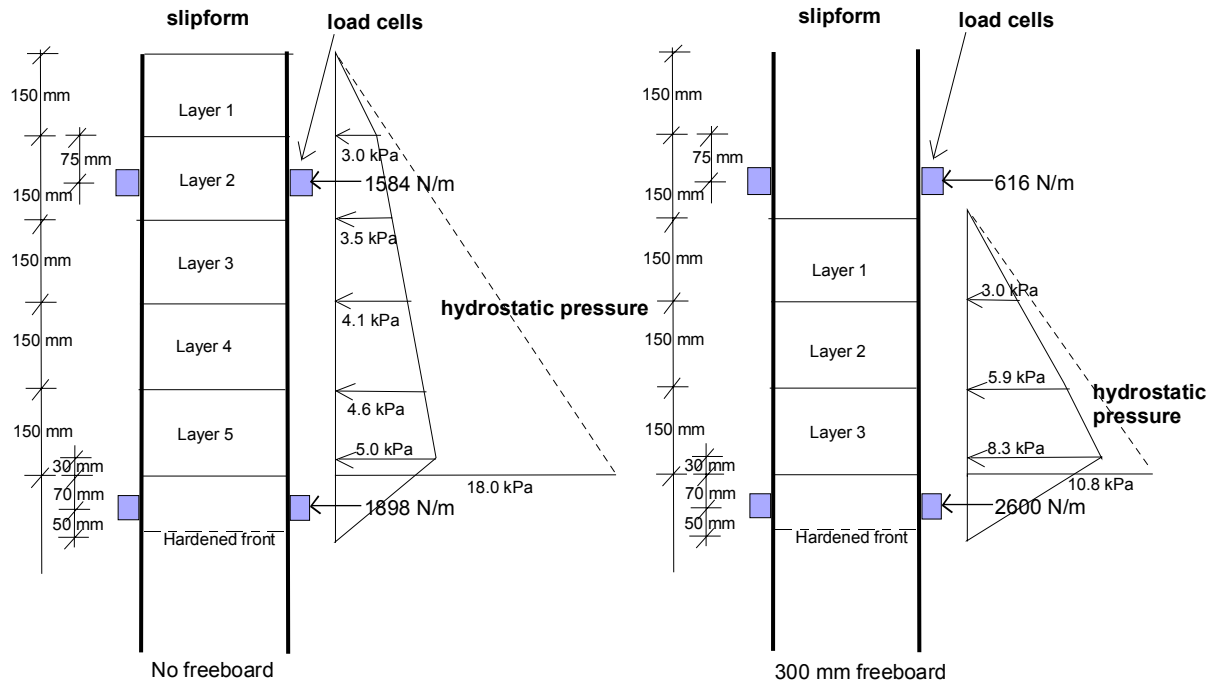
Table 7.26: Measured normal force and maximum friction at different freeboard (0.5 m wide test panel)

Time for each lift	Calculated freeboard [mm]	Measured normal force at upper load cells [N]	Measured normal force at lower load cells [N]	Measured maximum friction [N]
15:01	0	792	949	454
15:09	25	739	1010	441
15:17	50	691	1053	434
15:25	75	657	1048	426
15:34	100	597	1135	428
15:42	125	525	1064	421
15:50	150	488	1086	418
15:58	175	448	1115	415
16:07	200	397	1154	418
16:15	225	468	1228	410
16:25	250	389	1200	418
16:35	275	368	1299	446
16:46	300	308	1300	452
16:57	0	789	968	491

The measured normal force and the friction for each lift are shown in Table 7.26. The measurements in the table start with zero freeboard and are increasing with 25 mm for each lift. The result shows that the normal force at upper load cells is decreasing and the normal force at lower load cells is increasing with larger freeboard. This variation is in agreement with the static system for the slipform, see Figure 4.13. The friction is almost constant during the measurement period and is independent of the freeboard as expected, because the friction is low for newly placed concrete. The level of the friction is more related to the lifting frequency and the effective pressure for concrete layers in the transition period.

The pressure distribution in the slipform at 0 mm and 300 mm freeboard is calculated. The selected normal forces that are used in these calculations are marked bold in Table 7.26. These numbers represents the measured normal forces on the 0.5 m wide test panel and must be multiplied by 2 in order to calculate the normal pressure per meter slipform. The contact height between the slipform panel and the concrete is assumed to be from top and down to approximately the hardening front, which means a contact height of 850 mm with 0 mm freeboard and 550 mm contact height with 300 mm freeboard. The pressure distribution is calculated assuming that the normal pressure is approximately the same as the hydrostatic pressure and the layer thickness is 150 mm. The

calculated pressure distribution is presented in Figure 7.62 with 0 mm freeboard and in Figure 7.63 with 300 mm freeboard.



Figures 7.62 and 7.63: Calculated pressure distribution with 0 mm and 300 mm freeboard

The calculated pressure in Figure 7.62 with no freeboard show that only layer 1 has a pressure approximately at the same level as the hydrostatic pressure. For layer 2 to 5, the calculated pressure is 30 – 50 % of the hydrostatic pressure, which is lower than expected. It was assumed that the concrete pressure should be hydrostatically distributed (Reichverger et al., 1982).

The calculated pressure distribution with 300 mm freeboard is shown in Figure 7.63. The pressure is only slightly lower than the hydrostatic pressure for all layers, which is more as expected. The result shows that the total normal force at the walings is approximately at the same level as in Figure 7.62 with 0 mm freeboard. This means that the normal force is almost independent of the freeboard, which indicates that other parameters than the concrete pressure is affecting the measured normal force. The normal force is probably depending on the external loads such as the horizontal stability of the slipform, which may results in deformation in the walings or adjacent panels and affects the actual load on the test panel. The normal force, including the friction, should be measured on both side faces of the slipform at the same time because it will then be possible to detect more accurate the parameters affecting the normal force between the concrete and the slipform panel. Based on these measurements, it is difficult to conclude what range the normal forces have during slipforming.

7.6.3 Concrete tested in the slipform rig

The concrete mixes used in the field projects are tested in the slipform rig. The concrete used during the first meters at Sørkedalsv site is denoted mix 1 in Table 7.27 and the concrete replaced after mix 1 is denoted mix 2. It was approximately the same concrete constituents used in both mixes, but coarser aggregate was used in mix 2 and also the type and amount of superplasticizers were different, see Table 4.6. Melstab was used in mix 1 and Sika ViscoCrete 3 was used in mix 2. Also the concrete mix used in the slipform operation discussed in Section 7.6.2 at Tukthus site is tested. The required characteristic strength for all concretes tested were 45 MPa.

The same test set-up is used for all concrete tests. The concretes are tested as single layer tests, with 15 minutes between the lifts and 10 mm lifting height. With this chosen lifting height and period between the lifts, any difference between the concrete tests will be easier to detect and the result will also be comparable to earlier testing carried out in the vertical slipform rig and presented in previous sections. The initial inclination of the panel is -1.5 mm/m and the concrete is compacted by 2x15 sec vibration.

Table 7.27: Minimum pore water pressure and maximum net static/sliding lifting stress

	Sørkedalsv mix 1			Sørkedalsv mix 2		Tukthus site	
	VT237	VT243	VT247	VT242	VT244	VT248	VT249
Minimum pore water pressure [kPa]	-33.8	-32.9	-36.3	-19.9	-19.7	-18	-24.5
Maximum net static lifting stress [kPa]	19.9	29.9	27.4	15.1	17.5	14.6	17.6
Maximum net sliding lifting stress [kPa]	9.6	11.9	11.5	7.9	8.4	8.5	9.6

The results in Table 7.27 show that the maximum net static and sliding lifting stress is almost 100 % larger for mix 1 compared to mix 2 from Sørkedalsv site and the concrete from Tukthus site. The two latter concrete mixes have approximately the same lower level. Also the minimum pore water pressure for mix 1 is considerable lower compared to the other two mixes. However, even the lowest lifting stress levels can be considered to be higher than the basis concrete normally used in the previous sections.

The design of mix 1 and mix 2 from Sørkedals site is almost the same, see Table 4.6. The w/b-ratio is the same for both mixes, but the amount of cement and silica fume is higher for mix 2. This should theoretically result in a lower minimum pore water pressure for mix 2, but this is not the case here. Also the measured air content is at the same level for both mixes (1.1 to 1.5 %). Probably it is other parameters such as the effect of vibration on the initial air content that is the reason for the lower minimum capillary pressure for mix 1. In Section 7.2.3.2 it is shown that increased vibration time will have only a minor affect on the minimum pore water pressure in concrete with Sika ViscoCrete 3. This indicate that it can be the effect of the superplasticizers that is the main reason for the lower minimum pore water pressure and higher maximum net static/sliding lifting stress for mix 1.

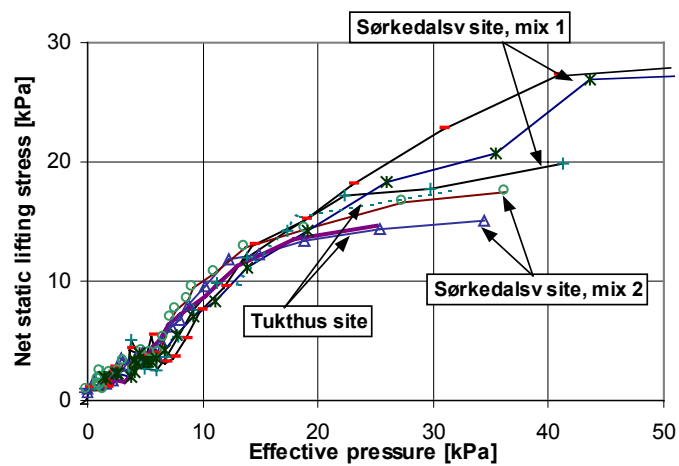


Figure 7.64: Net static lifting stress versus the effective pressure

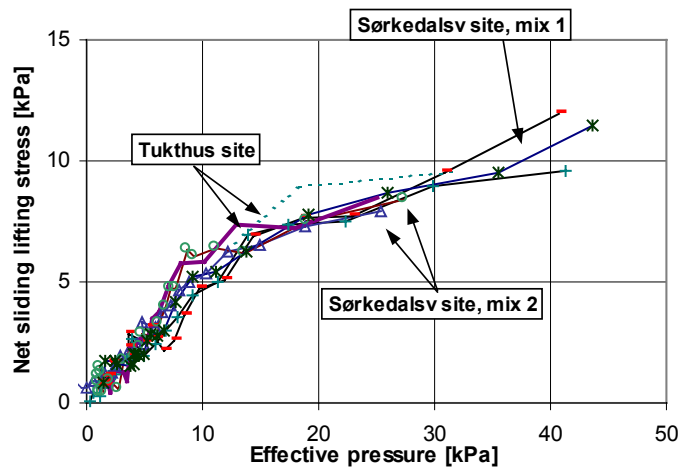


Figure 7.65: Net sliding lifting stress versus the effective pressure

The net static lifting stress versus the effective pressure is shown in Figure 7.64. The results show that all concrete mixes have the same lifting stress development until a period before maximum where the curves are leveling out. The same development for the concrete mixes can also be seen for the net sliding lifting stress in Figure 7.65. This means that all mixes show a similar static lifting stress response and sliding lifting response, respectively versus the effective pressure during lifting. This means the static friction coefficient is approximately the same for all mixes and the sliding friction coefficient is approximately the same for all mixes.

It can be concluded, based on the results, that all three concrete mixes show the same correlation between the net static lifting stress and the effective pressure and between the sliding lifting stress and the effective pressure. The difference is mainly the maximum net static and sliding lifting stress, where mix 1 from Sørkedalsv site show a considerably higher level compared to the other tested concrete mixes.

7.6.4 Surface quality

7.6.4.1 Tukthus site

The concrete surface was inspected during the slipform operations at Tukthus site. During these operations, some surface defects occurred during the start-up of the second slipform operation because of lack of vibration or difficulties to vibrate the previous concrete layer together with the new layer. This problem occurred because of too long time between the concrete layers. Except for these problems, which was not caused by the slipform itself, there were no serious surface defects like lifting cracks observed on the slipformed concrete surface. The surface smoothness varied during the slipform operations and it was observed that larger inclination of the slipform panel gave a rougher surface. Larger inclination will probably result in an earlier detach of the slipform panel from the concrete surface. This earlier detach time on the new hardened concrete surface is probably the cause of the rougher concrete surface.

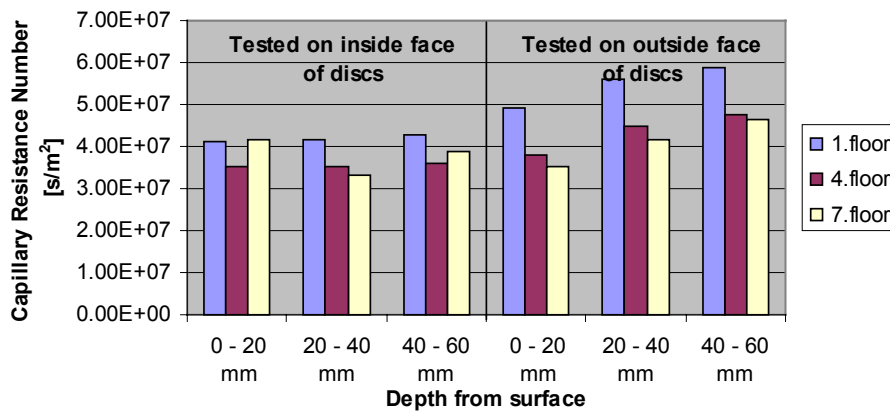


Figure 7.66: Capillary resistance number for slipform 1 at Tukthus site.

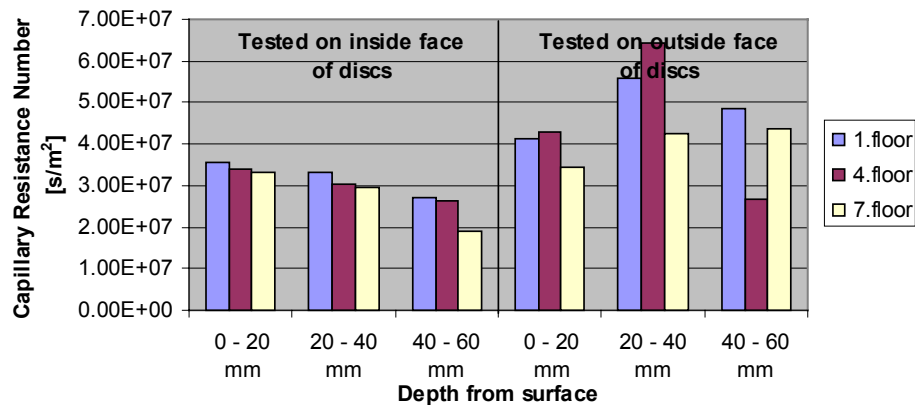


Figure 7.67: Capillary resistance number for slipform 2 at Tukthus site.

The quality of the concrete in the cover zone was also investigated on drilled cores. The cores were drilled straight through the 200 mm thick wall in both structures at different location, 1st, 4th and 7th floor, respectively. The cores were cut in 20 mm discs from each side (3 x 2 discs in total from each core) and tested for capillary water absorption as described in Section 4.4.4.1. The concrete was approximately 3 – 4 month old when tested. The capillary resistance number is calculated based on these tests, which reflects the fineness in the capillary system and it can be expected that the capillary resistance numbers have a correlation to the w/b-ratio. The capillary resistance number for the discs are shown in Figure 7.66 and 7.67. The results are detailed presented in Appendix B with the calculated absorption porosity and the estimated w/b-ratio for each disc.

The discs were tested first on the inside face and than at the outside face (inside face is towards the centre of the wall and outside face is toward the surface of the wall). The results from slipform 1 with a minimum characteristic strength of 45 MPa are shown in Figure 7.66. The results show that the capillary resistance numbers vary from 3.4 to 4.3 s/m² for testing carried out at the inside face of the discs. It can be seen that the resistance number is in general larger for the outside face compared to the inside face, except for disc representing 0 – 20 mm at 7th floor. The calculated w/b-ratio based on the measured results is in agreement with the actual w/b-ratio, see Appendix B. It can be concluded based on the results that the capillary resistance number is approximately the same at the surface as 40-60 mm inside, which indicates that the slipform operation has not affected the quality of the structure.

The results for slipform 2 with a minimum characteristic strength of 35 MPa, are shown in Figure 7.67. The results show that the capillary resistance numbers for the inside face is highest at the surface layer and is decreasing inside the cover zone. The results vary more for discs tested on the outside face, but in general a higher resistance number compared to the results from the inside face. The capillary resistance number is slightly lower for slipform 2 compared to slipform 1, which can be explained by the lower concrete grade for slipform 2. The capillary resistance at the surface is in

general at the same level or higher compared to 40-60 mm inside, which means that the quality of the concrete structure also here is not affected by the slipform operation.

The same concrete used in slipform 1 was also tested in the slipform rig, see Section 7.6.3. The testing was carried out with different slipform rate than in the field, but the properties for the mix relative the relative difference compared to the other concrete mixes tested. The results indicate that concrete with similar behavior in the vertical slipform rig as for this concrete used at Tukthus site, will have low risk for any surface quality reduction in slipform operations with the same slipform set-up and slipform rates used at Tukthus site.

7.6.4.2 Sørkedalsv site

Large surface damages occurred during the first meters of the slipform operation at Sørkedalsv site. After some meters with unsuccessful activities for solving the problems, the concrete mix was changed and an extensive surface cleaning of the slipform panel was carried out. This resulted in a considerably improved surface quality and the further operation to the top went successfully without any larger surface defects.

The damages at the beginning of the slipform operation was caused by lumps formed on the slipform panel, type 3 in Section 2.3.9. When lumps on the slipform panel occur, it can be observed on the slipformed concrete surface at the beginning as a very rough surface. As the slipform panel is lifted, the surface damages becomes deeper and wider, see Figure 7.68. The damages on the surface will continue until the lumps are completely removed from the slipform panel as a result of a difficult cleaning of the slipform panel.

The process behind the start of the lump growing is not fully known. It is assumed that a layer of cementitious grout that "sticks" to the slipform panel initiates the lump forming. As the panel is lifted, new layers of grout/concrete will stick to existing layer on the panel and a lump will be built up. It is assumed that the first layer of grout on the slipform panel is made when the friction between the slipform panel and the concrete is larger than the shear stress in the grout/concrete. After the first layer is adhered to the slipform panel, new layers will easily adhere to the existing layer because of increased roughness in the sliding zone. On Sørkedalsv site, the surface damages started after 1 – 1.5 meter, which indicates that the first layer of the lump was initiated during the start-up of the slipform operation and as the slipform panel was lifted, the lump was formed with surface damages as a result.

Both concrete mixes are tested in the slipform rig, see Section 7.6.3. The slipform rate during testing was different from the slipform rate in field, but the results will show the properties for the mixes relative to each other. Based on the results in Section 7.6.3, the correlation between the effective pressure and the lifting stress is similar for the mixes, but the maximum lifting stress is considerably higher for mix 1 as compared to mix 2. This indicates that mix 1 is more exposed for problems during slipforming and can be the trigger factor for lump forming on the slipform panel.

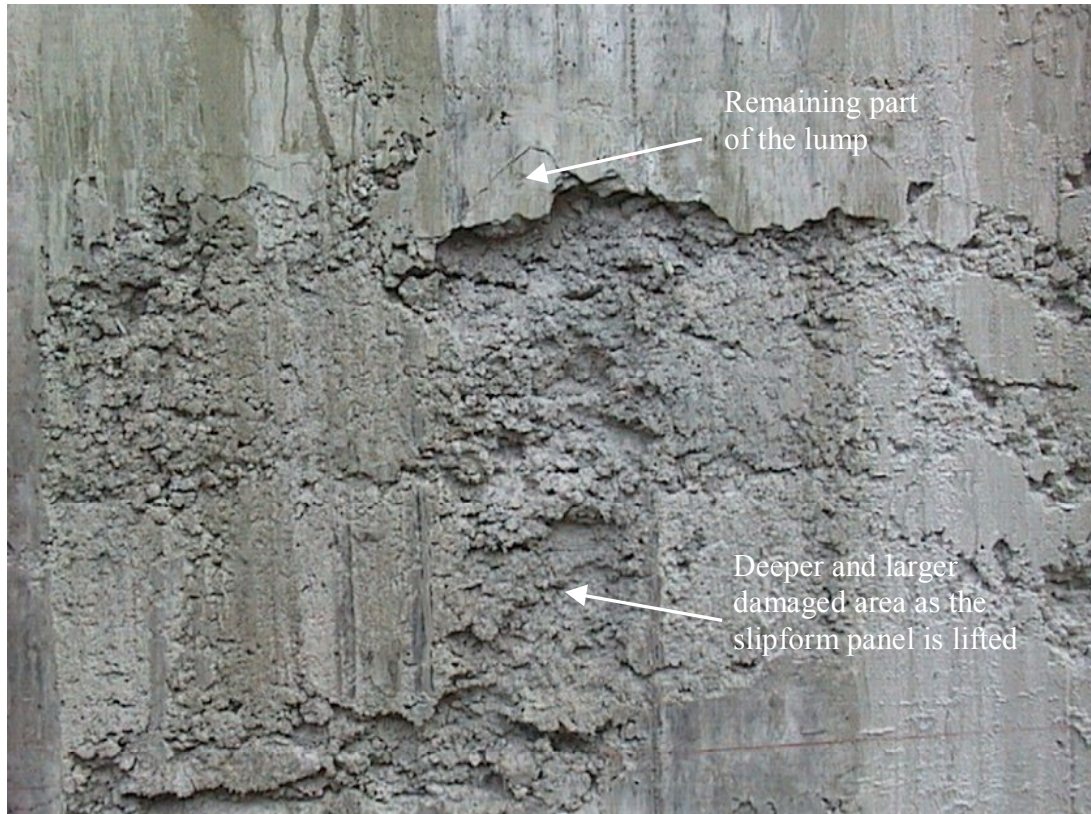


Figure 7.68: Picture of a damage area at Sørkedalsv site where mix 1 was used.

7.6.5 Summary

The results from the field investigations, where a test panel was used to measure the normal force and the friction force during slipforming, show that the measurements should be carried out on both wall faces at the same time. It seems that external loads may have affected the measurements and it is difficult to conclude what range the normal forces have during slipforming.

One concrete mix used at Tukthus site and two mixes used at Sørkedalsv site are tested in the slipform rig. The results show for all concrete mixes a similar correlation between the net static lifting stress and the effective pressure and also between the net sliding lifting stress and the effective pressure. The main difference is the maximum net static and sliding lifting stress that are considerably higher for the concrete mix used during the first meters at Sørkedalsv site (mix 1). This concrete resulted in large surface damages because of lump forming on the slipform panel at Sørkedalsv site. This indicates that concrete with high maximum lifting stress is more vulnerable for

problems during slipforming. The high lifting stress can be the trigger factor for lump forming on the slipform panel.

The surface quality was tested in the slipformed structures at Tukthus site. The results show that the quality of the concrete structure is not affected by the slipform operation. This indicates that similar slipform operations with the same concrete, slipform set-up and rates will probably have low risk for surface quality reduction during slipforming.

8 SUMMARY

8.1 Objectives and Scope

The prime objective of the research program has been to improve the understanding of the slipform technique as a construction method in order to ensure high quality concrete structures.

The objective has been to identify the parameters affecting the net lifting stress (friction) that occur during lifting of the slipform panel. Focus has been given to the importance of the concrete properties that will influence the forces that occur between the slipform panel and the concrete. Also any connection between the friction level and the surface damages has been investigated. Based on the result it should be possible to define requirements for materials, mix composition and method of execution to ensure that the specified quality in the structure is obtained.

The experimental program has been organized in two parts where the first and main part, has the focus on parameters that affect the friction. The second part has the focus on the connection between the friction and any surface damages. This part of the test program is primarily carried out during the field investigations. In order to simplify the test method, it is chosen to design slipform test rigs that can simulate the conditions one single layer of concrete is subjected to in a full-scale slipform.

8.2 The friction law

The lifting stress can be divided in static lifting stress and sliding lifting stress, where the static lifting stress represents the friction that has to be overcome in order to start sliding and the sliding lifting stress is the minimum friction that occurs during sliding. The difference between the static and sliding lifting stress is caused by the decreasing effective pressure during lifting at the sliding zone and the adhesion that occurs because of no movement of the slipform panel between two lifts. This difference starts at the beginning of the transition period and is increasing evenly with larger effective pressure until the maximum lifting stress, see Figure 8.1. Both static and sliding lifting stress are closely related, but the static lifting stress can be extremely large compared to the sliding lifting stress.

The friction law can be used to describe the correlation between the net lifting stress and the effective pressure. This correlation is almost linear and applicable for both the net static and sliding lifting stress. The effective pressure, which represents the pressure between the solid particles and the slipform panel, is the difference between the normal pressure (concrete pressure against the slipform panel) and the pore water pressure. It is primarily the pressure in the pore water that is responsible for most of the variation in the effective pressure during the plastic phase and the transition period, which means that it is mainly the variation in the pore water pressure that controls the level of the lifting stress. The pore water pressure is decreasing slightly in early phase because of the settlement in the concrete. During the transition period, the pore water pressure start to decrease faster as an effect of the chemical shrinkage that occurs because of the cement reaction.

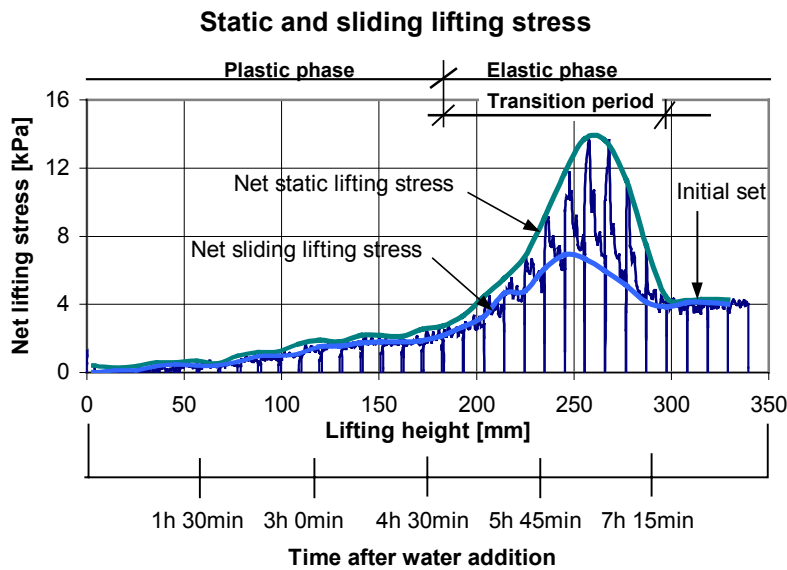


Figure 8.1: Typical static and sliding lifting stress development for single layer tests

8.3 The pore water pressure

The pore water pressure development can be characterised by the decrease rate of the pore water pressure and the minimum pore water pressure. The pore water pressure decrease rate is calculated as the average decrease rate at 0 kPa and at -10 kPa pore water pressure. The minimum pore water pressure is defined as the pore water pressure at the time of maximum lifting stress. The minimum pore water pressure occurs just before it increases or just disappears at the sliding zone close to the slipform panel. It is primarily the level of the minimum pore water pressure that will decide the maximum level of the static and sliding lifting stress.

The pore water pressure at the sliding zone is increasing during lifting of the slipform panel, which can explain the large difference between static and sliding lifting stress during the transition period, see Figure 8.1. When the concrete becomes denser, the period will be longer before the pore water pressure at the sliding zone is in equilibrium with the pore water pressure in the concrete. The minimum pore water pressure is probably reached when the period for equilibrium is longer than the period between two lifts. The pore water pressure will thereafter increase at the sliding zone, as the slipform panel is lifted (transition period finished).

The pore water pressure decrease rate and the minimum pore water pressure depends on the particle concentration and particle size distribution for the finer particles and also the air content. Higher particle concentration and finer particle size distribution will both result in a faster pore water pressure decrease rate and a lower minimum pore water pressure. A higher air content will reduce the effect of the chemical shrinkage because the existing air volume will act as a pressure release

volume, resulting in a lower pore water pressure decrease rate and a higher minimum pore water pressure.

Also the compaction method will have an impact on the decrease rate of the pore water pressure and the minimum pore water pressure, because the air content will be reduced with prolonged vibration time. Prolonged vibration will in general result in a higher lifting stress, depending on the response on the concrete during vibration. When lightweight aggregate is used in the concrete, the entrapped air in the lightweight aggregate will increase the pore water pressure and result in a lower lifting stress. Porous lightweight aggregate will have larger impact on the pore water pressure than denser lightweight aggregate.

Pressure gradients that occur between two concrete layers will affect the decrease rate of the pore water pressure. Water will “flow” from layers with younger concrete without any negative pressure to concrete layers with lower pore water pressure. This will reduce the decrease rate in the concrete layer that receives the water. At a later stage the same concrete that supplied the concrete layer below with water will receive water from the concrete layer above. The pressure gradient at the joint (between two concrete layers) will be more even as a result of the water communication between the concrete layers. Evaporation of water from a fresh concrete surface will result in a faster decrease rate and a lower minimum pore water pressure since the drying process will form menisci near the surface. The water communication is in general good in the concrete in this phase.

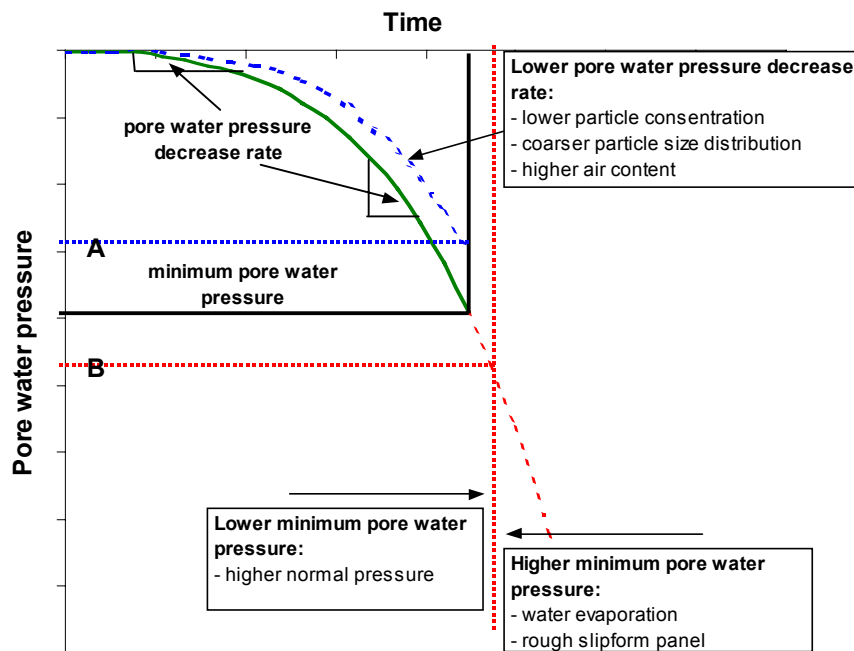


Figure 8.2: Parameters affecting the decrease rate of the pore water pressure and the time when the minimum pore water pressure occurs

- A: Higher minimum pore water pressure and lower decrease rate of the pore water pressure
- B: Lower minimum pore water pressure (because of delay)

The time at which the minimum pore water pressure occurs will also have an impact on the minimum pressure level. A shorter period of time from the minimum pore water pressure occur to the time of initial set will result in a relatively higher minimum pore water pressure and a lower lifting stress, see Figure 8.2. The minimum pore water pressure has occurred earlier when water has evaporated from an exposed concrete surface. Also when very rough slipform panel is used, the incipient vacuum between the slipform panel and the concrete is punctured early (collapse of the capillary system at the sliding zone) because of the rough panel surface and will result in a relative low lifting stress.

The time when the minimum pore water pressure occurs will be delayed compared to the time of initial set with increasing normal pressure. This will result in a lower minimum pore water pressure and higher lifting stress, see Figure 8.2.

8.4 Operational parameters

Both the lifting frequency and the lifting height has a considerable effect on the static lifting stress. Lower lifting height or decreased lifting frequency will both result in a lower pore water pressure and a higher static lifting stress. This is probably because the interface zone is disturbed each time the slipform panel is lifted. Less disturbance of the interface will result in a lower minimum pore water pressure. The lifting stress is decreasing during lifting as an effect of the decreasing effective pressure at the sliding zone and the reduced adhesion. The effective pressure at the sliding zone is probably at minimum and the adhesion is completely broken when the lifting stress is stabilized on a minimum level. The sliding lifting stress is also affected by the lifting frequency and the lifting height if not the minimum level is reached during the lift.

Most of the tests carried out in this research program have been with concrete in a single layer. It has been verified that the results from the single layer tests also represent each layer in a 3-layer test in the vertical slipform rig. (basically) The effect of the normal pressure and the water communication between the concrete layers are the difference between a single layer test and 3-layer test.

8.5 Connection between lifting stress (friction) and surface damages

Surface damages caused by high lifting stress are not demonstrated in the vertical slipform rig. However, similar concrete mix design that has been used in a field project, where surface damages occurred, has been tested in the vertical slipform rig. The concrete mix in this field project was replaced with a new concrete mix, where no or only minor surface damages occurred after the replacement. Both concrete mixes is tested in the vertical slipform rig and the result show a considerable higher static and sliding lifting stress for the concrete mix that was used when surface damages occurred. This indicates that there are a connection between high lifting stress and risk for surface damages. This means also that concrete mixes that obtains high lifting stress in the vertical slipform rig is more exposed to surface damages than concrete mixes that has obtained lower lifting stress.

8.6 The effect of combination of the parameters on the lifting stress

High content of fines in combination with low air content can potentially result in a high static and sliding lifting stress. This will result in a fast decrease rate of the pore water pressure and a lower minimum pore water pressure. If the slipform rate is also low when using this concrete, the minimum pore water pressure will be lower and result in high static and sliding lifting stresses. A concrete that has a moderate content of fines (e.g. washed sand and no silica fume) and a relative high air content will for comparison result in a considerable higher pore water pressure. This means that the lifting stress will be considerably lower and in particular in combination with higher slipform rates.

8.7 Confirmation of the hypotheses

All hypotheses in this research program have been confirmed. The main hypothesis that deals with the connection between lifting stress (friction) and surface damages has been indirectly confirmed by laboratory tests in combination with observation of surface damages that occurred at a field project, see Section 8.5.

9 CONCLUSIONS

The friction law can be used to describe the correlation between the lifting stress and the effective pressure between the slipform and the concrete. This correlation is almost linear and applicable for both the static and sliding lifting stress. The difference between the static and sliding lifting stress is caused by the decreasing effective pressure during lifting at the sliding zone and the adhesion that occurs because of no movements of the slipform panel between two lifts.

The effective pressure, which represents the pressure between the solid particles and the slipform panel, is the difference between the normal pressure (concrete pressure against the slipform panel) and the pore water pressure, which normally is negative during the setting period. It is primarily the pressure in the pore water that is responsible for most of the variation in the effective pressure, which means that it is mainly the variation in the pore water pressure that controls the level of the lifting stress.

The pore water pressure at the sliding zone is increasing during lifting of the slipform panel. When the concrete becomes denser, the time period will be longer before the pore water pressure at the sliding zone is in equilibrium with the pore water pressure in the concrete. The minimum pore water pressure is probably reached when the period for equilibrium is longer than the period between two lifts. The minimum pore water represents the pore water pressure at maximum lifting stress. It is primarily the minimum pore water pressure that will decide the maximum level of the static and sliding lifting stress. The minimum pore water pressure development depends on the particle concentration and particle size distribution of the finer particles and also the air content. Higher particle concentration and finer particle size distribution will both result in a lower minimum pore water pressure. A higher air content will reduce the effect of the chemical shrinkage because the existing air volume will act as a pressure release volume and result in a higher minimum pore water pressure.

Both the lifting frequency and the lifting height has a considerable effect on the static lifting stress. Lower lifting height or decreased lifting frequency will both result in a lower pore water pressure and a higher static lifting stress. This is probably because the interface zone between the slipform panel and the concrete is disturbed each time the slipform panel is lifted. Less disturbance of the interface will result in a lower minimum pore water pressure. The lifting stress is decreasing during lifting as an effect of the reduced adhesion and decreasing effective pressure at the sliding zone. The adhesion is completely broken and the effective pressure is reduced to a minimum when the lifting stress is stabilized on a minimum level. The sliding lifting stress is also affected by the lifting frequency and the lifting height if not the minimum level is reached during the lift.

Surface damages caused by high lifting stress are not demonstrated in the laboratory tests, but similar concrete that has been used in a field project, where surface damages occurred, has been tested in the vertical slipform rig. The tested concrete mix obtained a considerable higher lifting stress in the vertical slipform rig compared to concrete mix that has been successfully used during the same slipform operation in the field project. This indicates that there are a connection between high lifting stress and risk for surface damages. This means also that concrete mixes that obtains high lifting stress in the vertical slipform rig is more exposed for surface damages than concrete mixes that has obtained lower lifting stress, when it is used in field projects.

REFERENCES

- ADAM, Michel, 1976, "Realisation D'Ouvrages A L'Aide de Coffrages Glissants", Syndicat National du Beton Arme et des Techniques Industrialisees, No 341, July 1976, Paris, p 94.
- AİTCIN, P.C., "Autogenous shrinkage measurement", Proceeding in Autogenous Shrinkage of Concrete, edited by Tazawa. E & FN Spon, London, 1999, ISBN 0419238905, p. 257 – 268.
- ALEXANDRIDIS, A.; Gardner, N.J. 1981, "Mechanical Behavior of Fresh Concrete", Cement and Concrete research, vol.11, 1981, p. 323-339.
- BACHE, H.H. 1977, "Mekanisk stabilitet af frisk komprimeret beton" in Danish, Nordisk Betong, 1977, no. 6, p. 5-12.
- BACHE, H.H. 1987, "Flydeopførsel i beton ved betonfremstilling" in Danish, Cementfabrikkernes tekniske Oplysningskontor, Aalborg, 1987.
- BATTERHAM, R.G. 1980, "Slipform Concrete", The Construction Press Ltd ,1980, Lunesdale House, Horneby Lancaster, England. ISBN 0-86095-855-8
- BROOKS,J.J.; Cabrera, J.G.; Megat Johari,M.A., "Factors affecting the autogenous shrinkage of silica fume in high strength concrete", Proceeding in Autogenous Shrinkage of Concrete, edited by Tazawa. E & FN Spon, London, 1999, ISBN 0419238905, p. 195 – 202.
- DANIELSEN, S.W.; Hjermand, J.O. 1987, " In situ Strength of Concrete, Investigation at Gullfaks B", NOTEBY, 3 April 1987.
- DANIELSEN, S.W.; Hjermand, J.O.; Wick.S.O. 1989, "In situ Strength of Concrete, Investigation at Oseberg A", NOTEBY, 6 July 1987 and rev. Oct. 1989.
- DROZELLA, Rolf 1984, "Gleitschalung – Forschung und Anwendung", Deutscher Beton-Verein e.V, -DBV-, Wiesbaden, in-house publishing, 1984, p.397-410.
- GARDNER, N.J. 1985, "Pressure of Concrete on Formwork – A Review", ACI Journal, September – October 1985, p 744-753.
- HAMMER, T.A. 1999, " Test Methods for Linear Measurements of Autogenous Shrinkage before Setting", Proceeding in Autogenous Shrinkage of Concrete, edited by Tazawa. E & FN Spon, London, 1999, ISBN 0419238905, p. 143 – 154.
- HAMMER, T.A. 2000, "Effect of silica fume on the plastic shrinkage and pore water pressure of high-strength concretes", International RILEM Workshop on Shrinkage of Concrete, 16-17 October 2000, Paris, p 273-278.
- INGVARSON, Hans 1979, "Concrete Strength of a slipform Concreted structure", RILEM – Quality control of concrete structures, Stockholm, Sweden, June 17-21 1979.

JUSTNES, H. et al. 1999, "The influence of Cement Characteristics on Chemical Shrinkage", Proceeding in Autogenous Shrinkage of Concrete, edited by Tazawa. E & FN Spon, London, 1999, ISBN 0419238905, p. 71 – 80.

KASAI, Y.;Yokoyama, K.;Matsui, I. 1972," Tesile properties of early-age concrete", Proceedings of the 1971 International Conference on Mechanical Behaviour of Materials, Volume IV, 1972, Japan, pp. 288-299.

KLUGE, K.; Schmidt-Thrö, G.;Stöckl, S.; Kupfer, H. 1986 , "Ausziehversuche und Versuche an Übergreifungsstößen, Pronben in Berlin bzw. Köln hergestellt", in Versuche über das Verbundverhalten von Rippenstählen bei Anwendung des Gleitbauverfahrens, Lehrstuhl für Massivbau, Technische Universität München, 1986, Schriftenreihe des Deutschen Ausschusses für Stahlbeton, heft 378, p.63-110.

KOMPEN, Reidar 1995, "Bruk av glideforskaling til brusøyler og –tårn", Publikasjon nr. 77, Statens vegvesen, Veglaboratoriet, 1995, Oslo.

KORDINA, Karl; Droese, Siegfried 1984, "Korrosionsschutz von Bauwerken, die im Gleitschalungsbau errichtet wurden", Technische Universität Braunschweig, Institut für Baustoffe, Massivbau und Brandschutz, 1984, Schriftenreihe des Deutshen Ausschusses für Stahlbeton heft 365, ISBN 3-433-1356-X.

KORDINA, Karl; Droese Siegfried 1990, "Versuche zur Ermittlung von Schalungsdruck und Schalungsreibung im Gleitbau", Technische Universität Braunschweig, Institut für Baustoffe, Massivbau und Brandschutz, 1990, Schriftenreihe des Deutshen Ausschusses für Stahlbeton heft 414, ISBN 3-410-65614-6.

LANE, Ralph (chairman) 1993, "Behavior of Fresh Concrete During Vibration", ACI report 309.1R-93.

MITCHELL, J.K., 1993, "Fundamentals of soil behavior", Wiley, New York, 1993, ISBN 0471856401.

MØRK, Preben C. 1997, "Overflate og kolloidkjemi" in Norwegian, Norges teknisk-naturvitenskapelige universitet, Institutt for Industriell Kjemi, 5.utgave, 1997.

O'BRIEN. J.B. 1973, "Principles and Practice of Slipform", Symp. Concrete Research and Development 1970 – 1973, Cement and Concrete Association of Australia, Sydney, Sep 20 1973, p.20-26, ISBN:0-858-2250-349.

PARROTT, L.J.; Geiker, M.; Gutteridge, W.A.; Killoh, D. 1990, "Monitoring Portland Cement hydration: Comparison of methods", Cement and Concrete Research, v.20, no.6, 1990, p. 919-926.

POWERS, T.C. 1960, "Physical Properties of Cement Paste", Proceedings of the Fourth International Symposium on the Chemistry of Cement", Washington, October 2-7 1960, Issued 1962 of National Bureau of Standards Monograph 43 – volume 43, p. 577 – 609.

RADOCEA, Adrian 1992, "A study on the mechanism of plastic shrinkage of cement-based materials", Dr. These, Division of Building Materials, Chalmers University of Technology, Gothenburg, 1992, ISBN 91-7032-760-2.

RADOCEA, Adrian 1994 **A**, "A model of plastic shrinkage", Magazine of Concrete Research, 1994, v.46, no. 167, June, p. 125-132.

RADOCEA, Adrian 1994 **B**, "The influence of superplasticizers on the degree of flocculation of cement grains", Fourth CANMET/ACI International Conference on Superplasticizers and Other Chemical Admixtures in Concrete", Montreal, October 11-13, 1994, p. 45 – 56.

RADOCEA, Adrian 1998, "Autogenous volume change of concrete at very early age", Magazine of Concrete Research, 1998, v.50, no. 2, June, p. 107-113.

REDLUND, Margareta, 1994, "Stockholm högsta turistattraktion kläs med ny, stark betong", Byggindustrin, no.13, ISSN: 0349-3733, Stockholm, 1994, p. 22-24.

REICHVERGER, Z. 1979. "Interaction of casting and mould surfaces in slip-form technology". Magazine of Concrete Research, Sep. 1979, vol.31, no.108 p. 171-176.

REICHVERGER, Z.; Jaegermann C. 1982. "Friction and pressure of concrete in slip-form concreting". Colloque International Sur le beton, Jevne, Paris, 6-8 April 1982.

SANDVIK, Malvin 1997, "Durability of Offshore Concrete Platforms in the North Sea", Norwegian Ready Mixed Concrete Association, 1997, Oslo.

SMEPLASS, Sverre 1988, "Kapillærabsorpsjon som kvalitetskriterium", SINTEF rapport STF65 A88028, ISBN: 82-595-5218-31988, Trondheim, 1988.

SHAW, Duncan J. 1992, "Colloid & Surface Chemistry", Fourth edition, Butterworth Heinemann, ISBN 0750611820, 1992, Oxford

SCHMIDT-THRÖ, G.; Stöckl, S. 1986 **a**, "Ausziehversuche, Proben in Uttin hergestellt" in Versuche über das Verbundverhalten von Rippenstählen bei Anwendung des Gleitbauverfahrens", Lehrstuhl für Massivbau, Technische Universität München, 1986, Schriftenreihe des Deutscher Ausschusses für Stahlbeton, heft 378, p.9-38.

SCHMIDT-THRÖ, G.; Stöckl, S.; Kupfer, H. 1986 **b**, "Versuche zur Bestimmung charakteristischer Betoneigenschaften bei Anwendung des Gleitbauverfahrens", in Versuche über das Verbundverhalten von Rippenstählen bei Anwendung des Gleitbauverfahrens, Lehrstuhl für Massivbau, Technische Universität München, 1986, Schriftenreihe des Deutscher Ausschusses für Stahlbeton, heft 378, p.39-62.

STEINECKE, M.; Prokopowicz, J.; Bach, W. 1964, "Experimental Investigation of the Pressure Exerted on and the Friction Encountered by Sliding Formwork", Translation of the paper in German from Bauplanung-Bautechnik, vol. 18. No.7. July 1964 . pp. 342-344, no.8. August 1964. Pp. 395-397, no.9. September 1964. Pp. 446-449. Translation made by Armerongen, C.V., Cement and Concrete Association, 1968, London.

SPECH, Manfred 1973, "Die Belastung von Schalung und Rüstung durch Frischbeton", Lehrstuhl für Massivbau, Technische Universität Hannover, Werner-Verlag GmbH, 1973, Düsseldorf.

TAZAWA, Ei-ichi (Chairman) 1999, "Committee Report", Proceeding in Autogenous Shrinkage of Concrete, edited by Tazawa. E & FN Spon, London, 1999, ISBN 0419238905, p. 3 – 68.

TEIGLAND, Jarle 1991, "Vanninntrengning målt på kjerner utboret fra glideflater i lettbetong", Internal memo in Norwegian Contractors AS, 04 March 91.

YONG, Raymond N.; Warkentin, Benno P. 1966, "Introduction to Soil Behavior", The Macmillian Company, New York, 1966.

WITTMANN, F.H. 1976, "On the action of capillary pressure in fresh concrete", Cement and Concrete Research, 1976, v. 6,no.1, p. 49-56.

ØSTMOEN, Trond 1999, "Bestandige betonkonstruksjoner . Rapport 2.1- Erfaring fra bruer" NBI, Oslo 1999.

APPENDIX A

Overview of the tests from the test rigs

Table A-1: Overview of the tests from the friction rig

Nr	Concrete type	Air content %	w/b-ratio	Slump cm	Binder content litre	Cement kg/m ³	Silica fume %	Sand 0-8 mm kg/m ³	Sand 0-2 mm kg/m ³	Coarse aggr. 8-11 kg/m ³	Coarse aggr. 11-16 kg/m ³	Normal force N	Remarks
HT105	basis		0.40	23	300	393	5%	762	206	335	519	2500	reproducibility test
HT106	basis		0.40	21	300	393	5%	762	206	335	519	2500	reproducibility test
HT107	basis		0.40	21	300	393	5%	762	206	335	519	2500	reproducibility test
HT108	basis		0.40	21.5	300	393	5%	762	206	335	519	2500	reproducibility test
HT109	basis		0.40	26	300	-	5%	762	206	335	519	2500	cement substituted
HT112	basis		0.40	23	300	393	5%	762	206	335	519	2500	reference (New panel)
HT117	basis		0.40	21.5	300	393	5%	762	206	335	519	2500	30 min frequency and 35 mm sliding
HT118	basis		0.40	22.5	300	-	5%	762	206	335	519	2500	cement substituted with fly ash/ limestone
HT122	basis		0.40	24.5	300	393	5%	713 ^{*1}	247	342	519	2500	reference
HT124	mix V	1.2%	0.40	24	300	393	5%	713 ^{*1}	247 ^{*2}	342	519	2500	with Mylonitt
HT126	basis		0.40	23	300	393	5%	713	247	342	519	600	normal pressure
HT159	basis		0.40	21.5	300	393	5%	713	247	342	519	1600	normal pressure
HT160	basis	9.0%	0.40	22	300	393	5%	713	247	342	519	2500	air admixture added
HT161	mix I	3.0%	0.40	19	300	336	20%	713	247	342	519	2500	silica fume
HT162	mix I	2.0%	0.40	20	300	416	0%	713	247	342	519	2500	silica fume
HT164	mix III	2.6%	0.40	26	300	393	5%	961	0	342	519	2500	coarse sand
HT165	mix II	1.4%	0.40	20	250	327	5%	765	265	367	557	2500	low binder content
HT166	mix VI	1.0%	0.60	17	300	308	5%	713	247	342	519	2500	w/b-ratio high
HT167	mix VI	2.0%	0.30	25	300	455	5%	713	247	342	519	2500	w/b-ratio low
HT168	basis	3.1%	0.40	21.5	300	393	5%	713	247	342	519	2500	reference
HT169	basis	2.6%	0.40	22	300	393	5%	715	235	353	519	2500	reference
HT170	basis	4.3%	0.40	22	300	393	5%	715	235	353	519	stepwise up and down	air admixture added
HT171	basis	12.0%	0.40	18	300	393	5%	715	235	353	519	2500	air admixture added
HT172	basis	8.0%	0.40	23	300	393	5%	715	235	353	519	stepwise up and down	air admixture added
HT173	basis	4.3%	0.40	22.5	300	393	5%	715	235	353	519	2500	Rough slipform panel used

*1 0-2 mm 860 kg/m³ (Mylonitt aggregate)

*2 4-8 mm 141 kg/m³ (Mylonitt aggregate)

*3 8-12 mm 352 kg/m³ (Mylonitt aggregate)

*4 12-16 mm 498 kg/m³ (Mylonitt aggregate)

Table A-2: Overview of the tests from the vertical slipform rig

Nr	Concrete type	Air content %	w/b-ratio	Slump cm	Binder content litres	Cement kg/m ³	Silica fume %	Sand 0-8 mm kg/m ³	Sand 0-2 mm kg/m ³	Coarse aggr. > 11-16 kg/m ³	Density kg/m ³	Admixtures	Lifting height mm	Lifting frequency minutes	Inclin. mm/m	Measured stiffness [N/mm]	Remarks
VT108	basis	1.2%	0.40	15.5	300	392	5%	672	348	282	519	Sikament 92	10	8	-1.5	405	Reproducibility test
VT111	basis	1.0%	0.40	18	300	392	5%	672	348	282	519	Sikament 92	10	8	-1.5	405	Reproducibility test
VT112	basis	1.1%	0.40	17.5	300	392	5%	672	348	282	519	Sikament 92	10	8	-1.5	405	Reproducibility test
VT113	basis	1.0%	0.40	18	300	392	5%	672	348	282	519	Sikament 92	10	8	-1.5	405	Heavy vibration
VT114	basis	1.1%	0.40	16.5	300	392	5%	672	348	282	519	Sikament 92	10	8	-1.5	405	15 second vibration
VT115	basis	1.0%	0.40	14.5	300	392	5%	672	348	282	519	Sikament 92	10	8	-1.5	405	30 second vibration
VT116	basis	1.0%	0.40	18	300	392	5%	672	348	282	519	Sikament 92	10	8	-1.5	405	30 second vibration
VT117	basis	0.9%	0.40	19.5	300	392	5%	672	348	282	519	Sikament 92	10	8	-1.5	405	30 second vibration in two layers
VT118	basis	1.1%	0.40	17	300	392	5%	672	348	282	519	Sikament 92	10	8	-1.5	405	30 second vibration in two layers
VT121	basis	0.7%	0.40	23	300	392	5%	672	348	282	519	Sikament 92	10	8	-1.5	1568	Effect of slump
VT122	basis	1.0%	0.40	18	300	392	5%	672	348	282	519	Sikament 92	10	8	-1.5	1568	Effect of slump
VT123	basis	1.2%	0.40	16	300	392	5%	672	348	282	519	Sikament 92	10	8	-1.5	405	Effect of slump
VT124	basis	0.8%	0.40	20.5	300	392	5%	672	348	282	519	Sikament 92	10	8	-1.5	405	Effect of slump
VT126	basis	1.0%	0.40	17	300	392	5%	672	348	282	519	Sikament 92	10	8	-1.5	405	No plastic cover on concrete surface
VT127	basis	0.9%	0.40	17	300	392	5%	672	348	282	519	Sikament 92	10	8	-1.5	405	No plastic cover and a light installed.
VT128	basis	0.4%	0.40	27	300	392	5%	672	348	282	519	Scancem SSP2000	10	8	-1.5	405	Self-compacting concrete
VT130	basis	0.3%	0.40	27	300	392	5%	679	351	286	525	Scancem SSP2000	10	8	-1.5	405	Self-compacting concrete
VT131	basis	0.7%	0.40	23.5	300	392	5%	679	351	286	525	Scancem SSP2000	10	8	-1.5	405	Self-compacting concrete
VT137	basis	0.2%	0.40	25.5	300	392	5%	679	351	286	525	Scancem SSP2000	10	8	-1.5	405	Self-compacting concrete
VT139	mix III	1.0%	0.40	16	300	392	5%	1030	0	286	525	Sikament 92	10	8	-1.5	405	Coarse sieve curve
VT140	mix III	1.0%	0.40	9	300	392	5%	1030	0	286	525	Sikament 92	10	8	-1.5	405	Coarse sieve curve
VT142	basis	1.0%	0.40	25.5	300	392	5%	679	351	286	525	Sika ViskoCrete 3	10	8	-1.5	405	Self-compacting concrete reproducibility test
VT143	basis	1.0%	0.40	26	300	392	5%	679	351	286	525	Sika ViskoCrete 3	10	8	-1.5	405	Self-compacting concrete reproducibility test
VT144	basis	1.2%	0.40	25	300	392	5%	679	351	286	525	Sika ViskoCrete 3	10	8	-1.5	405	Self-compacting concrete reproducibility test
VT145	basis	1.0%	0.40	25	300	392	5%	679	351	286	525	Sika ViskoCrete 3	10	8	-1.5	405	Self-compacting concrete reproducibility test
VT146	basis	0.9%	0.40	26.5	300	392	5%	679	351	286	525	Sika ViskoCrete 3	10	30	-1.5	405	Effect of lifting frequency
VT147	basis	0.7%	0.40	26.5	300	392	5%	679	351	286	525	Sika ViskoCrete 3	10	30	-1.5	405	Effect of lifting frequency
VT148	basis	0.8%	0.40	25.5	300	392	5%	679	351	286	525	Sika ViskoCrete 3	10	5	-1.5	405	Effect of lifting frequency
VT150	basis	1.3%	0.40	25.5	300	392	5%	679	351	286	525	Sika ViskoCrete 3	10	15	-1.5	405	Reference
VT151	basis	1.0%	0.40	25.5	300	392	5%	679	351	286	525	Sika ViskoCrete 3	10	15	-1.5	405	Reference
VT152	basis	0.7%	0.40	27	300	392	5%	679	351	286	525	Sika ViskoCrete 3	5	15	-1.5	405	Effect of lifting height
VT153	basis	1.3%	0.40	26	300	392	5%	679	351	286	525	Sika ViskoCrete 3	20	15	-1.5	405	Effect of lifting height
VT159	basis	0.9%	0.40	25	300	392	5%	679	351	286	525	Sika ViskoCrete 3	5	15	-1.5	405	Effect of lifting height
VT161	basis	1.1%	0.40	25.5	300	392	5%	679	351	286	525	Sika ViskoCrete 3	10	15	1.9	405	Effect of panel inclination
VT162	basis	0.9%	0.40	24.5	300	392	5%	679	351	286	525	Sika ViskoCrete 3	10	15	3.8	405	Effect of panel inclination
VT163	basis	1.2%	0.40	26	300	392	5%	679	351	286	525	Sika ViskoCrete 3	10	15	5.5	405	Effect of panel inclination
VT164	basis	0.9%	0.40	24.5	300	392	5%	679	351	286	525	Sika ViskoCrete 3	10	15	5.5	405	Effect of panel inclination
VT165	basis	0.8%	0.40	27	300	392	5%	679	351	286	525	Sika ViskoCrete 3	10	15	1.9	405	Effect of panel inclination
VT166	basis	0.9%	0.40	26	300	392	5%	679	351	286	525	Sika ViskoCrete 3	10	15	0	405	Effect of panel inclination
VT167	basis	1.0%	0.40	26	300	392	5%	679	351	286	525	Sika ViskoCrete 3	10	15	-1.5	405	Reference
VT168	basis	0.8%	0.40	27.5	300	392	5%	679	351	286	525	Sika ViskoCrete 3	10	15	-1.5	405	Reference
VT169	lightwe.	5.0%	0.40	2.5	300	392	5%	153	306	115 *	383 **	Sika ViskoCrete 3	10	15	-1.5	405	Lightweight concrete, 508 litre of LWA
VT170	lightwe.	4.3%	0.40	17.5	300	392	5%	254	431	89 *	1688 **	Sika ViskoCrete 3	10	15	-1.5	405	Lightweight concrete, 423 litre of LWA
VT171	lightwe.	4.9%	0.40	20	300	392	5%	562	362	75 *	1849 **	Sika ViskoCrete 3	10	15	-1.5	405	Lightweight concrete, 331 litre of LWA
VT172	lightwe.	2.6%	0.40	20	300	392	5%	679	351	0 *	351 **	Sika ViskoCrete 3	10	15	-1.5	405	Lightweight concrete, 291 litre of LWA
VT175	basis	1.0%	0.40	26	300	392	5%	679	351	286	525	Sika ViskoCrete 3	10	15	-1.5	253	Panel stiffness test
VT176	basis	1.1%	0.40	25.5	300	392	5%	679	351	286	525	Sika ViskoCrete 3	10	15	-1.5	1568	Panel stiffness test

Nr	Concrete type	Air content %	w/b-ratio	Slump cm	Binder content litres	Cement kg/m ³	Silica fume %	Sand 0-8 mm kg/m ³	Sand 0-2 mm kg/m ³	Coarse aggr. 8-11 kg/m ³	Coarse aggr. 11-16 kg/m ³	Density kg/m ³	Admixtures	Lifting height mm	Lifting frequency min/utes	Inclin. mm/m	Measured stiffness [N/mm ²]	Remarks
VT177	basis	1.1%	0.40	27	300	392	5%	679	351	286	525	2422	Sika ViskoCrete 3	10	15	-1.5	11588	Panel stiffness test
VT180	basis	0.8%	0.40	26.5	300	392	5%	679	351	286	525	2436	Sika ViskoCrete 3	10	15	-1.5	145	Panel stiffness test
VT181	basis	0.7%	0.40	27	300	392	5%	679	351	286	525	2421	Sika ViskoCrete 3	10	15	-1.5	405	Reference
VT182	basis	1.0%	0.40	25.5	300	392	5%	679	351	286	525	2428	Sika ViskoCrete 3	10	15	-1.5	405	Reference
VT184	basis	1.9%	0.40	7	300	392	5%	679	351	286	525	2438	Sika ViskoCrete 3	10	15	-1.5	405	2 x 15 seconds vibration
VT185	basis	1.9%	0.40	11.5	300	392	5%	679	351	286	525	2430	Sika ViskoCrete 3	10	15	-1.5	405	2 x 30 seconds vibration
VT186	basis	1.9%	0.40	10	300	392	5%	679	351	286	525	2416	Scancem SSP 200	10	15	-1.5	405	2 x 30 seconds vibration
VT187	basis	1.8%	0.40	11	300	392	5%	679	351	286	525	2418	Scancem SSP 200	10	15	-1.5	405	2 x 15 seconds vibration
VT188	basis	1.2%	0.40	27	300	392	5%	679	351	286	525	2427	Sika ViskoCrete 3	10	15	-1.5	405	Reference
VT190	mix II	0.6%	0.40	27	350	457	5%	629	326	265	487	2391	Sika ViskoCrete 3	10	15	-1.5	405	Binder volume 350 litre
VT191	mix II	1.0%	0.40	25	350	457	5%	629	326	265	487	2400	Sika ViskoCrete 3	10	15	-1.5	405	Binder volume 350 litre
VT192	mix II	1.5%	0.40	23	275	359	5%	703	364	297	544	2437	Sika ViskoCrete 3	10	15	-1.5	405	Binder volume 275 litre
VT194	basis	1.6%	0.40	10	300	392	5%	679	351	286	525	2450	Sika ViskoCrete 3	10	15	-1.5	405	2 x 60 seconds vibration
VT200	basis	1.2%	0.40	27	300	392	5%	679	351	286	525	2414	Sika ViskoCrete 3	10	15	-1.5	405	Reference
VT201	lightwe.	4.2%	0.40	16	300	394	5%	562	362	75 *	250 **	1850	Sika ViskoCrete 3	10	30	-1.5	405	Lightweight concrete (VT171)
VT202	lightwe.	3.9%	0.40	13	300	394	5%	562	362	75 *	250 **	1861	Sika ViskoCrete 3	10	30	-1.5	405	Lightweight concrete (VT171)
VT205	mix I	1.5%	0.40	26	300	371	10%	679	351	286	525	2412	Sika ViskoCrete 3	10	15	0	405	10 % SF
VT206	basis	1.5%	0.40	26	300	392	5%	679	351	286	525	2388	Sika ViskoCrete 3	10	15	0	405	Reference
VT207	basis		0.40	27/28/26	300	392	5%	679	351	286	525	2388	Sika ViskoCrete 3	10	15	0	405	3 concrete layer
VT208	basis		0.40	26/26/26	300	392	5%	679	351	286	525	2388	Sika ViskoCrete 3	10	15	0	405	3 concrete layer
VT210	bas/mix I		0.40	26/26/26	300	392	5%/20%	679	351	286	525	2388	Sika ViskoCrete 3	10	15	0	405	3 concrete layer resp. 5, 20, 5 % SF
VT211	basis		0.40	26/26/27	300	392	5%	679	351	286	525	2412	Sika ViskoCrete 3	10	30	0	405	3 concrete layer
VT212	basis	1.0%	0.40	27	300	392	5%	679	351	286	525	2412	Sika ViskoCrete 3	10	15	0	405	Reference
VT215	mix I	1.5%	0.40	25.5	300	336	20%	679	351	286	525	2398	Sika ViskoCrete 3	10	15	0	405	20 % SF
VT216	basis		0.40	27/26/27	300	392	5%	679	351	286	525	2388	Sika ViskoCrete 3	10	15	0	405	3 concrete layer, dirty panel
VT217	mix I	2.5%	0.40	26	300	336	20%	679	351	286	525	2384	Sika ViskoCrete 3	20	15	0	405	20 % SF and 20 mm lifting heights
VT218	bas/mix I		0.40	27/27/26	300	392	5%/20%	679	351	286	525	2371	SVC/SSP	10	15	0	405	3 concrete layer resp. 5, 20, 5 % SF
VT219	basis		0.40	27/27/26	300	336	20%	679	351	286	525	2378	Sika ViskoCrete 3	10	15	3.8	405	3 concrete layers, vibrated
VT220	mix I	1.8%	0.40	26.5	300	336	20%	679	351	286	525	2378	Sika ViskoCrete 3	20	15	-1.5	405	20 % SF
VT221	basis	0.8%	0.40	27	300	392	5%	679	351	286	525	2336	Sika ViskoCrete 3	20	15	-1.5	405	Reference
VT223	basis	0.8%	0.40	27	300	392	5%	679	351	286	525	2400	Sika ViskoCrete 3	20	15	-1.5	405	Reference
VT224	basis	1.6%	0.40	27	300	392	5%	679	351	286	525	2400	Sika ViskoCrete 3	10	15	-1.5	405	Reference, new cement
VT225	mix I	2.1%	0.40	27	300	336	20%	679	351	286	525	2371	Sika ViskoCrete 3	10	15	-1.5	405	20 % SF
VT226	mix I	1.7%	0.40	27	300	336	20%	679	351	286	525	2392	Sika ViskoCrete 3	10	15	-1.5	405	20 % SF
VT227	basis	1.6%	0.40	27	300	392	5%	679	351	286	525	2404	Sika ViskoCrete 3	10	15	-1.5	405	Rough slipform panel
VT228	basis	1.4%	0.40	27	300	392	5%	679	351	286	525	2398	Sika ViskoCrete 3	10	15	-1.5	405	Rough slipform panel
VT230	basis	1.8%	0.40	25	300	392	5%	679	351	286	525	2405	Sika ViskoCrete 3	10	15	-1.5	405	Rough slipform panel
VT231	basis	2.1%	0.40	26	300	392	5%	679	351	286	525	2393	Sika ViskoCrete 3	10	15	-1.5	405	Reference
VT232	basis	1.1%	0.40	27	300	392	5%	679	351	286	525	2387	Sika ViskoCrete 3	10	15	-1.5	405	Reference
VT251	basis	1.1%	0.40	26	300	392	5%	679	351	286	525	2438	Sika ViskoCrete 3	10	15	-1.5	405	High concrete block
VT252	basis	1.6%	0.40	27	300	392	5%	679	351	286	525	2432	Sika ViskoCrete 3	10	15	-1.5	405	Low height of concrete block

* Leca 1-4 mm

** Liapor 7 4-10 mm

Nr	Concrete type	Air content %	w/b-ratio	Slump cm	Binder content litres	Cement kg/m ³	Silica fume %	Sand 0-2 mm kg/m ³	Sand 2-5 mm kg/m ³	Coarse aggr. 5-8 kg/m ³	Coarse aggr. 11-16 kg/m ³	Density kg/m ³	Admixtures	Lifting height mm	Lifting frequency minutes	Inclin. mm/m	Measured stiffness [N/mm]	Remarks
VT245	mix IV	1.2%	0.40	12	300	392	5%	486	448	187	747	2504	Sika ViskoCrete 3	10	15	-1.5	472	Crushed aggregate (Aggregate of Mylonitt)
VT246	mix IV	1.4%	0.40	14	300	392	5%	486	448	187	747	2497	Sika ViskoCrete 3	10	15	-1.5	472	Crushed aggregate (Aggregate of Mylonitt)

Nr	Concrete type	Air content %	w/b-ratio	Slump cm	Binder content litres	Cement kg/m ³	Silica fume %	Sand 0-8 mm kg/m ³	Coarse aggr. 8-14 kg/m ³	Coarse aggr. 14-24 kg/m ³	Density kg/m ³	Admixtures	Lifting height mm	Lifting frequency minutes	Inclin. mm/m	Measured stiffness [N/mm]	Remarks
VT237	SBL1	1.1%	0.48	17	313	370	2.7%	910	910	0	2420	R and Melstab 21	10	15	-1.5	472	Concrete used at Sørkedalsv. site
VT242	SBL2	1.3%	0.48	22.5	332	394	3.1%	895	562	298	2407	R and Sika ViskoC	10	15	-1.5	472	Concrete used at Sørkedalsv. site
VT243	SBL1	1.3%	0.48	16.5	313	370	2.7%	910	910	0	2428	R and Melstab 21	10	15	-1.5	472	Concrete used at Sørkedalsv. site
VT244	SBL2	1.5%	0.48	20	332	394	3.1%	895	562	298	2401	R and Sika ViskoC	10	15	-1.5	472	Concrete used at Sørkedalsv. site
VT247	SBL1	1.1%	0.48	20	313	370	2.7%	910	910	0	2423	R and Melstab 21	10	15	-1.5	472	Concrete used at Sørkedalsv. site

Nr	Concrete type	Air content %	w/b-ratio	Slump cm	Binder content litres	Cement kg/m ³	Silica fume %	Sand 0-7 mm kg/m ³	Sand 0-8 mm kg/m ³	Coarse aggr. 8-16 kg/m ³	Density kg/m ³	Admixtures	Lifting height mm	Lifting frequency minutes	Inclin. mm/m	Measured stiffness [N/mm]	Remarks
VT248	TUKT	2.1%	0.44	19	341	447	0%	452	452	835	2404	Scancem SP1	10	15	-1.5	472	Concrete used at Tukthus site
VT249	TUKT	1.9%	0.44	19	341	447	0%	452	452	835	2400	Scancem SP1	10	15	-1.5	472	Concrete used at Tukthus site

APPENDIX B

Results from the capillary absorption testing

Table B

The results from the capillary absorption testing

Layer	Floor	Capillary resistance number [s/m ²]	Absorption porosity [volume %]	Estimated w/b-ratio
Slipform 1: Tested on the inside face				
	1	4.11E+07	13.7	0.40
0-20 mm	4	3.53E+07	15.9	0.46
	7	4.15E+07	14.5	0.42
	1	4.17E+07	13.9	0.41
20-40 mm	4	3.51E+07	17.0	0.48
	7	3.33E+07	14.1	0.41
	1	4.29E+07	13.5	0.40
40-60 mm	4	3.60E+07	14.8	0.43
	7	3.88E+07	15.4	0.44
Slipform 1: Tested on the outside face				
	1	4.91E+07	13.8	0.41
0-20 mm	4	3.78E+07	16.1	0.46
	7	3.53E+07	14.3	0.42
	1	5.62E+07	13.9	0.41
20-40 mm	4	4.46E+07	16.1	0.46
	7	4.17E+07	15.4	0.44
	1	5.90E+07	14.9	0.43
40-60 mm	4	4.75E+07	15.0	0.44
	7	4.63E+07	15.8	0.45
Slipform 2: Tested on the inside face				
	1	3.57E+07	13.9	0.46
0-20 mm	4	3.38E+07	15.3	0.52
	7	3.32E+07	15.2	0.52
	1	3.33E+07	12.3	0.44
10-40 mm	4	3.02E+07	14.5	0.50
	7	2.96E+07	14.3	0.50
	1	2.71E+07	12.5	0.45
40-60 mm	4	2.61E+07	11.5	0.42
	7	1.91E+07	14.3	0.50
Slipform 2: Tested on the outside face				
	1	4.12E+07	14.3	0.50
0-20 mm	4	4.29E+07	15.4	0.52
	7	3.44E+07	15.3	0.53
	1	5.57E+07	12.6	0.45
20-40 mm	4	6.42E+07	15.1	0.51
	7	4.23E+07	14.5	0.50
	1	4.84E+07	12.9	0.46
40-60 mm	4	2.67E+07	15.0	0.51
	7	4.35E+07	14.9	0.52

APPENDIX C

Key results from each test used in the report

HT160

Time h:m	Lifting height mm	Lifting stress		Normal pressure kPa	Aver. Pore water pressure kPa	Effective pressure kPa	Temp °C
		static kPa	sliding kPa				
1:00	0	2.99	2.07	4.54	1.35	3.19	22.8
1:08	10	2.89	1.95	4.52	0.97	3.55	22.8
1:16	20	2.53	1.94	4.52	0.97	3.56	22.7
1:24	30	2.51	2.13	4.51	1.10	3.41	22.7
1:33	40	2.65	2.26	4.52	1.00	3.52	22.8
1:41	50	2.75	2.35	4.52	1.10	3.42	22.8
1:49	60	3.51	2.30	4.48	0.89	3.59	22.6
1:57	70	2.93	2.35	14.21	2.31	11.90	22.7
2:05	80	2.89	2.48	13.94	3.88	10.06	22.8
2:13	90	3.30	2.56	14.02	4.51	9.51	22.7
2:21	100	3.56	2.85	14.04	4.61	9.43	22.7
2:29	110	3.76	3.12	14.07	4.87	9.20	22.8
2:37	120	4.31	3.62	14.04	4.25	9.78	22.7
2:45	130	4.85	4.23	14.01	3.75	10.26	22.7
2:54	140	5.30	4.31	13.99	3.40	10.60	22.7
3:02	150	5.37	4.81	14.00	2.93	11.08	22.7
3:10	160	6.27	4.92	14.01	2.77	11.24	22.7
3:18	170	6.39	4.89	13.96	2.02	11.94	22.8
3:26	180	6.19	5.01	13.96	1.65	12.31	22.9
3:34	190	6.57	5.46	13.98	1.22	12.76	23.0
3:42	200	7.14	5.90	13.94	0.78	13.16	23.0
3:50	210	7.55	6.38	13.95	0.33	13.62	23.1
3:58	220	7.48	6.77	13.93	-0.08	14.01	23.1
4:06	230	8.04	6.92	14.01	-0.33	14.34	23.4
4:15	240	8.44	7.18	14.01	-0.61	14.62	23.4
4:23	250	8.63	7.40	14.03	-0.85	14.88	23.5
4:31	260	8.82	7.45	14.06	-1.13	15.19	23.7
4:39	270	8.58	7.39	14.02	-1.34	15.36	23.7
4:47	280	8.40	7.19	14.01	-1.56	15.58	23.9
4:55	290	8.03	7.02	14.01	-1.79	15.80	24.0
5:03	300	8.08	6.78	14.00	-2.04	16.04	24.1
5:11	310	7.39	6.53	14.00	-2.55	16.55	24.2
5:19	320	7.73	6.43	14.04	-3.56	17.60	24.4
5:27	330	6.85	6.48	14.10	-4.30	18.40	24.6
5:36	340	7.14	6.49	14.13	-5.55	19.68	24.7
5:44	350	7.39	6.54	14.18	-7.29	21.47	25.1
5:52	360	6.90	6.55	14.11	-9.65	23.76	25.3
6:00	370	6.77	6.30	14.18	-12.64	26.82	25.5
6:08	380	6.38	6.07	14.18	-15.59	29.77	25.8
6:16	390	6.10	5.91	14.18	-19.65	33.82	26.0
6:24	400	6.67	5.86	14.23	-15.67	29.90	26.2
6:32	410	6.06	5.89	14.23	-15.17	29.40	26.6
6:40	420	6.24	5.95	14.21	-21.39	35.60	26.9
6:48	430	6.45	6.04	14.24	-14.95	29.19	27.2
6:57	440	6.49	6.25	14.27	-14.77	29.04	27.5
7:05	450	6.81	6.24	14.31	-14.91	29.22	27.9
7:13	460	6.89	5.93	14.31	-20.09	34.40	28.3
7:21	470	6.11	5.77	14.30	-14.75	29.05	28.7
7:29	480	5.97	5.72	14.32	-18.83	33.15	29.0
7:37	490	5.86	5.66	14.33	-14.72	29.04	29.4

HT168

Time h:m	Lifting height mm	Lifting stress		Normal pressure kPa	Aver. Pore water pressure kPa	Effective pressure kPa	Temp °C
		static kPa	sliding kPa				
0:55	0	7.34	6.16	4.16	0.82	3.34	23.4
1:03	10	7.04	6.23	4.18	1.08	3.11	23.1
1:11	20	7.02	6.36	4.18	1.14	3.04	23.1
1:19	30	5.43	4.22	4.21	1.13	3.07	23.2
1:28	40	5.77	4.79	14.01	2.00	12.02	23.3
1:36	50	6.30	5.17	13.94	2.01	11.93	23.3
1:44	60	6.80	5.32	13.93	2.10	11.83	23.3
1:52	70	7.37	6.00	13.92	2.15	11.77	23.4
2:00	80	7.75	6.48	13.93	2.12	11.81	23.3
2:08	90	8.67	7.12	13.89	2.00	11.89	23.6
2:16	100	9.22	7.67	14.03	2.11	11.92	23.5
2:24	110	10.02	8.33	14.10	2.11	11.99	23.5
2:32	120	10.65	8.94	14.08	2.03	12.05	23.4
2:40	130	10.90	9.18	14.02	1.67	12.35	23.5
2:49	140	11.63	10.05	14.09	1.44	12.65	23.4
2:57	150	12.20	10.48	14.10	1.51	12.59	23.5
3:05	160	11.96	10.47	14.13	1.19	12.94	23.4
3:13	170	12.60	10.73	14.14	1.04	13.10	23.5
3:21	180	12.94	10.70	14.11	0.86	13.25	23.7
3:29	190	12.73	10.18	14.12	0.77	13.35	23.5
3:37	200	12.93	10.34	14.06	0.69	13.37	23.6
3:45	210	12.60	10.63	13.92	-0.02	13.94	23.5
3:53	220	12.89	10.59	13.86	-0.17	14.03	23.5
4:01	230	12.72	11.02	13.88	-0.28	14.15	23.9
4:10	240	12.86	10.90	14.09	-0.34	14.43	24.2
4:18	250	13.36	11.19	14.13	-0.24	14.37	23.8
4:26	260	13.78	11.57	14.13	-0.31	14.44	23.9
4:34	270	14.43	11.88	14.18	-0.20	14.38	24.1
4:42	280	13.88	11.95	14.27	-0.56	14.83	24.2
4:50	290	15.05	12.49	14.33	-0.76	15.09	24.3
4:58	300	15.50	12.25	14.35	-1.13	15.48	24.3
5:06	310	15.55	12.33	14.30	-1.33	15.63	24.6
5:14	320	15.90	12.79	14.25	-1.87	16.11	24.7
5:22	330	16.67	13.49	14.16	-2.49	16.64	24.7
5:31	340	17.76	14.33	14.15	-3.39	17.54	25.0
5:39	350	19.26	15.16	14.08	-4.91	18.99	25.1
5:47	360	20.74	15.95	14.13	-7.45	21.58	25.4
5:55	370	21.51	16.21	14.17	-10.40	24.57	25.5
6:03	380	21.60	15.22	14.18	-13.69	27.87	25.7
6:11	390	20.39	13.32	14.16	-12.66	26.82	25.7
6:19	400	18.45	10.56	14.10	-12.02	26.12	25.8
6:27	410	14.95	9.64	14.08	-11.22	25.31	26.4
6:35	420	12.85	9.38	14.11	-10.85	24.96	26.5
6:43	430	11.35	9.36	14.04	-10.80	24.84	26.5
6:52	440	9.96	9.29	14.01	-10.77	24.78	26.8
7:00	450	9.90	9.36	14.01	-10.77	24.78	27.0
7:08	460	9.68	9.37	14.01	-10.78	24.79	27.4
7:16	470	10.12	9.37	14.03	-10.79	24.82	27.8
7:24	480	9.58	9.33	14.04	-10.82	24.85	28.1
7:32	490	9.55	9.23	14.06	-18.48	32.53	28.4

HT169

Time h:m	Lifting height mm	Lifting stress		Normal pressure kPa	Aver. Pore water pressure kPa	Effective pressure kPa	Temp °C
		static kPa	sliding kPa				
1:00	0	3.40	2.49	4.24	0.92	3.32	22.0
1:08	10	3.26	2.40	4.10	1.05	3.05	22.8
1:16	20	3.18	2.44	4.16	1.18	2.98	23.1
1:24	30	2.18	1.74	4.13	1.31	2.81	23.4
1:33	40	2.63	2.09	14.05	2.60	11.45	23.9
1:41	50	3.12	2.02	14.23	1.53	12.70	24.1
1:49	60	3.20	2.27	14.18	1.62	12.56	24.0
1:57	70	3.56	2.82	14.23	1.68	12.55	24.1
2:05	80	4.29	3.01	14.19	1.75	12.44	24.0
2:13	90	4.71	3.22	14.16	1.86	12.30	24.0
2:21	100	5.24	3.91	14.04	2.02	12.02	23.9
2:29	110	6.16	4.90	14.10	2.11	11.99	23.9
2:37	120	6.92	5.00	14.00	2.28	11.72	24.1
2:45	130	7.57	5.55	14.08	2.10	11.98	24.0
2:54	140	8.27	6.49	14.00	2.07	11.93	23.9
3:02	150	9.07	7.52	14.05	1.95	12.10	23.8
3:10	160	9.89	7.19	14.03	1.38	12.65	23.8
3:18	170	9.80	7.34	13.92	1.15	12.77	23.8
3:26	180	10.23	7.95	13.94	1.06	12.88	23.9
3:34	190	11.05	7.95	13.98	1.03	12.95	23.9
3:42	200	11.01	8.54	13.96	0.95	13.01	23.8
3:50	210	11.56	8.58	13.97	0.89	13.08	23.9
3:58	220	11.65	9.24	14.03	0.82	13.21	23.9
4:06	230	11.35	9.20	14.00	0.75	13.25	24.0
4:15	240	12.38	9.50	13.99	0.65	13.34	23.9
4:23	250	12.37	9.42	13.93	-0.08	14.01	23.9
4:31	260	12.37	9.32	13.92	-0.15	14.07	24.0
4:39	270	11.75	9.28	13.87	-0.25	14.12	24.2
4:47	280	12.61	9.48	13.92	-0.21	14.13	24.4
4:55	290	11.93	9.60	13.96	-0.22	14.18	24.5
5:03	300	12.89	9.53	13.94	-0.20	14.14	24.5
5:11	310	13.11	9.64	13.93	-0.27	14.20	24.5
5:19	320	13.32	9.75	13.91	-1.16	15.06	24.5
5:27	330	13.67	10.33	14.08	-2.06	16.13	24.7
5:36	340	14.80	10.48	14.04	-3.14	17.17	24.8
5:44	350	15.06	10.93	13.99	-4.26	18.24	25.0
5:52	360	15.33	11.45	13.99	-5.56	19.55	25.0
6:00	370	15.08	11.07	14.00	-7.16	21.16	25.2
6:08	380	15.91	10.52	13.97	-10.38	24.35	25.3
6:16	390	15.48	9.56	13.97	-12.51	26.48	25.6
6:24	400	13.23	8.50	14.04	-13.39	27.42	25.7
6:32	410	11.41	7.20	14.06	-15.40	29.47	25.9
6:40	420	8.97	7.14	14.11	-15.28	29.40	26.0
6:48	430	8.60	7.21	14.20	-13.78	27.98	26.2
6:57	440	7.65	7.10	14.23	-13.81	28.03	26.4
7:05	450	7.54	7.10	14.25	-13.04	27.30	26.7
7:13	460	7.95	7.12	14.27	-10.94	25.21	27.0
7:21	470	7.31	7.00	14.25	-12.23	26.49	27.3
7:29	480	7.12	6.91	14.29	-13.78	28.07	27.5
7:37	490	7.42	7.01	14.28	-11.38	25.66	27.8
7:45	500	7.77	7.05	14.33	-13.52	27.85	28.1

HT170

Time h:m	Lifting height mm	Lifting stress		Normal pressure kPa	Aver. Pore water pressure kPa	Effective pressure kPa	Temp °C
		static kPa	sliding kPa				
1:10	0	4.94	4.21	3.60	1.16	2.43	23.6
1:18	10	4.87	4.13	3.61	1.07	2.53	23.7
1:26	20	4.73	4.24	3.59	1.06	2.53	23.8
1:34	30	4.03	3.39	3.58	1.04	2.55	23.8
1:43	40	3.83	3.31	7.79	1.20	6.59	23.8
1:51	50	3.94	3.37	7.82	1.25	6.58	23.8
1:59	60	3.82	3.45	7.85	1.13	6.71	23.9
2:07	70	4.06	3.53	7.86	1.20	6.66	23.9
2:15	80	4.09	3.55	7.85	1.23	6.62	23.8
2:23	90	4.21	3.82	7.85	1.31	6.54	23.8
2:31	100	4.75	4.21	7.85	1.29	6.56	23.8
2:39	110	5.07	4.27	7.83	1.14	6.69	23.8
2:47	120	5.62	4.98	7.86	1.00	6.86	23.8
2:55	130	6.16	5.21	7.82	0.95	6.87	23.9
3:04	140	6.68	5.55	7.83	0.96	6.87	23.9
3:12	150	7.83	6.20	11.13	1.57	9.56	23.9
3:20	160	7.78	6.07	11.21	1.58	9.63	23.9
3:28	170	7.83	5.91	11.19	1.53	9.65	23.9
3:36	180	8.11	6.35	11.22	1.36	9.86	24.0
3:44	190	8.47	7.05	11.24	1.15	10.08	24.0
3:52	200	9.19	7.57	11.24	0.85	10.38	24.1
4:00	210	9.80	7.35	11.22	0.37	10.85	24.0
4:08	220	10.09	7.86	11.21	0.36	10.85	24.1
4:16	230	10.25	8.25	11.19	0.22	10.97	24.1
4:25	240	10.43	8.56	11.24	-0.08	11.33	24.2
4:33	250	11.50	9.11	11.22	0.02	11.19	24.3
4:41	260	12.32	9.56	14.38	-0.05	14.44	24.3
4:49	270	12.88	9.96	14.49	-0.02	14.51	24.5
4:57	280	12.73	10.66	14.56	-0.10	14.65	24.6
5:05	290	13.21	10.54	14.55	-0.11	14.66	24.7
5:13	300	14.12	10.67	14.57	-0.14	14.71	24.7
5:21	310	14.50	10.91	14.56	-0.47	15.03	24.9
5:29	320	14.88	11.28	14.52	-0.87	15.39	25.0
5:37	330	15.40	11.67	14.50	-3.38	17.88	25.1
5:46	340	15.80	11.94	14.54	-4.58	19.12	25.2
5:54	350	15.92	12.37	14.54	-6.02	20.55	25.4
6:02	360	17.56	13.09	14.56	-7.90	22.46	25.5
6:10	370	17.86	12.32	14.57	-9.76	24.33	25.7
6:18	380	16.94	11.56	7.99	-7.82	15.81	25.9
6:26	390	16.44	10.15	8.10	-7.81	15.91	26.1
6:34	400	15.15	8.36	8.15	-7.81	15.96	26.3
6:42	410	11.36	7.70	8.19	-7.77	15.97	26.5
6:50	420	9.92	7.43	8.22	-7.81	16.03	26.8
6:58	430	8.44	7.58	8.22	-7.78	16.00	27.0
7:07	440	7.60	7.33	8.21	-7.81	16.02	27.3
7:15	450	7.78	7.46	3.98	-7.76	11.74	27.5
7:23	460	7.77	7.56	4.03	-7.84	11.87	27.8
7:31	470	7.72	7.48	4.06	-7.89	11.95	28.1
7:39	480	8.32	7.39	4.09	-8.01	12.09	28.4
7:47	490	8.37	7.43	4.09	-7.92	12.01	28.7
7:55	500	8.07	7.38	4.13	-7.92	12.05	29.0

HT172

Time h:m	Lifting height mm	Lifting stress		Normal pressure kPa	Aver. Pore water pressure kPa	Effective pressure kPa	Temp °C
		static kPa	sliding kPa				
1:10	0	5.80	4.97	4.88	1.27	3.62	23.0
1:18	10	5.60	4.84	4.47	1.33	3.15	23.0
1:26	20	5.61	4.57	4.40	1.11	3.29	23.0
1:34	30	4.80	4.19	4.38	1.00	3.38	23.0
1:43	40	4.79	3.97	8.17	1.39	6.78	23.0
1:51	50	4.68	4.16	7.39	1.02	6.38	23.1
1:59	60	5.01	4.42	7.22	1.15	6.08	23.1
2:07	70	4.95	4.42	7.27	1.38	5.88	23.1
2:15	80	5.21	4.42	7.32	1.24	6.07	23.2
2:23	90	5.46	4.75	7.23	1.18	6.05	23.1
2:31	100	5.52	5.14	7.34	1.25	6.09	23.1
2:39	110	6.03	5.15	7.32	1.03	6.29	23.2
2:47	120	5.83	5.47	7.27	0.87	6.40	23.2
2:55	130	6.38	5.41	7.29	0.87	6.42	23.2
3:04	140	6.30	5.67	10.95	1.40	9.55	23.2
3:12	150	6.78	6.12	10.95	1.51	9.43	23.3
3:20	160	7.09	6.29	11.01	1.41	9.60	23.3
3:28	170	7.56	6.55	11.03	1.45	9.58	23.3
3:36	180	7.43	6.92	11.06	1.37	9.70	23.3
3:44	190	7.98	7.27	11.05	1.12	9.93	23.3
3:52	200	8.69	7.74	11.07	0.78	10.30	23.3
4:00	210	9.23	7.68	11.08	0.81	10.27	23.4
4:08	220	9.14	7.87	11.07	0.52	10.55	23.4
4:16	230	9.50	8.19	11.07	0.25	10.81	23.5
4:25	240	9.48	8.58	11.07	0.19	10.88	23.6
4:33	250	10.60	9.54	13.82	0.05	13.77	23.7
4:41	260	11.62	9.91	14.13	-0.07	14.20	23.8
4:49	270	11.69	10.50	14.23	-0.47	14.70	23.9
4:57	280	12.27	10.94	14.21	-0.95	15.16	24.1
5:05	290	12.62	11.07	14.29	-1.41	15.70	24.2
5:13	300	13.06	11.33	14.28	-2.01	16.28	24.2
5:21	310	13.40	11.08	14.28	-2.73	17.01	24.4
5:29	320	13.35	11.10	14.22	-3.52	17.74	24.6
5:37	330	12.82	10.76	14.28	-4.56	18.83	24.8
5:46	340	12.44	10.05	14.30	-5.62	19.91	25.0
5:54	350	11.49	9.20	14.33	-6.97	21.30	25.1
6:02	360	11.47	8.89	14.35	-8.34	22.69	25.3
6:10	370	10.67	8.41	14.37	-9.51	23.88	25.5
6:18	380	9.14	8.24	8.06	-6.92	14.98	25.7
6:26	390	9.34	7.99	8.13	-7.07	15.20	25.9
6:34	400	8.08	7.79	8.19	-8.67	16.86	26.2
6:42	410	8.58	7.71	8.21	-8.39	16.60	26.4
6:50	420	7.74	7.48	8.24	-8.36	16.60	26.7
6:58	430	7.63	7.41	8.25	-8.33	16.58	27.0
7:07	440	7.77	7.49	4.59	-8.36	12.94	27.2
7:15	450	7.73	7.58	4.13	-8.37	12.50	27.5
7:23	460	7.67	7.53	4.16	-8.44	12.60	27.8
7:31	470	7.50	7.37	4.21	-8.50	12.71	28.1
7:39	480	7.85	7.29	4.23	-8.54	12.77	28.4
7:47	490	7.40	7.28	4.27	-8.48	12.74	28.8
7:55	500	7.81	7.24	4.28	-8.48	12.76	29.1

VT108

Time h:m	Lifting height mm	Lifting stress		Normal pressure kPa	Aver. Pore water pressure kPa	Effective pressure kPa	Deformation mm	Temp °C
		static kPa	sliding kPa					
0:47	0	2.17	1.42	7.43			0.00	Error in reading
0:55	10	1.40	1.32	7.41			0.03	
1:03	20	1.28	1.13	7.39	7.08	0.30	0.08	
1:11	31	1.11	1.03	7.37	6.75	0.62	0.12	
1:19	41	1.16	1.04	7.31	6.25	1.05	0.14	
1:26	51	1.20	1.00	7.26	5.82	1.44	0.15	
1:34	62	1.18	1.18	7.22	5.63	1.60	0.17	
1:42	72	1.32	1.32	7.15	5.32	1.84	0.18	
1:50	83	1.18	1.11	7.08	5.06	2.02	0.19	
1:58	93	1.29	1.29	7.04	4.97	2.07	0.20	
2:06	104	1.42	1.36	6.97	4.60	2.37	0.21	
2:14	114	1.44	1.39	6.89	4.24	2.65	0.22	
2:21	125	1.58	1.53	6.85	4.09	2.76	0.23	
2:29	135	1.83	1.59	6.78	3.90	2.88	0.24	
2:37	146	2.00	1.80	6.73	3.69	3.04	0.25	
2:45	156	2.13	1.90	6.71	3.62	3.09	0.25	
2:53	167	2.37	2.15	6.68	3.56	3.12	0.26	
3:01	177	2.54	2.28	6.62	3.44	3.18	0.27	
3:09	188	2.63	2.34	6.59	3.24	3.35	0.27	
3:16	198	2.66	2.66	6.56	3.19	3.37	0.27	
3:24	209	2.82	2.69	6.53	3.03	3.50	0.28	
3:32	219	2.93	2.74	6.52	2.87	3.65	0.28	
3:40	230	2.99	2.80	6.50	2.69	3.80	0.29	
3:48	240	3.28	3.24	6.47	2.74	3.73	0.29	
3:56	251	3.89	3.30	6.41	2.75	3.66	0.29	
4:04	261	3.18	3.00	6.38	2.72	3.66	0.29	
4:11	271	3.26	3.02	6.35	2.55	3.79	0.25	
4:19	282	3.13	2.91	6.33	2.37	3.96	0.30	
4:27	292	3.24	3.18	6.31	2.12	4.19	0.29	
4:35	303	3.11	2.74	6.30	1.82	4.47	0.27	
4:43	313	3.14	3.03	6.33	1.72	4.61	0.29	
4:51	323	3.63	3.11	6.46	1.38	5.09	0.30	
4:58	334	3.90	3.63	6.54	0.89	5.64	0.30	
5:06	345	4.17	4.09	6.54	0.27	6.27	0.30	
5:14	356	4.49	4.00	6.52	-0.21	6.73	0.31	
5:22	366	4.33	4.04	6.50	-0.42	6.92	0.32	
5:30	377	4.67	4.21	6.46	-0.51	6.97	0.33	
5:38	387	4.38	4.10	6.41	-0.68	7.09	0.34	
5:46	398	4.85	4.32	6.38	-0.99	7.37	0.35	
5:53	408	4.88	4.47	6.39	-1.51	7.90	0.35	
6:01	418	5.24	4.71	6.43	-2.17	8.60	0.36	
6:09	429	5.50	4.94	6.46	-3.02	9.48	0.36	
6:17	439	6.25	5.42	6.49	-3.99	10.49	0.36	
6:25	450	7.04	5.72	6.55	-5.08	11.63	0.37	
6:33	460	7.34	5.95	6.59	-6.13	12.73	0.37	
6:40	471	7.89	5.84	6.65	-7.28	13.93	0.37	
6:48	481	7.52	5.32	6.72	-8.82	15.53	0.37	
6:56	491	7.28	4.63	6.77	-10.25	17.02	0.37	
7:04	502	5.83	4.29	6.81	-11.84	18.65	0.38	
7:12	512	5.38	4.02	6.86	-17.54	24.39	0.38	
7:20	523	5.00	3.59	6.87	-23.30	30.17	0.38	
7:28	533	4.35	3.69	6.87	-28.94	35.81	0.38	
7:35	544	3.85	3.26	6.90	-34.56	41.45	0.38	
7:43	554	3.80	3.73	6.90	-41.82	48.72	0.39	
7:51	564	3.80	3.54	6.88	-46.99	53.88	0.39	
7:59	575	3.79	3.64	6.88	-53.28	60.17	0.39	
8:07	585	3.97	3.76	6.89	-58.87	65.76	0.39	
8:15	596	3.87	3.62	6.90	-63.50	70.41	0.40	
8:22	606	3.97	3.81	6.90	-66.67	73.56	0.40	
8:30	617	3.90	3.77	6.92	-67.71	74.63	0.40	
8:38	627	3.94	3.66	6.92	-66.28	73.20	0.41	
8:46	637	4.05	3.76	6.91	-63.71	70.62	0.41	
8:54	648	4.02	3.71	6.91	-60.76	67.67	0.41	
8:56	658	3.99	3.56	6.90	-59.49	66.39	0.41	

VT111

Time h:m	Lifting height mm	Lifting stress		Normal pressure kPa	Aver. Pore water pressure kPa	Effective pressure kPa	Deformation mm	Temp °C
		static kPa	sliding kPa					
0:36	0	1.41	0.92	7.18			0.00	23.1
0:44	11	1.02	0.75	7.14			0.01	23.1
0:52	21	0.87	0.78	7.09			0.01	23.2
1:00	32	0.96	0.68	7.05	7.05	0.01	0.01	23.2
1:08	42	0.92	0.66	7.01	6.64	0.36	0.01	23.3
1:15	52	1.04	0.97	6.95	6.38	0.56	0.02	23.4
1:23	63	0.89	0.83	6.89	6.13	0.76	0.02	23.4
1:31	73	1.22	0.87	6.79	5.98	0.81	0.02	23.5
1:39	84	1.09	0.99	6.73	5.73	1.00	0.02	23.5
1:47	94	1.18	1.16	6.70	5.42	1.28	0.02	23.5
1:55	105	1.51	1.25	6.63	5.19	1.45	0.02	23.5
2:03	115	1.38	1.34	6.57	5.00	1.57	0.02	23.6
2:10	126	1.67	1.38	6.56	4.70	1.85	0.03	23.6
2:18	136	1.63	1.34	6.49	4.47	2.02	0.03	23.4
2:26	147	1.92	1.79	6.42	4.25	2.17	0.03	23.4
2:34	157	1.86	1.65	6.37	4.08	2.29	0.03	23.5
2:42	168	2.11	2.11	6.31	3.96	2.35	0.03	23.5
2:50	178	1.96	1.83	6.26	3.75	2.51	0.04	23.6
2:58	189	2.46	2.24	6.22	3.61	2.61	0.04	23.6
3:05	199	2.75	2.26	6.18	3.35	2.82	0.04	23.6
3:13	210	2.34	1.99	6.14	3.32	2.82	0.06	23.6
3:21	220	2.32	2.32	6.13	3.12	3.01	0.06	23.7
3:29	231	2.31	2.26	6.10	2.89	3.21	0.06	23.7
3:37	241	2.38	2.37	6.06	2.84	3.22	0.06	23.7
3:45	252	2.48	2.48	6.04	2.88	3.16	0.06	23.8
3:53	262	2.54	2.47	6.02	2.63	3.39	0.06	23.8
4:00	272	2.98	2.91	5.99	2.62	3.37	0.05	23.9
4:08	283	2.85	2.69	5.98	2.23	3.76	0.06	23.9
4:16	293	2.84	2.58	5.96	1.96	4.00	0.06	23.9
4:24	304	2.95	2.78	5.98	1.74	4.24	0.07	23.9
4:32	314	2.75	2.75	6.05	1.32	4.73	0.07	24.0
4:40	325	2.96	2.86	6.19	0.94	5.25	0.07	24.0
4:47	335	3.43	3.35	6.27	0.46	5.81	0.07	24.1
4:55	346	4.00	3.84	6.27	-0.27	6.55	0.07	24.1
5:03	357	4.25	3.84	6.27	-0.70	6.98	0.07	24.2
5:11	367	4.31	4.05	6.24	-0.93	7.17	0.07	24.2
5:19	378	4.51	4.07	6.19	-1.16	7.34	0.08	24.3
5:27	388	4.61	4.26	6.13	-1.44	7.57	0.08	24.4
5:35	398	4.87	4.53	6.13	-1.79	7.93	0.08	24.5
5:42	409	5.26	4.83	6.15	-2.41	8.56	0.08	24.6
5:50	419	5.88	5.06	6.21	-3.16	9.38	0.08	24.7
5:58	430	6.57	6.14	6.25	-4.41	10.66	0.08	24.8
6:06	440	7.29	5.90	6.30	-5.60	11.90	0.08	25.0
6:14	451	8.08	6.32	6.33	-6.24	12.57	0.08	25.1
6:22	461	8.67	6.53	6.37	-8.65	15.03	0.08	25.2
6:30	471	9.93	5.85	6.43	-11.17	17.60	0.08	25.4
6:37	482	9.75	5.48	6.49	-14.58	21.07	0.08	25.5
6:45	492	7.87	4.11	6.53	-19.39	25.93	0.08	25.6
6:53	503	5.53	3.80	6.57	-25.00	31.57	0.08	25.7
7:01	513	4.58	3.39	6.60	-26.76	33.36	0.08	26.0
7:09	524	3.64	3.25	6.62	-32.98	39.61	0.08	26.2
7:17	534	3.70	3.63	6.67	-37.10	43.76	0.08	26.4
7:25	545	3.63	3.32	6.75	-41.32	48.07	0.08	26.6
7:32	555	3.83	3.56	6.81	-45.60	52.40	0.08	26.9
7:40	565	3.85	3.57	6.87	-45.68	52.55	0.08	27.2
7:48	576	3.97	3.90	6.93	-46.28	53.21	0.08	27.6
7:56	586	4.13	3.88	6.97	-47.90	54.87	0.08	27.8
8:04	597	4.23	3.99	7.02	-46.66	53.68	0.08	28.1
8:12	607	4.35	4.17	7.02	-47.09	54.11	0.08	28.4
8:19	618	4.36	4.21	7.03	-47.61	54.63	0.08	28.6
8:27	628	4.34	4.15	7.03	-48.16	55.19	0.08	28.9
8:35	638	4.27	3.96	7.02	-48.19	55.21	0.08	29.2
8:43	649	4.35	4.03	7.04	-48.08	55.12	0.08	29.5

VT112

Time h:m	Lifting height mm	Lifting stress		Normal pressure kPa	Aver. Pore water pressure kPa	Effective pressure kPa	Deformation mm	Temp °C
		static kPa	sliding kPa					
0:45	0	1.51	0.82	7.73			0.00	22.7
0:53	10	1.07	0.64	7.67			0.00	23.1
1:01	21	0.88	0.56	7.60	7.27	0.31	0.00	23.3
1:09	32	0.75	0.66	7.56	7.08	0.44	0.00	23.5
1:17	42	0.86	0.49	7.51	6.74	0.73	0.00	23.6
1:25	52	0.82	0.76	7.43	6.43	0.95	0.00	23.7
1:33	63	0.78	0.69	7.37	6.12	1.21	0.00	23.7
1:40	73	0.83	0.83	7.30	5.84	1.45	0.00	23.9
1:48	84	0.81	0.81	7.24	5.49	1.72	0.00	23.7
1:56	94	0.87	0.65	7.18	5.31	1.83	0.00	23.8
2:04	104	0.95	0.95	7.11	5.07	2.02	0.00	23.8
2:12	115	1.12	1.12	7.05	4.77	2.24	0.01	23.8
2:20	125	1.26	1.10	6.99	4.64	2.30	0.01	23.9
2:28	136	1.30	1.14	6.91	4.36	2.51	0.01	23.9
2:35	146	1.45	1.44	6.87	4.12	2.70	0.01	23.8
2:43	157	1.56	1.56	6.82	3.83	2.97	0.01	23.9
2:51	167	1.90	1.47	6.77	3.73	3.01	0.01	24.0
2:59	177	1.73	1.68	6.71	3.62	3.06	0.01	24.1
3:07	188	2.18	2.05	6.66	3.37	3.26	0.01	24.0
3:15	198	2.20	1.88	6.62	3.18	3.40	0.02	24.0
3:23	209	2.12	1.74	6.59	3.01	3.52	0.03	24.1
3:30	219	2.33	2.01	6.55	2.80	3.73	0.02	24.0
3:38	230	2.58	2.39	6.52	2.62	3.88	0.03	24.5
3:46	240	2.51	2.43	6.47	2.58	3.89	0.03	23.8
3:54	251	2.36	2.27	6.43	2.62	3.79	0.03	23.8
4:02	261	2.40	2.08	6.40	2.34	4.04	0.03	23.9
4:10	272	2.46	2.16	6.38	2.18	4.18	0.03	24.2
4:18	282	2.55	2.40	6.36	1.86	4.48	0.03	23.9
4:25	293	2.40	2.40	6.34	1.56	4.76	0.03	23.9
4:33	303	2.69	2.42	6.35	1.36	4.97	0.03	24.0
4:41	313	2.88	2.56	6.42	0.99	5.39	0.03	24.1
4:49	324	2.91	2.79	6.54	0.64	5.85	0.03	24.2
4:57	334	3.33	3.20	6.57	0.11	6.43	0.03	24.3
5:05	345	3.53	3.48	6.56	-0.49	7.05	0.03	24.3
5:13	356	3.87	3.64	6.56	-0.92	7.47	0.03	24.4
5:20	366	3.92	3.55	6.54	-1.08	7.61	0.03	24.5
5:28	377	4.02	3.85	6.52	-1.38	7.90	0.03	24.7
5:36	387	4.30	3.87	6.52	-1.78	8.30	0.03	24.8
5:44	398	4.39	4.11	6.55	-2.28	8.83	0.03	24.9
5:52	408	4.73	4.26	6.59	-2.88	9.47	0.03	25.0
6:00	419	5.43	4.57	6.65	-3.69	10.33	0.03	25.1
6:08	429	5.90	4.88	6.69	-4.70	11.39	0.03	25.2
6:15	440	6.40	5.18	6.75	-5.65	12.40	0.03	25.4
6:23	450	6.70	5.16	6.82	-7.79	14.60	0.03	25.5
6:31	461	6.58	4.37	6.85	-10.33	17.18	0.03	25.8
6:39	471	6.27	4.10	6.91	-13.60	20.51	0.03	25.8
6:47	481	5.39	3.69	6.97	-17.64	24.60	0.03	26.0
6:55	492	4.58	3.26	7.04	-23.21	30.24	0.03	26.1
7:03	502	3.73	3.07	7.12	-28.73	35.85	0.03	26.4
7:10	513	3.20	3.02	7.20	-34.84	42.04	0.03	26.6
7:18	523	3.20	3.11	7.28	-40.69	47.97	0.03	26.8
7:26	534	3.28	3.21	7.37	-43.52	50.90	0.03	27.1
7:34	544	3.39	3.14	7.45	-49.82	57.27	0.03	27.3
7:42	554	3.46	3.23	7.53	-51.87	59.38	0.03	27.6
7:50	565	3.42	3.12	7.58	-56.33	63.90	0.03	27.8
7:57	575	3.57	3.24	7.65	-56.64	64.29	0.03	28.1
8:05	586	3.63	3.36	7.73	-54.65	62.37	0.03	28.4
8:13	596	3.73	3.66	7.79	-44.03	51.81	0.03	28.7
8:21	606	3.77	3.77	7.83	-43.02	50.83	0.03	29.0
8:29	617	3.88	3.75	7.86	-41.50	49.37	0.03	29.3
8:37	627	3.83	3.76	7.90	-40.87	48.76	0.03	29.6
8:45	638	3.83	3.80	7.93	-35.89	43.82	0.03	29.9
8:52	648	3.82	3.72	7.93	-31.52	39.45	0.03	30.2
9:00	659	3.96	3.74	7.94	-30.59	38.52	0.03	30.5

VT113

Time	Lifting height	Lifting stress		Normal pressure	Aver. Pore water pressure	Effective pressure	Deformation	Temp
h:m	mm	static kPa	sliding kPa	kPa	kPa	kPa	mm	°C
0:40	0	1.34	0.67	8.17			0.00	23.1
0:48	10	0.67	0.59	8.12			0.00	23.4
0:56	21	0.63	0.56	8.01			0.00	23.6
1:03	32	0.70	0.50	7.94	7.44	0.47	0.00	23.8
1:11	42	0.70	0.67	7.89	7.28	0.58	0.01	23.9
1:19	52	0.84	0.63	7.86	6.86	0.96	0.01	24.0
1:27	64	0.81	0.58	7.79	6.70	1.08	0.01	24.1
1:35	74	0.81	0.57	7.72	6.61	1.09	0.01	24.1
1:43	84	0.98	0.74	7.67	6.31	1.33	0.01	24.2
1:51	94	1.01	0.98	7.60	6.21	1.37	0.01	24.2
1:59	105	0.90	0.90	7.56	5.78	1.75	0.01	24.2
2:06	116	1.15	1.08	7.50	5.60	1.87	0.01	24.3
2:14	126	1.44	1.12	7.43	5.54	1.86	0.02	24.3
2:22	136	1.60	1.33	7.37	5.29	2.04	0.02	24.3
2:30	147	1.41	1.32	7.32	5.11	2.19	0.01	24.4
2:38	157	1.66	1.43	7.27	4.86	2.38	0.02	24.5
2:46	168	1.63	1.63	7.23	4.67	2.52	0.02	24.5
2:54	178	1.72	1.70	7.18	4.48	2.67	0.02	24.5
3:01	189	2.26	2.25	7.13	4.26	2.83	0.02	24.6
3:09	199	2.52	2.09	7.08	4.23	2.82	0.03	24.5
3:17	210	2.26	2.19	7.05	3.99	3.02	0.03	24.5
3:25	220	2.60	2.50	7.01	3.79	3.18	0.03	24.5
3:33	231	2.59	2.48	6.96	3.49	3.46	0.03	24.5
3:41	241	2.94	2.72	6.93	3.37	3.55	0.04	24.6
3:49	252	2.85	2.78	6.90	3.31	3.57	0.04	24.7
3:56	262	2.88	2.88	6.85	2.92	3.89	0.04	24.6
4:04	273	2.78	2.63	6.81	2.58	4.20	0.04	24.6
4:12	283	2.87	2.70	6.78	2.24	4.51	0.02	24.7
4:20	294	2.94	2.89	6.80	1.70	5.08	0.03	24.8
4:28	304	3.04	2.79	6.82	1.26	5.53	0.04	24.7
4:36	314	3.50	3.50	6.96	0.81	6.08	0.04	24.9
4:43	325	3.95	3.92	7.09	0.27	6.78	0.04	24.9
4:51	336	4.68	4.50	7.10	-0.49	7.59	0.04	25.0
4:59	346	5.01	4.69	7.10	-0.87	7.96	0.05	25.1
5:07	357	5.14	4.67	7.08	-1.17	8.25	0.05	25.2
5:15	367	5.33	4.57	7.05	-1.52	8.57	0.05	25.3
5:23	378	5.13	4.68	7.02	-1.99	9.01	0.05	25.5
5:31	388	5.57	4.93	7.05	-2.47	9.52	0.05	25.6
5:38	399	6.18	5.30	7.08	-3.30	10.38	0.05	25.8
5:46	409	6.81	5.76	7.15	-4.76	11.90	0.05	25.9
5:54	420	8.12	6.37	7.19	-5.79	12.98	0.05	26.0
6:02	430	8.97	6.55	7.23	-8.97	16.19	0.05	26.2
6:10	440	10.27	6.95	7.29	-11.57	18.85	0.05	26.8
6:18	451	12.03	5.86	7.34	-15.52	22.86	0.05	26.3
6:26	461	8.87	4.16	7.39	-18.78	26.16	0.05	26.4
6:33	472	6.22	2.93	7.45	-22.30	29.75	0.04	26.7
6:41	482	3.65	3.22	7.50	-25.78	33.28	0.04	26.9
6:49	493	3.51	3.32	7.57	-29.39	36.96	0.04	27.2
6:57	503	3.56	3.08	7.64	-32.87	40.51	0.04	27.5
7:05	513	3.64	3.36	7.71	-35.96	43.67	0.04	27.9
7:13	524	3.73	3.57	7.77	-38.43	46.19	0.04	28.2
7:21	534	3.76	3.40	7.84	-40.74	48.58	0.04	28.4
7:28	545	3.85	3.69	7.91	-43.52	51.42	0.04	28.7
7:36	555	3.90	3.87	7.97	-44.70	52.67	0.04	29.1
7:44	566	3.95	3.82	8.05	-46.36	54.40	0.04	29.4
7:52	576	4.07	3.77	8.12	-46.86	54.98	0.04	29.7
8:00	586	4.16	3.87	8.18	-47.88	56.05	0.04	30.0
8:08	597	4.29	3.98	8.21	-48.56	56.76	0.04	30.3
8:15	607	4.29	4.20	8.21	-49.01	56.44	0.04	30.7

VT115

Time h:m	Lifting height mm	Lifting stress		Normal pressure kPa	Aver. Pore water pressure kPa	Effective pressure kPa	Deformation mm	Temp °C
		static kPa	sliding kPa					
0:53	0	2.03	1.16	7.96			0.00	23.6
1:03	10	1.62	1.14	7.79	5.42	2.37	1.20	23.7
1:10	21	1.37	1.28	7.71	5.25	2.45	1.22	23.7
1:18	32	1.69	0.88	7.67	4.95	2.69	1.23	23.8
1:26	43	1.62	1.62	7.64	4.72	2.91	1.26	23.8
1:34	53	1.64	1.64	7.54	4.66	2.87	1.26	23.8
1:42	63	1.66	0.93	7.52	4.05	3.47	1.27	23.9
1:50	74	1.90	1.00	7.47	3.89	3.58	1.31	23.9
1:58	84	1.47	1.16	7.40	3.72	3.68	1.32	23.9
2:05	95	1.47	1.40	7.37	3.48	3.86	1.32	23.9
2:13	105	1.80	1.50	7.30	3.17	4.11	1.33	24.0
2:21	116	1.80	1.70	7.26	2.87	4.36	1.46	24.0
2:29	126	1.82	1.77	7.21	2.65	4.53	1.47	24.0
2:37	137	2.11	1.91	7.13	2.44	4.67	1.47	24.0
2:45	147	2.06	2.06	7.08	2.26	4.81	1.47	24.0
2:53	158	2.17	1.95	7.05	1.96	5.07	1.49	24.0
3:01	168	2.05	1.88	7.01	1.73	5.26	1.50	24.1
3:08	179	2.34	2.06	6.97	1.53	5.41	1.52	24.1
3:16	189	2.48	2.12	6.92	1.33	5.58	1.51	24.1
3:24	200	2.54	2.02	6.90	1.17	5.71	1.51	24.1
3:32	210	2.79	2.79	6.87	0.96	5.89	1.52	24.2
3:40	220	3.40	2.97	6.83	0.87	5.96	1.55	24.1
3:48	231	3.16	2.78	6.82	0.59	6.22	1.55	24.2
3:56	241	3.21	1.81	6.81	0.49	6.31	1.56	24.2
4:03	252	3.01	3.00	6.78	0.33	6.45	1.56	24.2
4:11	262	3.44	2.94	6.78	0.06	6.72	1.56	24.3
4:19	272	3.65	3.65	6.79	-0.29	7.08	1.56	24.3
4:27	283	3.29	3.04	6.80	-0.77	7.56	1.53	24.4
4:35	293	3.33	3.11	6.83	-1.10	7.92	1.54	24.4
4:43	304	3.44	3.36	6.91	-1.49	8.36	1.55	24.5
4:51	314	3.87	3.41	7.06	-1.92	8.90	1.55	24.6
4:58	324	4.08	4.00	7.21	-2.49	9.58	1.56	24.7
5:06	335	4.62	4.18	7.22	-3.22	10.38	1.56	24.8
5:14	345	4.48	4.29	7.24	-3.60	10.84	1.56	24.9
5:22	355	4.94	4.09	7.35	-4.31	11.65	1.56	25.0
5:30	366	5.02	4.54	7.42	-5.32	12.74	1.56	25.1
5:38	376	5.58	4.93	7.44	-6.21	13.64	1.56	25.2
5:46	387	6.02	5.06	7.53	-7.11	14.63	1.56	25.4
5:53	397	6.09	5.16	7.64	-8.65	16.28	1.56	25.5
6:01	407	6.45	4.96	7.73	-10.54	18.26	1.56	25.7
6:09	418	6.45	4.94	7.82	-13.34	21.16	1.56	25.8
6:17	428	6.40	4.14	7.89	-16.97	24.86	1.56	26.0
6:25	439	6.06	4.42	7.94	-20.03	27.97	1.56	26.1
6:33	449	5.12	3.97	7.99	-23.04	31.03	1.56	26.3
6:41	459	4.50	3.54	8.06	-27.68	35.74	1.56	26.6
6:48	470	3.90	3.36	8.10	-34.68	42.76	1.57	27.1
6:56	480	3.61	3.28	8.10	-41.20	49.30	1.57	26.9
7:04	491	3.59	3.55	8.17	-47.46	55.63	1.56	27.1
7:12	501	3.58	3.43	8.23	-55.37	63.59	1.56	27.3
7:20	511	3.78	3.57	8.32	-61.28	69.59	1.56	27.6
7:28	522	3.69	3.50	8.40	-66.95	75.34	1.56	27.9
7:36	532	3.72	3.67	8.48	-70.93	79.40	1.56	28.3
7:43	543	3.83	3.72	8.54	-76.13	84.65	1.56	28.7
7:51	553	3.90	3.56	8.61	-78.21	86.80	1.56	28.9
7:59	564	3.85	3.52	8.68	-72.19	80.85	1.56	29.3
8:07	574	4.11	3.98	8.74	-71.60	80.31	1.56	29.6
8:15	585	4.11	3.83	8.80	-71.39	80.17	1.56	29.9
8:23	595	4.14	3.94	8.86	-69.81	78.66	1.56	30.2
8:31	605	4.08	4.01	8.88	-68.34	77.21	1.56	30.6

VT116

Time h:m	Lifting height mm	Lifting stress		Normal pressure kPa	Aver. Pore water pressure kPa	Effective pressure kPa	Deformation mm	Temp °C
		static kPa	sliding kPa					
0:40	0	1.63	1.25	8.17			0.00	22.8
0:48	9	1.34	1.01	8.16			0.02	23.1
0:56	20	1.12	1.12	8.13			0.02	23.3
1:04	30	1.24	0.90	8.07	5.83	2.22	0.02	23.5
1:12	41	1.08	1.08	8.03	5.62	2.39	0.02	23.6
1:19	51	1.47	1.12	7.97	5.28	2.67	0.02	23.7
1:27	62	1.20	0.98	7.91	5.12	2.78	0.02	23.8
1:35	73	1.09	0.97	7.89	4.71	3.17	0.02	23.8
1:43	83	1.18	1.09	7.83	4.69	3.13	0.03	23.9
1:51	94	1.21	1.09	7.78	4.36	3.40	0.03	23.9
1:59	104	2.09	1.73	7.73	4.11	3.60	0.03	24.0
2:07	115	1.84	1.71	7.68	3.70	3.96	0.03	24.0
2:15	126	2.12	1.80	7.64	3.67	3.95	0.04	24.1
2:22	136	2.61	2.28	7.61	3.27	4.33	0.04	24.0
2:30	147	2.74	2.65	7.57	2.94	4.62	0.05	24.1
2:38	157	2.90	2.51	7.54	2.75	4.77	0.06	24.1
2:46	167	2.93	2.68	7.52	2.51	5.00	0.06	24.2
2:54	178	3.10	2.67	7.48	2.29	5.17	0.07	24.1
3:02	188	3.07	2.98	7.43	2.04	5.38	0.08	24.2
3:10	199	3.38	3.28	7.41	1.81	5.58	0.08	24.2
3:17	209	3.66	3.35	7.39	1.71	5.68	0.08	24.2
3:25	219	4.07	3.75	7.36	1.52	5.85	0.09	24.2
3:33	230	4.23	3.74	7.36	1.36	6.00	0.11	24.3
3:41	240	4.18	3.88	7.33	1.21	6.10	0.07	24.3
3:49	251	3.75	3.62	7.32	0.79	6.52	0.08	24.3
3:57	261	3.45	3.28	7.30	0.46	6.83	0.09	24.4
4:05	272	3.70	3.70	7.28	0.16	7.11	0.11	24.4
4:13	282	3.60	3.50	7.33	-0.17	7.49	0.11	24.5
4:20	292	3.86	3.68	7.37	-0.47	7.82	0.12	24.5
4:28	303	4.22	4.14	7.55	-0.92	8.41	0.12	24.6
4:36	313	4.51	4.51	7.73	-1.53	9.16	0.11	24.7
4:44	323	4.89	4.17	7.75	-2.23	9.90	0.12	24.8
4:52	333	4.85	4.31	7.70	-2.76	10.46	0.12	24.9
5:00	343	4.91	4.34	7.75	-3.15	10.90	0.12	25.0
5:08	354	4.96	4.86	7.74	-3.57	11.31	0.12	25.1
5:15	364	5.38	4.64	7.71	-4.09	11.79	0.12	25.2
5:23	375	5.43	4.97	7.75	-4.89	12.65	0.12	25.4
5:31	385	6.19	5.67	7.85	-6.15	14.00	0.12	25.5
5:39	396	7.59	6.07	7.94	-7.75	15.69	0.12	25.6
5:47	406	7.66	6.48	8.03	-9.90	17.93	0.12	25.8
5:55	417	8.91	6.13	8.10	-12.50	20.60	0.12	26.0
6:03	427	9.60	6.92	8.18	-14.40	22.58	0.12	26.1
6:11	438	8.45	5.25	8.28	-19.57	27.85	0.12	26.3
6:18	448	8.85	4.99	8.34	-25.61	33.96	0.12	26.5
6:26	458	6.16	3.81	8.42	-28.38	36.80	0.12	26.7
6:34	469	4.49	3.68	8.51	-36.73	45.23	0.12	26.9
6:42	479	3.92	3.51	8.57	-43.14	51.71	0.12	27.2
6:50	490	3.81	3.78	8.67	-45.93	54.60	0.12	27.4
6:58	500	4.07	3.80	8.77	-52.24	61.00	0.12	27.6
7:06	510	4.07	3.81	8.85	-61.37	70.21	0.12	27.9
7:13	521	4.16	3.96	8.95	-65.94	74.88	0.12	28.1
7:21	531	4.25	4.15	9.05	-68.12	77.15	0.12	28.5
7:29	542	4.40	4.40	9.12	-71.13	80.23	0.12	28.7
7:37	552	4.46	3.94	9.19	-71.66	80.83	0.11	29.1
7:45	563	4.45	4.23	9.26	-74.41	83.64	0.11	29.4
7:53	573	4.53	4.36	9.31	-76.49	85.77	0.11	29.7
8:01	584	4.65	4.47	9.33	-78.20	87.51	0.11	30.1
8:08	594	4.67	4.52	9.35	-78.23	87.58	0.11	30.4
8:16	604	4.80	4.80	9.39	-79.14	88.52	0.11	30.7
8:24	615	4.93	4.92	9.42	-80.15	89.56	0.11	31.0
8:32	625	4.93	4.71	9.44	-79.91	89.33	0.11	31.4
8:40	636	4.89	4.72	9.43	-79.28	88.70	0.11	31.7
8:48	646	4.85	4.72	9.40	-78.75	88.08	0.11	32.1
8:56	657	5.04	4.84	9.38	-77.98	87.20	0.11	32.5

VT123

Time h:m	Lifting height mm	Lifting stress		Normal pressure kPa	Aver. Pore water pressure kPa	Effective pressure kPa	Deformation mm	Temp °C
		static kPa	sliding kPa					
0:47	0	4.01	3.78	7.70	6.56	1.14	0.00	23.5
0:55	11	3.72	3.70	7.55	7.50	0.05	0.00	23.7
1:03	21	3.97	3.80	7.50	7.43	0.07	0.00	23.8
1:11	32	3.40	3.32	7.41	7.33	0.08	0.00	23.9
1:19	42	3.31	3.28	7.29	7.21	0.08	0.00	24.0
1:27	52	3.37	3.32	7.14	7.10	0.04	0.00	24.1
1:35	63	3.64	3.49	7.07	7.00	0.07	0.00	24.1
1:43	73	3.52	3.43	6.98	6.90	0.08	0.00	24.2
1:51	84	3.41	3.17	6.88	6.69	0.19	0.00	24.2
1:58	94	3.74	3.32	6.72	6.47	0.25	0.00	24.3
2:06	105	3.74	3.24	6.57	6.27	0.31	0.00	24.3
2:14	115	3.72	3.40	6.55	6.10	0.46	0.00	24.3
2:22	126	3.83	3.83	6.53	5.87	0.66	0.00	24.3
2:30	136	3.76	3.44	6.49	5.67	0.82	0.00	24.3
2:38	147	3.85	3.81	6.50	5.45	1.05	0.01	24.4
2:46	157	4.26	4.18	6.47	5.27	1.19	0.01	24.4
2:53	168	4.30	4.14	6.42	5.07	1.35	0.01	24.4
3:01	178	4.47	4.47	6.46	4.92	1.55	0.01	24.4
3:09	189	4.73	4.38	6.45	4.68	1.76	0.01	24.4
3:17	199	4.55	4.30	6.36	4.54	1.82	0.01	24.4
3:25	210	4.73	4.73	6.46	4.31	2.15	0.02	24.4
3:33	220	4.91	4.77	6.45	4.13	2.32	0.02	24.5
3:41	230	5.35	5.15	6.43	3.92	2.50	0.02	24.5
3:49	241	5.31	4.99	6.37	3.70	2.67	0.02	24.5
3:56	251	5.14	4.94	6.39	3.49	2.90	0.03	24.6
4:04	262	5.52	5.52	6.49	3.23	3.26	0.03	24.6
4:12	272	5.83	5.60	6.68	2.84	3.84	0.04	24.6
4:20	283	6.24	6.11	6.81	2.57	4.24	0.04	24.7
4:28	293	6.32	6.27	7.28	2.20	5.08	0.04	24.8
4:36	304	6.92	6.92	8.02	1.64	6.38	0.03	24.8
4:44	314	8.18	8.16	8.92	1.08	7.84	0.03	24.9
4:52	324	9.06	9.06	9.81	0.44	9.36	0.03	25.0
4:59	334	9.63	9.59	10.12	-0.30	10.42	0.03	25.1
5:07	345	9.70	9.21	9.98	-0.73	10.71	0.04	25.2
5:15	355	9.21	8.71	9.50	-1.04	10.54	0.04	25.3
5:23	366	9.14	8.01	9.01	-1.37	10.37	0.04	25.4
5:31	376	9.27	7.93	8.43	-1.80	10.23	0.03	25.5
5:39	387	8.85	8.13	8.51	-2.35	10.86	0.03	25.6
5:47	397	10.03	8.64	8.90	-3.12	12.02	0.03	25.8
5:54	408	10.09	8.13	9.18	-4.19	13.38	0.02	25.9
6:02	418	12.07	8.20	9.53	-5.51	15.04	0.02	26.1
6:10	429	13.56	8.95	9.95	-7.13	17.08	0.02	26.3
6:18	439	13.56	8.36	10.15	-9.18	19.33	0.02	26.4
6:26	450	12.85	7.81	10.70	-12.16	22.86	0.02	26.6
6:34	460	12.85	8.12	11.38	-15.71	27.09	0.02	26.8
6:42	471	11.70	7.36	11.69	-20.02	31.71	0.02	27.0
6:50	481	10.79	8.22	12.34	-27.36	39.71	0.02	27.1
6:57	491	10.09	7.95	13.01	-33.44	46.45	0.02	27.3
7:05	502	9.52	8.43	13.33	-38.06	51.40	0.02	27.9
7:13	512	9.03	8.67	13.73	-44.36	58.09	0.02	27.6
7:21	523	9.20	8.61	14.21	-48.18	62.38	0.02	27.9
7:29	533	9.38	9.38	14.55	-52.18	66.73	0.02	28.2
7:37	544	9.65	9.40	14.61	-53.29	67.90	0.02	28.5
7:45	554	9.90	8.92	15.00	-56.55	71.55	0.02	28.9
7:52	564	10.08	9.92	15.21	-59.53	74.74	0.02	29.3
8:00	575	10.56	9.80	14.91	-61.71	76.62	0.02	29.6
8:08	585	10.43	9.49	15.00	-63.26	78.26	0.02	29.9
8:16	595	10.86	10.55	15.11	-64.16	79.27	0.02	30.3
8:24	606	10.89	10.50	14.94	-65.30	80.24	0.02	30.6
8:32	616	11.84	10.68	14.69	-66.32	81.01	0.02	30.9
8:40	627	11.84	10.82	14.76	-66.03	80.78	0.01	31.3
8:47	637	11.12	10.77	14.49	-65.27	79.76	0.01	31.7
8:55	648	11.22	10.95	14.16	-63.96	78.12	0.01	32.1
9:03	658	11.22	11.12	14.07	-61.59	75.66	0.01	32.4

VT126

Time h:m	Lifting height mm	Lifting stress		Normal pressure kPa	Aver. Pore water pressure kPa	Effective pressure kPa	Deformation mm	Temp °C
		static kPa	sliding kPa					
0:44	0	1.71	1.21	7.55			0.00	22.6
0:52	11	1.37	0.97	7.49			0.02	22.8
1:00	21	1.20	0.86	7.39	7.18	0.21	0.03	23.0
1:07	31	1.32	0.85	7.24	7.16	0.09	0.03	23.1
1:15	42	1.13	1.02	7.18	7.06	0.12	0.04	23.2
1:23	52	1.25	0.89	7.13	6.93	0.20	0.05	23.3
1:31	63	1.14	0.98	7.08	6.66	0.42	0.06	23.3
1:39	73	1.01	1.01	7.02	6.31	0.71	0.06	23.3
1:47	84	1.26	1.24	6.95	6.27	0.68	0.07	23.3
1:55	94	1.47	1.47	6.88	5.78	1.10	0.07	23.3
2:02	105	1.37	1.13	6.81	5.61	1.20	0.08	23.3
2:10	116	1.59	1.59	6.73	5.77	0.96	0.08	23.3
2:18	126	1.59	1.59	6.69	5.27	1.42	0.08	23.3
2:26	137	2.06	2.00	6.61	5.10	1.51	0.09	23.3
2:34	147	2.22	1.95	6.54	4.77	1.77	0.09	23.3
2:42	158	2.01	1.83	6.52	4.52	2.00	0.10	23.4
2:49	168	1.83	1.83	6.46	4.27	2.19	0.10	23.3
2:57	178	1.95	1.87	6.43	3.94	2.49	0.10	23.4
3:05	189	1.99	1.99	6.39	3.73	2.67	0.10	23.4
3:13	199	2.38	1.90	6.34	3.67	2.68	0.10	23.5
3:21	210	2.74	2.46	6.32	3.48	2.83	0.11	23.5
3:29	220	2.89	2.60	6.30	3.39	2.91	0.11	23.5
3:37	231	2.98	2.98	6.29	3.11	3.18	0.12	23.6
3:44	241	2.83	2.73	6.27	2.95	3.32	0.12	23.6
3:52	252	3.00	2.86	6.24	2.72	3.53	0.12	23.7
4:00	262	2.97	2.97	6.22	2.50	3.72	0.12	23.7
4:08	273	3.31	3.03	6.22	2.13	4.08	0.13	23.7
4:16	283	3.08	2.99	6.23	1.68	4.55	0.13	23.7
4:24	293	3.57	3.45	6.25	1.24	5.01	0.14	23.6
4:31	304	3.81	3.56	6.29	0.64	5.65	0.14	23.5
4:39	314	4.18	4.18	6.36	-0.06	6.43	0.14	23.6
4:47	324	4.64	4.26	6.49	-0.87	7.36	0.13	23.7
4:55	335	4.87	4.53	6.54	-1.66	8.20	0.13	23.8
5:03	345	5.64	4.99	6.54	-2.71	9.25	0.13	23.9
5:11	355	5.96	5.28	6.55	-3.72	10.27	0.14	24.0
5:19	366	6.02	5.56	6.60	-5.33	11.93	0.14	24.1
5:26	376	7.87	6.06	6.72	-6.95	13.67	0.14	24.3
5:34	386	8.25	6.89	6.84	-8.30	15.13	0.14	24.4
5:42	397	11.22	7.28	6.95	-11.71	18.66	0.14	24.5
5:50	407	11.55	7.89	7.10	-15.85	22.95	0.14	24.6
5:58	417	11.65	6.54	7.26	-20.77	28.03	0.14	24.7
6:06	428	11.65	3.98	7.34	-24.88	32.22	0.14	24.8
6:13	438	4.78	3.15	7.44	-30.33	37.77	0.14	25.0
6:21	449	3.66	3.44	7.54	-37.54	45.08	0.14	25.2
6:29	459	3.90	3.67	7.61	-41.53	49.15	0.14	25.4
6:37	470	4.01	3.64	7.70	-48.14	55.84	0.14	25.5
6:45	480	3.97	3.59	7.82	-52.24	60.05	0.14	25.7
6:53	490	4.13	3.63	7.93	-56.05	63.98	0.14	26.0
7:01	501	4.18	4.18	8.08	-59.61	67.69	0.14	26.2
7:08	511	4.25	4.21	8.22	-61.30	69.52	0.14	26.4
7:16	522	4.45	4.29	8.33	-61.11	69.43	0.14	26.6
7:24	532	4.59	4.41	8.46	-61.15	69.62	0.14	26.8
7:32	543	4.65	4.60	8.58	-60.47	69.05	0.14	27.0
7:40	553	4.84	4.59	8.67	-59.28	67.95	0.14	27.2
7:48	564	4.93	4.81	8.72	-58.75	67.47	0.13	27.5
7:55	574	5.11	4.89	8.78	-58.01	66.79	0.13	27.7
8:03	584	5.13	5.00	8.86	-57.23	66.08	0.13	28.0
8:11	595	5.21	4.90	8.89	-55.93	64.82	0.13	28.2
8:19	605	5.35	4.89	8.91	-55.47	64.38	0.13	28.5
8:27	616	5.33	5.32	8.95	-55.06	64.01	0.13	28.8
8:35	626	5.52	5.20	8.97	-54.88	63.85	0.13	29.0

VT127

Time	Lifting height	Lifting stress		Normal pressure	Aver. Pore water pressure	Effective pressure	Deformation	Temp
		static	sliding					
h:m	mm	kPa	kPa	kPa	kPa	kPa	mm	°C
0:41	0	1.14	0.71	7.60			0.00	23.1
0:49	11	0.85	0.42	7.46			0.01	23.4
0:57	21	0.58	0.58	7.38			0.01	23.5
1:04	31	0.75	0.53	7.26	7.09	0.17	0.01	23.7
1:12	42	0.99	0.53	7.16	7.07	0.09	0.02	23.8
1:20	53	0.74	0.56	7.11	6.95	0.17	0.02	23.8
1:28	63	0.85	0.66	7.06	6.59	0.47	0.02	23.9
1:36	74	1.11	0.79	6.97	6.36	0.61	0.02	23.9
1:44	84	1.31	1.18	6.91	5.96	0.95	0.02	24.0
1:52	94	1.24	1.02	6.83	5.89	0.94	0.02	24.0
1:59	105	1.18	1.16	6.73	5.69	1.03	0.03	24.0
2:07	115	1.08	1.01	6.66	5.36	1.30	0.03	24.0
2:15	126	1.37	1.20	6.58	5.12	1.46	0.03	24.0
2:23	136	1.36	1.34	6.49	4.76	1.73	0.03	24.0
2:31	147	1.63	1.60	6.44	4.53	1.92	0.03	24.1
2:39	157	1.52	1.50	6.37	4.38	1.99	0.03	24.1
2:47	168	1.71	1.64	6.33	4.11	2.22	0.03	24.1
2:55	178	1.92	1.77	6.30	3.83	2.46	0.03	24.1
3:02	189	2.11	1.88	6.25	3.62	2.64	0.04	24.1
3:10	199	2.18	2.18	6.20	3.34	2.86	0.04	24.2
3:18	210	2.51	2.41	6.18	3.15	3.03	0.04	24.2
3:26	220	2.57	2.41	6.14	2.86	3.28	0.04	24.2
3:34	231	2.51	2.26	6.12	2.61	3.51	0.04	24.2
3:42	241	2.76	2.45	6.11	2.41	3.70	0.04	24.2
3:50	252	2.83	2.66	6.08	1.99	4.09	0.04	24.2
3:57	262	3.07	2.77	6.06	1.57	4.50	0.04	24.2
4:05	272	3.26	2.86	6.06	1.01	5.06	0.04	24.3
4:13	283	3.33	2.92	6.10	0.17	5.93	0.04	25.0
4:21	293	3.57	3.39	6.16	-0.62	6.77	0.04	24.2
4:29	304	3.87	3.83	6.21	-1.67	7.88	0.04	24.2
4:37	314	4.91	4.54	6.32	-3.00	9.32	0.05	24.3
4:45	324	6.00	5.05	6.41	-4.69	11.10	0.05	24.4
4:52	335	7.29	5.80	6.43	-5.57	12.00	0.05	24.5
5:00	345	8.72	6.09	6.49	-7.61	14.10	0.05	24.6
5:08	355	11.50	7.19	6.60	-11.54	18.15	0.05	24.7
5:16	366	11.72	7.66	6.70	-15.90	22.60	0.05	24.9
5:24	376	13.83	8.19	6.86	-20.64	27.49	0.05	25.0
5:32	386	13.12	5.86	7.01	-26.30	33.31	0.05	25.2
5:40	397	7.74	3.57	7.14	-32.22	39.36	0.05	25.4
5:47	407	4.47	3.82	7.29	-37.70	44.99	0.05	25.6
5:55	418	4.04	3.86	7.38	-44.41	51.79	0.05	25.7
6:03	428	3.90	3.58	7.44	-52.90	60.34	0.05	25.9
6:11	439	3.80	3.75	7.51	-60.62	68.13	0.05	26.0
6:19	449	3.92	3.61	7.55	-67.98	75.53	0.05	26.2
6:27	459	4.01	3.88	7.59	-53.63	61.22	0.05	26.4
6:34	470	4.02	3.58	7.67	-49.60	57.27	0.05	26.6
6:42	480	4.16	3.68	7.77	-45.27	53.04	0.05	26.8
6:50	490	4.27	4.13	7.87	-23.79	31.66	0.04	27.1
6:58	501	4.36	4.36	8.01	-17.32	25.33	0.04	27.3
7:06	511	4.45	4.42	8.14	-20.14	28.27	0.04	27.6

VT137

Time h:m	Lifting height mm	Lifting stress		Normal pressure kPa	Aver. Pore water pressure kPa	Effective pressure kPa	Deformation mm	Temp °C
		static kPa	sliding kPa					
0:38	0	0.33	0.03	7.37			0.00	21.8
0:45	11	0.41	0.03	7.35			0.12	21.9
0:53	21	0.38	0.09	7.34			0.24	22.0
1:01	31	0.48	0.20	7.38	6.97	0.41	0.59	22.0
1:09	41	0.48	0.23	7.38	6.94	0.44	0.86	22.1
1:17	52	0.46	0.22	7.35	6.92	0.43	0.89	22.2
1:25	63	0.53	0.35	7.30	6.89	0.40	0.98	22.2
1:32	73	0.56	0.34	7.27	6.87	0.40	1.01	22.2
1:40	84	0.68	0.36	7.24	6.65	0.59	1.09	22.2
1:48	94	0.68	0.47	7.22	6.60	0.62	1.13	22.2
1:56	104	0.71	0.51	7.18	6.56	0.63	1.15	22.2
2:04	115	0.80	0.71	7.15	6.54	0.60	1.16	22.3
2:12	125	0.91	0.68	7.14	6.54	0.60	1.18	22.3
2:20	136	0.78	0.60	7.12	6.54	0.58	1.24	22.3
2:27	146	0.91	0.71	7.08	6.30	0.77	1.27	22.4
2:35	157	1.08	0.80	7.07	6.09	0.98	1.31	22.4
2:43	167	1.31	0.91	7.06	5.53	1.53	1.33	22.4
2:51	178	1.44	1.10	7.05	5.12	1.93	1.34	22.4
2:59	188	1.48	1.16	7.06	4.65	2.41	1.35	22.4
3:07	199	1.58	1.17	7.05	4.31	2.74	1.35	22.5
3:15	209	1.76	1.76	7.04	3.63	3.42	1.36	22.6
3:22	220	1.99	1.75	7.07	3.22	3.86	1.36	22.6
3:30	230	2.21	1.79	7.09	2.31	4.78	1.36	22.7
3:38	240	2.63	2.07	7.09	1.58	5.52	1.36	22.8
3:46	251	2.84	2.23	7.12	0.62	6.50	1.36	22.9
3:54	262	3.16	2.58	7.14	-0.39	7.53	1.36	22.9
4:02	272	4.54	3.17	7.17	-1.53	8.70	1.36	23.0
4:10	283	5.20	3.92	7.21	-2.80	10.01	1.35	23.1
4:17	293	6.12	4.72	7.23	-4.34	11.57	1.35	23.2
4:25	304	8.04	6.24	7.26	-6.18	13.44	1.35	23.4
4:33	314	10.89	7.56	7.26	-8.50	15.76	1.35	23.5
4:41	324	15.85	9.65	7.21	-11.46	18.67	1.35	23.6
4:49	334	22.97	11.78	7.17	-15.16	22.34	1.35	23.8
4:57	344	24.10	12.87	7.51	-21.32	28.83	1.35	24.0
5:05	355	26.69	13.04	7.64	-28.60	36.24	1.35	24.2
5:12	365	29.41	16.00	7.81	-35.86	43.67	1.34	24.4
5:20	376	31.66	15.34	7.94	-43.94	51.87	1.34	24.5
5:28	386	28.00	13.30	8.05	-50.85	58.91	1.35	24.7
5:36	397	23.11	7.40	7.87	-57.19	65.06	1.35	24.8
5:44	408	15.25	3.86	7.61	-61.71	69.32	1.35	24.9
5:52	418	4.61	4.14	7.65	-64.29	71.94	1.35	25.2
6:00	429	4.30	4.07	7.70	-66.62	74.32	1.35	25.4
6:07	439	4.41	4.39	7.75	-68.50	76.25	1.35	25.6
6:15	449	4.50	4.46	7.80	-68.29	76.09	1.35	25.8
6:23	460	4.58	4.32	7.86	-64.34	72.20	1.35	26.0
6:31	470	4.49	4.34	7.93	-58.86	66.80	1.34	26.3
6:39	481	4.54	4.40	7.99	-53.31	61.30	1.34	26.6
6:47	491	4.53	4.40	8.07	-49.67	57.74	1.34	26.8
6:55	502	4.55	4.39	8.13	-47.22	55.35	1.34	27.1
7:02	512	4.53	4.47	8.19	-45.75	53.94	1.34	27.4
7:10	522	4.68	4.41	8.26	-44.85	53.11	1.34	27.6
7:18	533	4.68	4.33	8.32	-44.20	52.53	1.34	27.9
7:26	543	4.46	4.36	8.39	-43.71	52.09	1.34	28.1
7:34	554	4.51	4.39	8.46	-43.34	51.79	1.34	28.4
7:42	564	4.45	4.27	8.51	-43.26	51.77	1.33	28.7
7:50	575	4.53	4.31	8.59	-43.26	51.85	1.33	28.9
7:57	585	4.44	4.30	8.65	-43.20	51.86	1.33	29.1
8:04	595	4.40	4.40	8.65	-43.13	51.79	1.33	29.4

VT143

Time h:m	Lifting height mm	Lifting stress		Normal pressure kPa	Aver. Pore water pressure kPa	Effective pressure kPa	Deformation mm	Temp °C
		static kPa	sliding kPa					
1:05	0	0.20	0.08	7.07	6.64	0.43	0.00	24.0
1:13	11	0.08	0.06	7.07	6.52	0.55	0.00	24.0
1:21	21	0.40	0.04	7.04	6.36	0.69	0.00	24.0
1:29	31	0.40	0.04	7.02	6.17	0.85	0.00	24.0
1:37	42	0.45	0.10	6.96	5.97	0.98	0.00	24.0
1:45	51	0.56	0.19	6.90	5.75	1.15	0.00	24.0
1:53	62	0.45	0.23	6.99	5.50	1.49	0.00	24.0
2:00	72	0.52	0.51	6.99	5.06	1.93	0.24	24.0
2:08	83	0.53	0.33	6.91	5.24	1.67	0.55	24.0
2:16	93	0.67	0.27	6.91	4.90	2.00	0.68	24.0
2:24	103	0.79	0.79	6.83	4.75	2.08	0.68	24.0
2:32	114	0.80	0.45	6.73	4.37	2.35	0.70	24.0
2:40	124	0.81	0.46	6.67	4.12	2.56	0.70	24.0
2:48	135	0.86	0.54	6.59	3.87	2.71	0.71	24.0
2:55	146	0.97	0.54	6.54	3.69	2.85	0.72	24.0
3:03	156	0.98	0.69	6.52	3.41	3.11	0.73	24.0
3:11	167	1.18	0.91	6.50	3.26	3.24	0.74	24.0
3:19	177	1.26	1.01	6.49	3.06	3.43	0.74	24.0
3:27	187	1.35	1.09	6.45	2.81	3.64	0.75	24.0
3:35	198	1.44	0.93	6.43	2.65	3.79	0.75	24.0
3:43	208	1.39	1.06	6.41	2.39	4.02	0.75	24.0
3:51	219	1.52	1.52	6.41	2.14	4.26	0.75	24.0
3:58	229	1.60	1.23	6.41	1.88	4.53	0.76	24.0
4:06	240	1.75	1.75	6.40	1.56	4.84	0.76	24.0
4:14	250	1.69	1.49	6.40	1.29	5.11	0.76	24.0
4:22	261	1.92	1.51	6.43	1.02	5.41	0.76	24.0
4:30	271	1.99	1.57	6.43	0.64	5.79	0.76	24.0
4:38	282	2.07	1.86	6.47	0.19	6.28	0.76	24.0
4:46	292	2.57	2.57	6.49	-0.29	6.78	0.76	24.0
4:53	302	2.93	2.21	6.53	-0.77	7.30	0.76	24.0
5:01	313	3.16	2.50	6.57	-1.38	7.95	0.75	24.0
5:09	324	3.57	3.29	6.59	-1.93	8.52	0.75	24.0
5:17	335	4.35	3.78	6.64	-2.59	9.22	0.75	24.0
5:25	345	5.83	4.03	6.70	-3.23	9.93	0.75	24.1
5:33	355	5.99	4.67	6.77	-3.98	10.75	0.75	24.1
5:41	365	6.46	5.51	6.82	-4.74	11.56	0.75	24.2
5:49	376	7.40	5.74	6.86	-5.63	12.49	0.75	24.3
5:56	386	6.70	5.51	6.90	-6.62	13.52	0.75	24.4
6:04	396	7.00	5.16	6.98	-7.90	14.87	0.75	24.5
6:12	407	6.81	5.67	7.04	-9.39	16.44	0.75	24.6
6:20	417	6.50	4.65	7.13	-11.13	18.26	0.75	24.7
6:28	427	5.64	4.25	7.20	-13.45	20.65	0.75	24.8
6:36	438	5.74	4.08	7.27	-16.56	23.83	0.75	25.0
6:44	448	5.25	4.51	7.33	-20.32	27.66	0.75	25.1
6:51	458	4.99	4.17	7.40	-24.58	31.98	0.75	25.3
6:59	469	4.56	3.91	7.48	-28.34	35.82	0.75	25.5
7:07	479	4.37	3.63	7.54	-33.50	41.04	0.75	25.6
7:15	489	4.28	4.24	7.64	-38.53	46.16	0.75	25.8
7:23	500	4.43	4.38	7.70	-43.20	50.90	0.75	26.0
7:31	510	4.51	4.18	7.76	-47.21	54.97	0.75	26.3
7:39	521	4.55	4.37	7.83	-50.60	58.43	0.75	26.5
7:46	531	4.58	4.42	7.89	-53.46	61.34	0.75	26.6
7:54	541	4.67	4.26	7.97	-55.92	63.88	0.75	26.9
8:02	552	4.74	4.55	8.05	-53.07	61.12	0.75	27.1
8:10	562	4.92	4.61	8.09	-54.56	62.65	0.75	27.3
8:18	573	4.72	4.63	8.15	-55.55	63.71	0.75	27.5
8:26	583	4.86	4.52	8.21	-50.97	59.19	0.75	27.7
8:34	593	4.73	4.46	8.26	-53.13	61.39	0.75	28.0
8:41	604	4.83	4.44	8.31	-54.74	63.04	0.74	28.1
8:49	614	4.87	4.70	8.31	-56.04	64.35	0.74	28.5

VT144

Time h:m	Lifting height mm	Lifting stress		Normal pressure kPa	Aver. Pore water pressure kPa	Effective pressure kPa	Deformation mm	Temp °C
		static kPa	sliding kPa					
0:35	0	0.45	0.00	7.08			0.00	22.0
0:43	11	0.37	0.02	7.05			0.00	22.1
0:51	21	0.37	0.08	7.03			0.01	22.2
0:58	32	0.37	0.03	7.00	5.84	1.15	0.01	22.2
1:06	43	0.77	0.37	6.96	5.72	1.24	0.01	22.3
1:14	53	0.84	0.52	6.94	5.57	1.37	0.01	22.4
1:22	63	0.84	0.59	6.91	5.63	1.28	0.01	22.4
1:30	73	0.81	0.35	6.87	5.30	1.57	0.01	22.4
1:38	83	0.95	0.57	6.84	5.25	1.59	0.01	22.5
1:46	93	0.94	0.59	6.82	5.06	1.75	0.01	22.5
1:54	103	0.88	0.77	6.78	4.99	1.80	0.03	22.5
2:02	114	0.90	0.57	6.79	4.58	2.21	0.04	22.5
2:09	125	1.04	0.58	6.73	4.72	2.01	0.05	22.5
2:17	135	0.96	0.93	6.69	4.49	2.20	0.05	22.6
2:25	146	1.13	0.74	6.66	4.16	2.49	0.05	22.6
2:33	156	1.13	0.91	6.62	3.95	2.67	0.05	22.6
2:41	167	1.18	0.86	6.58	3.80	2.77	0.05	22.6
2:49	177	1.26	0.93	6.55	3.67	2.88	0.05	22.6
2:57	188	1.17	0.96	6.51	3.45	3.06	0.05	22.6
3:05	198	1.30	0.90	6.48	3.23	3.25	0.05	22.6
3:12	208	1.34	1.21	6.46	2.89	3.58	0.05	22.7
3:20	219	1.53	1.38	6.43	2.89	3.54	0.05	22.7
3:28	229	1.61	1.23	6.43	2.70	3.73	0.06	22.7
3:36	240	1.66	1.66	6.41	2.50	3.91	0.06	22.8
3:44	250	1.39	1.28	6.41	2.28	4.13	0.06	22.7
3:52	261	1.80	1.61	6.39	2.24	4.15	0.06	22.8
4:00	271	1.88	1.58	6.41	2.07	4.34	0.06	22.8
4:08	282	1.64	1.39	6.41	1.83	4.57	0.07	22.8
4:15	292	1.89	1.33	6.42	1.59	4.83	0.07	22.8
4:23	303	2.02	1.54	6.43	1.31	5.12	0.07	22.8
4:31	313	1.82	1.67	6.46	0.99	5.47	0.07	22.9
4:39	324	1.86	1.73	6.49	0.69	5.80	0.07	22.9
4:47	334	2.23	1.90	6.53	0.24	6.29	0.07	23.0
4:55	344	2.88	2.48	6.58	-0.09	6.67	0.07	23.0
5:03	355	3.04	2.96	6.64	-0.69	7.33	0.07	23.1
5:11	365	3.56	3.08	6.66	-1.38	8.04	0.07	23.1
5:18	376	4.02	3.47	6.69	-1.90	8.59	0.07	23.2
5:26	386	4.23	3.86	6.72	-2.34	9.06	0.07	23.3
5:34	396	4.51	4.12	6.75	-2.70	9.45	0.08	23.4
5:42	407	5.07	4.33	6.82	-3.24	10.06	0.08	23.5
5:50	417	5.63	4.60	6.89	-3.90	10.79	0.08	23.6
5:58	427	6.28	5.33	6.92	-4.70	11.62	0.08	23.7
6:06	438	6.87	6.09	7.00	-5.65	12.65	0.08	23.8
6:13	448	7.03	5.22	7.06	-6.65	13.71	0.08	24.0
6:21	458	6.31	5.14	7.14	-7.92	15.06	0.08	24.1
6:29	469	6.15	4.88	7.21	-9.42	16.63	0.08	24.2
6:37	479	5.69	4.00	7.29	-11.05	18.34	0.08	24.4
6:45	489	5.46	4.57	7.37	-13.10	20.47	0.08	24.5
6:53	500	5.05	4.29	7.46	-15.62	23.07	0.08	24.7
7:01	510	4.80	4.19	7.52	-18.58	26.10	0.08	24.9
7:09	521	4.68	3.76	7.58	-21.59	29.17	0.08	25.0
7:16	531	4.45	4.12	7.67	-23.97	31.64	0.08	25.2
7:24	542	4.39	4.24	7.74	-25.48	33.22	0.08	25.4
7:32	552	4.38	3.89	7.81	-29.57	37.38	0.08	25.5
7:40	562	4.54	4.29	7.89	-34.50	42.39	0.08	25.8
7:48	573	4.39	4.24	7.95	-38.40	46.35	0.08	26.0
7:56	583	4.52	4.15	8.03	-33.96	41.99	0.08	26.2
8:04	593	4.42	4.18	8.11	-37.30	45.41	0.08	26.4
8:11	604	4.45	4.03	8.16	-40.41	48.57	0.08	26.6

VT145

Time h:m	Lifting height mm	Lifting stress		Normal pressure kPa	Aver. Pore water pressure kPa	Effective pressure kPa	Deformation mm	Temp °C
		static kPa	sliding kPa					
0:15	0	0.55	0.11	7.17			0.00	20.4
0:23	10	0.42	0.27	7.13			0.01	20.8
0:31	21	0.50	0.17	7.08			0.01	21.2
0:39	31	0.50	0.06	7.06			0.01	21.4
0:46	42	0.52	0.37	7.04			0.01	21.6
0:54	53	0.47	0.23	6.97			0.01	21.8
1:02	63	0.42	0.19	6.94	5.05	1.89	0.01	21.8
1:10	73	0.70	0.28	6.92	4.51	2.41	0.02	21.9
1:18	83	0.80	0.35	6.88	4.38	2.51	0.03	22.0
1:26	94	0.68	0.44	6.85	4.23	2.62	0.03	22.0
1:34	104	0.81	0.60	6.83	4.07	2.76	0.04	22.1
1:42	115	0.65	0.48	6.78	3.99	2.79	0.03	22.0
1:50	125	0.82	0.54	6.74	3.81	2.93	0.03	22.1
1:57	135	0.81	0.69	6.71	3.63	3.08	0.03	22.1
2:05	145	0.87	0.60	6.66	3.64	3.03	0.03	22.1
2:13	156	1.09	0.98	6.63	3.45	3.18	0.04	22.2
2:21	166	1.02	0.90	6.59	3.35	3.24	0.05	22.2
2:29	177	1.01	0.83	6.55	3.28	3.26	0.05	22.2
2:37	187	0.97	0.83	6.51	3.20	3.31	0.06	22.2
2:45	198	1.15	0.85	6.47	3.05	3.42	0.05	22.2
2:53	208	1.23	0.96	6.43	2.81	3.62	0.06	22.4
3:00	219	1.31	0.97	6.41	2.89	3.52	0.06	22.2
3:08	229	1.36	1.16	6.38	2.73	3.65	0.06	22.3
3:16	240	1.56	1.51	6.35	2.46	3.89	0.07	22.3
3:24	250	1.59	1.33	6.36	2.42	3.93	0.07	22.3
3:32	261	1.69	1.32	6.34	2.24	4.11	0.07	22.4
3:40	272	1.86	1.76	6.31	0.87	5.44	0.05	22.4
3:48	282	1.85	1.85	6.28	0.44	5.85	0.08	22.5
3:56	293	2.07	1.60	6.27	1.73	4.54	0.18	22.5
4:03	303	2.01	1.64	6.26	1.38	4.87	0.21	22.5
4:11	314	2.04	1.60	6.26	-0.06	6.32	0.22	22.5
4:19	324	2.04	1.75	6.26	-0.02	6.27	0.22	22.6
4:27	334	2.29	2.03	6.31	-0.33	6.64	0.22	22.6
4:35	345	2.74	2.37	6.34	-0.49	6.83	0.23	22.6
4:43	356	2.78	2.38	6.38	-0.63	7.01	0.23	22.7
4:51	366	2.65	2.45	6.40	-0.84	7.24	0.23	22.7
4:59	376	2.94	2.94	6.39	-1.02	7.42	0.23	22.7
5:06	387	3.04	3.04	6.42	-1.26	7.67	0.22	22.8
5:14	397	3.33	3.00	6.45	-1.35	7.80	0.22	22.9
5:22	407	3.82	3.42	6.48	-1.64	8.12	0.23	22.9
5:30	418	4.18	4.18	6.56	-1.93	8.49	0.22	23.0
5:38	428	4.48	3.91	6.61	-2.24	8.84	0.22	23.0
5:46	438	5.14	4.64	6.65	-2.38	9.03	0.22	23.1
5:54	448	5.60	5.06	6.73	-2.62	9.35	0.21	23.2
6:02	459	6.00	5.38	6.79	-3.05	9.84	0.21	23.3
6:09	469	6.40	5.18	6.86	-3.45	10.31	0.22	23.6
6:17	479	6.68	5.43	6.94	-3.47	10.41	0.21	23.3
6:25	490	7.33	5.83	7.02	-4.36	11.38	0.21	23.5
6:33	500	6.95	4.97	7.09	-4.58	11.68	0.22	23.6
6:41	510	6.29	4.46	7.17	-5.44	12.61	0.21	23.7
6:49	521	6.16	4.62	7.26	-5.62	12.88	0.21	23.8
6:57	531	5.64	4.88	7.33	-5.83	13.16	0.20	24.0
7:05	542	5.63	4.68	7.43	-6.68	14.12	0.20	24.2
7:12	552	4.88	4.45	7.53	-7.79	15.31	0.20	24.4
7:20	563	4.88	3.98	7.59	-9.22	16.81	0.20	24.5
7:28	573	4.70	4.02	7.68	-11.10	18.78	0.20	24.7
7:36	583	4.34	4.00	7.76	-13.41	21.16	0.20	24.9
7:44	594	4.58	3.92	7.83	-15.08	22.91	0.20	25.1

VT146

Time	Lifting height	Lifting stress		Normal pressure	Aver. Pore water pressure	Effective pressure	Deformation	Temp
h:m	mm	static kPa	sliding kPa	kPa	kPa	kPa	mm	°C
0:55	0	0.38	0.01	6.96	6.70	0.27	0.00	21.8
1:25	10	0.67	0.40	6.77	6.29	0.48	0.00	21.8
1:55	21	0.47	0.29	6.60	5.68	0.93	0.00	22.0
2:26	32	1.08	0.71	6.43	5.17	1.26	0.00	22.2
2:56	42	1.63	1.03	6.29	4.29	2.00	0.01	22.3
3:27	52	1.99	1.34	6.19	3.53	2.66	0.01	22.5
3:57	63	2.61	1.98	6.07	2.92	3.15	0.01	22.6
4:27	73	2.64	1.81	5.98	2.15	3.84	0.01	22.9
4:58	84	2.47	2.06	5.94	1.19	4.75	0.01	23.1
5:28	94	3.41	2.67	5.96	-0.07	6.03	0.01	23.3
5:58	105	5.57	3.94	5.99	-2.42	8.40	0.01	23.7
6:29	116	10.17	6.94	6.07	-6.69	12.77	0.01	24.1
6:59	126	16.47	12.09	6.09	-12.81	18.90	0.01	24.6
7:29	135	23.80	9.54	6.33	-29.18	35.50	0.01	25.2
8:00	146	22.48	7.52	6.27	-52.74	59.01	0.01	25.9
8:30	157	14.54	3.95	6.17	-69.12	75.30	0.01	26.8

VT147

Time h:m	Lifting height mm	Lifting stress		Normal pressure kPa	Aver. Pore water pressure kPa	Effective pressure kPa	Deformation mm	Temp °C
		static kPa	sliding kPa					
0:42	0	0.32	0.14	7.36	7.24	0.13	0.00	22.0
1:12	11	0.26	0.14	7.17	6.64	0.53	0.00	22.2
1:43	21	0.59	0.07	7.03	5.38	1.65	0.00	22.4
2:13	31	1.15	0.19	6.83	4.59	2.23	0.00	22.5
2:44	42	1.13	0.77	6.68	3.57	3.11	0.02	22.6
3:14	52	1.48	0.81	6.49	3.04	3.45	0.03	22.8
3:44	63	1.78	1.57	6.36	1.99	4.37	0.04	22.8
4:15	73	2.47	1.82	6.22	1.08	5.13	0.04	23.0
4:45	84	2.49	1.90	6.15	-0.32	6.47	0.05	23.2
5:15	94	3.46	3.27	6.14	-1.89	8.03	0.06	23.4
5:46	105	5.35	4.36	6.19	-4.11	10.30	0.06	23.7
6:16	116	9.56	7.96	6.20	-8.10	14.29	0.06	24.2
6:46	126	19.55	12.78	6.39	-14.43	20.82	0.06	24.8
7:17	136	23.85	10.07	6.76	-29.55	36.31	0.05	25.3
7:47	146	27.73	10.54	6.77	-52.11	58.88	0.05	26.3

VT148

Time	Lifting height	Lifting stress		Normal pressure	Aver. Pore water pressure	Effective pressure	Deformation	Temp
h:m	mm	static kPa	sliding kPa	kPa	kPa	kPa	mm	°C
0:52	0	0.28	0.13	7.28			0.00	22.0
0:57	21	0.24	0.05	7.26	7.09	0.17	0.00	22.1
1:03	41	0.26	0.08	7.25	6.98	0.27	0.00	22.2
1:08	62	0.23	0.02	7.18	6.88	0.31	0.00	22.3
1:13	83	0.38	0.05	7.14	6.78	0.36	0.00	22.4
1:18	104	0.44	0.08	7.10	6.66	0.44	0.00	22.5
1:24	115	0.44	0.30	7.04	6.53	0.51	0.00	22.5
1:32	125	0.59	0.17	7.00	6.43	0.57	0.01	22.5
1:40	136	0.62	0.29	6.95	6.13	0.82	0.00	22.5
1:48	146	0.56	0.33	6.92	5.94	0.98	0.02	22.6
1:57	157	0.73	0.40	6.89	5.84	1.05	0.02	22.6
2:05	167	0.57	0.47	6.85	5.68	1.17	0.02	22.7
2:13	177	0.71	0.40	6.81	5.55	1.26	0.02	22.7
2:21	188	0.72	0.54	6.79	5.44	1.35	0.02	22.7
2:30	198	0.68	0.51	6.75	5.33	1.42	0.02	22.7
2:38	209	0.95	0.55	6.67	5.16	1.51	0.02	22.7
2:43	219	0.95	0.76	6.67	5.08	1.59	0.02	22.8
2:49	230	1.00	0.94	6.66	5.05	1.61	0.03	22.8
2:54	240	1.00	1.00	6.63	4.97	1.66	0.04	22.8
2:59	251	1.05	0.81	6.63	4.88	1.75	0.04	22.8
3:04	261	1.08	0.71	6.61	4.79	1.82	0.04	22.8
3:09	272	1.08	0.73	6.58	4.71	1.87	0.04	22.9
3:14	282	1.13	0.73	6.58	4.59	1.99	0.04	22.9
3:20	293	1.22	0.84	6.56	4.55	2.01	0.04	22.9
3:25	303	1.39	0.93	6.55	4.46	2.09	0.04	22.9
3:30	314	1.31	1.00	6.54	4.34	2.20	0.04	22.9
3:35	324	1.38	1.27	6.56	4.23	2.32	0.05	23.0
3:40	334	1.76	1.33	6.57	4.06	2.51	0.05	23.0
3:45	345	1.88	1.76	6.57	3.88	2.70	0.05	23.0
3:50	356	1.88	1.65	6.57	3.73	2.84	0.05	23.0
3:56	366	1.70	1.53	6.59	3.54	3.05	0.05	23.0
4:01	376	1.89	1.54	6.62	3.37	3.24	0.05	23.1
4:06	387	1.89	1.62	6.63	3.29	3.33	0.05	23.1
4:11	397	1.84	1.51	6.64	3.19	3.45	0.05	23.1
4:16	408	1.85	1.50	6.66	3.09	3.57	0.05	23.1
4:21	418	1.96	1.71	6.69	3.01	3.68	0.05	23.2
4:26	428	2.08	1.77	6.71	2.94	3.78	0.05	23.2
4:32	439	2.08	1.75	6.74	2.84	3.90	0.05	23.2
4:37	449	2.20	1.78	6.78	2.72	4.06	0.05	23.3
4:42	459	2.38	1.98	6.80	2.59	4.21	0.05	23.3
4:47	470	2.38	2.09	6.83	2.43	4.40	0.05	23.3
4:52	480	2.53	2.29	6.88	2.27	4.61	0.05	23.4
4:57	490	2.70	2.19	6.90	2.02	4.88	0.05	23.4
5:02	501	2.70	2.30	6.95	1.85	5.09	0.05	23.4
5:08	511	3.08	2.55	7.00	1.63	5.37	0.05	23.5
5:13	522	3.33	2.76	7.04	1.45	5.59	0.05	23.5
5:18	532	3.49	2.94	7.10	1.26	5.84	0.05	23.6
5:23	542	3.71	3.49	7.15	1.06	6.09	0.05	23.6
5:28	553	4.38	3.65	7.21	0.84	6.37	0.05	23.7
5:33	563	4.41	3.84	7.28	0.52	6.76	0.05	23.8
5:38	573	4.96	4.33	7.38	0.15	7.23	0.05	23.8
5:44	584	5.32	4.74	7.44	-0.55	7.98	0.05	24.3
5:49	594	5.35	4.39	7.50	-0.65	8.16	0.05	23.8
5:54	604	5.93	4.60	7.61	-1.19	8.79	0.05	23.7
5:59	615	6.05	5.13	7.69	-1.50	9.19	0.05	24.1
6:04	625	6.22	5.49	7.79	-1.98	9.77	0.05	23.8
6:09	635	6.82	5.74	7.88	-2.33	10.21	0.05	23.9
6:15	646	7.18	5.86	7.92	-2.71	10.63	0.05	24.0
6:20	656	7.57	6.49	7.99	-3.11	11.11	0.05	24.1
6:25	667	7.62	6.24	8.05	-3.61	11.65	0.06	24.3
6:30	677	7.61	6.09	8.09	-4.19	12.28	0.06	24.4
6:35	688	7.23	5.28	8.19	-4.76	12.95	0.06	24.5
6:40	698	5.63	4.69	8.27	-5.40	13.67	0.06	24.5
6:45	708	4.81	3.80	8.27	-6.03	14.30	0.06	24.7

VT150

Time h:m	Lifting height mm	Lifting stress		Normal pressure kPa	Aver. Pore water pressure kPa	Effective pressure kPa	Deformation mm	Temp °C
		static kPa	sliding kPa					
1:58	0	0.49	0.15	6.63	6.58	0.05	0.00	21.6
2:00	11	0.37	0.37	6.59	6.29	0.29	0.00	21.6
2:03	21	0.43	0.00	6.58	5.98	0.60	0.00	21.7
2:05	32	0.43	0.12	6.57	5.67	0.90	0.01	21.7
2:11	42	0.58	0.15	6.52	5.43	1.10	0.01	21.7
2:16	52	0.58	0.27	6.52	5.09	1.43	0.01	21.8
2:22	63	0.58	0.34	6.48	4.69	1.79	0.01	21.8
2:28	73	0.62	0.32	6.43	4.53	1.90	0.02	21.9
2:38	84	0.84	0.75	6.36	4.08	2.28	0.02	21.9
2:54	95	1.31	0.79	6.26	3.53	2.73	0.03	22.0
3:09	105	1.44	1.12	6.15	3.19	2.95	0.04	22.0
3:24	116	1.41	0.97	6.12	2.65	3.47	0.05	22.1
3:40	126	1.70	1.47	6.03	2.15	3.88	0.05	22.2
3:55	136	2.13	1.74	5.96	1.84	4.12	0.06	22.3
4:11	147	1.99	1.52	5.93	1.29	4.64	0.06	22.3
4:26	157	2.28	1.71	5.92	0.99	4.94	0.07	22.4
4:42	168	2.46	1.84	5.89	0.47	5.42	0.07	22.5
4:57	178	2.79	2.22	5.91	-0.16	6.07	0.07	22.6
5:12	189	3.25	3.06	5.94	-1.05	6.99	0.07	22.7
5:28	200	4.02	3.77	5.98	-1.97	7.95	0.08	22.8
5:43	210	5.20	3.97	6.03	-3.22	9.25	0.08	22.8
5:59	221	6.66	5.07	6.08	-4.85	10.94	0.08	23.0
6:14	231	8.27	6.01	6.11	-6.90	13.01	0.08	23.3
6:30	242	11.28	6.32	6.18	-9.54	15.72	0.09	23.5
6:45	252	12.66	6.26	6.22	-12.54	18.76	0.09	23.9
7:00	262	11.72	5.02	6.29	-9.89	16.19	0.09	24.2
7:16	273	9.44	4.87	6.40	-13.06	19.46	0.08	24.7
7:31	283	6.95	4.48	6.47	-16.69	23.16	0.09	24.7
7:47	294	5.26	3.95	6.52	-20.18	26.69	0.09	25.1
8:02	304	4.34	4.21	6.60	-20.47	27.07	0.09	25.5
8:18	315	4.44	4.11	6.66	-20.64	27.30	0.09	25.9
8:33	325	4.24	4.09	6.72	-20.73	27.44	0.09	26.4
8:48	335	4.36	4.05	6.82	-20.76	27.57	0.09	26.9
9:04	346	4.62	4.32	6.91	-20.79	27.70	0.09	27.4

VT151

Time	Lifting height	Lifting stress		Normal pressure	Aver. Pore water pressure	Effective pressure	Deformation	Temp
		static	sliding					
h:m	mm	kPa	kPa	kPa	kPa	kPa	mm	°C
0:31	0	0.40	0.00	6.99			0.00	20.8
0:46	11	0.29	0.11	6.93			0.00	21.3
1:02	22	0.39	0.14	6.90	6.48	0.42	-0.01	21.6
1:17	32	0.61	0.39	7.04	6.15	0.89	0.03	21.7
1:33	42	0.60	0.49	6.98	5.73	1.25	0.46	21.9
1:48	53	0.70	0.42	6.89	5.46	1.43	0.46	21.9
2:04	64	0.54	0.41	6.80	5.15	1.65	0.47	22.0
2:19	74	0.99	0.63	6.71	4.71	2.01	0.47	22.1
2:34	84	1.20	0.94	6.62	4.38	2.24	0.47	22.2
2:50	95	1.23	0.99	6.53	3.93	2.60	0.47	22.3
3:05	105	1.67	1.10	6.44	3.56	2.88	0.47	22.3
3:21	116	1.89	1.50	6.38	3.18	3.20	0.47	22.3
3:36	126	1.81	1.53	6.33	2.63	3.70	0.47	22.4
3:52	137	2.17	1.74	6.28	2.22	4.06	0.47	22.5
4:07	147	2.18	1.78	6.26	1.67	4.59	0.48	22.6
4:23	158	2.10	1.80	6.25	1.08	5.17	0.48	22.7
4:38	168	2.52	1.86	6.25	0.34	5.92	0.48	22.7
4:53	179	2.72	2.14	6.28	-0.49	6.77	0.48	22.9
5:09	190	3.33	2.67	6.30	-1.49	7.79	0.48	23.0
5:24	201	4.46	3.28	6.36	-2.61	8.97	0.48	23.2
5:40	211	5.52	4.64	6.39	-3.97	10.36	0.48	23.4
5:55	221	6.78	4.76	6.46	-5.78	12.24	0.48	23.6
6:11	232	9.09	6.09	6.55	-8.30	14.85	0.48	23.9
6:26	242	11.74	6.92	6.63	-11.46	18.09	0.48	24.2
6:41	252	13.69	6.69	6.62	-15.96	22.59	0.48	24.4
6:57	262	13.65	5.97	6.73	-22.64	29.36	0.47	24.6
7:12	273	11.29	5.11	6.80	-23.97	30.78	0.47	25.1
7:28	284	7.49	4.13	6.87	-29.61	36.48	0.47	25.6
7:43	294	4.40	3.85	6.97	-35.04	42.01	0.47	25.9
7:59	305	4.23	4.10	7.04	-40.01	47.06	0.47	26.3
8:14	315	4.29	4.09	7.11	-43.98	51.09	0.47	26.9
8:29	326	4.26	4.01	7.21	-46.89	54.09	0.47	27.4

VT152

Time	Lifting height	Lifting stress		Normal pressure	Aver. Pore water pressure	Effective pressure	Deformation	Temp
		static	sliding					
h:m	mm	kPa	kPa	kPa	kPa	kPa	mm	°C
0:42	0	0.01	0.19	7.22			0.00	20.9
0:55	6	0.17	0.04	7.15			0.00	21.5
1:11	11	0.83	0.02	7.07	6.29	0.78	0.01	21.9
1:26	16	0.50	0.19	7.09	5.98	1.11	0.06	22.1
1:42	21	0.55	0.35	6.99	5.65	1.35	0.10	22.3
1:57	27	0.71	0.40	6.92	5.31	1.61	0.11	22.3
2:13	32	0.99	0.57	6.85	5.04	1.81	0.11	22.3
2:28	37	0.96	0.64	6.77	4.75	2.01	0.11	22.4
2:44	42	1.25	0.95	6.68	4.52	2.16	0.11	22.5
2:59	48	1.54	1.19	6.60	4.11	2.48	0.12	22.5
3:14	53	1.80	1.38	6.49	4.25	2.24	0.12	22.6
3:30	58	2.31	2.06	6.43	3.35	3.08	0.13	22.7
3:45	63	2.14	1.63	6.39	2.78	3.61	0.12	22.7
4:01	68	2.16	1.61	6.34	2.36	3.98	0.13	22.8
4:16	74	2.18	2.18	6.31	1.84	4.47	0.13	22.9
4:32	79	1.75	1.59	6.29	1.16	5.13	0.13	22.9
4:47	84	2.30	1.94	6.27	0.33	5.94	0.13	23.0
5:03	89	2.83	2.39	6.26	-0.67	6.93	0.13	23.2
5:18	95	3.73	3.04	6.30	-1.79	8.10	0.13	23.3
5:33	101	4.93	4.34	6.30	-3.09	9.39	0.13	23.6
5:49	106	6.71	5.62	6.31	-4.79	11.11	0.13	23.8
6:04	111	8.69	8.22	6.30	-7.13	13.44	0.12	24.1
6:20	116	12.77	11.80	6.40	-10.21	16.62	0.12	24.3
6:35	120	16.47	11.50	6.42	-14.30	20.71	0.12	24.5
6:51	125	17.44	12.83	6.48	-19.49	25.97	0.12	24.8
7:06	130	20.53	11.79	6.52	-27.96	34.48	0.12	25.4
7:21	135	21.85	13.89	6.68	-37.33	44.00	0.12	25.5
7:37	140	22.69	12.89	6.74	-46.50	53.24	0.12	26.0
7:52	146	18.66	10.08	6.61	-51.82	58.44	0.12	26.5
8:08	152	13.37	6.94	6.58	-57.92	64.49	0.12	27.1
8:23	158	4.94	3.99	6.63	-62.26	68.89	0.12	27.5
8:39	163	4.00	3.79	6.66	-64.57	71.23	0.12	28.0
8:54	168	4.10	3.92	6.70	-64.94	71.63	0.12	28.5
9:09	174	4.05	3.74	6.71	-64.55	71.26	0.12	29.1

VT153

Time h:m	Lifting height mm	Lifting stress		Normal pressure kPa	Aver. Pore water pressure kPa	Effective pressure kPa	Deformation mm	Temp °C
		static kPa	sliding kPa					
0:35	0	0.55	0.08	6.77			0.00	21.6
0:50	22	0.20	0.06	6.70			0.03	22.0
1:06	43	0.36	0.07	6.62	6.20	0.43	0.02	22.2
1:21	63	0.47	0.12	6.63	5.75	0.89	0.03	22.4
1:37	84	0.60	0.27	6.56	4.87	1.69	0.03	22.6
1:52	105	0.70	0.35	6.51	3.88	2.62	0.03	22.5
2:08	126	0.78	0.66	6.43	3.56	2.87	0.03	22.6
2:23	147	0.91	0.42	6.40	3.09	3.30	0.03	22.7
2:38	168	0.96	0.68	6.34	2.90	3.44	0.03	22.7
2:54	189	1.11	0.76	6.26	2.90	3.35	0.03	22.8
3:09	210	1.48	1.15	6.21	2.53	3.69	0.03	22.8
3:25	231	1.85	1.45	6.16	2.15	4.01	0.03	22.9
3:40	252	2.04	1.54	6.14	1.77	4.37	0.03	22.9
3:56	273	2.19	1.74	6.13	1.44	4.70	0.03	23.0
4:11	294	2.09	1.97	6.13	1.12	5.01	0.03	23.0
4:26	314	2.40	2.13	6.12	0.78	5.34	0.03	23.1
4:42	335	3.00	2.48	6.28	0.15	6.13	0.03	23.2
4:57	355	3.26	3.26	6.37	-0.83	7.20	0.03	23.3
5:13	376	3.64	3.17	6.36	-1.84	8.20	0.03	23.4
5:28	397	4.09	3.50	6.45	-2.46	8.91	0.03	23.5
5:44	418	4.62	4.17	6.59	-3.17	9.76	0.03	23.7
5:59	438	5.28	4.30	6.72	-4.27	11.00	0.03	24.0
6:15	459	6.16	4.64	6.87	-5.67	12.54	0.03	24.2
6:30	480	6.81	4.61	7.00	-7.36	14.36	0.03	24.4
6:45	500	6.07	4.18	7.11	-9.93	17.04	0.03	24.7
7:01	521	5.63	3.97	7.27	-12.65	19.92	0.03	24.9
7:16	542	4.86	3.70	7.45	-16.02	23.46	0.03	25.2
7:32	563	4.53	3.77	7.63	-20.05	27.68	0.03	25.7
7:47	583	4.29	4.04	7.78	-24.73	32.51	0.03	26.1
8:03	604	4.49	4.18	7.95	-30.93	38.88	0.03	26.5
8:18	625	4.61	4.55	8.08	-36.54	44.62	0.03	27.0

VT159

Time	Lifting height	Lifting stress		Normal pressure	Aver. Pore water pressure	Effective pressure	Deformation	Temp
		static	sliding					
h:m	mm	kPa	kPa	kPa	kPa	kPa	mm	°C
0:59	0	0.17	0.05	7.03	6.87	0.16	0.00	20.4
1:15	7	0.33	0.16	6.93	6.74	0.19	0.03	21.4
1:30	12	0.43	0.27	6.88	6.35	0.53	0.08	21.9
1:46	17	0.67	0.22	6.81	6.20	0.61	0.11	22.1
2:02	22	0.61	0.26	6.85	5.72	1.13	0.11	22.3
2:17	27	0.84	0.60	6.87	5.43	1.44	0.11	22.3
2:33	32	1.00	0.57	6.81	5.14	1.66	0.12	22.5
2:48	37	0.96	0.69	6.75	4.49	2.26	0.12	22.6
3:04	43	1.17	0.82	6.68	4.12	2.56	0.12	22.6
3:20	48	1.20	0.84	6.61	3.98	2.62	0.13	22.7
3:35	53	1.26	1.02	6.57	3.36	3.21	0.13	22.7
3:51	59	1.53	1.10	6.58	2.40	4.18	0.14	22.8
4:06	64	1.71	1.28	6.51	2.78	3.72	0.13	22.1
4:22	69	1.87	1.31	6.48	2.44	4.04	0.13	22.3
4:38	74	1.74	1.18	6.44	1.84	4.60	0.13	22.5
4:53	79	1.73	1.73	6.41	1.27	5.14	0.13	22.7
5:09	85	1.96	1.35	6.38	0.64	5.74	0.13	22.9
5:24	90	2.17	1.77	6.37	-0.05	6.43	0.13	23.0
5:40	95	2.51	2.31	6.39	-1.08	7.47	0.13	23.1
5:56	100	3.49	2.84	6.41	-2.42	8.82	0.13	23.3
6:11	106	4.65	4.32	6.40	-4.12	10.51	0.13	23.5
6:27	112	6.18	5.66	6.41	-6.52	12.93	0.13	23.7
6:42	117	9.02	8.11	6.44	-9.91	16.35	0.13	23.9
6:58	122	16.32	14.07	6.82	-14.39	21.21	0.13	24.1
7:14	126	21.58	13.25	6.88	-20.62	27.50	0.13	24.3
7:29	131	23.88	16.56	6.86	-28.55	35.41	0.13	24.6
7:45	136	24.43	13.50	7.00	-37.61	44.61	0.13	24.9
8:00	142	26.30	10.06	7.10	-47.53	54.62	0.13	25.4
8:16	147	27.77	8.21	7.09	-56.82	63.91	0.13	25.9
8:32	152	23.81	6.82	7.16	-64.67	71.83	0.13	26.3
8:47	158	13.26	3.48	6.53	-70.79	77.32	0.13	26.9
9:02	164	4.41	3.00	6.55	-75.36	81.91	0.13	27.4

VT161

Time h:m	Lifting height mm	Lifting stress		Normal pressure kPa	Aver. Pore water pressure kPa	Effective pressure kPa	Deformation mm	Temp °C
		static kPa	sliding kPa					
0:30	0	0.21	0.02	6.86			0.00	22.3
0:45	10	0.45	0.14	6.72			0.01	22.5
1:01	21	0.29	0.29	6.59	6.11	0.49	0.01	22.6
1:16	31	0.41	0.22	6.47	5.91	0.55	0.01	22.7
1:31	42	0.59	0.17	6.37	5.69	0.68	0.01	22.8
1:46	52	0.52	0.23	6.24	5.46	0.78	0.01	22.9
2:02	62	0.76	0.40	6.28	5.23	1.06	0.01	22.9
2:17	73	0.88	0.43	6.27	5.05	1.21	0.09	23.0
2:32	83	1.17	0.73	6.15	4.75	1.40	0.09	23.0
2:47	93	1.04	0.82	5.94	4.57	1.37	0.10	23.0
3:02	104	1.49	1.06	5.78	4.29	1.49	0.11	23.1
3:18	114	1.65	1.07	5.64	3.97	1.68	0.11	23.1
3:33	124	2.30	1.28	5.50	3.67	1.83	0.13	23.2
3:48	135	1.98	1.82	5.39	3.51	1.88	0.17	22.9
4:03	145	2.26	1.60	5.21	3.13	2.08	0.20	22.7
4:19	156	2.36	1.88	5.09	2.61	2.48	0.21	23.0
4:34	166	2.43	2.23	4.95	2.19	2.75	0.23	23.1
4:49	177	2.32	2.09	4.80	1.64	3.16	0.24	23.3
5:04	187	2.40	1.97	4.70	0.98	3.72	0.24	23.4
5:20	197	2.86	2.86	4.62	0.28	4.33	0.24	23.6
5:35	208	3.24	2.90	4.55	-0.54	5.09	0.24	23.7
5:50	219	4.61	4.03	4.49	-1.58	6.08	0.24	23.9
6:05	230	5.74	4.85	4.42	-2.95	7.38	0.24	24.1
6:21	240	7.17	4.62	4.38	-4.79	9.17	0.23	24.3
6:36	250	8.16	5.35	4.36	-7.55	11.91	0.23	24.7
6:51	261	8.12	5.44	4.34	-11.55	15.89	0.23	24.9
7:07	271	7.75	4.94	4.32	-16.38	20.70	0.23	25.2
7:22	282	6.82	4.60	4.30	-23.02	27.32	0.23	25.6
7:37	292	5.52	2.42	4.26	-30.13	34.39	0.23	26.0
7:52	302	3.11	2.26	4.21	-38.62	42.83	0.23	26.4
8:08	313	2.22	1.95	4.18	-47.11	51.29	0.24	26.8
8:23	323	2.07	1.71	4.14	-54.98	59.12	0.24	27.3
8:38	334	1.98	1.80	4.15	-61.51	65.66	0.23	27.8

VT162

Time	Lifting height	Lifting stress		Normal pressure	Aver. Pore water pressure	Effective pressure	Deformation	Temp
		static	sliding					
h:m	mm	kPa	kPa	kPa	kPa	kPa	mm	°C
0:47	0	0.24	0.12	6.61			0.00	23.0
1:02	10	0.25	0.07	6.46	6.20	0.26	0.00	23.1
1:17	20	0.38	0.06	6.26	5.72	0.54	0.01	23.2
1:32	31	0.30	0.18	6.14	5.22	0.93	0.01	23.4
1:47	41	0.51	0.51	6.20	4.71	1.48	0.01	23.4
2:03	51	0.81	0.37	6.22	4.20	2.02	0.05	23.4
2:18	62	1.17	0.49	6.10	4.13	1.97	0.05	23.5
2:33	72	0.95	0.47	5.90	3.71	2.19	0.06	23.5
2:48	83	1.02	0.53	5.68	3.54	2.14	0.10	23.6
3:04	93	1.28	0.83	5.56	3.06	2.50	0.14	23.6
3:19	104	1.53	0.85	5.34	2.77	2.57	0.17	23.6
3:34	114	2.24	1.23	5.18	2.48	2.69	0.20	23.7
3:49	125	1.61	1.17	4.98	2.06	2.91	0.26	23.8
4:04	135	1.88	1.36	4.81	1.80	3.01	0.31	23.9
4:20	146	2.14	1.46	4.63	1.11	3.52	0.35	24.0
4:35	156	1.96	1.55	4.46	0.83	3.62	0.38	24.1
4:50	167	1.92	1.63	4.26	0.40	3.86	0.39	24.2
5:05	177	2.18	1.69	4.10	-0.17	4.27	0.39	24.3
5:20	188	2.31	1.95	3.96	-0.72	4.68	0.39	24.4
5:36	198	2.82	2.40	3.83	-1.27	5.10	0.39	24.5
5:51	209	3.45	2.88	3.69	-2.02	5.71	0.39	24.7
6:06	220	4.52	3.49	3.57	-2.89	6.46	0.39	25.0
6:21	230	5.65	4.11	3.48	-4.17	7.65	0.39	25.2
6:36	241	7.27	4.30	3.42	-6.94	10.36	0.39	25.5
6:52	251	7.51	4.99	3.35	-6.30	9.65	0.40	25.8
7:07	262	6.05	3.18	3.28	-10.85	14.13	0.40	26.2
7:22	272	5.08	2.93	3.20	-14.94	18.14	0.39	26.6
7:37	282	4.11	1.88	3.13	-20.53	23.66	0.39	26.9
7:52	292	2.52	1.40	3.05	-26.04	29.08	0.39	27.4
8:08	302	1.43	1.34	2.97	-31.17	34.15	0.39	27.9
8:23	313	1.28	1.24	2.91	-26.85	29.77	0.39	28.4
8:38	323	1.38	1.14	2.86	-23.79	26.65	0.39	29.0

VT163

Time	Lifting height	Lifting stress		Normal pressure	Aver. Pore water pressure	Effective pressure	Deformation	Temp
		static	sliding					
h:m	mm	kPa	kPa	kPa	kPa	kPa	mm	°C
0:30	0	0.38	0.09	6.81			0.00	20.7
0:45	10	0.33	0.01	6.62	6.49	0.13	0.01	21.1
1:01	20	0.28	0.26	6.49	6.29	0.21	0.01	21.2
1:16	30	0.41	0.38	6.39	6.15	0.24	0.01	21.2
1:31	40	0.44	0.31	6.15	5.96	0.19	0.02	21.4
1:46	50	0.74	0.34	6.17	5.93	0.24	0.02	21.5
2:02	60	0.75	0.52	6.15	5.49	0.66	0.04	21.6
2:17	70	0.89	0.38	5.96	5.02	0.94	0.04	21.6
2:32	80	0.77	0.74	5.72	4.56	1.15	0.05	21.7
2:47	90	0.77	0.51	5.48	4.09	1.39	0.05	21.6
3:03	100	1.00	0.64	5.28	3.62	1.66	0.06	21.7
3:18	110	1.10	0.77	5.05	3.25	1.80	0.06	21.8
3:33	120	1.36	0.87	4.82	2.97	1.85	0.08	21.8
3:48	130	1.55	1.27	4.60	2.59	2.01	0.09	21.8
4:04	140	1.81	1.48	4.36	2.34	2.02	0.11	21.8
4:19	150	2.15	1.47	4.12	2.08	2.05	0.15	21.9
4:34	160	2.30	1.89	3.90	1.68	2.22	0.21	21.9
4:49	170	2.70	1.95	3.66	1.28	2.38	0.30	21.9
5:04	180	2.74	2.06	3.42	0.69	2.73	0.35	22.0
5:20	190	3.15	2.30	3.19	0.64	2.54	0.39	22.0
5:35	200	2.84	2.34	2.99	-0.07	3.06	0.43	22.1
5:50	210	2.70	2.11	2.80	-0.38	3.18	0.43	22.2
6:05	220	2.55	2.04	2.59	-0.84	3.43	0.44	22.4
6:21	230	2.32	2.08	2.40	-1.60	4.00	0.45	22.5
6:36	240	2.61	2.32	2.23	-2.54	4.77	0.46	22.5
6:51	250	3.05	2.34	2.07	-3.98	6.05	0.46	22.7
7:06	260	3.29	2.88	1.94	-5.63	7.56	0.47	23.0
7:21	270	3.82	2.90	1.80	-8.84	10.64	0.48	23.2
7:37	280	4.60	2.80	1.69	-13.58	15.28	0.48	23.5
7:52	290	4.83	2.42	1.60	-19.21	20.82	0.49	23.7
8:07	300	3.81	1.52	1.49	-25.93	27.42	0.49	24.0
8:22	310	2.25	0.48	1.37	-33.72	35.09	0.49	24.3

VT164

Time h:m	Lifting height mm	Lifting stress		Normal pressure kPa	Aver. Pore water pressure kPa	Effective pressure kPa	Deformation mm	Temp °C
		static kPa	sliding kPa					
0:30	0	0.04	0.01	7.02			0.00	21.7
0:45	10	0.29	-0.10	6.85			0.01	22.0
1:00	20	0.18	-0.11	6.71	6.50	0.21	0.01	22.2
1:15	30	0.36	0.00	6.57	6.24	0.32	0.01	22.3
1:31	40	0.56	0.28	6.47	6.28	0.19	0.01	22.5
1:46	50	0.54	0.21	6.52	6.20	0.32	0.01	22.5
2:01	60	0.58	0.21	6.41	5.91	0.49	0.02	22.5
2:16	70	0.61	0.30	6.17	5.50	0.67	0.02	22.6
2:32	80	0.75	0.49	5.94	5.09	0.86	0.02	22.7
2:47	90	1.22	0.75	5.77	4.77	1.00	0.02	22.7
3:02	100	1.42	0.82	5.53	4.38	1.16	0.02	22.8
3:17	110	1.59	0.99	5.32	4.08	1.24	0.02	22.8
3:32	120	1.51	1.15	5.08	3.72	1.36	0.02	22.9
3:48	130	1.46	1.07	4.87	3.28	1.59	0.02	23.0
4:03	140	1.58	1.22	4.67	1.94	2.74	0.07	23.7
4:18	150	1.74	1.21	4.44	1.89	2.54	0.06	23.1
4:33	160	2.15	1.36	4.22	1.68	2.54	0.08	22.4
4:49	170	2.18	1.51	4.00	1.66	2.34	0.08	21.6
5:04	180	2.20	1.75	3.71	1.11	2.59	0.06	21.2
5:19	190	2.29	1.86	3.47	0.62	2.85	0.05	21.7
5:34	200	2.36	1.93	3.26	0.20	3.06	0.05	22.2
5:49	210	2.21	2.13	3.06	-0.35	3.42	0.05	22.6
6:05	220	2.15	2.13	2.87	-0.82	3.69	0.05	22.8
6:20	230	2.58	2.14	2.71	-1.42	4.13	0.05	23.0
6:35	240	2.82	2.38	2.54	-2.19	4.72	0.05	23.3
6:50	250	3.35	3.14	2.39	-3.00	5.39	0.04	23.5
7:06	260	3.69	3.10	2.27	-4.29	6.56	0.04	23.7
7:21	270	4.00	3.21	2.16	-6.22	8.39	0.05	23.7
7:36	280	4.24	2.76	2.05	-9.32	11.38	0.04	24.0
7:51	290	4.51	2.91	1.93	-14.19	16.12	0.04	24.5
8:06	300	4.40	2.61	1.82	-20.08	21.89	0.04	24.8
8:22	310	3.37	1.82	1.71	-26.70	28.41	0.03	25.2
8:37	320	2.72	0.77	1.62	-33.53	35.15	0.03	25.6

VT165

Time h:m	Lifting height mm	Lifting stress		Normal pressure kPa	Aver. Pore water pressure kPa	Effective pressure kPa	Deformation mm	Temp °C
		static kPa	sliding kPa					
0:48	0	0.27	0.08	7.04			0.00	23.1
1:03	10	0.30	0.04	6.98	6.61	0.36	0.00	23.3
1:18	20	0.47	0.47	6.96	6.59	0.37	0.00	23.4
1:33	30	0.62	0.20	6.93	6.56	0.37	0.00	23.5
1:48	40	0.85	0.62	6.91	6.54	0.37	0.00	23.6
2:04	50	0.97	0.83	6.93	6.04	0.90	0.01	23.5
2:19	60	1.16	0.79	6.90	5.58	1.31	0.16	23.6
2:34	70	1.16	0.87	6.72	5.10	1.61	0.16	23.7
2:49	80	1.52	1.20	6.54	4.56	1.98	0.16	23.8
3:05	90	1.36	0.88	6.32	4.07	2.25	0.17	23.9
3:20	100	1.65	1.40	6.20	3.54	2.66	0.17	23.9
3:35	110	1.81	1.32	6.03	3.17	2.86	0.17	23.7
3:50	120	2.02	1.51	5.88	2.41	3.47	0.17	23.7
4:05	130	2.46	1.78	5.72	2.16	3.57	0.18	23.9
4:21	140	3.10	2.10	5.59	1.24	4.36	0.19	23.9
4:36	150	2.51	2.35	5.47	0.78	4.68	0.21	24.0
4:51	160	2.79	2.43	5.35	0.33	5.01	0.22	24.1
5:06	170	2.44	2.32	5.25	-0.25	5.50	0.23	24.2
5:22	180	2.86	2.46	5.18	-0.93	6.11	0.23	24.4
5:37	190	3.47	2.88	5.09	-1.55	6.65	0.23	24.6
5:52	200	3.83	3.83	5.07	-2.29	7.36	0.23	24.7
6:07	210	5.09	4.22	5.04	-3.22	8.26	0.23	24.9
6:22	220	6.10	4.99	4.99	-4.61	9.60	0.23	25.2
6:38	230	7.36	6.09	4.99	-6.69	11.68	0.23	25.3
6:53	240	8.56	6.62	4.98	-9.96	14.94	0.23	25.5
7:08	250	9.25	6.68	4.96	-15.13	20.10	0.23	25.7
7:23	260	10.37	6.06	4.96	-21.61	26.57	0.23	26.0
7:38	270	9.48	5.58	4.93	-28.36	33.28	0.23	26.5
7:54	280	6.77	4.27	4.86	-35.54	40.40	0.23	26.9
8:09	290	4.93	2.80	4.85	-35.80	40.65	0.23	27.4

VT166

Time h:m	Lifting height mm	Lifting stress		Normal pressure kPa	Aver. Pore water pressure kPa	Effective pressure kPa	Deformation mm	Temp °C
		static kPa	sliding kPa					
0:35	0	0.40	0.07	7.41			0.00	22.4
0:50	10	0.49	0.03	7.31			0.00	22.6
1:06	20	0.49	0.07	7.20	6.87	0.33	0.00	22.8
1:21	30	0.48	0.16	7.06	6.84	0.22	0.00	22.9
1:36	40	0.76	0.56	6.99	6.62	0.36	0.00	23.0
1:51	50	0.83	0.78	6.90	6.61	0.29	0.00	23.0
2:07	60	0.91	0.80	7.09	6.71	0.38	0.01	23.1
2:22	70	1.07	0.76	7.02	6.57	0.45	0.07	23.2
2:37	80	1.18	1.08	6.90	6.15	0.75	0.14	23.3
2:52	90	1.44	1.34	6.77	5.66	1.11	0.14	23.3
3:08	100	1.24	1.02	6.62	5.37	1.25	0.15	23.4
3:23	110	1.79	1.46	6.50	4.87	1.63	0.15	23.4
3:38	120	1.75	1.48	6.37	4.69	1.68	0.16	23.5
3:53	130	1.74	1.28	6.26	4.30	1.96	0.18	23.6
4:08	140	2.18	1.79	6.20	3.58	2.62	0.20	23.6
4:24	150	2.78	2.41	6.10	3.36	2.74	0.21	23.7
4:39	160	2.80	2.25	6.03	2.83	3.21	0.22	23.8
4:54	170	2.81	2.33	5.98	2.48	3.50	0.23	23.8
5:09	180	2.72	2.31	5.91	1.74	4.17	0.23	23.8
5:25	190	2.79	2.51	5.88	1.11	4.78	0.23	24.0
5:40	200	2.95	2.58	5.88	0.37	5.50	0.23	24.1
5:55	210	3.47	2.94	5.89	-0.48	6.37	0.23	24.2
6:10	220	4.23	3.49	5.87	-1.33	7.20	0.22	24.5
6:26	230	5.16	4.81	5.87	-2.29	8.17	0.22	24.7
6:41	240	6.51	5.70	5.90	-3.57	9.46	0.22	24.9
6:56	250	8.19	6.18	5.94	-5.33	11.27	0.22	25.1
7:11	260	9.41	6.40	5.97	-7.83	13.80	0.22	25.2
7:26	270	11.85	6.10	6.04	-10.89	16.93	0.22	25.5
7:42	280	11.84	5.91	6.06	-14.27	20.33	0.22	25.8
7:57	290	7.83	4.63	6.08	-19.63	25.71	0.22	26.1
8:12	300	5.86	3.78	6.11	-25.38	31.49	0.22	26.4
8:27	310	4.54	3.51	6.16	-30.62	36.78	0.22	27.1
8:43	320	3.59	3.30	6.20	-35.19	41.39	0.22	27.6

VT167

Time h:m	Lifting height mm	Lifting stress		Normal pressure kPa	Aver. Pore water pressure kPa	Effective pressure kPa	Deformation mm	Temp °C
		static kPa	sliding kPa					
0:28	0	0.36	0.02	7.56			0.00	22.6
0:44	10	0.48	0.19	7.47			0.00	23.0
0:59	20	0.50	0.19	7.37	7.03	0.34	0.00	23.3
1:14	30	0.65	0.35	7.29	6.77	0.52	0.01	23.5
1:29	40	1.19	0.53	7.24	6.50	0.74	0.02	23.6
1:45	50	1.07	1.06	7.18	6.23	0.95	0.02	23.6
2:00	60	1.32	0.87	7.16	5.98	1.18	0.02	23.6
2:15	70	1.27	1.00	7.15	5.85	1.29	0.03	23.6
2:30	80	1.51	1.17	7.03	5.24	1.79	0.08	23.6
2:46	90	2.03	1.29	6.96	4.57	2.39	0.08	23.6
3:01	100	1.86	1.55	6.85	4.31	2.54	0.09	23.6
3:16	110	2.09	1.74	6.78	3.83	2.95	0.09	23.6
3:31	120	2.58	2.02	6.71	3.78	2.93	0.09	23.6
3:47	130	2.55	1.96	6.62	3.32	3.29	0.09	23.6
4:02	140	2.55	2.31	6.54	3.02	3.52	0.11	23.6
4:17	150	2.85	2.77	6.48	2.64	3.84	0.12	23.7
4:32	160	3.07	2.63	6.43	2.17	4.26	0.12	23.9
4:47	170	3.09	2.75	6.40	1.87	4.52	0.12	23.8
5:03	180	3.24	2.77	6.41	1.32	5.09	0.12	24.0
5:18	190	2.95	2.46	6.41	0.64	5.77	0.12	24.1
5:33	200	3.20	2.89	6.41	0.03	6.38	0.12	24.2
5:48	210	3.88	3.25	6.45	-0.66	7.11	0.12	24.4
6:04	220	4.75	3.97	6.48	-1.45	7.93	0.12	24.5
6:19	230	5.59	4.54	6.53	-2.35	8.88	0.12	24.7
6:34	240	6.95	5.59	6.61	-3.55	10.15	0.11	24.9
6:49	250	8.41	5.97	6.67	-5.08	11.75	0.11	25.2
7:05	260	10.04	7.07	6.73	-7.02	13.75	0.11	25.5
7:20	270	11.47	6.30	6.81	-9.49	16.29	0.11	25.8
7:35	280	11.51	6.33	6.89	-13.03	19.92	0.11	26.2
7:50	290	7.37	4.99	6.97	-18.02	24.99	0.11	26.5
8:05	300	6.49	5.09	7.09	-26.13	33.22	0.11	26.8
8:21	310	6.04	4.77	7.19	-35.58	42.77	0.12	27.4

VT169

Time h:m	Lifting height mm	Lifting stress		Normal pressure kPa	Aver. Pore water pressure kPa	Effective pressure kPa	Deformation mm	Temp °C
		static kPa	sliding kPa					
0:45	0	3.06	2.76	5.48			0.00	23.5
1:00	10	3.11	3.11	5.20	1.34	3.86	0.03	23.7
1:15	20	3.15	2.60	4.96	0.44	4.52	0.10	23.9
1:31	30	3.40	2.80	4.83	0.17	4.66	0.12	24.0
1:46	40	3.07	2.62	4.74	-0.14	4.88	0.14	24.1
2:01	50	3.08	2.81	4.65	-0.19	4.84	0.15	24.2
2:16	60	2.94	2.88	4.61	-0.41	5.03	0.14	24.2
2:32	70	3.21	2.76	4.56	-0.63	5.18	0.16	24.4
2:47	80	3.25	2.91	4.51	-0.57	5.09	0.18	24.5
3:02	90	3.24	3.24	4.48	-0.84	5.32	0.18	24.6
3:17	100	3.24	3.05	4.46	-1.14	5.59	0.20	24.7
3:33	110	3.43	3.09	4.49	-1.46	5.94	0.21	24.8
3:48	120	3.71	3.30	4.49	-1.98	6.47	0.21	24.9
4:03	130	3.84	3.75	4.49	-2.74	7.23	0.21	25.0
4:18	140	4.26	3.61	4.51	-3.54	8.05	0.21	25.3
4:34	150	4.59	3.59	4.53	-4.15	8.68	0.21	25.6
4:49	160	4.63	3.78	4.56	-4.65	9.21	0.21	25.9
5:04	170	4.66	3.24	4.59	-5.18	9.78	0.21	26.3
5:20	180	3.79	3.08	4.64	-5.63	10.27	0.21	26.7
5:35	190	3.57	2.62	4.67	-6.04	10.71	0.21	27.2
5:50	200	3.25	2.48	4.72	-6.42	11.14	0.21	27.8
6:05	210	3.10	2.88	4.76	-6.82	11.59	0.21	28.4
6:21	220	2.96	2.60	4.79	-7.32	12.10	0.22	29.5
6:36	230	2.80	2.58	4.82	-7.70	12.52	0.22	29.8
6:51	240	2.82	2.54	4.84	-8.10	12.94	0.22	30.9
7:06	250	2.84	2.60	4.86	-8.35	13.21	0.22	31.6
7:22	260	2.88	2.79	4.88	-8.76	13.65	0.22	32.6
7:37	270	2.89	2.78	4.91	-9.16	14.07	0.22	33.6
7:52	280	2.89	2.71	4.93	-9.65	14.58	0.22	34.6
8:07	290	3.05	2.95	5.02	-10.22	15.24	0.22	35.6

VT170

Time	Lifting height	Lifting stress		Normal pressure	Aver. Pore water pressure	Effective pressure	Deformation	Temp
		static	sliding					
h:m	mm	kPa	kPa	kPa	kPa	kPa	mm	°C
1:09	0	3.25	2.75	5.63	0.83	4.81	0.00	23.8
1:25	10	3.20	2.64	5.46	0.92	4.54	0.04	23.8
1:40	20	3.29	2.72	5.27	0.42	4.85	0.21	24.0
1:55	30	3.19	3.03	5.13	0.06	5.07	0.23	24.0
2:11	40	3.63	3.05	5.02	0.21	4.80	0.19	24.1
2:26	50	3.71	3.29	4.98	-0.17	5.15	0.20	24.0
2:41	60	3.82	3.42	4.94	-0.44	5.39	0.20	24.2
2:56	70	3.64	3.55	4.94	-0.71	5.65	0.19	24.3
3:12	80	3.38	3.24	4.92	-1.11	6.02	0.21	24.5
3:27	90	3.53	3.02	4.91	-1.45	6.36	0.22	24.6
3:42	100	3.45	3.12	4.95	-1.78	6.73	0.23	24.8
3:58	110	3.84	3.84	5.00	-2.17	7.18	0.24	25.0
4:13	120	4.25	3.90	5.05	-2.67	7.72	0.24	25.3
4:28	130	4.69	4.28	5.14	-3.25	8.39	0.24	25.6
4:43	140	4.64	4.28	5.23	-3.79	9.02	0.24	25.9
4:59	150	4.90	4.09	5.35	-4.26	9.61	0.24	26.3
5:14	160	4.87	3.84	5.45	-4.77	10.23	0.24	26.7
5:29	170	4.35	3.42	5.54	-5.24	10.78	0.24	27.2
5:44	180	3.65	2.64	5.66	-5.79	11.44	0.24	28.1
6:00	190	3.29	2.78	5.78	-6.21	11.99	0.24	28.1
6:15	200	3.53	3.10	5.85	-6.76	12.61	0.24	28.8
6:30	210	3.58	3.24	5.91	-7.32	13.23	0.24	29.7
6:45	220	3.71	3.26	5.93	-7.81	13.75	0.24	30.1
7:01	230	3.81	3.81	5.96	-8.46	14.42	0.24	31.2
7:16	240	3.84	3.45	5.99	-8.77	14.76	0.24	31.8
7:31	250	3.72	3.06	6.07	-9.30	15.37	0.24	32.8
7:46	260	3.86	3.41	6.12	-9.84	15.97	0.24	33.7

VT171

Time	Lifting height	Lifting stress		Normal pressure	Aver. Pore water pressure	Effective pressure	Deformation	Temp
h:m	mm	static kPa	sliding kPa	kPa	kPa	kPa	mm	°C
0:48	0	1.25	1.15	6.24			0.00	22.9
1:03	10	1.99	1.78	5.97	3.95	2.02	0.01	23.0
1:18	20	2.72	2.49	5.71	3.15	2.56	0.00	23.2
1:33	30	2.77	2.49	5.54	2.49	3.05	0.10	23.3
1:49	40	3.22	2.93	5.41	2.16	3.25	0.11	23.5
2:04	50	3.93	3.75	5.27	1.79	3.48	0.10	23.6
2:19	60	4.22	4.22	5.16	1.35	3.81	0.11	23.7
2:34	70	4.57	3.91	5.08	0.88	4.20	0.10	23.8
2:50	80	4.56	3.97	5.03	0.59	4.44	0.11	23.9
3:05	90	4.50	4.17	5.00	0.21	4.79	0.09	24.0
3:20	100	4.95	4.21	5.00	-0.06	5.06	0.08	24.1
3:35	110	4.41	4.03	4.97	-0.55	5.52	0.08	24.3
3:51	120	4.34	3.97	4.95	-0.99	5.94	0.08	24.4
4:06	130	4.16	3.76	4.95	-1.33	6.28	0.09	24.4
4:21	140	4.42	3.62	4.98	-1.67	6.65	0.12	24.6
4:36	150	4.50	3.57	5.04	-2.14	7.17	0.13	24.8
4:52	160	4.59	4.06	5.12	-2.73	7.85	0.14	24.8
5:07	170	4.82	4.52	5.21	-3.14	8.35	0.14	24.9
5:22	180	5.52	4.09	5.32	-3.66	8.98	0.14	25.2
5:38	190	5.41	4.42	5.41	-4.15	9.56	0.14	25.5
5:53	200	5.37	4.06	5.58	-4.63	10.21	0.14	25.7
6:08	210	4.85	3.97	5.77	-5.10	10.87	0.14	26.1
6:23	220	4.86	3.89	5.92	-5.59	11.51	0.14	26.4
6:39	230	4.37	3.32	6.05	-6.08	12.14	0.14	26.7
6:54	240	4.19	3.80	6.19	-6.52	12.71	0.14	27.1
7:09	250	4.13	4.13	6.28	-7.49	13.77	0.14	27.5
7:24	260	4.17	3.91	6.35	-8.29	14.63	0.14	28.0
7:40	270	4.16	3.76	6.44	-9.14	15.58	0.14	28.5
7:55	280	4.27	4.07	6.49	-10.04	16.54	0.14	29.0

VT172

Time	Lifting height	Lifting stress		Normal pressure	Aver. Pore water pressure	Effective pressure	Deformation	Temp
		static	sliding					
h:m	mm	kPa	kPa	kPa	kPa	kPa	mm	°C
0:46	0	3.63	2.79	6.97			0.00	22.7
1:01	10	3.20	2.78	6.50	2.15	4.35	0.02	23.1
1:16	20	3.45	2.97	6.20	1.73	4.47	0.05	23.3
1:32	30	3.43	3.39	6.01	0.86	5.15	0.00	23.4
1:47	40	3.51	3.05	5.81	0.40	5.41	0.03	23.5
2:02	50	3.46	3.42	5.66	0.14	5.52	0.02	23.7
2:17	60	3.90	3.67	5.53	-0.15	5.68	0.06	23.7
2:33	70	4.55	4.17	5.48	-0.45	5.93	0.05	23.8
2:48	80	4.40	3.64	5.34	-0.96	6.31	0.07	23.9
3:03	90	4.52	3.76	5.29	-1.56	6.85	0.09	24.0
3:19	100	4.60	3.88	5.27	-2.37	7.64	0.06	24.1
3:34	110	4.33	3.68	5.27	-3.30	8.57	0.05	24.2
3:49	120	4.83	4.26	5.28	-4.53	9.82	0.07	24.4
4:04	130	5.00	4.53	5.33	-5.77	11.10	0.09	24.5
4:20	140	5.48	4.62	5.38	-7.17	12.55	0.09	24.8
4:35	150	6.70	5.13	5.47	-8.59	14.06	0.08	25.0
4:50	160	6.56	4.21	5.56	-9.88	15.45	0.08	25.3
5:05	170	6.06	3.76	5.63	-11.06	16.69	0.08	25.6
5:21	180	4.59	3.87	5.75	-12.31	18.07	0.09	25.9
5:36	190	4.22	4.03	5.86	-13.56	19.42	0.09	26.2
5:51	200	4.44	3.83	5.94	-15.10	21.04	0.09	26.7
6:06	210	4.65	3.74	6.00	-16.38	22.38	0.09	27.2
6:22	220	4.83	4.03	6.12	-17.59	23.71	0.09	27.8
6:37	230	4.86	4.12	6.17	-18.66	24.83	0.09	28.3
6:52	240	4.50	4.06	6.18	-19.88	26.06	0.09	28.9
7:07	250	4.58	4.23	6.21	-21.14	27.35	0.09	29.5
7:23	260	4.79	4.17	6.23	-22.23	28.46	0.09	30.1
7:38	270	4.79	4.57	6.27	-23.70	29.97	0.09	30.8
7:53	280	4.83	4.50	6.33	-24.99	31.32	0.09	31.5

VT175

Time h:m	Lifting height mm	Lifting stress		Normal pressure kPa	Aver. Pore water pressure kPa	Effective pressure kPa	Deformation mm	Temp °C
		static kPa	sliding kPa					
0:32	0	0.10	0.28	7.39			0.00	23.6
0:47	10	0.03	0.21	7.28			0.00	23.8
1:02	19	0.05	0.09	7.20	5.50	1.70	0.01	23.8
1:18	29	0.11	0.04	7.12	4.93	2.19	0.03	24.0
1:33	39	0.28	0.22	7.28	4.45	2.84	0.05	24.1
1:48	49	0.54	0.17	7.26	3.89	3.37	0.07	24.3
2:03	58	0.60	0.35	7.17	3.30	3.87	0.08	24.1
2:19	68	0.75	0.44	7.12	2.82	4.30	0.10	24.3
2:34	78	0.98	0.63	7.00	3.11	3.89	0.12	24.5
2:49	88	0.94	0.82	6.93	2.72	4.21	0.15	24.6
3:05	97	1.53	1.27	6.90	2.24	4.66	0.17	24.7
3:20	107	1.77	1.49	6.85	1.85	5.01	0.19	24.7
3:35	117	1.77	1.61	6.81	1.68	5.12	0.20	24.8
3:50	127	2.17	1.88	6.79	1.28	5.50	0.22	24.7
4:06	136	2.35	2.04	6.78	0.87	5.91	0.23	24.6
4:21	146	2.51	2.30	6.80	0.26	6.54	0.25	24.9
4:36	156	2.80	2.48	6.83	-0.42	7.25	0.26	25.0
4:51	165	3.44	3.15	6.90	-1.07	7.96	0.27	25.1
5:07	175	4.44	4.14	6.99	-1.67	8.66	0.27	25.3
5:22	186	6.26	5.34	7.09	-3.05	10.14	0.28	25.5
5:37	196	7.83	6.32	7.24	-4.26	11.51	0.29	25.8
5:52	206	9.94	6.78	7.43	-7.00	14.43	0.29	26.1
6:08	215	11.04	5.53	7.59	-10.57	18.17	0.30	26.4
6:23	225	10.32	4.43	7.76	-15.97	23.72	0.31	26.8
6:38	235	7.85	4.47	7.90	-22.24	30.14	0.31	27.2
6:53	245	6.57	3.92	8.02	-32.33	40.35	0.31	27.6
7:09	254	4.71	3.59	8.10	-29.60	37.70	0.32	28.1
7:24	264	4.17	3.61	8.18	-29.65	37.83	0.32	28.6
7:39	274	4.10	3.58	8.22	-33.91	42.13	0.32	29.2
7:54	283	3.84	3.34	8.25	-37.06	45.32	0.33	29.7
8:10	293	3.83	3.49	8.28	-39.37	47.65	0.33	30.3

VT176

Time h:m	Lifting height mm	Lifting stress		Normal pressure kPa	Aver. Pore water pressure kPa	Effective pressure kPa	Deformation mm	Temp °C
		static kPa	sliding kPa					
0:27	0	2.27	1.58	7.53			0.00	23.2
0:43	10	2.05	1.73	7.42			0.26	23.8
0:58	19	2.06	1.73	7.27	6.16	1.11	0.31	24.2
1:13	29	2.16	1.89	7.16	5.67	1.49	0.33	24.3
1:28	39	2.35	2.06	7.10	5.19	1.91	0.35	24.5
1:44	48	2.43	2.22	6.99	4.71	2.28	0.37	24.5
1:59	58	2.37	2.22	6.98	4.27	2.71	0.40	24.6
2:14	68	2.62	2.34	6.83	3.89	2.94	0.40	24.7
2:30	78	2.96	2.69	6.68	3.01	3.67	0.42	24.7
2:45	87	3.25	3.12	6.56	2.62	3.94	0.43	24.6
3:00	97	3.68	3.29	6.48	2.41	4.07	0.44	24.5
3:15	107	4.06	3.44	6.37	2.18	4.19	0.44	24.6
3:31	117	4.17	3.59	6.25	1.90	4.35	0.45	24.5
3:46	126	4.40	3.78	6.21	1.64	4.57	0.46	24.3
4:01	136	4.11	3.78	6.06	1.17	4.89	0.46	24.5
4:16	146	4.52	3.82	6.01	0.72	5.28	0.47	24.6
4:32	156	4.52	4.42	6.02	0.30	5.72	0.49	24.8
4:47	166	5.23	4.36	6.03	-0.15	6.18	0.49	24.8
5:02	176	6.16	4.84	6.10	-0.74	6.84	0.45	25.0
5:17	186	6.67	5.14	6.29	-1.37	7.66	0.47	25.1
5:33	196	6.81	5.62	6.54	-2.11	8.66	0.46	25.3
5:48	205	7.67	6.89	6.83	-3.10	9.93	0.47	25.5
6:03	215	9.65	6.74	7.20	-4.39	11.59	0.47	25.8
6:18	225	11.43	7.70	7.71	-5.52	13.23	0.47	26.1
6:34	234	11.70	7.71	8.36	-7.33	15.69	0.47	26.5
6:49	243	11.98	7.76	8.76	-10.55	19.31	0.47	26.9
7:04	253	11.86	6.26	8.99	-17.27	26.26	0.47	27.1
7:20	263	9.45	5.96	9.88	-24.51	34.38	0.48	27.5
7:22	273	6.84	6.56	9.88	-24.68	34.56	0.48	27.7

VT177

Time	Lifting height	Lifting stress		Normal pressure	Aver. Pore water pressure	Effective pressure	Deformation	Temp
h:m	mm	static kPa	sliding kPa	kPa	kPa	kPa	mm	°C
0:23	0	2.27	1.92	7.97			0.00	23.4
0:38	10	2.28	1.90	7.86			0.03	23.9
0:54	20	2.33	2.03	7.73	6.12	1.61	0.04	24.2
1:09	30	2.22	2.03	7.62	5.67	1.95	0.03	24.4
1:24	40	2.44	2.06	7.46	5.22	2.24	0.04	24.5
1:40	49	2.36	2.05	7.36	4.78	2.58	0.03	24.6
1:55	59	2.44	2.27	7.34	4.43	2.91	0.04	24.7
2:10	69	2.53	2.34	7.13	4.05	3.08	0.04	24.7
2:26	78	2.59	2.52	6.90	2.89	4.01	0.04	24.7
2:41	87	2.87	2.87	6.83	3.14	3.69	0.06	24.7
2:56	97	3.39	3.03	6.78	2.07	4.71	0.07	24.8
3:12	107	3.31	3.16	6.62	1.65	4.97	0.06	24.8
3:27	117	3.94	3.79	6.67	1.34	5.34	0.06	24.9
3:42	127	4.51	3.97	6.68	0.73	5.96	0.06	24.9
3:57	136	4.43	4.12	6.49	0.24	6.25	0.06	25.0
4:13	146	4.48	4.20	6.53	-0.13	6.65	0.07	25.0
4:28	156	4.90	4.53	6.49	-0.51	7.00	0.07	25.1
4:43	166	5.30	4.76	6.47	-0.98	7.44	0.09	25.1
4:59	176	5.86	5.11	6.49	-1.54	8.03	0.09	25.2
5:14	186	6.42	5.35	6.68	-2.11	8.79	0.10	25.3
5:29	196	7.17	5.47	7.18	-2.76	9.93	0.10	25.5
5:44	206	8.24	6.01	7.56	-3.51	11.06	0.09	25.6
6:00	215	9.50	7.05	7.80	-4.56	12.37	0.09	25.8
6:15	225	10.90	8.41	8.63	-5.99	14.62	0.09	26.0
6:30	234	12.21	8.49	9.29	-7.88	17.16	0.09	26.3
6:46	243	13.09	8.71	10.38	-10.41	20.79	0.09	26.6
7:01	253	13.40	8.53	11.06	-13.76	24.82	0.09	27.0
7:16	263	12.44	7.90	11.74	-16.41	28.15	0.09	27.3
7:31	273	11.65	8.92	12.69	-25.83	38.51	0.09	27.8
7:47	282	11.32	8.62	14.09	-34.01	48.10	0.09	28.3
8:02	292	11.19	9.61	15.30	-41.17	56.47	0.10	28.8
8:17	302	10.88	9.66	15.78	-52.16	67.94	0.10	29.4
8:33	311	10.98	9.96	16.08	-61.71	77.79	0.10	30.0

VT180

Time h:m	Lifting height mm	Lifting stress		Normal pressure kPa	Aver. Pore water pressure kPa	Effective pressure kPa	Deformation mm	Temp °C
		static kPa	sliding kPa					
0:40	0	0.82	0.00	6.85			0.00	24.6
0:55	9	0.46	0.06	6.79	6.73	0.05	0.03	25.0
1:10	20	0.48	0.29	6.71	6.34	0.37	0.15	25.1
1:25	29	0.85	0.41	6.68	5.77	0.91	0.22	25.2
1:41	39	0.80	0.80	6.77	5.54	1.23	0.21	25.3
1:56	48	0.84	0.77	6.71	5.06	1.65	0.18	25.4
2:11	58	0.89	0.57	6.67	4.63	2.04	0.28	25.4
2:27	68	1.12	0.62	6.67	4.14	2.54	0.34	25.4
2:42	77	1.31	0.88	6.66	3.72	2.95	0.39	25.4
2:57	87	1.15	0.83	6.61	3.36	3.25	0.48	25.4
3:13	97	1.70	1.27	6.61	2.74	3.87	0.50	25.5
3:28	106	1.98	1.49	6.62	2.40	4.22	0.56	25.7
3:43	116	2.17	2.07	6.59	2.30	4.29	0.60	25.4
3:58	126	2.19	2.04	6.59	1.96	4.63	0.62	25.4
4:14	135	2.41	2.07	6.58	1.72	4.86	0.64	25.5
4:29	146	2.46	1.98	6.58	1.50	5.09	0.65	25.5
4:44	156	2.53	2.27	6.58	1.07	5.52	0.65	25.6
5:00	165	2.60	2.39	6.62	0.73	5.89	0.69	25.8
5:15	175	3.13	2.71	6.63	0.42	6.22	0.68	25.3
5:30	185	3.59	3.19	6.66	-0.18	6.84	0.67	25.6
5:46	194	4.20	3.66	6.72	-0.74	7.46	0.65	25.8
6:01	204	5.24	4.43	6.78	-1.45	8.22	0.61	26.0
6:16	213	6.28	5.08	6.85	-2.42	9.26	0.58	26.2
6:32	223	7.63	5.49	6.94	-3.75	10.69	0.53	26.5
6:47	232	8.61	5.37	7.03	-6.65	13.68	0.47	26.8
7:02	242	8.54	4.77	7.12	-12.03	19.15	0.40	27.1
7:17	252	7.14	4.16	7.20	-18.34	25.54	0.31	27.5
7:33	261	5.72	3.47	7.28	-25.76	33.04	0.20	27.9
7:48	271	4.65	2.95	7.34	-34.08	41.42	0.11	28.3
8:03	281	3.22	3.16	7.42	-33.97	41.39	0.04	28.8

VT181

Time h:m	Lifting height mm	Lifting stress		Normal pressure kPa	Aver. Pore water pressure kPa	Effective pressure kPa	Deformation mm	Temp °C
		static kPa	sliding kPa					
0:27	0	0.56	0.33	7.52			0.00	23.7
0:42	11	0.85	0.47	7.45			0.00	24.3
0:57	20	0.99	0.67	7.42	6.64	0.78	0.00	24.6
1:12	30	1.15	0.82	7.35	6.20	1.15	0.00	24.8
1:28	40	1.24	0.93	7.30	5.78	1.51	0.06	24.9
1:43	49	1.29	1.28	7.38	5.30	2.09	0.06	24.9
1:58	59	1.32	1.23	7.38	4.91	2.47	0.06	25.0
2:13	69	1.60	1.41	7.26	4.32	2.93	0.06	25.1
2:29	78	1.72	1.43	7.14	3.89	3.25	0.06	25.0
2:44	88	2.14	1.95	7.03	3.60	3.43	0.07	25.0
2:59	98	2.44	2.10	6.93	2.73	4.20	0.07	25.1
3:15	107	2.90	2.18	6.83	2.38	4.45	0.07	25.1
3:30	117	2.80	2.26	6.73	2.16	4.57	0.12	25.1
3:45	127	3.19	2.91	6.64	1.75	4.89	0.13	25.2
4:01	137	3.74	3.29	6.56	1.49	5.06	0.13	25.2
4:16	146	4.09	3.42	6.50	1.02	5.48	0.13	25.3
4:31	156	3.85	3.66	6.49	0.51	5.98	0.12	25.4
4:47	166	3.99	3.44	6.50	-0.01	6.51	0.12	25.4
5:02	176	4.53	4.44	6.56	-0.53	7.09	0.13	25.6
5:17	186	5.03	4.65	6.66	-1.06	7.72	0.12	25.7
5:32	196	6.47	5.33	6.79	-1.66	8.45	0.13	25.8
5:48	206	7.88	5.95	6.96	-2.41	9.38	0.13	26.2
6:03	216	9.69	6.70	7.18	-3.63	10.81	0.13	26.4
6:18	226	12.53	7.98	7.44	-5.51	12.95	0.13	26.6
6:34	235	13.47	8.44	7.67	-8.29	15.96	0.13	27.0
6:49	245	13.18	7.41	7.93	-12.45	20.39	0.13	27.3
7:04	255	12.32	6.55	8.04	-16.50	24.54	0.13	27.7
7:20	265	10.00	6.87	8.22	-23.54	31.76	0.13	28.2
7:35	274	7.81	5.73	8.40	-30.16	38.57	0.13	28.7
7:50	284	6.23	5.16	8.54	-39.40	47.94	0.13	29.2
8:05	293	5.53	4.57	8.67	-48.15	56.82	0.13	29.8
8:21	303	5.44	4.86	8.79	-57.48	66.27	0.13	30.3
8:36	313	5.54	5.33	8.86	-65.31	74.17	0.13	31.0
8:51	322	5.78	4.94	8.95	-70.55	79.50	0.13	31.6
9:07	332	6.05	5.48	9.02	-73.56	82.58	0.13	32.2
9:22	342	5.79	5.52	9.07	-75.66	84.73	0.13	33.0
9:37	351	5.78	5.67	9.15	-73.59	82.74	0.13	33.5
9:52	361	5.81	5.36	9.22	-72.71	81.93	0.14	34.2
10:08	371	5.69	5.66	9.28	-58.65	67.94	0.14	34.9
10:23	381	6.02	5.81	9.34	-46.57	55.92	0.14	35.6

VT182

Time h:m	Lifting height mm	Lifting stress		Normal pressure kPa	Aver. Pore water pressure kPa	Effective pressure kPa	Deformation mm	Temp °C
		static kPa	sliding kPa					
0:25	0	0.81	0.52	7.41			0.00	23.1
0:40	10	0.98	0.63	7.37			0.00	23.8
0:56	20	1.04	0.95	7.25	6.51	0.74	0.01	24.1
1:11	30	1.16	1.12	7.18	5.94	1.24	0.01	24.4
1:26	39	1.13	1.13	7.11	5.34	1.77	0.02	24.7
1:42	49	1.38	1.24	7.04	4.98	2.07	0.02	24.2
1:57	58	1.59	1.31	7.05	4.37	2.67	0.02	24.3
2:12	68	1.60	1.60	6.98	4.06	2.91	0.02	24.5
2:28	78	1.61	1.41	6.91	2.94	3.97	0.02	24.6
2:43	88	1.77	1.60	6.80	3.06	3.74	0.02	24.7
2:58	97	1.98	1.60	6.70	2.50	4.20	0.02	24.7
3:14	107	2.21	1.96	6.65	2.22	4.43	0.02	24.8
3:29	116	2.56	2.31	6.60	1.60	5.00	0.02	24.8
3:44	126	2.74	2.56	6.52	1.23	5.29	0.02	24.8
4:00	136	2.75	2.48	6.48	1.02	5.46	0.02	24.9
4:15	146	3.00	2.79	6.39	0.93	5.46	0.03	25.0
4:30	156	3.18	3.04	6.36	0.62	5.75	0.03	25.0
4:45	165	3.39	3.11	6.35	0.33	6.02	0.03	25.0
5:01	175	3.49	3.14	6.36	-0.19	6.56	0.02	25.0
5:16	185	3.84	3.41	6.39	-0.36	6.75	0.03	25.1
5:31	195	4.41	3.65	6.46	-0.62	7.08	0.03	25.2
5:47	205	4.47	3.74	6.55	-1.01	7.56	0.03	25.3
6:02	215	5.34	4.11	6.67	-1.37	8.03	0.03	25.4
6:17	225	5.59	4.97	6.82	-1.84	8.66	0.03	25.5
6:32	234	6.81	5.85	6.97	-2.59	9.56	0.03	25.7
6:48	244	8.56	6.84	7.13	-3.41	10.55	0.03	25.9
7:03	254	10.28	6.77	7.34	-5.61	12.94	0.03	26.1
7:18	264	11.45	7.23	7.55	-5.57	13.12	0.03	26.3
7:34	274	10.17	6.09	7.83	-7.66	15.50	0.03	26.6
7:49	284	8.29	6.04	7.93	-11.10	19.03	0.03	27.0

VT184

Time h:m	Lifting height mm	Lifting stress		Normal pressure kPa	Aver. Pore water pressure kPa	Effective pressure kPa	Deformation mm	Temp °C
		static kPa	sliding kPa					
0:36	0	2.16	1.58	7.43			0.00	22.5
0:51	10	2.12	1.65	7.11			0.09	22.7
1:06	19	1.75	1.23	7.02	5.80	1.22	0.10	22.7
1:22	30	1.53	1.19	6.91	4.65	2.26	0.11	23.1
1:37	40	1.69	1.30	6.83	3.99	2.84	0.11	23.1
1:52	49	1.58	1.34	6.71	3.78	2.93	0.11	23.1
2:08	59	2.01	2.01	6.65	3.30	3.34	0.12	23.1
2:23	68	1.44	1.32	6.58	2.63	3.95	0.13	23.2
2:38	78	1.90	1.90	6.48	2.12	4.36	0.14	23.3
2:54	87	1.85	1.37	6.45	1.50	4.95	0.15	23.4
3:09	97	2.02	1.72	6.46	0.80	5.66	0.16	23.6
3:24	107	2.52	2.10	6.52	0.04	6.47	0.17	23.6
3:40	116	3.21	2.83	6.63	-0.96	7.59	0.18	23.8
3:55	127	3.73	3.53	6.78	-1.93	8.71	0.18	24.0
4:10	137	4.90	4.38	6.97	-2.96	9.92	0.19	24.1
4:26	146	6.45	5.69	7.15	-4.75	11.91	0.19	24.5
4:41	157	8.33	5.64	7.37	-8.11	15.48	0.19	24.8
4:56	166	9.53	5.80	7.61	-12.75	20.36	0.20	25.1
5:12	176	8.89	5.72	7.90	-18.39	26.30	0.20	25.4
5:27	186	8.75	5.12	8.14	-28.27	36.41	0.20	25.8
5:42	196	6.22	4.47	8.36	-41.92	50.28	0.21	26.4
5:57	205	4.91	4.53	8.55	-58.65	67.20	0.21	26.8
6:13	215	5.13	4.76	8.72	-58.60	67.32	0.21	27.4
6:28	224	5.16	4.66	8.85	-63.06	71.91	0.21	28.0
6:43	234	5.42	5.07	8.94	-64.01	72.94	0.21	28.6
6:59	244	5.35	5.21	8.99	-63.85	72.84	0.21	29.2
7:14	253	5.46	5.41	9.07	-63.22	72.29	0.21	29.8
7:29	263	5.60	5.37	9.07	-62.76	71.83	0.21	30.4
7:45	273	5.77	5.50	9.13	-62.25	71.38	0.21	31.0
8:00	282	5.70	5.52	9.22	-61.95	71.17	0.21	31.5
8:15	292	5.90	5.57	9.28	-61.76	71.04	0.21	32.1

VT185

Time	Lifting height	Lifting stress		Normal pressure	Aver. Pore water pressure	Effective pressure	Deformation	Temp
		static	sliding					
h:m	mm	kPa	kPa	kPa	kPa	kPa	mm	°C
0:53	0	2.58	1.60	7.20	6.70	0.50	0.00	23.9
1:09	9	2.06	1.37	7.10	5.96	1.14	0.15	24.1
1:24	19	1.61	1.49	6.98	6.28	0.70	0.16	24.3
1:39	29	2.20	1.69	6.84	5.49	1.35	0.17	24.4
1:55	39	2.23	1.90	6.77	5.09	1.69	0.16	24.3
2:10	48	2.86	2.52	6.73	4.26	2.46	0.17	24.5
2:25	58	2.29	2.29	6.64	3.44	3.19	0.17	24.5
2:41	67	2.12	1.78	6.60	2.34	4.26	0.16	24.6
2:56	77	2.28	1.93	6.58	1.64	4.94	0.16	24.8
3:11	87	2.69	2.34	6.56	1.17	5.39	0.15	25.0
3:27	96	3.34	3.06	6.66	-0.74	7.41	0.15	25.2
3:42	106	4.13	3.35	6.79	-2.07	8.87	0.15	25.4
3:57	117	5.63	4.36	6.94	-3.57	10.52	0.15	25.7
4:13	127	7.32	5.42	7.15	-5.58	12.72	0.15	26.1
4:28	136	8.23	5.96	7.37	-9.19	16.56	0.15	26.6
4:43	146	10.90	6.27	7.62	-15.32	22.93	0.15	27.0
4:58	155	11.53	6.10	7.86	-26.02	33.88	0.15	27.5
5:14	165	9.16	4.72	8.13	-40.39	48.52	0.15	28.0
5:29	175	5.47	4.15	8.37	-47.00	55.37	0.15	28.6
5:44	185	5.30	5.06	8.62	-52.08	60.70	0.15	29.3
6:00	194	5.57	4.97	8.84	-55.84	64.68	0.15	29.8
6:15	204	5.78	5.62	8.99	-54.89	63.87	0.15	30.5
6:30	214	5.94	5.17	9.13	-46.04	55.17	0.15	31.0
6:45	223	5.80	5.35	9.30	-44.00	53.30	0.15	31.7
7:01	233	5.92	5.60	9.38	-42.71	52.09	0.14	32.3
7:16	243	5.99	5.71	9.43	-41.89	51.33	0.14	33.0

VT186

Time h:m	Lifting height mm	Lifting stress		Normal pressure kPa	Aver. Pore water pressure kPa	Effective pressure kPa	Deformation mm	Temp °C
		static kPa	sliding kPa					
0:46	0	2.06	1.41	7.24	5.32	1.92	0.00	25.0
1:01	9	1.79	1.65	7.01	5.30	1.71	0.19	25.2
1:16	19	2.01	1.60	6.89	4.42	2.47	0.27	25.3
1:32	28	1.94	1.67	6.81	3.71	3.11	0.50	25.4
1:47	38	2.43	2.43	6.71	3.22	3.49	0.50	25.5
2:02	48	2.54	2.21	6.64	2.21	4.43	0.51	25.7
2:18	57	2.29	2.07	6.61	1.37	5.24	0.51	25.6
2:33	67	2.27	1.94	6.60	0.20	6.40	0.51	25.7
2:48	77	2.69	2.69	6.62	-1.19	7.82	0.51	25.9
3:04	86	3.50	3.08	6.76	-2.97	9.73	0.51	26.2
3:19	96	4.41	4.15	6.89	-5.13	12.02	0.50	26.5
3:34	107	6.86	5.20	7.02	-8.61	15.64	0.50	26.7
3:50	117	9.09	7.43	7.21	-15.37	22.57	0.50	27.1
4:05	127	13.34	7.42	7.44	-30.63	38.07	0.50	27.5
4:20	135	20.53	5.95	7.55	-51.20	58.75	0.50	28.1
4:36	144	11.93	4.13	7.86	-65.73	73.59	0.50	28.9
4:51	155	4.85	4.52	8.10	-73.38	81.48	0.50	28.7
5:06	165	4.79	4.69	8.35	-76.65	85.00	0.50	29.6
5:21	174	5.26	5.12	8.59	-72.59	81.18	0.49	30.0
5:37	184	5.49	4.89	8.78	-60.01	68.79	0.49	30.6
5:52	194	5.62	5.20	8.97	-49.86	58.82	0.49	31.0
6:07	204	5.83	5.22	9.12	-43.46	52.58	0.49	31.7
6:23	213	5.95	5.95	9.18	-40.24	49.42	0.49	32.4
6:38	223	6.20	5.86	9.24	-37.65	46.89	0.49	33.0
6:53	233	6.09	5.36	9.39	-34.87	44.26	0.48	33.9
7:09	242	5.90	5.39	9.42	-31.42	40.84	0.48	34.5
7:24	252	5.95	5.39	9.50	-27.71	37.20	0.48	35.3

VT187

Time h:m	Lifting height mm	Lifting stress		Normal pressure kPa	Aver. Pore water pressure kPa	Effective pressure kPa	Deformation mm	Temp °C
		static kPa	sliding kPa					
0:42	0	2.11	1.35	6.93			0.00	24.2
0:57	11	1.71	1.22	6.76	4.95	1.81	0.09	24.5
1:12	20	1.73	1.36	6.66	4.77	1.88	0.10	24.7
1:28	30	2.00	1.30	6.54	3.89	2.66	0.10	24.9
1:43	40	2.79	2.11	6.47	2.96	3.50	0.10	25.0
1:58	49	2.44	2.00	6.37	2.30	4.07	0.11	25.1
2:14	58	2.51	2.51	6.34	1.13	5.22	0.11	25.1
2:29	68	2.41	2.09	6.35	0.10	6.25	0.11	25.3
2:44	77	2.49	2.49	6.38	-1.19	7.58	0.11	25.5
3:00	87	3.17	3.04	6.48	-2.62	9.10	0.11	25.7
3:15	97	4.03	4.03	6.65	-4.32	10.97	0.11	25.8
3:30	108	5.88	4.43	6.79	-6.47	13.27	0.11	26.1
3:45	117	7.28	5.39	7.01	-11.33	18.34	0.11	26.5
4:01	127	9.34	6.52	7.20	-20.11	27.31	0.10	26.7
4:16	137	11.84	6.68	7.36	-33.26	40.61	0.10	27.1
4:31	146	11.45	4.79	7.60	-50.14	57.74	0.11	27.6
4:47	156	5.88	4.85	7.88	-68.08	75.96	0.11	28.1
5:02	166	5.18	5.02	8.10	-79.21	87.31	0.11	28.7
5:17	176	5.28	5.02	8.32	-64.95	73.27	0.10	29.2
5:32	185	5.51	5.46	8.53	-63.13	71.65	0.10	29.9
5:48	195	5.91	5.27	8.69	-60.14	68.84	0.10	30.5
6:03	204	5.76	5.40	8.86	-58.51	67.37	0.10	31.1
6:18	214	6.06	5.75	9.00	-58.43	67.42	0.10	31.8
6:33	224	6.11	5.62	9.12	-57.88	67.01	0.09	32.4
6:49	233	6.18	5.71	9.22	-57.19	66.41	0.09	33.1
7:04	243	6.13	5.64	9.35	-56.27	65.62	0.09	33.7
7:19	253	6.20	5.37	9.41	-55.13	64.54	0.09	34.3

VT188

Time h:m	Lifting height mm	Lifting stress		Normal pressure kPa	Aver. Pore water pressure kPa	Effective pressure kPa	Deformation mm	Temp °C
		static kPa	sliding kPa					
0:33	0	0.34	0.04	6.93			0.00	22.5
0:48	11	0.37	0.36	6.82			0.01	22.9
1:04	20	0.60	0.18	6.73	6.73	0.00	0.01	23.1
1:19	29	0.54	0.46	6.63	6.59	0.04	0.02	23.2
1:34	39	0.65	0.32	6.89	6.81	0.08	0.02	23.3
1:50	48	0.89	0.45	6.84	6.38	0.46	0.14	23.4
2:05	58	0.90	0.78	6.74	6.46	0.28	0.14	23.4
2:20	68	0.92	0.87	6.63	6.01	0.63	0.14	23.6
2:36	77	1.12	0.96	6.52	5.66	0.86	0.15	23.7
2:51	87	1.39	0.90	6.43	5.14	1.29	0.15	23.6
3:06	97	1.51	1.33	6.34	4.74	1.60	0.15	23.7
3:21	106	1.87	1.33	6.25	4.17	2.07	0.15	23.8
3:37	116	2.36	1.79	6.14	3.96	2.18	0.16	23.9
3:52	126	2.36	1.80	6.06	3.53	2.54	0.17	23.9
4:07	135	2.59	1.87	5.98	3.07	2.91	0.19	24.0
4:23	145	2.80	2.34	5.92	3.04	2.88	0.20	24.0
4:38	155	3.52	2.81	5.88	2.73	3.15	0.20	24.1
4:53	165	3.61	3.40	5.88	1.65	4.24	0.20	24.2
5:08	175	3.54	3.54	5.89	0.90	4.99	0.21	24.4
5:24	185	3.85	3.60	5.95	0.14	5.81	0.21	24.6
5:39	195	4.51	3.75	6.04	-0.61	6.65	0.22	24.8
5:54	205	5.15	3.99	6.14	-1.40	7.54	0.22	25.0
6:09	214	5.96	4.85	6.24	-2.50	8.75	0.22	25.2
6:25	224	7.28	5.86	6.38	-4.07	10.46	0.22	25.4
6:40	234	8.80	6.25	6.53	-5.94	12.47	0.22	25.7
6:55	243	10.55	5.83	6.72	-9.11	15.83	0.22	25.9
7:11	253	10.24	6.10	6.94	-14.15	21.09	0.22	26.2
7:26	263	9.62	4.80	7.13	-19.93	27.06	0.22	26.6
7:41	272	7.55	4.58	7.30	-15.64	22.94	0.22	27.1
7:56	282	5.45	4.22	7.50	-18.76	26.26	0.22	27.5
8:12	292	4.53	4.15	7.68	-22.02	29.70	0.22	28.1

VT190

Time h:m	Lifting height mm	Lifting stress		Normal pressure kPa	Aver. Pore water pressure kPa	Effective pressure kPa	Deformation mm	Temp °C
		static kPa	sliding kPa					
0:34	0	0.47	0.05	7.14			0.00	21.0
0:49	10	0.36	0.04	7.01			0.01	23.2
1:04	19	0.49	0.26	6.88	6.87	0.01	0.02	23.5
1:20	30	0.65	0.21	6.80	6.46	0.34	0.02	23.7
1:35	40	0.68	0.43	6.80	5.95	0.85	0.03	23.7
1:50	49	0.78	0.39	6.90	5.28	1.62	0.03	23.7
2:06	58	0.86	0.49	6.73	4.96	1.78	0.03	23.8
2:21	68	0.91	0.55	6.63	4.50	2.13	0.03	23.8
2:36	77	1.01	0.80	6.49	3.80	2.69	0.04	23.9
2:52	87	1.21	0.79	6.40	3.39	3.01	0.05	23.9
3:07	96	1.59	0.95	6.21	3.08	3.13	0.06	24.0
3:22	105	1.80	1.20	6.12	2.77	3.35	0.07	24.2
3:38	115	1.88	1.44	6.06	2.48	3.58	0.13	24.3
3:53	124	1.79	1.51	6.00	1.72	4.28	0.13	24.4
4:08	134	2.59	1.70	5.90	2.02	3.88	0.13	24.5
4:23	144	2.62	2.04	5.88	1.17	4.71	0.13	24.7
4:39	153	2.80	2.26	5.90	0.68	5.22	0.13	24.8
4:54	163	3.17	2.89	5.95	0.07	5.87	0.13	24.9
5:09	173	3.62	3.62	6.03	-0.55	6.58	0.13	25.1
5:25	183	5.15	4.01	6.13	-1.20	7.33	0.13	25.3
5:40	192	6.17	5.15	6.22	-2.32	8.53	0.13	25.6
5:55	202	9.04	6.96	6.35	-3.78	10.13	0.13	26.0
6:10	212	12.19	9.00	6.44	-5.79	12.23	0.13	26.3
6:26	221	15.41	9.40	6.35	-11.04	17.40	0.13	26.6
6:41	230	15.47	8.40	6.57	-19.63	26.20	0.14	27.0
6:56	240	19.06	8.46	6.72	-27.74	34.46	0.14	27.2
7:11	250	15.88	6.96	7.16	-37.21	44.37	0.14	27.5
7:27	260	13.83	3.97	7.28	-44.87	52.15	0.14	27.9
7:42	270	4.55	4.05	7.49	-47.45	54.94	0.13	28.3
7:57	280	4.54	4.16	7.61	-43.47	51.08	0.13	28.8
8:13	289	4.57	3.97	7.74	-46.20	53.93	0.13	29.6

VT191

Time h:m	Lifting height mm	Lifting stress		Normal pressure kPa	Aver. Pore water pressure kPa	Effective pressure kPa	Deformation mm	Temp °C
		static kPa	sliding kPa					
1:09	0	0.83	0.33	5.82	5.77	0.05	0.00	25.6
1:25	9	0.75	0.70	5.65	5.45	0.20	0.01	25.8
1:40	19	0.91	0.53	5.52	4.70	0.83	0.01	25.9
1:55	29	1.12	0.87	5.53	3.96	1.57	0.06	25.9
2:11	39	1.43	0.91	5.33	3.22	2.11	0.07	25.9
2:26	48	1.83	0.99	5.21	2.47	2.74	0.09	26.0
2:41	57	2.07	1.37	5.09	2.39	2.70	0.10	26.1
2:57	67	2.00	1.38	4.98	1.36	3.62	0.12	26.2
3:12	77	2.37	1.80	4.88	1.42	3.46	0.13	26.3
3:27	86	2.91	2.55	4.80	1.19	3.60	0.15	26.3
3:42	96	3.27	2.40	4.74	0.87	3.87	0.16	26.5
3:58	106	3.14	2.56	4.73	0.33	4.41	0.18	26.6
4:13	116	3.20	2.41	4.78	-0.20	4.97	0.18	26.7
4:28	125	3.58	3.00	4.85	-0.76	5.62	0.19	27.0
4:44	136	4.65	4.00	4.95	-1.58	6.53	0.19	27.2
4:59	146	6.73	5.77	5.07	-3.09	8.16	0.20	27.5
5:14	155	8.46	7.03	5.19	-5.91	11.10	0.20	27.8
5:29	165	11.94	8.11	5.30	-10.55	15.86	0.21	28.1
5:45	174	17.78	8.61	5.46	-17.22	22.68	0.21	28.6
6:00	183	16.98	6.29	5.71	-27.34	33.05	0.21	29.1
6:15	194	12.55	3.85	5.96	-38.87	44.83	0.22	29.4
6:30	204	4.35	3.36	6.19	-50.49	56.68	0.22	29.9
6:46	214	3.82	3.60	6.41	-61.04	67.45	0.22	30.7
7:01	223	3.90	3.80	6.57	-69.72	76.28	0.22	31.5
7:16	233	4.00	3.83	6.70	-75.53	82.23	0.22	32.4
7:32	243	4.15	4.03	6.84	-79.37	86.21	0.22	33.3
7:47	252	4.26	4.12	6.95	-81.44	88.39	0.22	34.2

VT192

Time h:m	Lifting height mm	Lifting stress		Normal pressure kPa	Aver. Pore water pressure kPa	Effective pressure kPa	Deformation mm	Temp °C
		static kPa	sliding kPa					
0:42	0	1.47	0.92	7.65			0.00	24.2
0:58	10	1.09	0.96	7.53			0.02	24.5
1:13	20	0.96	0.95	7.63	6.91	0.72	0.02	24.7
1:28	30	1.08	0.67	7.55	6.12	1.43	0.42	24.7
1:44	41	0.96	0.51	7.48	5.00	2.48	0.40	24.8
1:59	52	1.05	0.84	7.42	4.68	2.74	0.40	24.8
2:14	62	1.19	0.88	7.34	4.31	3.03	0.41	24.8
2:30	72	1.17	0.79	7.32	4.09	3.23	0.41	24.9
2:45	81	1.27	1.27	7.28	3.76	3.52	0.42	25.0
3:00	91	1.47	1.34	7.18	3.38	3.80	0.42	24.9
3:15	100	1.93	1.53	7.12	2.95	4.17	0.42	25.1
3:31	110	1.97	1.59	7.08	2.67	4.41	0.42	25.0
3:46	120	2.34	2.34	7.04	2.14	4.91	0.43	25.0
4:01	129	2.36	1.98	7.02	1.51	5.51	0.42	25.0
4:17	139	2.34	2.05	7.00	1.07	5.93	0.43	25.1
4:32	149	2.64	2.38	7.02	0.22	6.79	0.43	25.3
4:47	159	2.98	2.61	7.06	-0.61	7.67	0.44	25.4
5:02	168	3.26	2.94	7.14	-1.58	8.72	0.43	25.5
5:18	176	4.20	3.68	7.27	-2.37	9.64	0.43	25.7
5:33	183	5.44	4.47	7.41	-3.61	11.02	0.43	25.9
5:48	193	6.68	5.62	7.55	-6.07	13.62	0.43	26.1
6:04	203	7.86	6.58	7.71	-10.69	18.39	0.43	26.3
6:19	212	9.66	6.47	7.90	-16.99	24.90	0.43	26.4
6:34	222	11.94	5.45	8.09	-27.29	35.39	0.43	26.8
6:50	232	11.64	5.31	8.31	-38.79	47.10	0.43	27.0
7:05	241	7.87	5.25	8.51	-50.66	59.17	0.42	27.7
7:20	251	6.18	4.66	8.72	-60.64	69.36	0.42	28.1
7:35	261	5.39	5.01	8.91	-69.02	77.93	0.42	28.6

VT194

Time h:m	Lifting height mm	Lifting stress		Normal pressure kPa	Aver. Pore water pressure kPa	Effective pressure kPa	Deformation mm	Temp °C
		static kPa	sliding kPa					
1:03	0	2.49	1.87	7.93	4.66	3.27	0.00	25.9
1:18	10	2.46	1.70	7.81	4.41	3.40	0.10	26.0
1:33	19	2.49	1.75	7.70	3.65	4.05	0.13	26.2
1:49	30	2.24	1.92	7.61	2.85	4.76	0.15	26.1
2:04	39	2.50	1.78	7.51	2.07	5.44	0.16	26.3
2:19	49	2.75	2.44	7.43	1.80	5.64	0.23	26.4
2:35	59	2.57	2.31	7.39	0.88	6.51	0.23	26.6
2:50	68	3.01	3.01	7.40	0.07	7.33	0.23	26.7
3:05	78	4.00	4.00	7.51	-0.61	8.12	0.23	27.0
3:21	88	6.15	5.25	7.67	-1.58	9.25	0.23	27.2
3:36	98	9.64	6.50	7.84	-4.17	12.01	0.23	27.8
3:51	108	16.34	9.48	8.49	-9.78	18.26	0.23	27.7
4:06	116	21.62	9.83	8.40	-21.58	29.98	0.24	28.0
4:22	125	26.20	11.34	8.61	-32.97	41.58	0.24	28.3
4:37	135	24.50	8.07	8.65	-26.49	35.15	0.24	28.7
4:52	145	14.66	4.17	8.65	-29.56	38.21	0.23	29.3
5:08	156	5.60	5.34	8.87	-30.68	39.55	0.23	29.9
5:23	166	5.92	5.79	9.09	-31.06	40.15	0.23	30.7
5:38	175	6.31	6.14	9.26	-31.06	40.32	0.23	31.2
5:54	185	6.26	5.67	9.44	-28.82	38.25	0.23	31.7
6:09	195	6.38	6.14	9.55	-23.57	33.12	0.23	32.5
6:24	204	6.65	6.37	9.64	-17.77	27.41	0.23	33.1
6:40	214	6.89	6.60	9.76	-11.83	21.59	0.22	33.8
6:55	224	7.32	6.93	9.84	-6.41	16.25	0.22	34.7
7:10	233	7.27	6.72	9.93	-3.25	13.18	0.22	35.6
7:26	243	7.29	6.27	10.02	-1.88	11.90	0.22	36.4
7:41	253	7.16	6.60	10.08	-1.40	11.48	0.22	37.2

VT200 (reference for 3-layer tests)

Time h:m	Lifting height mm	Lifting stress		Normal pressure kPa	Pore water pressure				Effective pressure kPa	Deformation mm	Temp °C
		static kPa	sliding kPa		no.1 kPa	no.2 kPa	no.3 kPa	no.4 kPa			
0:53	0	0.17	-0.34	7.37	2.54	6.20			1.17	0.00	25.1
1:09	10	0.19	0.01	7.30	2.56	6.28			1.02	0.01	25.0
1:24	20	0.33	0.01	7.24	2.54	6.23			1.01	0.01	24.9
1:39	30	0.35	0.16	7.30	2.62	6.48			0.82	0.03	24.9
1:55	40	0.35	0.15	7.22	2.71	6.19			1.04	0.03	24.7
2:10	50	0.67	0.20	7.13	2.61	6.13			1.00	0.04	25.0
2:25	60	0.71	0.43	7.06	2.60	6.06			1.00	0.05	25.0
2:41	70	0.95	0.63	6.97	2.54	6.05			0.92	0.05	25.2
2:56	80	1.88	0.70	6.89	2.48	5.87			1.02	0.06	25.3
3:11	90	1.22	0.99	6.81	2.45	5.77			1.04	0.10	25.4
3:26	100	1.67	1.24	6.75	2.44	5.62			1.13	0.11	25.7
3:42	110	1.84	1.70	6.66	2.43	5.56			1.11	0.15	25.4
3:57	120	1.81	1.51	6.59	2.37	5.35			1.24	0.18	25.5
4:12	130	1.96	1.85	6.54	2.25	5.25			1.29	0.21	25.6
4:28	140	2.62	2.14	6.46	2.14	5.05			1.42	0.23	25.7
4:43	150	2.74	2.25	6.42	1.99	4.66			1.76	0.25	25.8
4:58	160	2.92	2.91	6.40	1.67	4.04			2.36	0.27	25.9
5:14	170	2.99	2.59	6.39	1.28	3.16			3.22	0.29	26.0
5:29	180	3.19	2.44	6.43	0.62	1.73			4.70	0.29	26.1
5:44	190	4.00	3.28	6.45	-0.05	0.23			6.22	0.29	26.2
5:59	200	5.33	4.60	6.50	-0.87	-1.48			7.97	0.29	26.4
6:15	210	7.45	6.20	6.55	-2.02	-3.69			10.24	0.29	26.4
6:30	220	9.73	5.97	6.55	-3.82	-6.73			13.28	0.29	26.7
6:45	230	10.32	6.34	6.56	-6.24	-10.31			16.87	0.29	26.9
7:01	240	9.94	6.30	6.61	-9.11	-14.40			21.00	0.29	27.3
7:16	250	8.13	5.18	6.86	-12.46	-18.51			25.37	0.29	27.6
7:31	260	7.04	4.29	6.84	-19.70	-24.32			31.17	0.29	28.1
7:46	270	5.81	3.62	6.92	-31.20	-31.92			38.84	0.29	28.4
8:02	280	3.64	3.31	6.99	-42.57	-33.10			40.09	0.29	29.0
8:17	290	3.75	3.20	7.11	-52.59	-26.82			33.93	0.29	29.5
8:32	300	3.89	3.89	7.21	-61.08	-23.48			30.69	0.29	30.1

VT201

Time	Lifting height	Lifting stress		Normal pressure	Aver. Pore water pressure	Effective pressure	Deformation	Temp
h:m	mm	static kPa	sliding kPa	kPa	kPa	kPa	mm	°C
0:55	0	2.30	1.90	5.63	4.42	1.20	0.00	24.4
0:58	10	1.68	1.27	5.50	4.21	1.30	0.23	24.4
1:26	20	2.54	1.93	5.08	2.35	2.73	0.49	24.5
1:56	30	3.39	2.81	4.82	1.30	3.52	0.48	24.6
2:26	40	4.04	3.24	4.63	0.85	3.78	0.48	24.6
2:57	50	3.87	3.31	4.54	-0.30	4.84	0.49	24.7
3:27	60	3.69	3.24	4.51	-1.19	5.69	0.50	24.6
3:58	70	3.43	3.34	4.48	-2.23	6.72	0.51	25.2
4:28	80	4.13	3.49	4.51	-3.24	7.75	0.51	25.7
4:59	90	5.71	4.74	4.58	-4.32	8.90	0.51	26.3
5:29	100	8.22	5.16	4.67	-5.41	10.08	0.51	27.1
5:59	110	8.04	4.16	4.76	-6.45	11.21	0.51	28.0
6:30	120	5.47	2.38	4.85	-7.69	12.54	0.51	29.1
7:00	130	3.25	2.50	4.94	-9.05	13.98	0.51	30.5

VT202

Time h:m	Lifting height mm	Lifting stress		Normal pressure kPa	Aver. Pore water pressure kPa	Effective pressure kPa	Deformation mm	Temp °C
		static kPa	sliding kPa					
0:47	0	2.23	2.23	5.81	4.81	1.00	0.00	24.2
1:11	10	2.66	2.23	5.25	3.06	2.19	0.50	24.5
1:35	20	2.94	2.94	4.98	1.85	3.13	0.51	24.8
1:59	30	4.34	3.40	4.77	1.14	3.64	0.62	25.0
2:23	40	4.37	3.96	4.63	0.55	4.08	0.69	25.2
2:47	50	4.37	3.64	4.55	-0.37	4.93	0.72	25.2
3:12	60	4.30	3.68	4.53	-1.07	5.60	0.72	25.2
3:36	70	3.96	3.49	4.52	-1.94	6.47	0.73	25.5
4:00	80	5.00	3.78	4.55	-2.75	7.30	0.76	25.7
4:24	90	5.92	4.19	4.61	-3.78	8.39	0.78	25.9
4:48	100	6.68	3.73	4.65	-4.87	9.52	0.79	26.1
5:12	110	7.06	3.95	4.71	-6.03	10.74	0.79	26.5
5:36	120	6.37	2.60	4.79	-7.12	11.91	0.79	27.0
6:00	130	3.96	2.19	4.86	-8.14	13.01	0.79	27.5
6:24	140	2.67	2.41	4.95	-9.22	14.17	0.80	28.3
6:48	150	2.63	2.31	5.08	-10.53	15.61	0.79	29.5

VT205

Time h:m	Lifting height mm	Lifting stress		Normal pressure kPa	Aver. Pore water pressure kPa	Effective pressure kPa	Deformation mm	Temp °C
		static kPa	sliding kPa					
0:56	0	0.02	0.00	7.36	7.31	0.06	0.00	24.2
1:11	10	0.17	-0.05	7.31	7.26	0.05	0.01	24.5
1:27	20	0.44	0.01	7.47	7.38	0.09	0.02	24.7
1:42	30	0.30	0.01	7.54	7.28	0.26	0.63	25.1
1:58	40	0.38	0.13	7.42	6.91	0.51	0.66	25.1
2:13	50	0.44	0.42	7.36	6.39	0.97	0.68	25.1
2:29	60	0.52	0.21	7.26	5.20	2.07	0.70	25.2
2:45	70	0.52	0.35	7.17	5.15	2.02	0.73	25.2
3:00	80	0.66	0.42	7.14	4.38	2.76	0.75	25.1
3:16	90	0.74	0.53	7.06	4.29	2.77	0.77	25.1
3:31	100	0.89	0.69	7.05	3.82	3.23	0.80	25.1
3:47	110	1.09	0.96	7.02	3.45	3.57	0.82	25.1
4:02	120	1.38	1.21	6.95	3.31	3.63	0.86	25.1
4:18	130	1.46	1.28	6.90	2.87	4.03	0.90	25.2
4:33	140	1.58	1.27	6.88	2.58	4.31	0.92	25.2
4:49	150	1.41	1.39	6.86	2.38	4.48	0.95	25.1
5:04	160	1.70	1.40	6.86	1.98	4.88	0.98	25.2
5:20	170	1.91	1.78	6.91	1.66	5.25	0.99	25.2
5:35	180	2.55	2.55	6.87	1.06	5.81	1.00	25.2
5:51	190	2.70	2.57	6.92	0.44	6.48	1.01	25.3
6:06	200	3.13	2.86	6.97	-0.41	7.38	1.01	25.4
6:22	210	4.14	3.67	7.04	-1.37	8.42	1.01	25.5
6:37	220	5.43	4.94	7.13	-2.53	9.66	1.02	25.6
6:53	230	7.61	5.81	7.22	-4.12	11.35	1.02	25.8
7:08	240	9.49	6.19	7.34	-6.23	13.58	1.02	26.0
7:24	250	10.51	6.45	7.41	-9.88	17.29	1.02	26.3
7:39	260	10.72	6.69	7.46	-15.21	22.66	1.02	26.6
7:55	270	12.24	6.75	7.54	-22.68	30.22	1.03	26.9
8:11	280	10.12	4.77	7.62	-32.93	40.56	1.03	27.3
8:26	290	6.19	3.79	7.77	-44.76	52.52	1.04	27.8
8:42	300	5.33	3.65	7.98	-54.08	62.06	1.04	28.8
8:52	310	4.00	3.76	7.98	-59.14	67.12	1.04	29.4

VT206

Time h:m	Lifting height mm	Lifting stress		Normal pressure kPa	Aver. Pore water pressure kPa	Effective pressure kPa	Deformation mm	Temp °C
		static kPa	sliding kPa					
0:37	0	0.35	0.30	7.32			0.00	21.1
0:52	10	0.00	0.25	7.26	7.26	0.00	0.04	24.0
1:08	20	0.29	-0.04	7.19	6.99	0.20	0.07	24.7
1:24	30	0.24	0.24	7.09	6.60	0.49	0.08	24.8
1:39	40	0.51	0.30	7.08	6.20	0.88	0.09	24.8
1:55	50	0.42	0.17	6.98	5.79	1.19	0.10	24.8
2:10	60	0.64	0.34	6.90	5.36	1.54	0.11	24.8
2:26	70	0.88	0.47	6.85	5.08	1.77	0.12	24.9
2:41	80	0.83	0.71	6.75	4.28	2.46	0.13	24.9
2:57	90	1.03	1.03	6.65	4.22	2.43	0.14	24.8
3:12	100	1.15	0.91	6.58	3.69	2.89	0.15	24.9
3:28	110	1.73	1.33	6.47	3.30	3.17	0.16	24.9
3:43	120	1.85	1.60	6.43	2.81	3.61	0.18	24.9
3:59	130	2.32	1.81	6.38	2.39	4.00	0.21	25.0
4:15	140	2.46	2.12	6.34	2.07	4.27	0.22	25.0
4:30	150	2.71	2.61	6.28	2.15	4.13	0.27	25.1
4:46	160	2.86	2.86	6.26	1.85	4.41	0.27	25.1
5:01	170	2.79	2.51	6.27	1.79	4.48	0.29	25.2
5:17	180	2.83	2.76	6.30	1.48	4.82	0.29	25.4
5:32	190	3.42	2.81	6.33	1.18	5.15	0.30	25.5
5:48	200	4.31	3.83	6.40	0.70	5.70	0.31	25.7
6:03	210	5.32	5.06	6.48	0.18	6.30	0.32	25.8
6:19	220	6.40	5.20	6.60	-0.48	7.08	0.32	26.0
6:34	230	6.77	5.43	6.76	-0.66	7.42	0.32	26.0
6:50	240	7.80	5.57	6.93	-1.72	8.64	0.33	26.5
7:05	250	7.61	5.72	7.08	-3.55	10.63	0.33	27.0
7:21	260	8.08	4.33	7.24	-5.67	12.92	0.33	27.4
7:36	270	5.39	4.05	7.38	-8.63	16.01	0.33	27.7
7:52	280	4.76	3.80	7.54	-13.35	20.90	0.34	28.6
8:07	290	3.72	3.42	7.66	-18.64	26.30	0.34	29.2
8:23	300	3.79	3.46	7.88	-26.22	34.10	0.34	29.9
8:35	310	4.02	3.78	7.88	-31.64	39.51	0.34	30.6

VT208 (3-layer test)

Time h:m	Lifting height mm	Lifting stress		Normal pressure kPa	Pore water pressure				Temp layer 3 °C	Temp layer 1 °C
		static kPa	sliding kPa		no.1 kPa	no.2 kPa	no.3 kPa	no.4 kPa		
0:34	0	-0.34	-1.11	5.36			2.08		20.9	21.9
0:50	10	0.08	-0.06	5.33			1.92		20.8	23.9
1:05	20	0.05	0.05	5.30			1.81		20.8	24.6
1:21	30	0.14	0.40	5.44			1.82		20.7	24.8
1:37	40	0.35	0.19	5.54			1.86		21.5	25.0
1:52	50	0.40	0.01	5.50			1.79		21.6	25.0
2:08	60	0.32	0.25	4.93			1.74		21.7	24.8
2:23	70	0.31	0.03	5.42		1.85	5.93	3.55	21.8	24.3
2:39	80	0.79	0.17	5.43		2.06	5.67	3.41	21.7	24.2
2:54	90	0.65	0.37	5.36		2.07	5.47	3.28	21.9	24.1
3:10	100	0.92	0.39	5.26		2.02	5.34	3.02	22.3	24.1
3:25	110	0.80	0.80	5.19		1.99	5.19	2.05	22.3	23.9
3:41	120	1.10	0.92	5.14		1.96	5.00	1.50	22.4	24.1
3:56	130	0.87	0.56	4.85		1.94	4.79	0.94	22.5	24.1
4:12	140	1.16	0.96	5.22		5.25	2.05	-1.85	22.6	23.9
4:27	150	1.14	0.94	5.30	2.32	5.50	3.44	-0.54	23.2	24.0
4:43	160	1.34	1.21	5.32	2.51	5.23	3.61	-0.52	23.2	24.1
4:58	170	1.66	1.37	5.28	2.54	4.94	3.41	-0.58	23.3	24.2
5:14	180	2.03	2.03	5.25	2.53	4.72	3.25	-0.73	23.4	24.2
5:29	190	2.28	1.82	5.25	2.45	4.39	2.75	-1.24	23.5	24.4
5:45	200	2.91	2.86	5.22	2.34	4.11	2.33	-1.78	23.6	24.6
6:00	210	2.55	2.21	5.20	2.86	3.93	1.57	-2.65	23.6	24.7
6:16	220	2.89	2.50	5.20	2.47	3.38	1.11	-3.22	23.5	25.0
6:32	230	3.66	3.42	5.18	2.27	2.85	0.56	-3.77	23.6	25.2
6:47	240	4.13	3.59	5.22	1.99	2.34	-0.06	-4.46	23.7	25.5
7:03	-14	4.67	3.59	5.25	1.62	1.70	-0.80	-5.38	23.8	25.9
7:18	260	5.16	4.36	5.37	1.28	0.89	-1.80	-6.96	23.9	26.3
7:34	270	5.93	4.17	5.40	0.81	-0.27	-3.37	-9.45	24.0	26.6
7:49	280	5.32	4.12	5.31	0.33	-1.60	-5.11	-12.58	24.1	26.2
8:05	290	5.38	3.78	5.34	-0.46	-3.49	-7.37	-16.60	24.1	26.7
8:20	300	5.45	4.07	5.39	-1.29	-5.53	-9.89	-21.93	24.3	28.1
8:36	310	5.55	3.66	5.48	-2.62	-7.96	-12.56	-27.97	24.4	28.8
8:51	320	5.66	3.60	5.56	-4.28	-10.65	-15.44	-35.48	24.5	29.5
9:07	330	4.57	3.49	5.66	-6.26	-13.56	-18.43	-42.64	24.7	30.0
9:22	340	5.29	3.67	5.75	-8.59	-16.73	-21.44	-50.67	24.9	30.7
9:38	350	4.52	3.46	5.86	-11.50	-20.27	-24.32	-57.88	25.1	31.3
9:53	360	4.37	3.45	5.97	-16.22	-24.98	-27.12	-66.56	25.4	31.7
10:09	370	4.32	2.76	6.05	-24.80	-32.18	-30.49	-58.47	25.7	32.5
10:24	380	3.36	3.12	6.13	-36.57	-41.72	-34.13	-69.53	26.0	33.0
10:40	390	3.23	3.17	6.19	-50.82	-51.94	-37.83	-70.51	26.4	34.1
10:55	400	3.34	3.21	6.26	-63.21	-61.56	-41.19	-72.35	26.9	35.2
11:11	410	3.43	3.19	6.37	-79.01	-69.41	-44.08	-73.70	27.3	35.7
11:17	420	3.43	3.15	6.37	-83.47	-71.90	-44.75	-73.28	27.6	36.6

VT209

Time h:m	Lifting height mm	Lifting stress		Normal pressure kPa	Aver. Pore water pressure kPa	Effective pressure kPa	Deformation mm	Temp °C
		static kPa	sliding kPa					
1:40	0	0.34	0.22	7.67	7.63	0.04	Error in reading	25.3
1:56	10	0.36	0.10	7.57	7.57	0.01		25.6
2:12	20	0.40	0.24	7.46	7.45	0.01		25.8
2:27	30	0.39	0.12	7.40	7.37	0.03		25.9
2:43	40	0.45	0.37	7.36	7.33	0.03		26.0
2:58	50	0.68	0.46	7.25	7.01	0.24		26.1
3:14	60	0.75	0.56	7.19	6.96	0.23		26.2
3:29	70	0.90	0.72	7.09	6.61	0.47		26.2
3:45	80	1.07	0.75	7.02	6.12	0.89		26.2
4:01	90	1.47	1.23	6.97	5.66	1.31		26.3
4:16	100	1.68	1.30	6.94	5.05	1.89		26.3
4:32	110	1.92	1.60	6.89	4.56	2.33		26.3
4:47	120	2.31	2.29	6.92	3.97	2.94		26.4
5:03	130	2.58	2.26	6.91	3.18	3.73		26.7
5:18	140	2.80	2.80	6.98	2.21	4.77		26.4
5:34	150	3.41	2.95	7.05	1.46	5.59		25.9
5:49	160	5.02	4.03	7.16	0.40	6.76		26.1
6:05	170	5.98	4.87	7.29	-0.90	8.18		26.4
6:20	180	7.04	5.53	7.44	-2.62	10.06		26.7
6:36	190	9.93	6.54	7.62	-5.53	13.14		27.0
6:51	200	10.14	5.65	7.82	-10.17	17.98		27.4
7:07	210	10.94	4.63	7.99	-18.78	26.78		27.8
7:23	220	8.36	4.01	8.14	-33.68	41.82		28.1
7:38	230	4.51	3.99	8.30	-52.91	61.21		28.6
7:54	240	4.67	4.45	8.44	-70.27	78.71		29.1
8:09	250	4.79	4.68	8.57	-73.95	82.51		29.8
8:25	260	4.94	4.24	8.77	-74.82	83.59		30.5

VT211(3-layer test)

Time h:m	Lifting height mm	Lifting stress		Normal pressure kPa	Pore water pressure				Temp layer 1 °C	Temp layer 3 °C
		static kPa	sliding kPa		no.1 kPa	no.2 kPa	no.3 kPa	no.4 kPa		
0:58	0	0.34	-0.08	4.45			1.72		18.1	23.7
1:29	10	0.01	-0.02	4.52			1.75		22.1	24.5
2:00	20	0.20	0.04	4.55			1.69		22.3	24.3
2:31	30	0.79	0.01	6.09			6.01	6.52	22.3	24.0
3:02	40	0.41	0.04	6.11		1.92	5.61	5.54	22.4	24.1
3:33	50	0.81	0.25	6.03		2.02	5.69	4.56	22.6	24.2
4:04	60	0.60	0.22	6.20		2.09	5.70	3.50	22.6	24.3
4:35	70	0.54	0.13	6.34	2.57	6.56	8.88	3.16	24.4	25.1
5:06	80	0.84	0.43	6.31	2.69	6.56	8.54	2.03	24.5	24.8
5:37	90	1.53	1.18	6.23	2.69	6.50	7.70	0.92	24.5	24.7
6:08	100	2.10	1.72	6.21	2.68	6.29	6.41	-0.47	24.6	24.9
6:39	110	2.97	2.57	6.18	2.68	5.92	5.08	-1.87	24.3	24.9
7:10	120	3.04	2.94	6.19	2.65	5.09	3.60	-3.69	24.6	25.3
7:40	130	5.24	4.93	6.20	2.61	3.69	2.01	-5.96	24.6	25.9
8:11	140	7.76	5.80	6.14	1.80	1.52	-0.21	-9.98	24.7	26.6
8:42	150	9.58	6.61	6.15	0.55	-1.40	-3.09	-17.16	24.9	27.5
9:13	160	11.49	7.08	6.13	-1.72	-6.22	-7.06	-29.93	25.1	28.5
9:44	170	12.71	7.03	6.18	-6.40	-13.76	-12.17	-47.55	25.5	29.6
10:15	180	12.87	6.22	6.26	-18.18	-26.39	-19.01	-56.24	25.9	30.9
10:46	190	15.25	6.99	6.50	-41.36	-45.06	-27.97	-30.01	26.7	32.1
11:17	200	13.91	3.84	6.58	-3.69	-58.98	-35.99	-30.30	27.6	31.0

VT212

Time h:m	Lifting height mm	Lifting stress		Normal pressure kPa	Aver. Pore water pressure kPa	Effective pressure kPa	Deformation mm	Temp °C
		static kPa	sliding kPa					
0:40	0	0.09	-0.02	7.39			0.00	24.5
0:56	10	0.28	0.02	7.35	7.20	0.15	0.00	25.1
1:11	20	0.17	0.11	7.30	7.14	0.15	0.00	25.1
1:27	30	0.35	0.10	7.26	7.08	0.18	0.00	25.1
1:42	40	0.51	0.26	7.26	7.04	0.22	0.02	25.1
1:58	50	0.40	0.20	7.21	6.94	0.27	0.05	25.3
2:13	60	0.50	0.15	7.10	6.62	0.48	0.06	25.4
2:29	70	0.45	0.27	6.99	6.34	0.66	0.08	25.2
2:44	80	0.65	0.23	6.91	6.03	0.88	0.08	25.5
3:00	90	0.90	0.44	6.83	5.68	1.15	0.09	25.2
3:16	100	0.93	0.93	6.74	5.31	1.43	0.10	25.3
3:31	110	1.16	0.77	6.67	4.93	1.74	0.10	25.4
3:47	120	1.32	1.01	6.59	4.46	2.13	0.11	25.3
4:02	130	1.39	1.10	6.51	4.15	2.36	0.08	25.3
4:18	140	1.81	1.63	6.47	3.80	2.67	0.10	25.4
4:33	150	2.07	1.66	6.43	3.45	2.98	0.11	25.4
4:49	160	2.30	1.96	6.36	3.28	3.09	0.11	25.6
5:04	170	2.28	1.95	6.36	2.53	3.83	0.14	25.8
5:20	180	2.74	2.22	6.35	2.05	4.29	0.15	25.8
5:35	190	2.81	2.46	6.39	1.42	4.97	0.16	25.8
5:51	200	3.17	2.83	6.44	0.65	5.80	0.15	25.8
6:06	210	4.03	3.78	6.52	-0.15	6.67	0.15	25.9
6:22	220	5.05	4.27	6.60	-1.11	7.71	0.15	25.9
6:37	230	5.91	4.95	6.71	-2.26	8.98	0.15	26.1
6:53	240	7.51	5.27	6.82	-3.83	10.66	0.14	26.3
7:08	250	7.94	6.44	6.96	-6.27	13.22	0.14	26.6
7:24	260	9.78	6.41	7.12	-10.14	17.27	0.14	26.9
7:39	270	10.45	5.77	7.31	-15.17	22.48	0.14	27.3
7:55	280	8.42	4.12	7.45	-22.67	30.12	0.14	27.7
8:10	290	5.25	3.50	7.57	-30.76	38.33	0.14	28.1
8:26	300	4.09	3.29	7.75	-43.05	50.80	0.14	28.8
8:29	310	4.06	3.82	7.75	-38.13	45.87	0.14	28.9

VT215

Time h:m	Lifting height mm	Lifting stress		Normal pressure kPa	Aver. Pore water pressure kPa	Effective pressure kPa	Deformation mm	Temp °C
		static kPa	sliding kPa					
0:47	0	0.72	0.28	8.04			0.00	24.8
1:03	10	0.62	0.37	8.02	7.76	0.26	0.00	25.2
1:18	20	0.72	0.48	7.98	7.79	0.19	0.02	25.5
1:34	30	0.63	0.46	8.00	7.72	0.28	0.03	25.6
1:49	40	0.74	0.01	7.93	7.49	0.44	0.03	25.7
2:05	50	0.71	0.58	7.92	6.98	0.94	0.06	25.7
2:20	60	1.07	0.75	7.84	6.70	1.14	0.05	25.8
2:36	70	1.02	0.97	7.75	6.55	1.20	0.06	25.8
2:51	80	1.26	1.26	7.69	6.29	1.39	0.07	25.9
3:07	90	1.41	1.19	7.65	5.85	1.80	0.07	26.0
3:23	100	1.65	1.44	7.59	5.48	2.11	0.07	26.0
3:38	110	1.63	1.11	7.58	5.01	2.57	0.08	26.0
3:54	120	1.29	1.29	7.53	4.30	3.22	0.08	26.1
4:09	130	1.62	1.29	7.48	3.80	3.68	0.09	26.1
4:25	140	1.88	1.69	7.50	2.90	4.60	0.09	26.1
4:40	150	2.62	2.13	7.61	1.95	5.66	0.10	26.2
4:56	160	2.79	2.49	7.66	0.70	6.96	0.10	26.3
5:11	170	3.28	2.92	7.78	-0.39	8.17	0.10	26.4
5:27	180	4.27	3.23	7.93	-1.31	9.24	0.10	26.5
5:42	190	4.89	3.71	8.11	-2.41	10.51	0.10	26.7
5:57	200	6.83	4.50	8.30	-4.03	12.33	0.10	27.0
6:13	210	8.29	5.68	8.55	-6.72	15.27	0.10	27.1
6:28	220	10.27	7.18	8.90	-11.43	20.33	0.10	27.3
6:44	230	14.06	7.01	9.11	-18.94	28.05	0.10	27.6
6:59	240	18.80	8.23	9.26	-29.35	38.61	0.10	27.8
7:15	250	18.75	9.27	9.39	-41.80	51.19	0.09	28.1
7:30	260	17.59	8.90	9.48	-53.62	63.09	0.09	28.5
7:46	270	16.05	6.83	9.48	-63.74	73.22	0.09	28.9
8:01	280	7.15	4.32	9.26	-63.06	72.32	0.09	29.4
8:17	290	4.81	4.54	9.25	-62.57	71.83	0.09	30.0
8:32	300	5.26	4.69	9.42	-58.39	67.81	0.08	30.6
8:42	310	5.38	5.21	9.42	-56.40	65.83	0.08	30.9

VT216 (3-layer test)

Time h:m	Lifting height mm	Lifting stress		Normal pressure kPa	Pore water pressure				Temp layer 1 °C	Temp layer 3 °C
		static kPa	sliding kPa		no.1 kPa	no.2 kPa	no.3 kPa	no.4 kPa		
0:36	0	0.32	-0.14	4.93			1.38		24.0	18.2
1:08	10	2.25	0.73	4.99			1.36		24.1	21.8
1:38	20	2.78	1.65	5.15			1.31		24.4	22.0
2:09	30	1.48	0.45	5.32			1.38		24.0	18.5
2:40	40	1.58	1.07	6.08		1.86	5.63	5.08	23.9	21.2
3:11	50	2.04	1.51	6.01		1.80	5.74	5.75	24.3	21.6
3:42	60	2.78	1.65	5.92		1.80	5.71	4.45	24.5	21.9
4:13	70	2.27	1.52	6.53		1.82	5.67	3.23	24.7	19.5
4:44	80	2.75	2.02	7.15	2.16	5.87	5.99	0.75	24.4	23.8
5:15	90	4.16	3.15	7.08	2.50	5.71	6.45	1.84	24.4	22.9
5:45	100	5.73	3.60	6.99	2.31	5.50	5.92	1.32	24.7	22.8
6:16	110	5.36	3.43	6.95	2.31	5.14	4.66	0.32	24.8	22.7
6:47	120	5.39	4.14	6.91	2.31	4.85	3.36	-0.65	24.9	22.7
7:18	130	6.54	4.55	6.94	2.19	3.88	1.83	-1.75	25.2	22.7
7:49	140	7.82	4.63	7.04	2.04	2.89	0.04	-3.25	25.7	22.8
8:20	150	7.91	4.39	7.24	1.40	1.50	-2.53	-7.36	26.1	22.9
8:51	160	7.10	4.18	7.48	-0.21	-0.22	-6.82	-15.99	26.8	23.0
9:22	170	7.50	4.41	7.92	-2.49	-4.68	-13.87	-30.55	27.6	23.4
9:52	180	6.67	4.81	8.34	-10.89	-13.00	-22.31	-49.06	28.4	23.6
10:23	190	6.36	5.13	8.72	-30.11	-26.28	-34.12	-66.29	29.4	24.2
10:54	200	7.08	5.15	9.07	-29.22	-8.42	-46.67	-77.85	30.6	24.8
11:25	210	6.40	5.20	9.30	-17.97	-7.51	-56.21	-81.06	31.7	25.7
11:56	220	6.07	5.50	9.44	-8.87	-6.64	-61.42	-81.38	33.5	26.8
12:24	230	5.90	5.14	9.60	-6.25	-5.74	-63.95	-81.84	34.9	27.9

VT217

Time h:m	Lifting height mm	Lifting stress		Normal pressure kPa	Aver. Pore water pressure kPa	Effective pressure kPa	Deformation mm	Temp °C
		static kPa	sliding kPa					
0:47	0	0.56	0.16	7.18			0.00	24.8
1:03	20	0.75	0.64	7.13	7.12	0.00	0.00	25.0
1:19	40	0.94	0.66	7.06	7.05	0.01	0.00	25.2
1:35	60	1.21	0.97	7.08	6.98	0.10	0.04	25.3
1:50	80	1.30	1.08	6.96	6.80	0.16	0.04	25.4
2:06	100	1.44	1.08	6.87	6.87	0.00	0.04	25.5
2:22	120	1.60	0.92	6.83	6.68	0.15	0.04	25.5
2:38	140	1.76	0.97	6.76	6.38	0.37	0.05	25.5
2:53	160	1.66	1.33	6.68	6.03	0.65	0.05	25.5
3:09	180	1.76	1.56	6.64	5.44	1.20	0.05	25.6
3:25	200	1.98	1.84	6.60	4.43	2.17	0.05	25.7
3:41	220	2.00	1.58	6.63	3.23	3.40	0.05	25.7
3:56	240	2.21	1.97	6.68	3.23	3.45	0.05	25.8
4:12	260	2.69	2.53	6.76	2.79	3.97	0.05	25.8
4:28	280	3.63	3.57	6.93	1.90	5.03	0.04	25.9
4:44	300	4.58	4.27	7.09	0.07	7.02	0.04	26.1
4:59	320	5.17	4.20	7.27	-1.15	8.42	0.04	26.2
5:15	340	5.73	3.99	7.47	-2.18	9.65	0.04	26.4
5:31	360	7.04	4.81	7.68	-3.37	11.05	0.04	26.5
5:47	380	10.57	4.50	7.89	-5.19	13.07	0.04	26.7
6:02	400	9.43	5.63	8.15	-8.41	16.56	0.04	27.0
6:18	420	13.52	5.62	8.39	-14.38	22.77	0.04	27.2
6:34	440	14.06	6.78	8.56	-25.67	34.23	0.04	27.6
6:50	460	11.96	5.81	8.73	-43.95	52.68	0.04	28.0
7:05	480	8.14	6.26	8.80	-58.56	67.37	0.03	28.4
7:21	500	7.55	6.67	8.79	-65.34	74.13	0.03	28.8
7:37	521	8.43	6.78	8.76	-61.75	70.51	0.02	29.3
7:53	540	7.42	6.86	8.68	-51.40	60.08	0.02	29.8
8:08	560	7.87	7.40	8.78	-30.01	38.79	0.02	30.2
8:10	580	7.87	7.87	8.78	-28.86	37.64	0.02	30.3

VT218 (3-layer test)

Time h:m	Lifting height mm	Lifting stress		Normal pressure kPa	Pore water pressure				Temp layer 3 °C	Temp layer 1 °C
		static kPa	sliding kPa		no.1 kPa	no.2 kPa	no.3 kPa	no.4 kPa		
0:29	0	1.35	1.01	6.58			1.92			24.5
0:45	10	1.06	1.06	5.72			1.77			24.1
1:00	20	0.96	0.16	5.56			1.90			24.0
1:16	30	0.86	0.51	5.42			1.95			23.8
1:32	40	0.99	0.24	5.45			1.95			23.7
1:48	50	0.37	0.00	7.11			1.94			23.5
2:03	60	0.22	0.22	7.13			6.56	7.51		25.0
2:19	70	1.80	1.16	6.88		1.08	6.15	6.89		24.4
2:35	80	1.26	0.87	6.81		1.26	6.26	6.89		24.4
2:51	90	1.65	0.86	6.83		1.45	6.23	6.93		24.4
3:06	100	1.84	1.62	6.83		1.53	6.26	6.84		24.5
3:22	110	1.97	1.97	6.86		1.53	6.21	6.56		24.5
3:38	120	2.51	2.18	7.01		1.49	6.14	6.14		24.6
3:54	130	1.39	1.16	8.54		1.45	5.96	5.45		24.6
4:09	140	1.89	1.37	8.63	2.31	5.95	10.44	10.86	25.6	24.6
4:25	150	1.73	1.32	8.33	2.38	5.47	10.45	9.50	25.6	24.8
4:41	160	2.17	1.92	8.09	2.52	5.13	10.29	8.38	25.6	24.8
4:57	170	2.52	1.85	8.02	2.55	4.62	10.01	7.10	25.7	24.9
5:12	180	2.90	2.29	8.00	2.53	3.96	9.65	5.88	25.7	25.1
5:28	190	2.98	2.67	8.07	2.51	3.25	7.89	3.94	25.6	25.2
5:44	200	3.62	3.35	8.15	2.47	2.13	5.62	2.16	25.6	25.4
6:00	210	4.60	4.18	8.23	2.40	0.58	2.86	0.18	25.6	25.5
6:15	220	5.52	4.56	8.34	2.32	-1.09	-0.08	-1.68	25.7	25.7
6:31	230	7.88	5.72	8.46	2.15	-3.52	-3.89	-4.23	25.8	26.0
6:47	240	10.12	6.52	8.55	1.99	-5.80	-8.91	-7.13	25.8	26.3
7:03	250	10.89	7.16	8.63	1.61	-8.31	-14.13	-11.32	26.0	26.7
7:18	260	13.78	8.08	8.65	1.14	-11.09	-21.24	-17.58	26.0	27.1
7:34	270	13.34	7.01	8.68	0.46	-14.32	-29.20	-24.27	26.2	27.5
7:50	280	12.06	5.91	8.61	-0.12	-17.73	-37.16	-28.18	26.2	28.0
8:05	290	6.97	6.00	8.69	-0.71	-21.38	-44.37	-29.84	26.4	28.5
8:21	300	6.55	6.23	8.82	-1.68	-25.33	-51.10	-30.06	26.6	30.4
8:37	310	6.68	5.63	8.94	-3.86	-29.54	-56.99	-30.26	26.8	31.6
8:53	320	6.75	5.71	9.09	-7.91	-33.78	-61.60	-30.06	27.1	32.6
9:08	330	6.50	5.71	9.21	-15.01	-37.85	-64.24	-29.84	27.4	33.5
9:24	340	6.56	6.10	9.32	-26.52	-41.77	-66.05	-29.75	27.6	34.2
9:40	350	6.52	5.70	9.43	-43.33	-45.37	-66.69	-29.61	28.0	34.8
9:56	360	6.43	6.19	9.50	-62.93	-48.72	-66.24	-31.13	28.6	35.2
10:11	370	6.24	6.00	9.57	-83.29	-51.75	-64.02	-32.19	29.3	35.8
10:27	380	6.23	5.86	9.67	-91.16	-54.44	-60.39	-32.70	29.8	36.2
10:43	390	6.17	6.11	9.80	-94.36	-56.79	-55.77	-32.50	30.3	36.5

VT219 (3-layer test)

Time h:m	Lifting height mm	Lifting stress		Normal pressure kPa	Pore water pressure				Temp layer 3 °C	Temp layer 1 °C
		static kPa	sliding kPa		no.1 kPa	no.2 kPa	no.3 kPa	no.4 kPa		
0:28	0	-0.26	-0.86	4.42	Error in reading			2.17		25.8
0:44	10	-0.32	-0.46	4.43				1.93		25.3
1:00	20	-0.06	-0.68	4.36				2.02		25.0
1:16	30	-0.11	-0.53	4.36				2.06		24.8
1:31	40	0.07	-0.69	4.41				2.09		24.8
1:47	50	0.04	-0.19	4.61				2.04		24.6
2:03	60	0.24	-0.36	5.91				2.04		24.5
2:19	70	0.68	0.19	5.96			2.37	5.79	6.69	24.2
2:35	80	0.61	0.13	5.81			2.49	5.48	6.64	24.4
2:50	90	0.72	0.25	5.67			2.57	5.37	6.41	24.5
3:06	100	0.59	-0.01	5.58			2.58	5.29	5.99	24.6
3:22	110	0.90	0.58	5.46			2.59	5.24	5.66	24.6
3:38	120	1.33	0.26	5.41			2.58	5.22	5.27	24.7
3:53	130	0.83	0.37	3.78			2.60	5.20	4.63	24.8
4:09	140	0.91	0.44	6.77			2.60	5.18	3.75	24.7
4:25	150	1.03	0.51	6.64			7.03	8.06	7.33	24.6
4:41	160	1.11	0.74	6.50			7.04	7.84	4.92	24.0
4:57	170	2.33	1.38	6.32			6.98	7.63	4.27	24.4
5:12	180	2.38	1.60	6.16			6.95	7.33	2.99	24.4
5:28	190	2.64	1.71	6.00			6.89	7.11	1.97	24.4
5:44	200	2.50	1.77	5.87			6.83	6.79	0.89	24.3
6:00	210	2.35	2.35	5.73			6.64	6.42	-0.21	24.4
6:16	220	2.75	2.42	5.58			6.28	6.05	-1.25	24.0
6:31	230	3.07	2.47	5.45			5.68	5.72	-2.41	24.0
6:47	240	2.95	2.88	5.33			4.89	5.48	-3.51	24.2
7:03	250	4.07	3.62	5.23			4.01	5.05	-4.79	24.4
7:19	260	4.99	4.04	5.15		2.87	4.94	-6.00	24.4	
7:34	270	5.32	3.99	5.09		1.79	4.70	-7.80	24.5	
7:50	280	5.80	4.64	5.01		0.51	4.32	-11.02	24.6	
8:06	290	5.74	3.96	4.94		-1.00	3.80	-15.68	24.6	
8:22	300	6.06	4.49	4.89		-2.86	3.15	-21.56	24.8	
8:38	310	5.78	4.11	4.83		-4.98	2.44	-29.52	24.8	
8:53	320	5.85	4.84	4.79		-7.51	1.63	-39.34	24.9	
9:09	330	6.03	4.68	4.73		-10.58	0.27	-50.08	25.1	
9:25	340	5.63	4.09	4.70		-14.25	-1.95	-61.82	25.2	
9:41	350	5.15	3.27	4.68		-18.89	-5.83	-72.06	25.4	
9:56	360	4.61	2.75	4.61		-24.75	-11.20	-78.44	25.6	
10:12	370	4.27	2.42	4.56		-32.23	-19.68	-79.29	26.1	
10:28	380	2.40	2.40	4.49		-40.42	-2.45	-80.25	26.5	
10:44	390	2.43	1.96	4.45		-48.29	-2.21	-81.58	27.0	
10:59	400	2.33	2.15	4.40		-53.82	-1.93	-82.72	27.4	
11:15	410	2.59	2.01	4.36		-55.93	-1.71	-83.47	27.8	

VT221 (reference for 3-layer tests)

Time h:m	Lifting height mm	Lifting stress		Normal pressure kPa	no.1 kPa	Pore water pressure				Effective pressure kPa	Deformation mm	Temp °C
		static kPa	sliding kPa			no.2 kPa	no.3 kPa	no.4 kPa				
0:47	0	0.56	0.10	7.29	Error in reading	6.30	7.76		0.98	0.00	23.8	
1:03	20	0.79	0.44	7.34		5.92	7.91		1.42	0.01	24.1	
1:19	40	0.71	0.46	7.32		5.97	7.97		1.35	0.01	23.8	
1:34	60	0.89	0.24	7.26		6.04	8.07		1.22	0.02	23.5	
1:50	80	0.67	0.40	7.29		6.15	8.18	11.80	1.15	0.08	23.7	
2:06	100	0.87	0.46	7.22		6.00	8.13	11.21	1.21	0.09	23.9	
2:22	120	1.28	1.03	7.13		6.03	8.11	10.90	1.10	0.10	24.1	
2:37	140	1.36	1.08	7.08		5.96	8.06	10.17	1.12	0.11	24.1	
2:53	160	1.28	0.88	7.07		5.94	8.05	9.04	1.13	0.13	24.3	
3:09	180	1.39	1.13	6.97		5.91	8.09	8.37	1.05	0.13	24.4	
3:25	200	1.51	1.33	6.85		5.89	8.11	7.95	0.96	0.14	24.4	
3:40	220	1.73	1.35	6.81		5.79	8.06	6.62	1.02	0.15	24.5	
3:56	240	1.89	1.89	6.79		5.64	7.88	5.76	1.16	0.17	24.4	
4:12	260	2.27	1.79	6.80		5.48	7.63	5.29	1.32	0.18	24.5	
4:27	280	2.37	1.99	6.80		4.92	7.18	4.51	1.88	0.19	24.5	
4:43	300	2.82	2.05	6.78		4.14	6.57	3.66	2.63	0.22	24.6	
4:59	320	3.09	2.86	6.83		3.23	5.87	2.39	3.59	0.23	24.7	
5:15	340	3.95	3.04	6.88		2.36	4.96	1.22	4.52	0.24	24.7	
5:30	360	4.48	3.70	6.92		1.24	3.80	0.06	5.68	0.24	24.8	
5:46	380	5.05	4.05	7.00		0.17	2.43	-0.87	6.83	0.25	24.9	
6:02	400	5.90	4.36	7.16		-1.42	0.26	-2.29	8.58	0.25	25.1	
6:18	420	7.32	5.25	7.32		-3.51	-1.88	-4.00	10.83	0.25	25.1	
6:33	440	8.38	5.44	7.47		-6.62	-5.11	-6.91	14.09	0.25	25.2	
6:49	460	9.90	5.41	7.61		-11.05	-9.67	-11.67	18.66	0.25	25.3	
7:05	481	9.41	5.29	7.53		-16.92	-16.03	-17.71	24.46	0.25	25.5	
7:21	501	7.35	4.59	7.57		-24.16	-24.83	-26.56	31.74	0.25	25.7	
7:36	521	7.07	4.51	7.63		-32.99	-35.77	-36.98	40.62	0.25	26.0	
7:52	540	6.04	4.51	7.71		-41.97	-45.72	-48.82	49.68	0.26	26.3	
8:08	560	4.70	4.46	7.85		-50.24	-52.17	-61.12	58.10	0.26	26.6	
8:24	580	4.72	4.60	7.98		-57.46	-56.98	-72.70	65.44	0.26	27.0	
8:39	600	4.98	4.56	8.10		-63.15	-60.88	-77.41	71.25	0.26	27.4	
8:52	620	4.91	4.64	8.13		-66.67	-63.45	-75.92	74.80	0.26	27.8	

VT223 (reference for 3-layer tests)

Time h:m	Lifting height mm	Lifting stress		Normal pressure kPa	Pore water pressure				Effective pressure kPa	Deformation mm	Temp °C
		static kPa	sliding kPa		no.1 kPa	no.2 kPa	no.3 kPa	no.4 kPa			
0:49	0	0.18	-0.23	7.57	2.41	7.51	8.79		0.06	0.00	23.7
1:05	20	0.40	0.33	7.54	2.32	7.21	8.54		0.33	0.00	23.8
1:21	40	0.65	0.22	7.51	2.26	7.24	8.55		0.27	0.00	23.9
1:37	60	1.36	0.38	7.49	2.28	7.23	8.59		0.25	0.00	24.1
1:52	80	0.87	0.28	7.55	2.29	7.22	8.50		0.32	0.00	24.1
2:08	100	0.79	0.46	7.46	2.30	7.30	8.59	11.68	0.17	1.73	24.3
2:24	120	0.89	0.53	7.40	2.27	7.23	8.46	10.98	0.17	1.75	24.3
2:40	140	0.96	0.64	7.37	2.24	7.16	8.40	10.29	0.21	1.75	24.3
2:55	160	1.02	0.65	7.31	2.25	7.17	8.42	9.45	0.14	1.76	24.3
3:11	180	1.10	1.02	7.17	2.23	7.12	8.37	8.43	0.05	1.76	24.3
3:27	200	1.19	0.71	7.07	2.25	7.08	8.41	8.32	0.00	1.77	24.6
3:43	220	1.28	0.74	7.01	2.22	7.01	8.32	7.25	0.00	1.79	24.1
3:58	240	1.52	1.01	6.95	2.24	6.84	8.24	6.28	0.11	1.81	24.2
4:14	260	2.13	1.82	6.94	2.20	6.65	8.20	6.18	0.29	1.82	24.1
4:30	280	2.16	1.62	6.89	2.14	6.32	7.83	4.95	0.57	1.84	23.7
4:46	300	2.51	1.94	6.86	2.07	5.26	7.52	4.41	1.60	1.85	23.9
5:01	320	2.79	2.31	6.84	1.83	4.76	6.79	3.39	2.07	1.86	24.2
5:17	340	2.99	2.48	6.90	1.40	4.09	5.91	2.32	2.81	1.87	24.4
5:33	360	3.22	2.86	6.89	0.67	3.23	4.86	1.02	3.65	1.88	24.4
5:49	380	3.59	2.90	6.95	-0.01	2.75	3.97	0.71	4.20	1.88	24.6
6:04	400	3.87	3.13	7.06	-0.70	0.08	3.04	0.00	6.97	1.89	24.8
6:20	420	4.44	3.12	7.17	-1.48	-1.18	1.98	-0.86	8.35	1.89	24.9
6:36	440	5.34	4.63	7.31	-2.35	-2.67	0.75	-1.79	9.98	1.90	25.1
6:52	460	6.28	4.53	7.49	-3.36	-3.89	-0.67	-2.72	11.38	1.90	25.2
7:07	480	6.77	4.91	7.67	-4.65	-4.23	-2.62	-3.97	11.90	1.90	25.4
7:23	501	7.22	4.50	7.84	-6.56	-4.21	-5.41	-6.28	12.05	1.90	25.5
7:39	521	7.10	4.60	8.05	-9.47	-3.99	-9.38	-9.65	12.04	1.90	25.7
7:54	540	6.89	4.54	8.23	-14.52	-3.62	-14.48	-14.75	11.85	1.90	26.0
8:10	560	6.81	3.65	8.43	-24.44	-6.91	-7.37	-22.17	15.34	1.90	26.4
8:26	580	6.26	4.06	8.60	-40.74	-14.18	-5.06	-31.97	22.78	1.90	26.8
8:42	600	6.66	4.22	8.73	-52.44	-16.57	2.77	-38.16	25.30	1.91	27.3
8:57	620	4.80	4.56	8.79	-64.84	-24.83	2.78	-50.84	33.62	1.91	27.8
9:13	641	4.80	4.38	8.93	-38.53	-33.52	2.78	-58.98	42.45	1.91	28.3
9:29	661	5.08	4.64	8.84	-23.53	-42.61	2.79	-64.02	51.45	1.91	28.7

VT224 (reference for 3-layer tests)

Time h:m	Lifting height mm	Lifting stress		Normal pressure kPa	Pore water pressure				Effective pressure kPa	Deformation mm	Temp °C
		static kPa	sliding kPa		no.1 kPa	no.2 kPa	no.3 kPa	no.4 kPa			
1:24	0	0.48	0.02	7.31	2.03	7.16	9.47		0.15	0.00	0.0
1:39	10	0.49	0.30	7.27	1.90	5.89	8.66		1.38	0.03	23.9
1:55	20	0.89	0.61	7.27	2.19	5.55	8.30		1.71	0.06	24.0
2:11	30	0.93	0.41	7.30	2.25	5.24	8.00	12.07	2.06	0.09	24.2
2:26	40	1.18	0.91	7.32	2.30	5.40	8.86	11.29	1.92	0.17	24.3
2:42	50	1.09	0.84	7.22	2.29	5.18	8.16	10.51	2.04	0.23	24.2
2:58	60	1.20	0.92	7.15	2.28	5.06	7.81	9.73	2.08	0.24	24.3
3:14	70	1.57	1.19	7.07	2.24	4.94	7.43	8.89	2.13	0.25	24.4
3:29	80	1.62	1.35	7.07	2.20	4.81	7.04	8.08	2.26	0.28	24.4
3:45	90	2.04	1.60	6.92	2.17	4.72	6.81	7.51	2.20	0.28	24.4
4:01	100	1.98	1.98	6.84	2.09	4.62	6.42	6.79	2.22	0.29	24.4
4:17	110	2.10	2.10	6.78	2.02	4.46	5.90	6.07	2.33	0.29	24.4
4:32	120	2.61	2.15	6.72	2.00	4.22	4.87	5.50	2.50	0.27	24.3
4:48	130	2.83	2.20	6.77	1.76	3.80	4.00	4.68	2.97	0.30	24.6
5:04	140	2.80	2.40	6.79	1.42	3.23	3.08	3.81	3.56	0.32	24.7
5:20	150	3.11	3.11	6.75	1.19	2.89	2.98	3.57	3.86	0.33	24.8
5:35	160	3.62	3.62	6.82	0.52	1.84	1.34	2.00	4.98	0.34	24.9
5:51	170	4.09	4.09	6.92	-0.22	0.77	0.19	1.02	6.15	0.34	25.1
6:07	180	5.03	4.17	7.03	-1.11	-0.49	-1.11	-0.05	7.53	0.34	25.2
6:23	190	5.75	5.13	7.22	-2.18	-1.98	-2.61	-1.35	9.20	0.35	25.4
6:38	200	6.78	5.56	7.42	-3.37	-3.20	-4.68	-3.30	10.62	0.35	25.6
6:54	210	7.50	6.66	7.68	-5.17	-3.54	-7.39	-6.19	11.22	0.36	25.7
7:10	220	8.73	7.49	7.89	-8.60	-3.52	-7.86	-9.79	11.41	0.36	26.0
7:26	230	9.64	7.51	8.16	-16.09	-3.30	-7.42	-14.63	11.46	0.36	26.3
7:41	240	10.12	6.44	8.44	-25.00	-2.93	-6.82	-20.99	11.36	0.37	26.5
7:57	250	8.14	4.27	8.72	-33.87	-6.22	-6.21	-28.80	14.94	0.37	27.0
8:13	260	4.90	4.06	8.95	-46.83	-13.49	-5.37	-36.24	22.44	0.37	27.2
8:29	270	4.90	4.54	9.19	-58.28	-15.89	-4.41	-44.55	25.07	0.37	27.5
8:44	280	5.09	4.94	9.42	-67.50	-18.31	-3.29	-50.24	27.74	0.38	27.9
9:00	290	5.27	4.48	9.61	-74.07	-16.83	-2.04	-50.78	26.44	0.38	28.4
9:16	300	5.48	5.48	9.66	-78.46	-16.92	-1.30	-54.31	26.58	0.38	28.9

VT225

Time h:m	Lifting height mm	Lifting stress		Normal pressure kPa	Aver. Pore water pressure kPa	Effective pressure kPa	Temp °C
		static kPa	sliding kPa				
0:40	0	0.21	0.02	7.28			24.1
0:42	10	0.21	0.38	7.27			24.1
0:58	20	0.29	0.19	7.27	7.24	0.02	24.5
1:14	30	0.44	0.00	7.29	7.25	0.04	24.8
1:29	40	0.27	0.15	7.27	7.20	0.08	24.8
1:45	50	0.32	0.23	7.24	7.11	0.13	24.8
2:01	60	0.33	0.97	7.21	6.96	0.25	24.8
2:17	70	0.48	0.23	7.18	6.85	0.33	25.0
2:32	80	0.37	0.11	7.11	6.76	0.34	25.0
2:48	90	0.63	0.16	7.07	6.63	0.44	25.1
3:04	100	0.59	0.30	7.05	6.66	0.40	25.1
3:20	110	0.53	0.16	7.03	6.43	0.60	25.2
3:35	120	0.74	0.23	7.10	6.21	0.89	25.2
3:51	130	0.64	0.30	7.07	5.93	1.14	25.2
4:07	140	0.72	0.47	7.09	5.50	1.60	25.3
4:23	150	0.93	0.51	7.13	5.11	2.02	25.3
4:38	160	1.23	0.68	7.11	4.80	2.32	25.4
4:54	170	1.32	0.01	7.17	3.94	3.23	25.5
5:10	180	1.58	1.58	7.27	3.31	3.95	25.5
5:25	190	2.25	1.54	7.37	2.31	5.06	25.7
5:41	200	2.85	2.08	7.49	1.17	6.32	25.8
5:57	210	3.12	2.69	7.65	-0.44	8.09	26.0
6:13	220	4.37	3.30	7.84	-2.42	10.26	26.2
6:28	230	5.31	4.42	8.03	-5.24	13.27	26.3
6:44	240	6.75	4.94	8.24	-9.47	17.71	26.6
7:00	250	8.52	5.35	8.48	-16.61	25.09	26.8
7:16	260	12.63	6.03	8.67	-26.71	35.38	27.0
7:31	270	13.60	7.30	8.72	-35.35	44.08	27.3
7:47	280	14.92	6.94	8.87	-47.58	56.46	27.7
8:03	290	13.38	5.27	9.04	-55.71	64.75	28.1
8:18	300	5.26	5.25	9.16	-60.47	69.64	28.5
8:34	310	5.50	5.16	9.34	-63.13	72.47	29.1
8:39	320	5.35	4.83	9.33	-63.68	73.01	29.1

VT226

Time	Lifting height	Lifting stress		Normal pressure	Aver. Pore water pressure	Effective pressure	Temp
		static	sliding				
h:m	mm	kPa	kPa	kPa	kPa	kPa	°C
0:31	0	0.59	0.06	7.79			24.4
0:47	10	0.53	0.01	7.73			24.5
1:03	20	0.58	0.24	7.82	7.73	0.09	24.8
1:19	30	0.61	0.30	7.75	7.69	0.05	24.9
1:34	40	0.61	0.21	7.63	7.60	0.02	25.1
1:50	50	0.70	0.51	7.63	7.56	0.07	25.2
2:06	60	0.80	0.57	7.60	7.53	0.07	25.1
2:21	70	0.96	0.53	7.58	7.50	0.08	25.2
2:37	80	0.82	0.64	7.59	7.53	0.06	25.3
2:53	90	0.87	0.60	7.58	7.38	0.20	25.4
3:08	100	0.93	0.81	7.55	7.30	0.24	25.5
3:24	110	1.17	0.62	7.55	6.87	0.69	25.6
3:40	120	0.77	0.65	7.56	6.58	0.98	25.6
3:56	130	1.17	1.17	7.56	6.01	1.55	25.7
4:11	140	1.06	0.92	7.60	5.72	1.87	25.7
4:27	150	1.18	1.00	7.61	5.22	2.39	25.8
4:43	160	1.38	1.13	7.67	4.51	3.16	25.9
4:58	170	1.92	1.50	7.73	3.87	3.86	25.9
5:14	180	2.26	1.71	7.77	3.48	4.29	25.9
5:30	190	2.37	2.01	7.88	2.49	5.39	26.1
5:45	200	3.18	2.37	8.02	1.58	6.44	26.3
6:01	210	4.01	3.27	8.10	0.42	7.68	26.5
6:17	220	5.36	3.98	8.26	-1.15	9.41	26.5
6:32	230	7.40	4.80	8.37	-3.39	11.75	26.6
6:48	240	9.28	5.55	8.46	-6.51	14.98	26.9
7:04	250	12.46	6.29	8.60	-10.87	19.47	27.1
7:19	260	16.96	8.17	8.79	-17.17	25.96	27.3
7:35	270	21.01	8.40	8.87	-25.95	34.82	27.4
7:51	280	17.16	8.80	8.98	-35.30	44.28	27.7
8:06	290	18.06	7.67	9.07	-46.98	56.05	27.9
8:22	300	14.02	5.03	9.16	-57.80	66.96	28.3
8:36	310	5.76	5.02	9.28	-65.02	74.30	28.7

VT227

Time h:m	Lifting height mm	Lifting stress		Normal pressure kPa	Aver. Pore water pressure kPa	Effective pressure kPa	Temp °C
		static kPa	sliding kPa				
0:26	0	0.25	0.12	7.69			24.4
0:42	10	0.90	0.54	7.61			24.9
0:57	20	1.17	0.19	7.58			25.4
1:13	30	1.12	0.52	7.69	7.33	0.36	25.6
1:29	40	1.59	0.48	7.72	7.38	0.33	25.8
1:45	50	1.52	0.96	7.68	7.05	0.63	25.7
2:00	60	1.53	0.63	7.63	6.82	0.80	25.9
2:16	70	1.67	0.80	7.56	6.59	0.97	26.0
2:32	80	1.75	1.11	7.47	6.18	1.29	26.0
2:48	90	2.00	0.89	7.38	5.92	1.46	26.1
3:03	100	1.98	1.06	7.31	5.39	1.92	26.0
3:19	110	2.50	1.31	7.30	4.90	2.40	26.1
3:35	120	2.42	1.57	7.22	4.22	3.00	26.1
3:51	130	2.61	1.80	7.16	4.04	3.12	26.2
4:06	140	2.82	1.97	7.13	3.66	3.47	26.2
4:22	150	3.14	2.41	7.08	3.23	3.85	26.3
4:38	160	3.80	2.71	7.02	2.77	4.26	26.3
4:54	170	4.05	2.69	7.00	2.34	4.66	26.4
5:09	180	5.38	4.05	6.96	1.77	5.19	26.6
5:25	190	5.92	4.15	6.92	1.16	5.76	26.6
5:41	200	6.87	4.58	6.94	0.59	6.36	26.7
5:57	210	7.33	4.56	6.97	-0.20	7.17	26.9
6:12	220	7.95	3.25	7.09	-1.25	8.34	27.1
6:28	230	6.15	3.21	7.24	-2.49	9.73	27.2
6:44	240	6.07	2.65	7.32	-4.53	11.85	27.4
6:59	250	3.36	2.88	7.44	-8.55	15.99	27.8
7:15	260	3.50	3.22	7.55	-14.38	21.93	28.1
7:31	270	4.50	3.26	7.62	-23.64	31.26	28.5
7:47	280	4.32	3.04	7.73	-35.43	43.15	29.0
8:02	290	3.64	3.26	7.85	-47.87	55.72	29.5
8:15	300	3.62	2.86	7.85	-56.98	64.82	29.9

VT228

Time	Lifting height	Lifting stress		Normal pressure	Aver. Pore water pressure	Effective pressure	Temp
		static	sliding				
h:m	mm	kPa	kPa	kPa	kPa	kPa	°C
0:27	0	0.23	-0.13	7.43			24.5
0:43	10	0.79	0.04	7.39			25.1
0:59	20	0.78	0.34	7.35			25.5
1:15	30	1.21	0.22	7.39	7.09	0.30	25.7
1:30	40	1.08	0.37	7.43	7.07	0.36	25.8
1:46	50	1.20	0.42	7.44	7.09	0.35	25.9
2:02	60	1.00	0.65	7.38	7.06	0.32	25.9
2:17	70	1.43	0.84	7.32	6.77	0.55	26.1
2:33	80	1.27	0.67	7.25	6.42	0.83	25.7
2:49	90	1.31	0.70	7.17	6.00	1.17	25.9
3:05	100	1.96	0.89	7.11	5.82	1.29	25.9
3:20	110	1.78	1.23	7.08	5.39	1.69	26.0
3:36	120	1.59	1.23	7.03	4.80	2.22	26.1
3:52	130	1.93	1.68	6.98	4.72	2.26	26.1
4:08	140	2.41	1.65	6.93	4.20	2.73	26.1
4:23	150	2.99	1.98	6.88	3.97	2.91	26.2
4:39	160	3.27	2.07	6.83	3.50	3.32	26.5
4:55	170	3.66	2.37	6.80	3.02	3.78	26.4
5:10	180	4.94	3.62	6.76	2.94	3.82	26.5
5:26	190	5.42	4.14	6.72	2.27	4.45	26.7
5:42	200	5.41	3.91	6.71	1.49	5.23	26.8
5:58	210	6.29	3.72	6.73	0.83	5.90	26.9
6:13	220	7.61	4.28	6.77	0.00	6.77	27.0
6:29	227	6.57	3.43	6.87	-1.06	7.93	27.1
6:45	237	5.48	2.65	7.00	-2.31	9.31	27.3
7:00	247	2.97	2.28	7.11	-4.36	11.48	27.5
7:16	257	4.76	2.35	7.19	-8.23	15.42	27.8
7:32	267	4.88	2.93	7.30	-13.66	20.96	28.0
7:48	277	3.14	2.73	7.39	-21.65	29.04	28.5
8:03	287	3.40	2.81	7.43	-33.14	40.57	28.9
8:19	297	4.50	3.35	7.49	-46.04	53.53	29.4
8:35	307	4.42	3.08	0.00	-58.63	58.63	29.9

VT230

Time h:m	Lifting height mm	Lifting stress		Normal pressure kPa	Aver. Pore water pressure kPa	Effective pressure kPa	Temp °C
		static kPa	sliding kPa				
0:47	0	1.17	0.37	7.66			24.6
1:03	10	0.95	0.44	7.64	7.37	0.27	25.5
1:19	20	1.00	0.44	7.63	7.28	0.34	25.2
1:34	30	1.62	0.72	7.68	7.09	0.59	25.5
1:50	40	1.36	0.68	7.72	6.76	0.96	25.6
2:06	50	1.20	0.48	7.68	6.67	1.00	25.7
2:22	60	1.40	0.84	7.61	6.48	1.13	25.9
2:37	70	1.41	1.27	7.57	6.20	1.37	25.9
2:53	80	1.43	1.24	7.49	5.93	1.56	25.9
3:09	90	1.67	1.52	7.42	5.55	1.87	26.0
3:25	100	1.79	1.75	7.37	5.10	2.27	26.3
3:40	110	2.18	1.63	7.35	4.51	2.84	25.9
3:56	120	2.43	1.85	7.32	4.35	2.97	25.8
4:12	130	2.98	2.08	7.27	3.77	3.50	25.7
4:28	140	3.26	2.40	7.24	3.37	3.87	25.5
4:43	150	3.38	2.53	7.20	2.70	4.50	25.7
4:59	160	3.41	2.92	7.17	1.73	5.44	25.6
5:15	170	4.02	3.42	7.16	1.03	6.13	25.7
5:31	180	4.98	3.89	7.17	0.49	6.69	25.7
5:46	190	5.65	4.36	7.20	-0.46	7.66	25.9
6:02	200	6.19	4.72	7.21	-1.60	8.81	26.0
6:18	210	7.93	3.75	7.29	-3.11	10.39	26.4
6:34	220	5.49	2.63	7.37	-5.67	13.04	26.7
6:49	230	6.77	3.34	7.47	-9.93	17.40	27.2
7:05	240	5.54	3.96	7.55	-16.27	23.82	27.6
7:21	250	4.83	4.03	7.65	-25.53	33.18	28.0
7:36	260	4.38	4.01	7.73	-38.23	45.96	28.5
7:52	270	4.60	3.96	7.80	-53.80	61.60	29.0
8:08	280	4.26	3.64	7.88	-62.37	70.26	29.6
8:24	290	4.50	4.30	7.94	-66.32	74.26	30.2
8:39	300	4.34	3.90	8.01	-68.47	76.48	31.0

VT231

Time	Lifting height	Lifting stress		Normal pressure	Aver. Pore water pressure	Effective pressure	Temp
		static	sliding				
h:m	mm	kPa	kPa	kPa	kPa	kPa	°C
0:14	0	0.03	0.44	0.00			23.8
0:30	10	0.51	0.10	7.36			24.1
0:46	20	0.43	0.01	7.32			24.7
1:01	30	0.71	0.29	7.34	7.07	0.27	24.5
1:17	40	0.64	0.03	7.41	6.84	0.57	24.7
1:33	50	0.64	0.18	7.35	6.47	0.88	24.7
1:49	60	0.67	0.43	7.29	6.08	1.21	24.8
2:04	70	0.70	0.57	7.23	5.65	1.57	25.0
2:20	80	0.75	0.45	7.14	5.55	1.59	24.9
2:36	90	1.23	0.52	7.07	4.97	2.09	25.0
2:52	100	1.46	0.90	6.98	4.89	2.09	25.2
3:07	110	1.48	1.22	6.94	4.49	2.46	25.3
3:23	120	1.25	1.08	6.90	4.63	2.27	25.3
3:39	130	1.69	1.69	6.84	3.69	3.14	25.4
3:55	140	1.84	1.60	6.82	3.32	3.50	25.2
4:10	150	1.91	1.80	6.75	2.88	3.87	25.3
4:26	160	2.42	1.91	6.70	2.50	4.20	25.2
4:42	170	2.42	1.84	6.68	1.85	4.83	25.3
4:57	180	2.13	1.94	6.68	1.07	5.60	25.5
5:13	190	2.77	2.58	6.69	0.36	6.33	25.6
5:29	200	3.59	3.26	6.70	-0.56	7.26	25.7
5:45	210	4.64	4.12	6.72	-1.78	8.49	25.9
6:00	220	5.61	4.71	6.79	-3.40	10.19	26.2
6:16	230	6.82	5.26	6.90	-5.92	12.82	26.3
6:32	240	8.86	5.51	7.03	-9.62	16.65	26.5
6:47	250	10.07	6.52	7.13	-15.86	22.98	26.8
7:03	260	10.97	5.55	7.25	-24.86	32.11	27.0
7:19	270	8.61	4.02	7.36	-36.08	43.44	27.4
7:35	280	5.13	3.21	7.50	-48.27	55.77	27.7
7:50	290	3.79	3.09	7.65	-60.67	68.31	28.3
8:06	300	3.94	3.72	7.87	-70.14	78.01	28.6
8:14	310	4.10	3.60	4.69	-73.35	78.04	28.9

VT232

Time h:m	Lifting height mm	Lifting stress		Normal pressure kPa	Aver. Pore water pressure kPa	Effective pressure kPa	Temp °C
		static kPa	sliding kPa				
0:27	0	0.07	0.01	0.00			23.3
0:28	0	0.07	-0.02	7.47			23.3
0:43	10	0.58	-0.18	7.42			23.6
0:59	20	0.52	0.05	7.38	5.99	1.38	23.9
1:15	30	0.67	0.08	7.42	6.50	0.92	24.2
1:31	40	0.67	0.13	7.44	4.48	2.96	24.5
1:46	50	0.83	0.36	7.35	3.43	3.92	24.5
2:02	60	0.87	0.31	7.31	3.31	4.00	24.5
2:18	70	0.65	0.43	7.25	3.51	3.74	24.6
2:34	80	0.87	0.82	7.17	3.03	4.14	24.6
2:49	90	1.32	0.96	7.12	3.04	4.08	24.7
3:05	100	1.13	1.03	7.03	2.86	4.18	24.8
3:21	110	1.34	0.99	6.97	2.65	4.32	24.7
3:37	120	1.58	1.15	6.89	2.75	4.14	24.7
3:52	130	1.65	1.45	6.83	2.68	4.15	24.8
4:08	140	2.10	1.54	6.76	2.50	4.26	24.9
4:24	150	2.16	2.16	6.73	2.24	4.49	24.6
4:40	160	2.32	1.84	6.67	2.21	4.46	24.7
4:55	170	2.53	1.89	6.66	2.21	4.45	24.8
5:11	180	2.67	2.43	6.63	2.06	4.57	24.8
5:27	190	2.31	1.78	6.61	1.61	5.00	24.8
5:42	200	2.18	2.18	6.63	1.27	5.36	25.0
5:58	210	2.80	2.58	6.67	0.78	5.89	24.9
6:14	220	3.47	2.81	6.71	0.15	6.57	25.3
6:30	230	4.69	3.95	6.74	-0.60	7.35	25.1
6:45	240	5.99	4.67	6.81	-1.78	8.60	25.3
7:01	250	6.96	5.99	6.89	-3.10	10.00	25.7
7:17	260	8.72	5.90	7.00	-5.78	12.78	25.6
7:33	270	11.06	7.60	7.12	-10.16	17.28	25.7
7:48	280	11.74	6.72	7.25	-14.78	22.03	25.9
8:04	290	13.20	6.18	7.24	-20.88	28.11	26.2
8:20	300	10.07	4.02	7.30	-28.30	35.60	26.5
8:35	310	4.46	3.26	4.34	-36.07	40.41	26.9
8:51	320	3.67	3.06	4.47	-42.58	47.04	27.4
9:07	330	3.95	3.59	4.55	-47.49	52.03	28.0
9:23	340	3.92	3.44	4.60	-48.63	53.24	28.4
9:38	350	4.09	4.09	4.69	-38.88	43.58	28.9
9:54	360	4.19	3.77	4.74	-35.21	39.95	29.5

VT236

Time	Lifting height	Lifting stress		Normal pressure	Aver. Pore water pressure	Effective pressure	Temp
		static	sliding				
h:m	mm	kPa	kPa	kPa	kPa	kPa	°C
0:29	0	0.51	0.23	7.02			22.2
0:45	10	0.36	-0.41	7.00			22.7
1:00	20	0.73	0.50	6.95	6.07	0.88	23.0
1:15	30	0.70	0.39	6.94	6.06	0.88	23.2
1:31	40	0.73	0.26	7.00	6.10	0.91	23.3
1:46	50	0.73	0.53	6.95	5.92	1.03	23.4
2:01	60	0.80	-0.04	6.93	5.74	1.19	23.4
2:16	70	0.82	0.27	6.85	5.59	1.26	23.2
2:32	80	0.88	0.23	6.77	5.22	1.55	23.3
2:47	90	1.05	0.78	6.71	5.10	1.61	23.3
3:02	100	1.27	0.96	6.67	4.79	1.87	23.3
3:18	110	1.23	1.22	6.60	4.33	2.26	23.3
3:33	120	1.60	1.08	6.52	4.23	2.30	23.5
3:48	130	1.63	1.40	6.47	3.81	2.65	23.5
4:03	140	1.63	1.38	6.39	3.81	2.58	23.5
4:19	150	1.96	1.55	6.36	3.19	3.18	23.5
4:34	160	2.14	2.10	6.34	2.68	3.66	23.6
4:49	170	2.38	2.16	6.29	2.16	4.13	23.8
5:04	180	2.42	1.99	6.31	1.57	4.74	23.7
5:20	190	2.71	2.10	6.28	1.04	5.23	23.9
5:35	200	2.40	2.23	6.26	0.20	6.06	23.9
5:50	210	2.57	2.49	6.31	-0.52	6.83	24.0
6:05	220	3.29	2.91	6.36	-1.45	7.81	24.2
6:21	230	3.78	3.78	6.44	-2.64	9.09	24.2
6:36	240	4.89	4.24	6.52	-4.29	10.80	24.4
6:51	250	5.78	4.46	6.64	-6.07	12.71	24.5
7:06	260	6.98	5.35	6.79	-9.03	15.83	24.6
7:22	270	7.33	4.90	6.91	-13.53	20.44	24.7
7:37	280	7.42	5.24	7.05	-19.40	26.45	24.9
7:52	290	7.70	5.02	7.21	-27.54	34.74	25.3
8:07	300	6.64	4.31	7.37	-37.40	44.77	25.4
8:23	310	4.43	3.92	4.32	-48.95	53.27	25.7

VT237

Time h:m	Lifting height mm	Lifting stress		Normal pressure kPa	Aver. Pore water pressure kPa	Effective pressure kPa	Temp °C
		static kPa	sliding kPa				
0:51	0	0.23	0.08	7.48			21.6
1:07	10	0.01	-0.07	7.41	7.21	0.20	21.7
1:22	20	0.95	0.07	7.43	7.16	0.27	21.8
1:37	30	1.31	0.44	7.31	6.78	0.54	21.9
1:52	40	1.23	0.28	7.24	6.12	1.12	21.9
2:08	50	1.78	0.73	7.16	5.95	1.21	22.0
2:23	60	1.75	0.87	7.01	5.90	1.11	22.0
2:38	70	2.46	1.18	6.92	5.56	1.37	22.1
2:54	80	2.12	1.14	6.83	4.93	1.91	22.1
3:09	90	2.46	1.17	6.73	4.30	2.42	22.3
3:24	100	2.64	1.68	6.65	3.93	2.73	22.2
3:40	110	2.51	1.77	6.58	3.11	3.46	22.3
3:55	120	5.03	2.64	6.50	2.64	3.86	22.5
4:10	130	2.62	1.93	6.46	1.52	4.94	22.6
4:26	140	2.54	2.44	6.47	0.50	5.97	23.7
4:41	150	3.61	3.00	6.51	-0.33	6.84	22.6
4:56	160	5.30	3.56	6.60	-1.25	7.85	22.1
5:11	170	7.55	4.44	6.66	-2.51	9.17	22.8
5:27	180	9.81	5.01	6.76	-4.48	11.24	22.7
5:42	190	11.90	6.91	6.88	-7.01	13.88	23.1
5:57	200	14.25	7.33	7.03	-10.36	17.39	23.5
6:13	210	17.15	7.53	7.13	-15.17	22.30	23.7
6:28	220	17.71	8.94	7.47	-22.33	29.80	24.2
6:43	230	19.93	9.56	7.50	-33.80	41.31	24.6
6:59	240	19.64	7.31	7.56	-48.17	55.73	25.0
7:14	250	15.03	4.47	7.78	-59.12	66.90	25.4
7:29	260	6.72	3.91	7.85	-70.96	78.81	25.8
7:45	270	4.10	3.69	7.97	-78.83	86.79	26.2
8:00	280	4.16	3.58	8.08	-81.63	89.71	26.7
8:15	290	4.11	3.91	5.01	-82.87	87.88	27.1

VT242

Time h:m	Lifting height mm	Lifting stress		Normal pressure kPa	Aver. Pore water pressure kPa	Effective pressure kPa	Temp °C
		static kPa	sliding kPa				
0:26	0	0.71	0.51	7.55			20.7
0:41	10	0.94	0.90	7.38			21.4
0:56	20	1.03	0.65	7.28	7.20	0.08	21.8
1:12	30	0.93	0.62	7.20	7.15	0.06	22.1
1:27	40	1.74	0.90	7.32	6.71	0.61	22.2
1:42	50	1.57	0.83	7.44	6.14	1.30	22.3
1:58	60	1.47	1.20	7.31	5.65	1.66	22.4
2:13	70	1.65	1.27	7.21	4.99	2.23	22.4
2:28	80	2.39	1.53	7.12	4.62	2.50	22.5
2:43	90	3.53	1.97	6.96	4.09	2.87	22.5
2:59	100	2.91	2.04	6.88	3.38	3.50	22.6
3:14	110	3.63	2.45	6.79	2.50	4.29	22.7
3:29	120	3.20	2.43	6.72	1.76	4.95	22.9
3:44	130	4.03	3.31	6.65	1.84	4.81	22.9
4:00	140	3.86	3.13	6.59	0.67	5.92	23.0
4:15	150	4.89	3.75	6.59	0.11	6.48	23.2
4:30	160	6.18	4.05	6.56	-0.67	7.23	23.2
4:46	170	6.78	4.63	6.53	-1.46	7.99	23.3
5:01	180	7.97	5.00	6.57	-2.21	8.78	23.5
5:16	190	9.58	5.35	6.82	-3.44	10.26	23.6
5:31	200	11.83	6.24	6.87	-5.31	12.18	23.8
5:47	210	12.26	6.54	7.09	-7.82	14.91	24.0
6:02	220	13.35	7.26	7.45	-11.35	18.80	24.2
6:17	230	14.32	7.88	7.49	-17.94	25.43	24.4
6:32	240	15.05	7.16	7.57	-26.80	34.37	24.7
6:48	250	11.32	4.09	7.55	-36.41	43.97	24.9
7:03	260	6.42	4.17	7.64	-46.28	53.92	25.3
7:18	270	5.27	4.57	7.76	-55.64	63.40	25.6
7:33	280	4.82	4.14	7.83	-63.75	71.58	26.0
7:49	290	4.84	4.65	7.96	-71.52	79.49	26.4
8:04	300	4.93	4.62	8.03	-77.54	85.57	26.7

VT243

Time h:m	Lifting height mm	Lifting stress		Normal pressure kPa	Aver. Pore water pressure kPa	Effective pressure kPa	Temp °C
		static kPa	sliding kPa				
0:21	0	1.02	0.71	7.43			19.9
0:36	10	1.23	0.72	7.32			20.9
0:52	20	1.47	0.61	7.26	5.78	1.48	21.0
1:07	30	1.28	0.81	7.22	5.71	1.51	21.9
1:22	40	1.50	1.03	7.22	5.58	1.65	21.2
1:38	50	2.12	1.11	7.14	5.30	1.85	21.4
1:53	60	2.65	1.60	7.10	4.84	2.25	21.5
2:08	70	2.28	1.66	7.03	4.91	2.12	21.6
2:23	80	2.72	1.97	6.92	3.09	3.82	21.7
2:39	90	2.61	2.26	6.84	3.15	3.70	21.5
2:54	100	4.28	2.83	6.73	3.08	3.65	21.6
3:09	110	3.69	2.49	6.63	1.56	5.07	21.8
3:24	120	5.39	3.09	6.58	1.08	5.51	22.0
3:40	130	3.77	2.62	6.56	0.57	5.98	22.1
3:55	140	3.08	2.18	6.53	-0.13	6.66	22.3
4:10	150	3.59	2.56	6.52	-0.95	7.47	22.4
4:25	160	5.01	3.58	6.56	-1.91	8.47	22.8
4:41	170	7.42	4.71	6.57	-3.14	9.71	22.4
4:56	180	9.44	5.10	7.04	-4.78	11.82	22.4
5:11	190	12.97	6.84	7.14	-7.17	14.32	23.3
5:26	200	15.11	7.67	7.41	-11.34	18.74	22.7
5:42	210	18.01	7.69	7.56	-15.32	22.89	23.0
5:57	220	22.66	9.53	7.73	-23.08	30.80	24.0
6:12	230	27.22	11.94	7.79	-32.93	40.72	23.0
6:27	240	27.94	8.87	7.84	-42.69	50.54	23.6
6:43	250	25.64	6.92	7.97	-52.10	60.07	24.1
6:58	260	11.38	3.57	7.63	-58.97	66.60	24.4
7:13	270	4.57	4.12	7.74	-64.53	72.27	24.8
7:28	280	4.72	4.68	7.82	-68.67	76.49	25.2
7:44	290	4.77	4.54	7.97	-72.13	80.10	25.7
7:59	300	4.89	4.33	8.08	-73.83	81.92	26.1

VT244

Time h:m	Lifting height mm	Lifting stress		Normal pressure kPa	Aver. Pore water pressure kPa	Effective pressure kPa	Temp °C
		static kPa	sliding kPa				
0:22	0	0.90	0.41	7.56			20.9
0:37	10	1.24	1.09	7.44			21.6
0:53	20	1.12	0.42	7.34	6.24	1.11	21.9
1:08	30	1.69	0.80	7.27	6.22	1.05	22.1
1:23	40	1.81	1.27	7.39	6.13	1.26	22.2
1:38	50	2.37	1.42	7.28	6.14	1.14	22.1
1:54	60	2.27	0.87	7.15	5.13	2.01	22.1
2:09	70	2.40	0.56	7.02	4.22	2.80	22.2
2:24	80	3.18	1.71	6.88	3.74	3.14	22.3
2:39	90	2.51	1.87	6.79	2.65	4.14	22.3
2:55	100	2.87	2.28	6.70	2.11	4.58	22.3
3:10	110	4.08	2.85	6.64	1.83	4.81	22.4
3:25	120	3.89	2.75	6.58	1.08	5.50	22.5
3:40	130	3.25	2.67	6.51	0.47	6.04	22.6
3:56	140	3.90	3.28	6.48	0.22	6.26	22.7
4:11	150	5.19	3.94	6.48	-0.28	6.76	22.8
4:26	160	6.86	4.73	6.54	-0.71	7.25	22.9
4:41	170	7.67	4.73	6.64	-1.10	7.74	23.0
4:57	180	8.51	6.35	6.96	-1.75	8.70	23.2
5:12	190	9.50	6.07	6.93	-2.30	9.23	23.6
5:27	200	10.64	6.41	7.00	-4.12	11.12	23.4
5:42	210	12.87	6.19	7.30	-6.34	13.64	23.6
5:58	220	14.41	7.50	7.61	-11.37	18.98	24.0
6:13	230	16.61	8.41	7.69	-19.74	27.44	24.4
6:28	240	17.47	7.63	7.74	-28.54	36.28	24.7
6:43	250	15.68	4.91	7.81	-38.33	46.15	25.1
6:59	260	7.15	3.96	7.74	-48.45	56.19	25.2
7:14	270	4.58	4.12	7.90	-56.81	64.71	25.5
7:22	280	4.71	4.51	7.90	-60.60	68.50	25.8

VT245

Time h:m	Lifting height mm	Lifting stress		Normal pressure kPa	Aver. Pore water pressure kPa	Effective pressure kPa	Temp °C
		static kPa	sliding kPa				
0:33	0	3.35	2.91	7.92			21.6
0:48	10	4.63	4.20	7.65			22.0
1:03	20	4.35	3.29	7.52	6.92	0.60	22.2
1:18	30	3.30	2.84	7.56	6.83	0.73	22.3
1:34	40	3.40	2.85	7.58	6.70	0.89	22.5
1:49	50	3.11	2.80	7.59	6.03	1.56	22.5
2:04	60	3.12	2.68	7.64	5.63	2.01	22.6
2:20	70	3.30	2.80	7.59	5.26	2.33	22.6
2:35	80	3.44	3.03	7.50	3.48	4.02	22.6
2:50	90	3.24	2.97	7.41	3.91	3.50	22.7
3:05	100	3.30	3.05	7.35	3.07	4.28	22.7
3:20	110	3.68	3.68	7.25	2.19	5.06	22.7
3:36	120	4.34	3.68	7.19	1.89	5.30	22.7
3:51	130	5.03	4.12	7.07	1.65	5.42	22.7
4:06	140	4.33	3.93	7.04	1.56	5.48	22.8
4:21	150	4.30	3.92	7.03	1.53	5.50	22.9
4:37	160	4.63	4.46	7.01	1.49	5.52	22.9
4:52	170	4.92	4.39	6.97	1.33	5.64	22.9
5:07	180	5.26	5.16	6.94	1.19	5.75	23.0
5:22	190	5.43	4.80	6.94	0.99	5.95	23.0
5:38	200	6.19	5.30	6.97	0.54	6.43	23.0
5:53	210	6.98	5.72	7.04	0.33	6.71	23.1
6:08	220	7.97	5.94	7.06	-0.40	7.46	23.0
6:23	230	8.50	6.47	7.15	-1.74	8.90	23.1
6:39	240	10.16	6.87	7.41	-4.01	11.42	23.2
6:54	250	11.85	7.27	7.80	-6.51	14.31	23.3
7:09	260	13.47	8.40	8.02	-9.65	17.67	23.4
7:24	270	15.30	9.80	8.20	-13.65	21.85	23.6
7:40	280	18.10	9.17	8.36	-19.36	27.72	23.9
7:55	290	19.80	10.50	8.49	-22.17	30.67	24.1
8:10	300	18.82	8.49	8.57	-21.00	29.57	24.2
8:25	310	12.57	5.77	5.40	-25.92	31.32	24.4

VT246

Time h:m	Lifting height mm	Lifting stress		Normal pressure kPa	Aver. Pore water pressure kPa	Effective pressure kPa	Temp °C
		static kPa	sliding kPa				
0:31	0	3.72	2.94	7.69			21.8
0:45	10	3.46	1.73	7.59			22.2
1:01	20	3.27	2.96	7.52	6.39	1.14	22.5
1:16	30	3.36	2.85	7.52	5.85	1.68	22.7
1:31	40	2.96	2.96	7.51	5.28	2.23	23.1
1:47	50	3.51	3.40	7.46	4.42	3.03	22.5
2:02	60	3.20	2.92	7.40	3.65	3.75	22.6
2:17	70	3.30	3.17	7.33	2.61	4.72	22.7
2:32	80	3.37	3.08	7.23	3.30	3.92	22.7
2:48	90	3.88	3.41	7.16	3.02	4.13	22.7
3:03	100	4.17	3.82	7.08	2.57	4.50	22.8
3:18	110	3.61	3.45	7.04	2.58	4.46	22.8
3:33	120	3.46	3.24	6.96	2.17	4.79	22.9
3:49	130	3.80	3.25	6.88	2.43	4.45	23.0
4:04	140	3.77	3.36	6.83	2.26	4.57	23.0
4:19	150	4.23	3.56	6.80	2.04	4.75	22.9
4:34	160	4.22	3.64	6.77	1.80	4.97	23.0
4:49	170	4.90	4.10	6.80	1.54	5.25	22.9
5:05	180	5.14	4.74	6.82	1.28	5.54	23.0
5:20	190	6.08	5.16	6.88	0.84	6.04	23.0
5:35	200	7.47	5.15	6.92	0.24	6.68	23.0
5:50	210	7.61	5.72	7.01	-0.44	7.45	23.2
6:06	220	8.26	6.23	7.03	-1.48	8.52	23.1
6:21	230	10.32	6.85	7.11	-2.66	9.77	23.1
6:36	240	11.41	6.27	7.34	-5.36	12.70	23.3
6:51	250	12.64	7.46	7.71	-9.39	17.10	23.4
7:07	260	15.01	8.54	7.87	-15.46	23.33	23.5
7:22	270	16.22	6.97	7.94	-22.82	30.76	23.7
7:37	280	16.01	5.95	7.97	-30.57	38.54	24.0
7:52	290	9.53	4.86	7.99	-39.52	47.51	24.3
8:08	300	5.41	4.81	8.22	-48.75	56.97	24.5
8:23	310	5.17	5.05	5.10	-57.67	62.77	24.8

VT247

Time h:m	Lifting height mm	Lifting stress		Normal pressure kPa	Aver. Pore water pressure kPa	Effective pressure kPa	Temp °C
		static kPa	sliding kPa				
0:35	0	1.80	1.43	7.40			22.0
0:50	10	1.93	0.82	7.24			22.3
1:05	20	1.84	1.72	7.08	5.52	1.56	22.6
1:21	30	2.29	1.72	7.02	4.61	2.41	22.7
1:36	40	2.27	1.59	6.92	4.29	2.63	22.9
1:51	50	1.99	1.54	6.83	3.02	3.81	22.8
2:06	60	2.33	1.99	6.74	2.68	4.06	22.9
2:21	70	3.44	1.57	6.64	2.55	4.10	23.0
2:37	80	3.15	1.98	6.51	2.27	4.24	23.0
2:52	90	3.88	1.94	6.41	1.87	4.53	23.1
3:07	100	3.28	2.04	6.29	1.36	4.93	23.1
3:22	110	3.25	2.55	6.24	1.03	5.21	23.2
3:37	120	3.21	2.82	6.16	0.63	5.53	23.3
3:52	130	3.47	2.75	6.12	0.08	6.03	23.4
4:08	140	4.25	2.98	6.11	-0.62	6.73	23.5
4:23	150	5.52	4.16	6.14	-1.61	7.75	23.6
4:38	160	7.02	5.24	6.20	-2.92	9.12	23.7
4:53	170	8.37	5.44	6.52	-4.58	11.09	23.8
5:08	180	11.08	6.24	6.74	-7.10	13.84	24.0
5:23	190	14.27	7.77	6.94	-12.13	19.08	24.1
5:39	200	18.25	8.70	7.14	-18.87	26.00	24.4
5:54	210	20.74	9.51	7.18	-28.30	35.47	24.6
6:09	220	26.84	11.48	7.34	-36.31	43.65	24.9
6:24	230	27.38	10.32	7.13	-47.59	54.72	25.3
6:39	240	21.04	5.74	7.23	-56.23	63.45	25.5
6:54	250	8.18	4.02	7.49	-34.76	42.25	25.7
7:10	260	4.61	4.27	7.67	-35.63	43.30	26.0
7:25	270	4.56	3.98	7.79	-35.77	43.56	26.3

VT248

Time h:m	Lifting height mm	Lifting stress		Normal pressure kPa	Aver. Pore water pressure kPa	Effective pressure kPa	Temp °C
		static kPa	sliding kPa				
0:31	0	1.61	0.78	7.42			23.0
0:46	10	1.38	0.42	7.25			23.4
1:01	20	1.64	1.34	7.10	4.63	2.48	23.7
1:16	30	1.60	1.25	6.98	3.80	3.18	23.9
1:31	40	1.90	0.87	6.86	3.39	3.46	23.9
1:47	50	2.32	2.32	6.70	2.97	3.73	24.0
2:02	60	2.51	2.10	6.60	2.49	4.11	24.1
2:17	70	3.05	2.58	6.49	2.17	4.33	24.3
2:32	80	2.99	2.68	6.40	1.65	4.75	24.2
2:47	90	3.31	2.47	6.37	1.20	5.17	24.4
3:03	100	4.51	3.46	6.34	0.70	5.63	24.6
3:18	110	5.01	3.76	6.37	0.12	6.26	24.9
3:33	120	6.38	4.88	6.42	-0.65	7.07	25.1
3:48	130	7.21	5.76	6.47	-1.61	8.08	25.2
4:03	140	8.74	5.85	6.80	-3.34	10.14	25.5
4:19	150	11.20	7.35	6.92	-6.03	12.95	25.6
4:34	160	13.57	7.20	7.04	-10.92	17.96	25.9
4:49	170	14.62	8.46	7.15	-17.97	25.12	26.3
5:04	180	13.62	6.60	7.30	-25.45	32.74	26.7
5:19	190	13.65	4.38	7.00	-32.02	39.03	27.2
5:35	200	4.80	3.86	7.22	-41.09	48.30	27.7
5:50	210	4.30	3.54	7.41	-50.65	58.06	28.2
6:05	220	4.48	4.00	7.57	-59.55	67.12	28.7
6:20	230	4.62	4.32	7.76	-43.41	51.17	29.1
6:35	240	4.75	4.54	7.94	-45.69	53.63	29.7
6:51	250	5.01	4.88	8.09	-46.95	55.04	30.1
7:06	260	5.19	5.06	8.27	-47.68	55.94	30.7

VT249

Time h:m	Lifting height mm	Lifting stress		Normal pressure kPa	Aver. Pore water pressure kPa	Effective pressure kPa	Temp °C
		static kPa	sliding kPa				
			Power failure				
4:55	0	9.72	6.58	7.14	-5.73	12.87	23.5
5:11	10	15.50	8.97	7.27	-11.04	18.31	24.8
5:26	20	17.59	9.59	7.34	-24.49	31.83	25.7
5:41	30	16.34	5.32	7.55	-35.93	43.48	26.3
5:56	40	6.30	4.86	7.78	-47.40	55.18	26.9
6:11	50	6.02	4.86	7.95	-58.80	66.75	27.4
6:27	60	5.18	4.90	8.08	-69.10	77.18	28.0
6:42	70	5.51	5.51	8.24	-36.46	44.70	28.3
6:57	80	5.77	5.56	8.37	-38.99	47.36	28.9
7:12	90	6.06	5.66	8.46	-40.53	49.00	29.5
7:27	100	6.09	5.78	8.53	-41.53	50.06	30.0

VT251

Time h:m	Lifting height mm	Lifting stress		Normal pressure kPa	Aver. Pore water pressure kPa	Effective pressure kPa	Temp °C
		static kPa	sliding kPa				
0:31	0	0.33	0.03	9.76			24.2
0:46	10	0.86	0.15	9.64			24.4
1:01	20	0.84	0.25	9.54	8.71	0.83	24.6
1:16	30	0.76	0.33	9.44	8.68	0.76	24.8
1:32	40	0.82	0.22	9.37	8.67	0.70	24.8
1:47	50	0.98	0.61	9.29	8.68	0.61	24.9
2:02	60	0.95	0.81	9.30	8.69	0.61	24.9
2:17	70	1.04	0.97	9.20	8.68	0.52	25.0
2:33	80	1.20	0.85	9.16	7.51	1.65	25.0
2:48	90	1.36	0.96	9.12	6.66	2.46	25.1
3:03	100	1.40	1.07	9.07	6.13	2.95	25.1
3:18	110	1.59	1.39	9.00	5.70	3.29	25.2
3:34	120	1.65	1.52	8.97	5.44	3.53	25.2
3:49	130	1.63	1.51	8.93	4.81	4.12	25.2
4:04	140	1.79	1.53	8.91	4.53	4.38	25.1
4:19	150	2.13	2.04	8.91	3.90	5.00	25.2
4:34	160	2.06	1.85	8.91	3.76	5.15	24.5
4:50	170	2.13	2.13	8.94	3.05	5.89	24.8
5:05	180	2.33	1.94	8.90	2.83	6.07	24.8
5:20	190	2.29	2.07	8.90	2.59	6.32	24.8
5:35	200	2.80	2.31	8.89	2.40	6.49	24.9
5:51	210	3.08	2.45	8.88	2.11	6.78	25.0
6:06	220	3.38	2.50	8.89	1.76	7.13	25.1
6:21	230	3.81	3.03	8.89	1.23	7.66	25.1
6:36	240	4.97	3.37	8.88	0.68	8.21	25.0
6:51	250	5.36	3.57	8.88	-0.04	8.92	25.3
7:07	260	6.10	4.39	8.87	-0.77	9.63	25.1
7:22	270	6.55	5.11	8.84	-1.82	10.67	25.1
7:37	280	7.54	5.44	8.90	-3.07	11.98	25.2
7:52	290	9.28	5.76	8.99	-5.27	14.26	25.2
8:07	300	9.35	6.18	9.10	-8.43	17.53	25.1
8:23	310	11.05	7.41	9.26	-12.68	21.94	25.3
8:38	320	12.99	7.03	9.22	-14.89	24.10	25.3
8:53	330	11.82	6.96	9.36	-18.47	27.82	25.5
9:08	340	12.60	5.64	9.39	-22.57	31.96	25.8
9:24	350	9.22	4.48	9.26	-27.25	36.50	26.0
9:39	360	6.39	4.80	9.29	-31.75	41.04	26.3
9:54	370	5.62	4.75	9.36	-35.07	44.43	26.5
10:09	380	5.23	4.73	9.45	-36.50	45.95	26.9

VT252

Time h:m	Lifting height mm	Lifting stress		Normal pressure kPa	Aver. Pore water pressure kPa	Effective pressure kPa	Temp °C
		static kPa	sliding kPa				
0:33	0	0.47	0.20	5.33	5.24	0.10	22.6
0:48	10	0.91	0.67	5.24	5.06	0.19	23.2
1:03	20	0.67	0.59	5.14	4.93	0.22	23.5
1:18	30	0.92	0.74	5.18	5.02	0.16	23.7
1:33	40	1.02	0.65	5.30	5.13	0.18	23.8
1:49	50	1.23	1.23	5.22	5.07	0.15	23.9
2:04	60	0.87	0.36	5.14	4.98	0.15	24.1
2:19	70	1.06	0.76	5.07	4.96	0.11	23.9
2:34	80	1.03	0.74	5.00	4.90	0.10	24.0
2:50	90	1.10	0.81	4.93	4.81	0.13	24.0
3:05	100	1.35	0.64	4.88	4.22	0.67	24.0
3:20	110	1.39	0.83	4.82	4.02	0.80	24.1
3:35	120	1.54	1.04	4.76	3.69	1.07	24.4
3:50	130	1.20	0.50	4.69	3.91	0.78	23.7
4:06	140	1.19	1.06	4.65	3.35	1.29	23.8
4:21	150	1.42	0.91	4.64	3.01	1.63	23.6
4:36	160	1.66	0.91	4.63	2.76	1.87	23.8
4:51	170	1.83	1.49	4.63	2.30	2.33	23.7
5:07	180	2.09	1.52	4.64	1.96	2.69	23.6
5:22	190	2.33	1.75	4.66	1.51	3.15	23.4
5:37	200	2.70	2.19	4.69	1.15	3.55	23.4
5:52	210	2.47	1.72	4.74	0.50	4.24	23.0
6:07	220	2.92	2.40	4.76	0.08	4.68	23.6
6:23	230	3.44	2.56	4.83	-0.67	5.50	22.8
6:38	240	3.62	3.31	4.88	-1.69	6.57	23.6
6:53	250	3.46	2.82	4.92	-3.14	8.06	23.7
7:08	260	3.89	3.59	4.93	-5.03	9.96	23.6
7:23	270	4.75	3.31	4.91	-7.57	12.47	23.6
7:39	280	5.89	4.45	4.88	-11.28	16.15	23.8
7:54	290	6.51	3.19	4.78	-16.21	20.98	24.0
8:09	300	5.14	1.70	4.72	-22.04	26.76	24.1
8:24	310	3.22	2.25	4.75	-28.51	33.26	22.4
8:39	320	2.61	2.27	4.87	-35.91	40.77	23.2
8:55	330	2.36	2.15	5.03	-44.14	49.17	24.5
9:10	340	2.44	1.90	5.10	-52.32	57.42	24.8
9:25	350	2.41	2.20	5.19	-59.58	64.77	25.4
9:40	360	2.82	2.40	5.42	-65.56	70.98	25.7
9:53	370	2.97	2.50	5.51	-69.22	74.73	26.0

**DEPARTMENT OF STRUCTURAL ENGINEERING
NORWEGIAN UNIVERSITY OF SCIENCE AND TECHNOLOGY**

N-7491 TRONDHEIM, NORWAY
Telephone: +47 73 59 47 00 Telefax: +47 73 59 47 01

- "Reliability Analysis of Structural Systems using Nonlinear Finite Element Methods",
C. A. Holm, 1990:23, ISBN 82-7119-178-0.
- "Uniform Stratified Flow Interaction with a Submerged Horizontal Cylinder",
Ø. Arntsen, 1990:32, ISBN 82-7119-188-8.
- "Large Displacement Analysis of Flexible and Rigid Systems Considering Displacement-
Dependent Loads and Nonlinear Constraints", K. M. Mathisen, 1990:33, ISBN 82-7119-189-6.
- "Solid Mechanics and Material Models including Large Deformations",
E. Levold, 1990:56, ISBN 82-7119-214-0, ISSN 0802-3271.
- "Inelastic Deformation Capacity of Flexurally-Loaded Aluminium Alloy Structures",
T. Welo, 1990:62, ISBN 82-7119-220-5, ISSN 0802-3271.
- "Visualization of Results from Mechanical Engineering Analysis",
K. Aamnes, 1990:63, ISBN 82-7119-221-3, ISSN 0802-3271.
- "Object-Oriented Product Modeling for Structural Design",
S. I. Dale, 1991:6, ISBN 82-7119-258-2, ISSN 0802-3271.
- "Parallel Techniques for Solving Finite Element Problems on Transputer Networks",
T. H. Hansen, 1991:19, ISBN 82-7119-273-6, ISSN 0802-3271.
- "Statistical Description and Estimation of Ocean Drift Ice Environments",
R. Korsnes, 1991:24, ISBN 82-7119-278-7, ISSN 0802-3271.
- "Turbidity Current Modelling",
B. Brørs, 1991:38, ISBN 82-7119-293-0, ISSN 0802-3271.
- "Zero-Slump Concrete: Rheology, Degree of Compaction and Strength. Effects of Fillers as Part
Cement-Replacement",
C. Sørensen, 1992:8, ISBN 82-7119-357-0, ISSN 0802-3271.
- "Nonlinear Analysis of Reinforced Concrete Structures Exposed to Transient Loading",
K. V. Høiseh, 1992:15, ISBN 82-7119-364-3, ISSN 0802-3271.
- "Finite Element Formulations and Solution Algorithms for Buckling and Collapse Analysis of Thin
Shells", R. O. Bjærum, 1992:30, ISBN 82-7119-380-5, ISSN 0802-3271.
- "Response Statistics of Nonlinear Dynamic Systems",
J. M. Johnsen, 1992:42, ISBN 82-7119-393-7, ISSN 0802-3271.
- "Digital Models in Engineering. A Study on why and how engineers build and operate digital
models for decision support", J. Høyte, 1992:75, ISBN 82-7119-429-1, ISSN 0802-3271.

- "Sparse Solution of Finite Element Equations",
A. C. Damhaug, 1992:76, ISBN 82-7119-430-5, ISSN 0802-3271.
- "Some Aspects of Floating Ice Related to Sea Surface Operations in the Barents Sea",
S. Løset, 1992:95, ISBN 82-7119-452-6, ISSN 0802-3271.
- "Modelling of Cyclic Plasticity with Application to Steel and Aluminium Structures",
O. S. Hopperstad, 1993:7, ISBN 82-7119-461-5, ISSN 0802-3271.
- "The Free Formulation: Linear Theory and Extensions with Applications to Tetrahedral Elements with Rotational Freedoms", G. Skeie, 1993:17, ISBN 82-7119-472-0, ISSN 0802-3271.
- "Høyfast betongs motstand mot piggdekkslitasje. Analyse av resultater fra prøving i Veisliter'n",
T. Tveter, 1993:62, ISBN 82-7119-522-0, ISSN 0802-3271.
- "A Nonlinear Finite Element Based on Free Formulation Theory for Analysis of Sandwich Structures", O. Aamlid, 1993:72, ISBN 82-7119-534-4, ISSN 0802-3271.
- "The Effect of Curing Temperature and Silica Fume on Chloride Migration and Pore Structure of High Strength Concrete", C. J. Hauck, 1993:90, ISBN 82-7119-553-0, ISSN 0802-3271.
- "Failure of Concrete under Compressive Strain Gradients",
G. Markeset, 1993:110, ISBN 82-7119-575-1, ISSN 0802-3271.
- "An experimental study of internal tidal amphidromes in Vestfjorden",
J. H. Nilsen, 1994:39, ISBN 82-7119-640-5, ISSN 0802-3271.
- "Structural analysis of oil wells with emphasis on conductor design",
H. Larsen, 1994:46, ISBN 82-7119-648-0, ISSN 0802-3271.
- "Adaptive methods for non-linear finite element analysis of shell structures",
K. M. Okstad, 1994:66, ISBN 82-7119-670-7, ISSN 0802-3271.
- "On constitutive modelling in nonlinear analysis of concrete structures",
O. Fyrilev, 1994:115, ISBN 82-7119-725-8, ISSN 0802-3271.
- "Fluctuating wind load and response of a line-like engineering structure with emphasis on motion-induced wind forces",
J. Bogunovic Jakobsen, 1995:62, ISBN 82-7119-809-2, ISSN 0802-3271.
- "An experimental study of beam-columns subjected to combined torsion, bending and axial actions", A. Aalberg, 1995:66, ISBN 82-7119-813-0, ISSN 0802-3271.
- "Scaling and cracking in unsealed freeze/thaw testing of Portland cement and silica fume concretes", S. Jacobsen, 1995:101, ISBN 82-7119-851-3, ISSN 0802-3271.
- "Damping of water waves by submerged vegetation. A case study of laminaria hyperborea",
A. M. Dubi, 1995:108, ISBN 82-7119-859-9, ISSN 0802-3271.
- "The dynamics of a slope current in the Barents Sea",
Sheng Li, 1995:109, ISBN 82-7119-860-2, ISSN 0802-3271.
- "Modellering av delmaterialenes betydning for betongens konsistens",
Ernst Mørtzell, 1996:12, ISBN 82-7119-894-7, ISSN 0802-3271.

- "Bending of thin-walled aluminium extrusions",
Birgit Søvik Opheim, 1996:60, ISBN 82-7119-947-1, ISSN 0802-3271.
- "Material modelling of aluminium for crashworthiness analysis",
Torodd Berstad, 1996:89, ISBN 82-7119-980-3, ISSN 0802-3271.
- "Estimation of structural parameters from response measurements on submerged floating tunnels",
Rolf Magne Larssen, 1996:119, ISBN 82-471-0014-2, ISSN 0802-3271.
- "Numerical modelling of plain and reinforced concrete by damage mechanics",
Mario A. Polanco-Loria, 1997:20, ISBN 82-471-0049-5, ISSN 0802-3271.
- "Nonlinear random vibrations - numerical analysis by path integration methods",
Vibeke Moe, 1997:26, ISBN 82-471-0056-8, ISSN 0802-3271.
- "Numerical prediction of vortex-induced vibration by the finite element method",
Joar Martin Dalheim, 1997:63, ISBN 82-471-0096-7, ISSN 0802-3271.
- "Time domain calculations of buffeting response for wind sensitive structures",
Ketil Aas-Jakobsen, 1997:148, ISBN 82-471-0189-0, ISSN 0802-3271.
- "A numerical study of flow about fixed and flexibly mounted circular cylinders",
Trond Stokka Meling, 1998:48, ISBN 82-471-0244-7, ISSN 0802-3271.
- "Estimation of chloride penetration into concrete bridges in coastal areas",
Per Egil Steen, 1998:89, ISBN 82-471-0290-0, ISSN 0802-3271.
- "Stress-resultant material models for reinforced concrete plates and shells",
Jan Arve Øverli, 1998:95, ISBN 82-471-0297-8, ISSN 0802-3271.
- "Chloride binding in concrete. Effect of surrounding environment and concrete composition",
Claus Kenneth Larsen, 1998:101, ISBN 82-471-0337-0, ISSN 0802-3271.
- "Rotational capacity of aluminium alloy beams",
Lars A. Moen, 1999:1, ISBN 82-471-0365-6, ISSN 0802-3271.
- "Stretch Bending of Aluminium Extrusions",
Arild H. Clausen, 1999:29, ISBN 82-471-0396-6, ISSN 0802-3271.
- "Aluminium and Steel Beams under Concentrated Loading",
Tore Tryland, 1999:30, ISBN 82-471-0397-4, ISSN 0802-3271.
- "Engineering Models of Elastoplasticity and Fracture for Aluminium Alloys",
Odd-Geir Lademo, 1999:39, ISBN 82-471-0406-7, ISSN 0802-3271.
- "Kapasitet og duktilitet av dybelforbindelser i trekonstruksjoner",
Jan Siem, 1999:46, ISBN 82-471-0414-8, ISSN 0802-3271.
- "Etablering av distribuert ingeniørarbeid; Teknologiske og organisatoriske erfaringer fra en norsk ingeniørbedrift", Lars Line, 1999:52, ISBN 82-471-0420-2, ISSN 0802-3271.
- "Estimation of Earthquake-Induced Response",
Símon Ólafsson, 1999:73, ISBN 82-471-0443-1, ISSN 0802-3271.

- “Coastal Concrete Bridges: Moisture State, Chloride Permeability and Aging Effects”
Ragnhild Holen Relling, 1999:74, ISBN 82-471-0445-8, ISSN 0802-3271.
- ”Capacity Assessment of Titanium Pipes Subjected to Bending and External Pressure”,
Arve Bjørset, 1999:100, ISBN 82-471-0473-3, ISSN 0802-3271.
- “Validation of Numerical Collapse Behaviour of Thin-Walled Corrugated Panels”,
Håvar Ilstad, 1999:101, ISBN 82-471-0474-1, ISSN 0802-3271.
- “Strength and Ductility of Welded Structures in Aluminium Alloys”,
Miroslaw Matusiak, 1999:113, ISBN 82-471-0487-3, ISSN 0802-3271.
- “Thermal Dilation and Autogenous Deformation as Driving Forces to Self-Induced Stresses in High Performance Concrete”,
Øyvind Bjøntegaard, 1999:121, ISBN 82-7984-002-8, ISSN 0802-3271.
- “Some Aspects of Ski Base Sliding Friction and Ski Base Structure”,
Dag Anders Moldestad, 1999:137, ISBN 82-7984-019-2, ISSN 0802-3271.
- "Electrode reactions and corrosion resistance for steel in mortar and concrete",
Roy Antonsen, 2000:10, ISBN 82-7984-030-3, ISSN 0802-3271.
- "Hydro-Physical Conditions in Kelp Forests and the Effect on Wave Damping and Dune Erosion. A case study on Laminaria Hyperborea",
Stig Magnar Løvås, 2000:28, ISBN 82-7984-050-8, ISSN 0802-3271.
- "Random Vibration and the Path Integral Method",
Christian Skaug, 2000:39, ISBN 82-7984-061-3, ISSN 0802-3271.
- "Buckling and geometrical nonlinear beam-type analyses of timber structures",
Trond Even Eggen, 2000:56, ISBN 82-7984-081-8, ISSN 0802-3271.
- ”Structural Crashworthiness of Aluminium Foam-Based Components”,
Arve Grønsund Hanssen, 2000:76, ISBN 82-7984-102-4, ISSN 0809-103X.
- “Measurements and simulations of the consolidation in first-year sea ice ridges, and some aspects of mechanical behaviour”,
Knut V. Høyland, 2000:94, ISBN 82-7984-121-0, ISSN 0809-103X.
- ”Kinematics in Regular and Irregular Waves based on a Lagrangian Formulation”,
Svein Helge Gjørund, 2000-86, ISBN 82-7984-112-1, ISSN 0809-103X.
- ”Self-Induced Cracking Problems in Hardening Concrete Structures”,
Daniela Bosnjak, 2000-121, ISBN 82-7984-151-2, ISSN 0809-103X.
- "Ballistic Penetration and Perforation of Steel Plates",
Tore Børvik, 2000:124, ISBN 82-7984-154-7, ISSN 0809-103X
- "Freeze-Thaw resistance of Concrete. Effect of: Curing Conditions, Moisture Exchange and Materials",
Terje Finnerup Rønning, 2001:14, ISBN 82-7984-165-2, ISSN 0809-103X
- "Structural behaviour of post tensioned concrete structures. Flat slab. Slabs on ground",
Steinar Trygstad, 2001:52, ISBN 82-471-5314-9, ISSN 0809-103X.